

**AMINOSTRATIGRAPHY, GEOCHRONOLOGY AND GEOCHEMISTRY OF FOSSILS
FROM LATE CENOZOIC MARINE UNITS IN SOUTHEASTERN VIRGINIA**

By
June Elizabeth Mirecki

A dissertation submitted to the Faculty of the University of Delaware
in partial fulfillment of the requirements for the degree of
Doctor of Philosophy in Geology

June 1990

**AMINOSTRATIGRAPHY, GEOCHRONOLOGY AND GEOCHEMISTRY OF FOSSILS
FROM LATE CENOZOIC MARINE UNITS IN SOUTHEASTERN VIRGINIA**

By

June Elizabeth Mirecki

Approved: _____

Billy P. Glass, Ph.D.
Chairman of the Department of Geology

Approved: _____

Carol E. Hoffecker, Ph.D.
Acting Associate Provost for Graduate Studies

AMINOSTRATIGRAPHY, GEOCHRONOLOGY AND GEOCHEMISTRY OF FOSSILS
FROM LATE CENOZOIC MARINE UNITS IN SOUTHEASTERN VIRGINIA

By

June Elizabeth Mirecki

I certify that I have read this dissertation and that in my opinion it meets the academic and professional standard required by the University as a dissertation for the degree of Doctor of Philosophy.

Signed: _____

John F. Wehmiller, Ph.D.
Professor in charge of dissertation

I certify that I have read this dissertation and that in my opinion it meets the academic and professional standard required by the University as a dissertation for the degree of Doctor of Philosophy.

Signed: _____

Billy P. Glass, Ph.D.
Chairman of the Department of Geology and member of dissertation committee

I certify that I have read this dissertation and that in my opinion it meets the academic and professional standard required by the University as a dissertation for the degree of Doctor of Philosophy.

Signed: _____

Dr. Peter B. Leavens, Ph.D.
Member of dissertation committee

I certify that I have read this dissertation and that in my opinion it meets the academic and professional standard required by the University as a dissertation for the degree of Doctor of Philosophy.

Signed: _____

Dr. Noreen Tuross, Ph.D.
Member of dissertation committee

I certify that I have read this dissertation and that in my opinion it meets the academic and professional standard required by the University as a dissertation for the degree of Doctor of Philosophy.

Signed: _____

Dr. Harold White, Ph.D.
Member of dissertation committee

TABLE OF CONTENTS

List of Tables.....	
List of Figures.....	
CHAPTER 1: INTRODUCTION AND STATEMENT OF PURPOSE.....	
CHAPTER 2: ANALYTICAL METHODS I: SEPARATION AND QUANTIFICATION OF AMINO ACIDS.....	
2.1: Sample Preparation.....	
2.2: System Description.....	
2.2.1: A Note on Reagent and Laboratory Glassware Quality.....	
2.3: Calculation of Amino Acid Concentration.....	
CHAPTER 3: EVALUATION OF AMINO ACID DATA.....	
3.1: Introduction and Structure of Chapter.....	
3.2: Chromatographic Criteria.....	
3.3: Precision of ILC Molluscan Shell Powder Analyses.....	
3.3.1: Precision of Amino Acid Concentrations From ILC-B Molluscan Shell Powders.....	
3.3.2: Precision of Amino Acid Fractions From ILC-B Molluscan Shell Powders.....	
3.3.3: Precision of Free/Total Amino Acid Values From ILC-B Molluscan Shell Powders.....	
3.3.4: Precision of ALLO/ISO Values From ILC-B Molluscan Shell Powders.....	
3.3.5: Accuracy of ALLO/ISO Values from ILC-B Molluscan Shell Powders.....	
3.4: Precision of Fossil Sample Analyses.....	
3.4.1: Comparison of Fossil Sample and ILC Standard Data Run Concurrently.....	
CHAPTER 4: ANALYTICAL METHODS II: ATOMIC ABSORPTION SPECTROMETRY, X-RAY DIFFRACTION, SCANNING ELECTRON MICROSCOPY AND WEIGHT GAIN/LOSS EXPERIMENTS.....	
4.1: Introduction and Structure of Chapter.....	
4.2: Atomic Absorption Spectrometry Methods: Calcium, Strontium, Manganese and Iron.....	
4.2.1: Estimation of Dilution Error.....	
4.2.2: Comments for Future Work.....	

- 4.3: Scanning Electron Microscopy.....
- 4.4: X-Ray Diffraction Methods.....
- 4.5: Water Weight Gain/Loss Experiments.....

**CHAPTER 5: GEOLOGIC HISTORY OF THE PLEISTOCENE UNITS
FOUND IN THE OUTER COASTAL PLAIN OF
SOUTHEASTERN VIRGINIA.....**

- 5.1: Introduction.....
- 5.2: Lithostratigraphy of Pleistocene Units in Southeastern Virginia
(Oaks and Coch,1973).....
- 5.3: Reinterpretations Considering Timing and Magnitude of Sea Level
Rise.....
- 5.4: Lithostratigraphy of Related Field Sites in Virginia: Norris
Bridge and Yadkin Pit.....
 - 5.4.1: The Norris Bridge Locality.....
 - 5.4.2: The Yadkin Pit Locality.....
- 5.5: Comparison of Stratigraphic Frameworks Applied in Southeastern
Virginia.....
 - 5.5.1: Definition of Lithostratigraphic Frameworks in
Southeastern Virginia.....
 - 5.5.2: Definition of Biostratigraphic Frameworks in
Southeastern Virginia.....
 - 5.5.3: Definition of an Allostratigraphic Framework in
Southeastern Virginia, and Its Relationship to
Aminostratigraphy.....

**CHAPTER 6: AMINOSTRATIGRAPHY OF THE PLEISTOCENE UNITS
FOUND IN THE OUTER COASTAL PLAIN OF SOUTH-
EASTERN VIRGINIA.....**

- 6.1: Introduction.....
- 6.2: Aminostratigraphy of Gomez Pit.....
- 6.3: Aminostratigraphy of the Yadkin Pit and Norris Bridge Localities..
- 6.4: Calibration of ALLO/ISO Values in Southeastern Virginia.....
 - 6.4.1: Uranium Series Ages.....
- 6.5: Age Estimates Using the ESR (Electron Spin Resonance) Dating
Method.....
- 6.6: Age Options for Aminozones Defined in Southeastern Virginia.....
 - 6.6.1: Aminozone IIa.....
 - 6.6.2: Aminozone IIc.....
 - 6.6.3: Aminozone IId.....
 - 6.6.4: Aminozone IIe.....
- 6.7: Concluding Remarks.....

**CHAPTER 7: AGE ESTIMATES FOR AMINOZONES DEFINED IN SOUTH-
EASTERN VIRGINIA USING THE NON-LINEAR MODEL
OF ISOLEUCINE EPIMERIZATION.....**

- 7.1: Introduction.....

(7.1: Introduction.....) *je*
 7.2: Modeling Temperature History.....
 7.3: The Quantitative Non-Linear Model of Isoleucine Epimerization.....
 7.4: Amino Acid Epimerization Age Estimates for Aminozones Ilc and Ild in Southeastern Virginia.....
 7.4.1: Age Estimates Using Aminozone Ila Calibrated By 70.2 ka Uranium Series Dates.....
 7.4.2: Age Estimates Using Aminozone Ila Calibrated By Substage 5e (120 ka) High Sea Stand.....
 7.5: Summary.....

CHAPTER 8: DIAGENETIC MODIFICATION OF MOLLUSC SHELL: ANALYSIS OF AMINO ACID COMPOSITION, ELEMENTAL CONCENTRATIONS, MINERALOGY AND TEXTURES IN LATE CENOZOIC MOLLUSCS

8.1: Introduction.....
 8.2: Definition of Shell Quality.....
 8.2.1: Relationship Between Shell Quality and Shell Porosity: Water Weight Gain/Loss Experiments.....
 8.2.2: Relationship Between Shell Age and Shell Micro-textures: SEM Observations.....
 8.3: A Generalized Model of Diagenetic Hydrolysis and Epimerization.....
 8.4: Toward a Leaching Model for Molluscan Shell Amino Acids.....
 8.5: Variations in Amino Acid Composition with Condition.....
 8.5.1: Gomez Pit Aminozone Ila.....
 8.5.2: Comparison of Amino Acid Data Between Gomez Pit Ilc and Yadkin Pit Ilc.....
 8.5.3: Comparison of Amino Acid Data Between Norris Bridge Ild and Gomez Pit Ild.....
 8.6: Variations in Amino Acid Composition with Time.....
 8.6.1: Changes in Amino Acid Concentrations and Their Distribution in Free and Bound States.....
 8.7: Sr Concentrations and Sr/Ca Values with Time, and Condition.....

CHAPTER NINE: SUMMARY AND FUTURE WORKS.....

REFERENCES CITED.....

Appendix A: ILC Data and Experiments

- Appendix A.1: Total and Free ILC-B Concentration Data.
- Appendix A.2: Total and Free ILC-B Concentration Data
- Appendix A.3: Free/Total Values for ILC-B Samples
- Appendix A.4: Hydrolysis Experiment Data

LIST OF TABLES

- Table 3-1:** Sample description for ILC standard molluscan shell powders.....
- Table 3-2:** Statistical summary describing precision of ILC-B Free/Total values for each amino acid.....
- Table 3-3:** Comparison of mean ALLO/ISO values and standard deviations with published data.....
- Table 4-1:** Summary of techniques used to determine diagenetic changes in molluscan shell carbonate.....
- Table 4-2:** Operating parameters for elemental analyses using flame atomic absorption spectrometry.....
- Table 4-3:** Statistics describing 10 analyses of the ILC-D powder to determine dilution error.....
- Table 6-1:** Statistics describing four aminozones found in southeastern Virginia and the Delmarva peninsula.....
- Table 6-2:** Uranium series ages obtained from fossil corals collected from localities described in the text.....
- Table 6-3:** Electron spin resonance age estimates and (ALLO/ISO)TOTAL values obtained from analyses of mollusc valves collected from Gomez Pit.....
- Table 7-1:** Range of (ALLO/ISO)TOTAL values and corresponding y values for each aminozone defined in Gomez Pit.....
- Table 7-2:** The range of age estimates (in ka) calculated for aminozone IIc (above) and aminozone IId (below) in Gomez Pit using maximum, mean and minimum values of y_1 and y_2 as applied to the non-linear kinetic model of isoleucine epimerization.....

Table 7-3: The range of age estimates (in ka) calculated for aminozone IIc (above) and aminozone II d (below) in Gomez Pit using maximum, mean and minimum values of y_1 and y_2 as applied to the non-linear kinetic model of isoleucine epimerization.....

Appendix Table A.1-1: Total ILC-B Concentration data
Appendix Table A.1-2: Free ILC-B Concentration data

Appendix Table A.2-1: Total ILC-B Fraction data
Appendix Table A.2-2: Free ILC-B Fraction data

Appendix Table A.3-1: Free/Total Values for ILC-B Samples
Appendix Table A.4-1: Hydrolysis Experiment Data

Appendix Table A.5-1: Glassware Adsorption Data

Appendix Table C.1-1: Ca, Fe, Mn and Sr concentrations ($\mu\text{g/g}$ shell) in mollusc shells

Appendix Table C.2-1: R values for calcite/aragonite mixtures, obtained from X-ray diffraction

Appendix Table C.3-1: Raw data from long-term weight gain/loss experiment

Appendix Table C.3-2: Raw data from short-term weight gain/loss experiment

Appendix Table E.1-1: Uranium concentrations used to calculate internal dose in shell samples for ESR dating

Appendix Table E.1-2: Element concentrations in sediment for each UDAMS site from which shells were analyzed

Appendix Table F.1-1: Values of constants a and b for the kinetic equation for isoleucine epimerization

< Need Table 8-1
Caption
Table 8-2
Caption

LIST OF FIGURES

- Fig. 1-1:** L- and D- stereoisomers of the amino acid isoleucine.....
- Fig. 1-2:** Area of study.....
- Fig. 2-1:** Flow chart showing laboratory analyses of a molluscan fossil.....
- Fig. 2-2:** Typical chromatogram of an ILC-B total hydrolysate sample.....
- Fig. 2-3:** Sample calculation of amino acid concentration from peak area raw data.....
- Fig. 3-1:** Plots showing precision of ALLO/ISO values obtained from both total (above) and free (below) samples of ILC-B molluscan shell powders.....
- Fig. 3-2:** Comparison of fossil sample ALLO/ISO values with ILC-B standard data run concurrently.....
- Fig. 4-1:** Plot showing the relationship between % calcite and calculated R value for powder mixtures with varying proportions of calcite and aragonite.....
- Fig. 5-1:** A comparison of stratigraphic interpretations used to describe the late Pleistocene units of southeastern Virginia.....
- Fig. 5-2:** A comparison of stratigraphic interpretations used in southeastern Virginia, as seen in Yadkin Pit.....
- Fig. 6-1:** Frequency diagrams showing the distribution of (ALLO/ISO)TOTAL and (ALLO/ISO)FREE values in Gomez Pit.....
- Fig. 6-2:** Gomez Pit exposure showing superposed aminozones IIa and IIc....
- Fig. 6-3:** Gomez Pit exposure showing aminozone IIa above the reworked horizon.....
- Fig. 6-4:** Synthesis of lithostratigraphy and aminostratigraphy at Gomez Pit.....

- Fig. 6-5:** Aminostratigraphic options describing the spatial relationship between aminozones IIc and IIId as exposed in Gomez Pit.....
- Fig. 6-6:** A comparison of ALLO/ISO TOTAL values with ESR age estimates (a) and uranium concentrations (ppm; b) obtained from both in-place and re-worked valves in Gomez Pit.....
- Fig. 7-1:** The non-linear curve describing changing rates of the epimerization reaction over time.....
- Fig. 7-2:** Relationship between the oxygen isotope curve and age assignments for aminozones defined in southeastern Virginia.....
- Fig. 8-1:** Examples of shell qualities used in this work.....
- Fig. 8-2:** Comparison of % weight change from initial weight in the long-term (2 month) water weight gain/loss experiment.....
- Fig. 8-3:** Comparison of % weight change from initial weight in the short-term (approximately one month) experiment.....
- Fig. 8-4:** Diagrammatic cross-section of *Mercenaria*, showing the location of outer prismatic, and homogeneous layers in the shell.....
- Fig. 8-5:** Photomicrographs of lamellar features in the homogeneous layer of *Mercenaria*
- Fig. 8-6:** Diagenetic processes of epimerization, protein hydrolysis and amino acid leaching in mollusc shell.....
- Fig. 8-7:** Amino acid abundances for free and total samples for all aminozones in Gomez Pit.....
- Fig. 8-8:** Comparison of amino acid concentrations by shell condition in both total and free samples.....
- Fig. 8-9:** Comparison of amino acid fractions by shell condition in both total and free samples.....
- Fig. 8-10:** Photograph of leached, in-place *Mercenaria* collected from the upper part (approximately +1m above MSL) of aminozone IIa in Gomez Pit.....
- Fig. 8-11:** Plot of (ALLO/ISO)TOTAL (•) and (ALLO/ISO)FREE (0) values versus stratigraphic position in aminozone IIa.....

- Fig. 8-12:** Comparison of amino acid concentrations (left) and amino acid fractions (right) between valves collected from Yadkin Pit and Gomez Pit, both representing aminozone IIc.....
- Fig. 8-13:** Comparison of amino acid concentrations (left) and amino acid fractions (right) between valves collected from Gomez Pit and Norris Bridge, representing aminozone II d.....
- Fig. 8-14:** Comparison of amino acid concentrations among valves from all aminozones in Gomez Pit.....
- Fig. 8-15:** Comparison of amino acid fractions among valves from all aminozones in Gomez Pit.....
- Fig. 8-16:** Sr concentrations (a. $\mu\text{g/g}$ shell), and Sr/Ca values (b.) for mollusc valves from Gomez Pit (GP), Yadkin Pit (YP), the Chowan River Formation (CR) and Norris Bridge (NB).....

CHAPTER 1

INTRODUCTION AND STATEMENT OF PURPOSE

The study of amino acid diagenesis in mollusc shells originated with Abelson (1954), who observed changes in amino acid concentration and composition in *Mercenaria* shells spanning Cenozoic time. Abelson (1954) suggested that diagenetic reactions of amino acids protected within shell carbonate could serve as a dating method. Racemization of amino acids is one reaction that has been used previously for dating carbonate fossils. In life, all amino acids have the L- (or levo-) stereochemical configuration. After death of the organism and over time, these L-amino acids racemize or invert to the D- (or dextro-) stereochemical configuration (Fig. 1-1). Racemization occurs about the alpha carbon atom which serves as the center of asymmetry in the amino acid molecule. Some amino acids (for example, isoleucine) have more than one center of asymmetry at which racemization can occur. Racemization in these types of amino acids is called epimerization, and epimerization of L-isoleucine results in the diagenetic production of D-alloisoleucine (Fig. 1-1). The concentration of D-stereoisomers increases with fossil age, so that ratio of D-stereoisomer to L-stereoisomer (or D/L value) is a measure of time. In this work, the ratio of D-alloisoleucine to L-isoleucine (or ALLO/ISO value) is measured in mollusc shell protein.

The rate of racemization of amino acids in fossils is controlled primarily by the post-depositional temperature history that a fossil has endured (Wehmiller and Belknap, 1982; Wehmiller *et al.*, 1988). However, it has been recognized that peptide

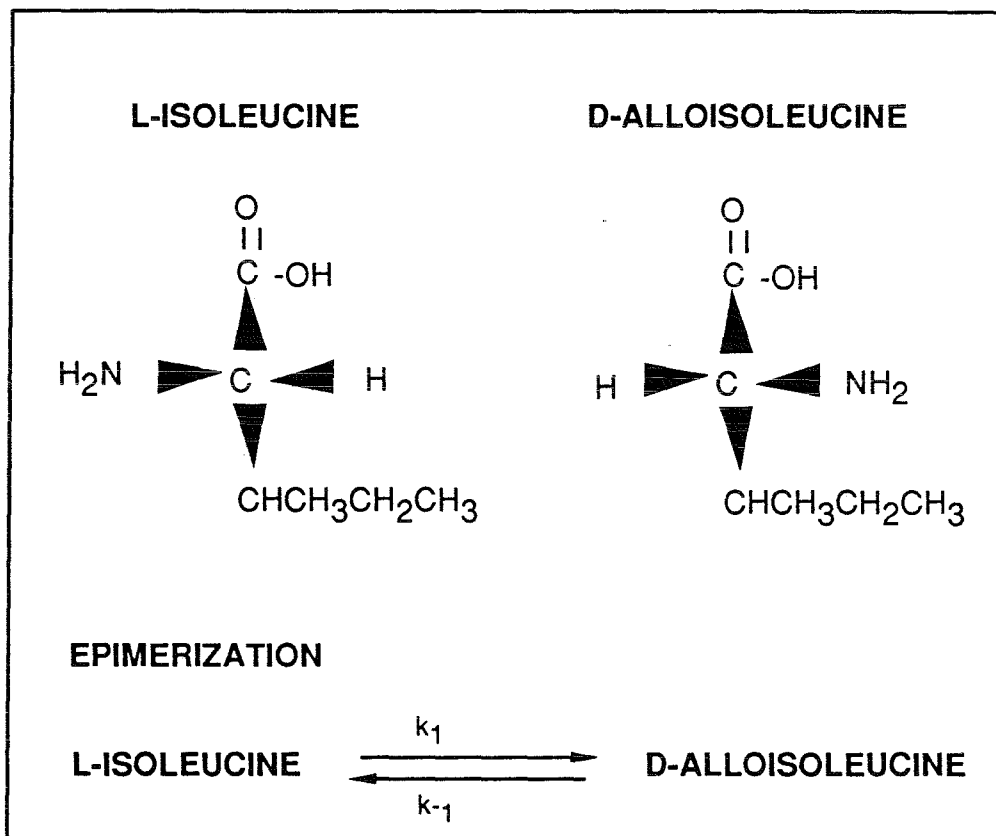


Fig. 1-1. L- and D- stereoisomers of the amino acid isoleucine.

bond hydrolysis, resulting in the production of extensively racemized free amino acids from peptide-bound amino acids also exerts a rate-controlling influence on the racemization reaction (Kriausakul and Mitterer, 1980b).

Another consequence of protein hydrolysis is that liberated free amino acid molecules are most likely to be removed or altered during fossilization. Peptide bonds impart stability to bound amino acids; as peptide bonds are hydrolyzed, free amino acids can be leached from the shell.

Leaching and decomposition of amino acids can have significant effects on amino acid composition. Specifically, these processes can affect the resolution of the amino acid dating method, because leaching may preferentially remove the most extensively racemized free amino acids (D-alloisoleucine, for example). Therefore, it is important to define criteria that allow recognition of the effects of diagenetic leaching and decomposition on amino acid data.

The hypothesis guiding this inquiry can be stated as follows: molluscan shell proteins hydrolyze yielding free amino acids, and these free amino acids represent the most extensively racemized and labile fraction in the shell. If extensively racemized free amino acids are most easily removed from the shell by groundwater leaching, then the amino acid composition of leached shell should show these two following characteristics. First, the shell should show lower concentrations of amino acids in the labile (free) sample, and second, the shell should show lower ALLO/ISO values in the free sample under relatively mild leaching conditions, and ultimately, lower ALLO/ISO values in the total (or bulk) sample under more severe leaching conditions. Therefore, shells of the same age can show different ALLO/ISO values if leaching is severe. This hypothesis

is based on previous work by Müller (1985), studying amino acid compositions of foraminifera, and Boutin (1989) whose work with Quaternary molluscs from Peru provide a "best-case" example of molluscan shell preservation and which serves as a model of amino acid diagenesis in venerid molluscs.

The work presented in this dissertation is closely follows that of Weiner and Lowenstam (1982), at least in philosophy. Weiner and Lowenstam (1982) compared fossil and modern bivalve and ammonid molluscs using amino acid analyses, carbon isotope, trace metal (Mg and Sr), and x-ray diffraction measurements in order to define chemical characteristics representing diagenetic change. The difference between this work and that of Weiner and Lowenstam (1982) is that they compared analyses of Upper Cretaceous species with closely related (but not identical) modern species, preserved in different sedimentary matrices. Upper Cretaceous specimens are beyond the range of amino acid racemization dating, so that the amino acid data obtained by Weiner and Lowenstam (1982) cannot be applied directly to this study. However, they suggest that well-preserved organic matrices (of equal age) show lower ALLO/ISO values than poorly preserved organic matrices. This chemical criteria for well-preserved mollusc shells will be applied to molluscs of late Cenozoic age analyzed in this work.

The protein-rich organic matrix of shell serves as a template on which biomineralization can occur (Weiner and Hood, 1975). Although the relationship between intact shell protein and shell carbonate is not well-defined at the molecular level, a degree of stability is imparted by the association of protein with carbonate at the Ca²⁺-binding site. Because of this association, changes in organic matrix composition can often accompany textural changes in shell carbonate. Chemical analyses and physical characterization of shell carbonate may provide criteria that allow recognition of

characterization of shell carbonate may provide criteria that allow recognition of diagenetic effects in shells showing textural change.

In this study, four sites located on the coastal plain of Virginia and North Carolina (Fig. 1-2) were sampled intensively to provide a large population of shells of increasing age, and which showed a wide range of textural characteristics. Previous work had shown that up to four aminozones (or strata characterized by similar ALLO/ISO values) were present within this region (Belknap, 1982; Mirecki, 1985), and that these aminozones seemed to appear in stratigraphic superposition at the Gomez Pit locality. Therefore, the Gomez Pit locality serves as an important (although ephemeral) reference site for aminostratigraphic work in the mid-Atlantic coastal plain. The Yadkin Pit, Norris Bridge and Chowan River Formation localities reveal stratigraphic sections which are less complex (generally showing only one or two aminozones present at Gomez Pit), but these localities also yield molluscan fossils which can best be described as "end-members" of the preservation spectrum - Yadkin Pit fossils representing the most poorly preserved samples of the collection, and Norris Bridge samples representing the finest molluscan samples.

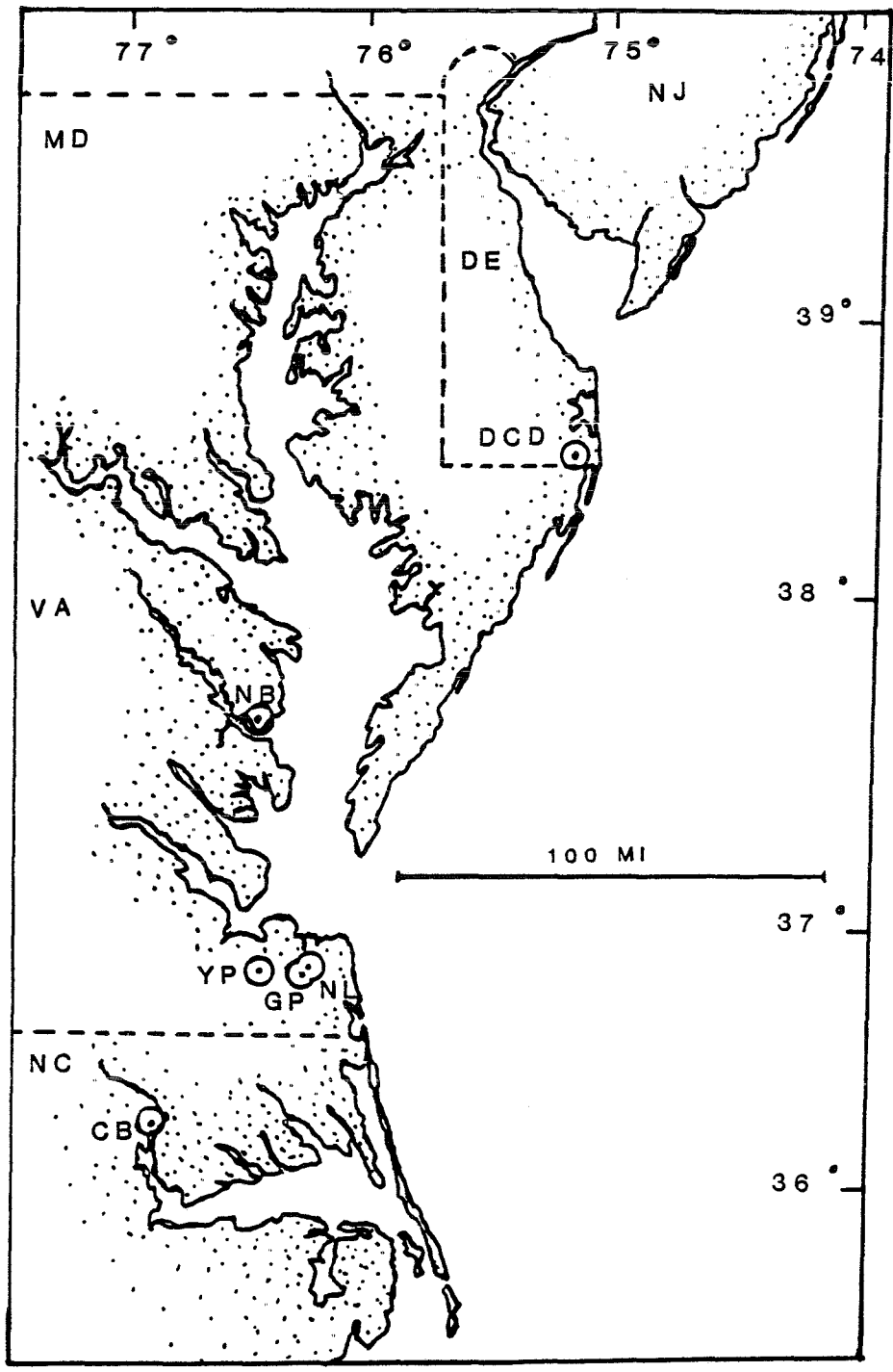


Fig. 1-2. Area of study. Sites discussed in the text are abbreviated as follows: DCD: Dirickson Creek Ditch; NB: Norris Bridge; YP: Yadkin Pit; GP: Gomez Pit; NL: New Light Pit; CB: Colerain Beach locality for the Chowan River Formation in North Carolina.

The goals of this project can be summarized in the following points:

1. To document aminostratigraphic relationships among aminozones in Gomez Pit, southeastern Virginia, so that this site can be used as reference site for future aminostratigraphic work in the region.
2. To compare age estimates obtained from several dating methods (amino acid racemization, uranium-series, ESR) for these strata, in order to better understand the timing of high sea levels in the southeastern Virginia coastal plain. Once age options are developed, these data can be interpreted in the context of the more complete record of Quaternary sea levels provided by the deep-sea oxygen isotope curve.
3. To understand relationships between amino acid composition, elemental composition and the degree of preservation of the molluscan fossil. Fossils from each aminozone were subjectively graded into four conditions based on physical appearance. This gradation allowed a comparison of amino acid and element data among shells of different condition, but having similar age.
4. To observe mollusc shell microstructure for evidence to suggest leaching of either organic matrix or shell carbonate.

CHAPTER 2

ANALYTICAL METHODS I: SEPARATION AND QUANTIFICATION OF AMINO ACIDS

2.1: Sample Preparation

Two adjacent transverse slices were cut with a Buehler wafer saw, extending from hinge to margin in each mollusc valve; one slice each for free and total amino acid analyses. Hinge sections of each slice were used for routine analysis (Fig. 2-1), and the remainder of each slice was retained for other work. Shell fragments were mechanically cleaned with a dental drill. Periostracum and the darker outer prismatic layer were removed, along with any chalkiness on the shell interior. Shell fragments were then chemically cleaned with alternating rinses of triple-distilled water and 1.0 N HCl, and dried under low temperature (<40° C) in a vacuum. After this point, preparation of free and total samples differed.

Total samples consisted of amino acids released by acid hydrolysis of molluscan shell proteins and represent bulk amino acid composition of the shell fragment. Total samples were prepared as follows. A clean, weighed (about 0.2g) shell fragment was dissolved in a stoichiometric volume of ultraclean 12N HCl, resulting in a solution having a final concentration of 6N HCl.

The hydrolysate solution was capped under N₂ and placed in a heating block at 110° C for 22 hours. After hydrolysis, 0.1 ml of hydrolysate was dried down in a new culture tube under N₂ with 0.4 ml deionized water. The dried hydrolyzate was diluted to 2.0 ml with pH2 buffer.

Free samples consist of amino acids which have been released from molluscan shell proteins by diagenetic hydrolysis. Free samples were obtained through dissolution in the following manner. A clean, weighed (about 0.15g) shell fragment was covered with 0.5 ml of deionized water in a culture tube, and placed into an ice bath. The fragment was then slowly dissolved in a stoichiometric volume of ultraclean 12N HCl. After complete dissolution, 0.20 ml of the dissolved sample was dried down in a separate culture tube under N₂ with 0.4 ml of deionized water. The dried free sample was diluted with 2.0 ml of pH2 buffer.

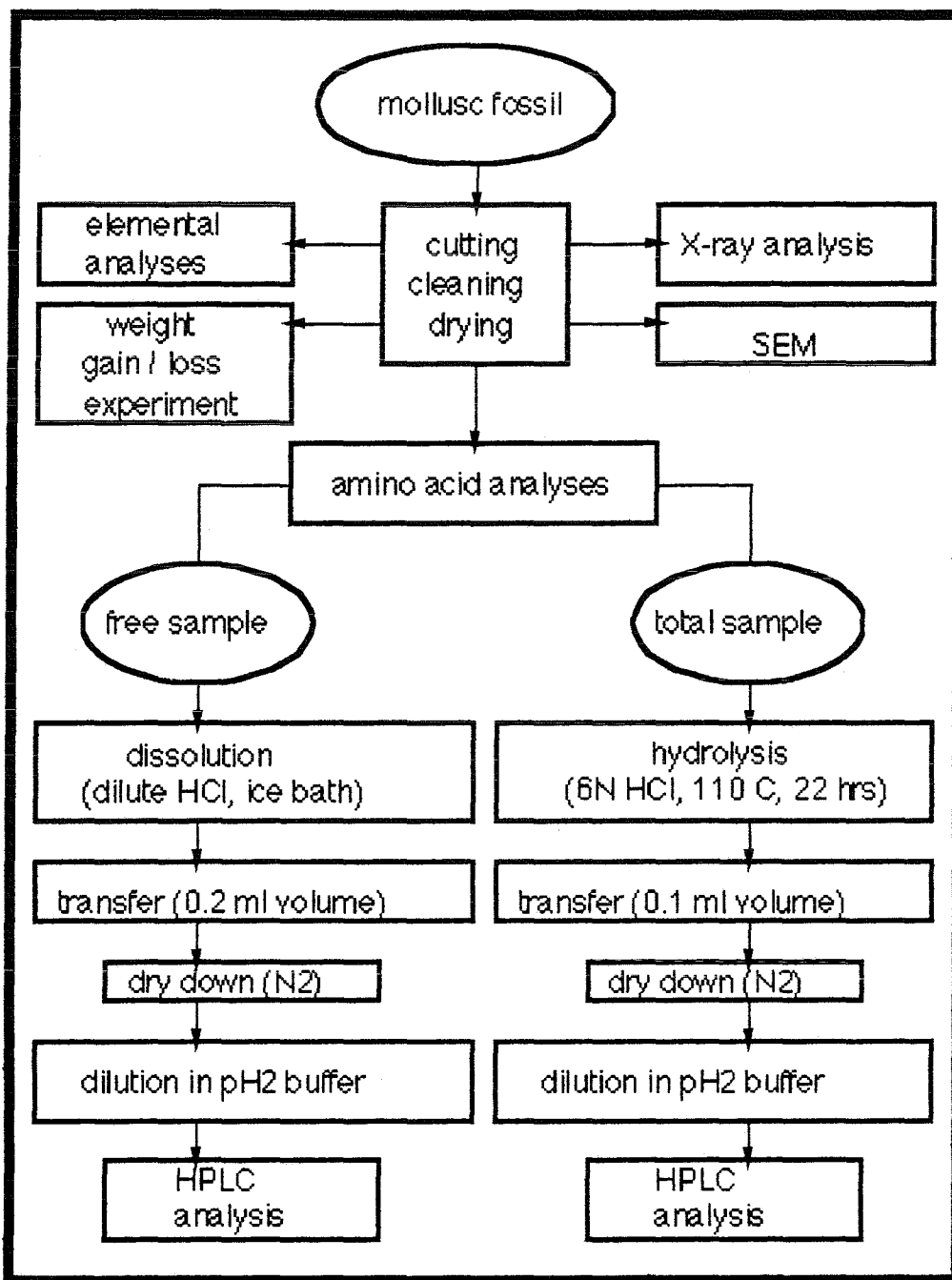


Fig. 2-1. Flow chart showing laboratory analyses of a molluscan fossil. Circles represent samples, rectangles represent actions

2.2: System Description

Amino acids obtained from molluscan shell protein hydrolyzates were analyzed using a high-performance liquid chromatography (HPLC) system developed at the Carnegie Institution of Washington (Benson and Hare, 1975; Hare *et al.*, 1985). Dilute samples were loaded onto a 50 μ l loop, then eluted under pressure (usually 1000 to 1200 psi) through a thermostatted narrow bore ion-exchange column packed with a polystyrene/divinyl benzene cation exchange resin (St. John Associates, Adelphi, MD). Amino acids were detected post-column with *o*-phthalaldehyde/2-mercaptoethanol (OPA; Benson and Hare, 1975) derivatization, which yielded a fluorescent isoindole derivative of the primary amino acid detected at a wavelength of 340 nm.

Samples were run continually with the help of a Micromeritics autosampler. Each sample run consisted of two injections. Free and total samples from the same shell were run as a pair. Shell samples were usually prepared in batches of twenty, accompanied by two Interlaboratory Comparison (ILC) shell powders (Wehmiller, 1984). A quantitative amino acid standard mixture (Sigma Chemical Company, St. Louis, MO) was diluted to 2.50 nanomoles/ml for each amino acid and analyzed after each pair of free and total samples (or four injections). The published detection limit for this system is 10 picomoles/ml (Hare *et al.*, 1985). Typical amino acid concentrations in shell samples were in the nanomole/ml range. A chromatogram obtained from a total hydrolyzate of ILC-B shell powder is shown in Fig. 2-2.

Fourteen amino acids were well-resolved using this system; however only concentrations of amino acids ASP, GLU, GLY, ALA, VAL, ALLO, ISO, LEU and PHE are

reported. Basic amino acids HIS, ARG, and LYS were poorly resolved by this method and THR and SER are not reported because resolution of these peaks varies with column efficiency. Optimum column efficiency is shown by a symmetrical, well-resolved THR+SER doublet. When the column does not show optimum resolution (e.g. in an older column), the THR+SER doublet can appear as one peak, and does not accurately represent THR and SER concentrations in the sample.

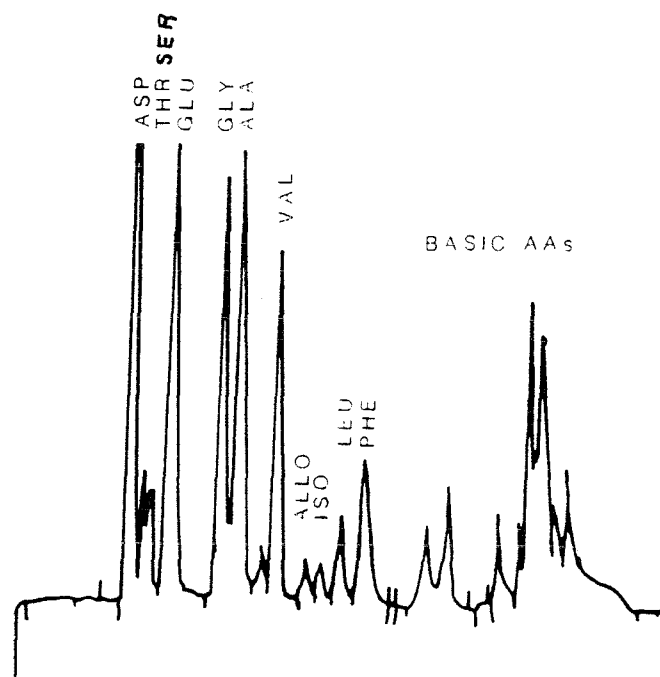


Fig. 2-2. Typical chromatogram of an ILC-B total hydrolysate sample. Shown here is ILC-B12/10T (UDAALAB No. 87071; redrawn from the original chromatogram) run 18 January, 1988. Standard abbreviations for amino acids will be used throughout the text: ASP = aspartic acid, THR = threonine, SER = serine, GLU = glutamic acid, GLY = glycine, ISO = isoleucine, LEU = leucine, TYR = tyrosine, phe = phenylalanine. Basic amino acids histidine, arginine and lysine are poorly resolved and were quantified.

MET and TYR are two other amino acids which yield well-resolved peaks, but these peaks do not accurately represent actual concentrations in shell protein. MET and TYR are both thermally unstable. MET concentrations often vary by 25% or more between injections of the same sample, so MET concentration is not considered in the data set. TYR has been shown to be thermally unstable during experimental pyrolysis of *Mercenaria* shell (Vallentyne, 1969), and also degrades during hydrolysis of total samples (Appendix A.3). TYR also will not be considered in the data set.

2.2.1: A Note on Reagent and Laboratory Glassware Quality

Triple-distilled water was used for all reagents in the chemical cleaning step. Commercial buffer concentrates (Beckman; Palo Alto, CA) and pH2 buffer were diluted in Millipore deionized water. HCl used for dissolution, hydrolysis and preparation of pH2 buffer was condensed from HCl gas in Millipore deionized water. Spectroscopically pure reagents were used for the OPA fluorescent tag. PVC gloves were always worn during sample cutting and wet chemical preparation to prevent contamination by fingerprint-borne L-amino acids. Culture tubes used for dissolution and hydrolysis were always baked at least 24 hours at 300° C prior to use. If culture tubes were recycled, they were rinsed and soaked in 3N HNO₃ for several days before baking. Recycled culture tube caps have been a source of hydrolyzate contamination; reuse of cleaned caps is not advised for hydrolysis.

2.3: Calculation of Amino Acid Concentration

Amino acid concentrations of mollusk samples were calculated from peak area output on HPLC chromatograms. Integration of peak area provided a more accurate measurement of amino acid concentration than peak height measurement; however, a linear relationship between peak area and peak height was observed.

Calculation of amino acid concentration in mollusk samples was based on comparison of sample peak areas with peak areas obtained from a quantitative standard of known concentration (2.50 nanomoles/ml for each amino acid). A sample calculation is shown in Fig. 2-3. The peak area number in the quantitative standard term is the average of four injections; this peak area term is also corrected for dilution by a factor of four. The peak area number in the fossil sample term is an average of two injections. Peak areas obtained from fossil samples are corrected for dilution, hydrolyzate (or dissolution) volume and initial shell mass, resulting in a concentration of each amino acid in nanomoles/g shell. Calculations are facilitated by a spreadsheet program written by John Wehmiller for the Apple Macintosh™ personal computer.

$$\begin{aligned}
 & \frac{(\text{average ASP peak area})_{\text{fossil}}}{(\text{average ASP peak area})_{\text{quant std}} \cdot 4} = W \\
 & \left[\frac{0.05 \text{ ml}}{2.0 \text{ ml}} \right] \frac{\text{injection volume}}{\text{dilute sample volume}} = X \\
 & \left[\frac{0.10 \text{ ml}}{0.75 \text{ ml}} \right] \frac{\text{transfer volume}}{\text{hydrolysis volume}} = Y \\
 & \text{sample mass (g shell)} = Z \\
 & W \cdot \left[\frac{1}{X \cdot Y \cdot Z} \right] = \text{Concentration of ASP (nanomole/g shell)}
 \end{aligned}$$

Fig. 2-3. Sample calculation of amino acid concentration from peak area raw data.

CHAPTER 3

EVALUATION OF AMINO ACID DATA

3.1: Introduction and Structure of Chapter

The precision of amino acid analyses needs evaluation before these data can be interpreted in a geologic context. The first step toward determination of analytical precision is to define a set of chromatographic criteria to distinguish good from lesser quality chromatographic data (Section 3.2). To determine chromatographic variability during the two-year period of this project, the precision of ILC molluscan shell powder analyses will be assessed (Section 3.3). The ILC powder data set will provide a basis to which the precision of fossil sample analyses can be compared. This comparison will be discussed in later chapters where analytical precision is considered within each of the defined aminozones. Factors contributing to poor precision of some sample analyses will be considered in Section 3.4. The use of internal standards to improve analytical precision is discussed in Section 3.5.

3.2: Chromatographic Criteria

It is necessary to define "high-quality" data on the basis of chromatogram characteristics. Data not fulfilling most of the six criteria listed below are discarded, or at least regarded as suspect. A high-quality chromatogram shows the following characteristics: 1) a stable baseline; 2) well-resolved THR + SER and TYR + PHE doublet peaks; 3) valleys between peaks which extend to the baseline; 4) consistent retention times for each amino acid; 5) no evidence of peak broadening, such as "tails"

on peaks or peak area/height ratios >0.8 , and 6) no evidence of contamination, shown by anomalous peaks or "shoulders" on amino acid peaks. A high-quality chromatogram is shown in Fig. 2-2. Personal experience has shown that the characteristic which varies most commonly during routine operation is broadening of peaks. It is beyond the scope of this discussion to provide advice on "troubleshooting". The reader is referred to HPLC operation manuals, Parris (1984) and Parente (1987) for discussion of practical techniques applied to HPLC operation.

3.3: Precision of ILC Molluscan Shell Powder Analyses

Interlaboratory Comparison (ILC) molluscan shell powders are used to determine precision and accuracy of analyses for HPLC operation over long periods of time, and to allow comparison of amino acid data between laboratories. Wehmiller (1984) has published a compilation and analysis of ILC enantiomeric data obtained by gas chromatography (GC) and high-performance liquid chromatography (HPLC) methods from several amino acid laboratories. Three shell powders of different ages were analyzed continually during this study (Table 3-1).

At least one free and one total ILC standard powder were prepared with each batch of fossil samples. ILC-B was always run, often accompanied by either ILC-A or ILC-C. ILC-B free and total data are used here to determine the precision of amino acid data obtained during the period extending from 6/14/86 through 5/15/88.

Four types of ILC-B data are considered for analysis of precision: amino acid concentrations, relative abundance of amino acids (termed amino acid fractions), Free/Total values for each amino acid, and ALLO/ISO values.

is not as obvious in the absence of hydrolysis. %CVs for all thermally stable amino acids range from 40% to 43%, again suggesting that these amino acid concentrations co-vary.

To summarize, precision of absolute amino acid concentration in both free and total samples is poor, despite the acquisition of high quality data. High %CVs for each amino acid preclude their use as indicators of HPLC performance over time. Poor reproducibility among ILC-B analyses may be due in part to pipetting error in the transfer step during sample preparation (Fig. 2-1). For example, a difference of 0.03ml (ca. one drop) can result in a 20% difference in concentration of all amino acids in a sample. Reproducibility can be affected to a lesser extent by other instrumental parameters, including age (and hence performance) of the ion-exchange resin and the ultraviolet lamp.

3.3.2: Precision of Amino Acid Fractions From ILC-B Molluscan Shell Powders

Amino acid fractions are calculated from the sum of all stable amino acid concentrations, as shown by the equation:

$$\text{Fraction [X]} = \frac{\text{[X]}}{\text{[ASP + GLU + GLY + ALA + VAL + ALLO + ISO + LEU + PHE]}}$$

THR and SER are excluded because their concentration is dependent upon complete resolution of the doublet peak. MET and TYR are excluded because they have been shown to decompose during hydrolysis (Appendix A.4). Amino acid fractions are tabulated for ILC-B total samples in Appendix Table A.2-1, and for ILC-B free samples in Appendix Table A.2-2. Variation in the calculated fraction of each amino acid is shown by the %CV. There was no need to selectively remove poor data because %CVs of amino acid fractions

are relatively low.

ILC-B data show greater precision when each amino acid is normalized to a sum value. %CVs for amino acid fractions in total samples range from 5% to 11%. Precision of PHE is still poor (%CV = 39.0) probably reflecting poor resolution of the TYR+PHE doublet. All amino acid fractions in free samples show good precision, with %CV ranging from 4% to 13%. When amino acid data are normalized to a sum value, variability resulting from pipetting error is eliminated. Because the relative abundance of each amino acid in ILC-B samples remains relatively constant throughout the duration of this study, preferential loss of any one amino acid during wet chemical preparation is unlikely. Data supporting this conclusion are discussed in Appendix A.5.

3.3.3: Precision of Free/Total Amino Acid Values From ILC-B Molluscan Shell Powders

The ratio of an amino acid concentration in the free versus total sample can indicate the extent of diagenetic hydrolysis. When calculating the mean Free/Total value of each amino acid, Free/Total values greater than 1.0 are excluded because Free/Total values greater than 1.0 are not theoretically possible.

Free/Total values, like amino acid concentrations are very variable. When the entire ILC-B data set is considered, %CVs for Free/Total values of all amino acids range from 45 to 50%. Because Free/Total values may be a useful quantity to determine the extent of protein hydrolysis, several attempts were made to systematically identify and eliminate poor or spurious data. These attempts include the removal of statistical outliers, and removal of low-quality data. Further discussion of these techniques is found in section 3.4.

Statistical outliers were identified as those points lying off of a generally straight, sloping trend as determined on a probability plot. The advantage of this method is that precision is increased with the removal of few data points, yet these points do not necessarily correspond with low-quality data. Removal of low-quality data results in a significant decrease in sample population; almost half of the data set was removed for some amino acids. In any case, neither method of data reduction reduces variability of Free/Total values to acceptable levels (Table 3-2). It seems that this variability is at least partly inherent in the fossil molluscan samples.

F/T ASP	X	S.D.	%CV	n	F/T GLU	X	S.D.	%CV	n
All data	0.527	0.258	48.9	25	All data	0.236	0.117	49.5	25
-Outliers	0.507	0.243	47.9	24	-Outliers	0.196	0.076	38.8	21
-Poor Data	0.494	0.203	41.0	14	-Poor Data	0.246	0.105	42.7	15
F/T GLY					F/T ALA				
All data	0.601	0.285	47.4	25	All data	0.744	0.339	45.5	25
-Outliers	0.473	0.167	35.3	19	-Outliers	0.595	0.204	34.2	19
-Poor Data	0.599	0.209	34.9	14	-Poor Data	0.681	0.231	34.9	13
F/T VAL					F/T ALLO				
All data	0.491	0.233	47.4	25	All data	0.653	0.319	48.8	25
-Outliers	0.428	0.163	38.1	22	-Outliers	0.51	0.172	33.7	19
-Poor Data	0.508	0.21	41.3	15	-Poor Data	0.583	0.203	34.8	13
F/T ISO					F/T LEU				
All data	0.334	0.154	46.1	25	All data	0.493	0.226	45.8	25
-Outliers	0.293	0.111	37.9	22	-Outliers	0.433	0.163	37.6	22
-Poor Data	0.352	0.145	41.2	15	-Poor Data	0.511	0.199	38.9	15
F/T PHE									
All data	0.445	0.215	48.3	25					
-Outliers	0.371	0.137	36.9	21					
-Poor Data	0.463	0.199	42.9	15					

Table 3-2. Statistical summary describing precision of ILC-B Free/Total values for each amino acid. Data are abbreviated as X (Mean), S.D. (Standard Deviation), %CV (Coefficient of Variation) and n (number of samples). Refer to Section 3.4 for discussion.

3.3.4: Precision of ALLO/ISO Values From ILC-B Molluscan Shell Powders

ALLO/ISO values obtained from both free and total ILC-B samples provide a convenient way to assess HPLC performance. ILC-B samples having ALLO/ISO values which deviate substantially from University of Delaware mean ALLO/ISO values are suspect, as are all accompanying fossil samples. Plots of ILC-B ALLO/ISO values obtained during this study can also be used to determine long-term trends in HPLC performance. ALLO/ISO values obtained from ILC-B samples are shown in Fig. 3-1.

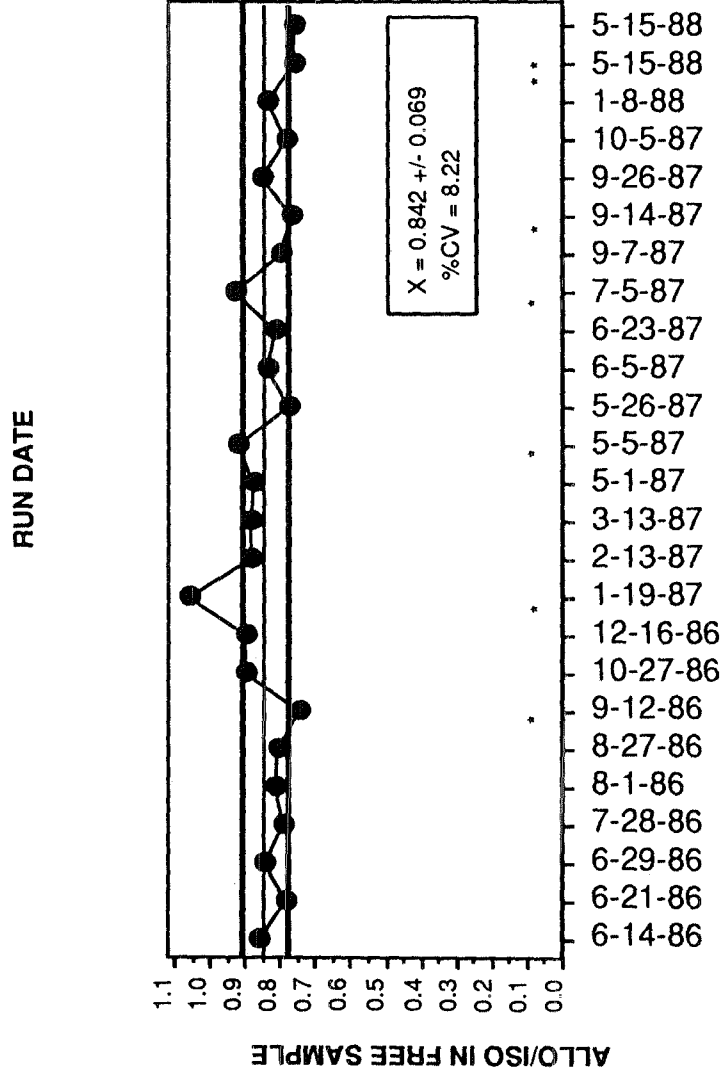
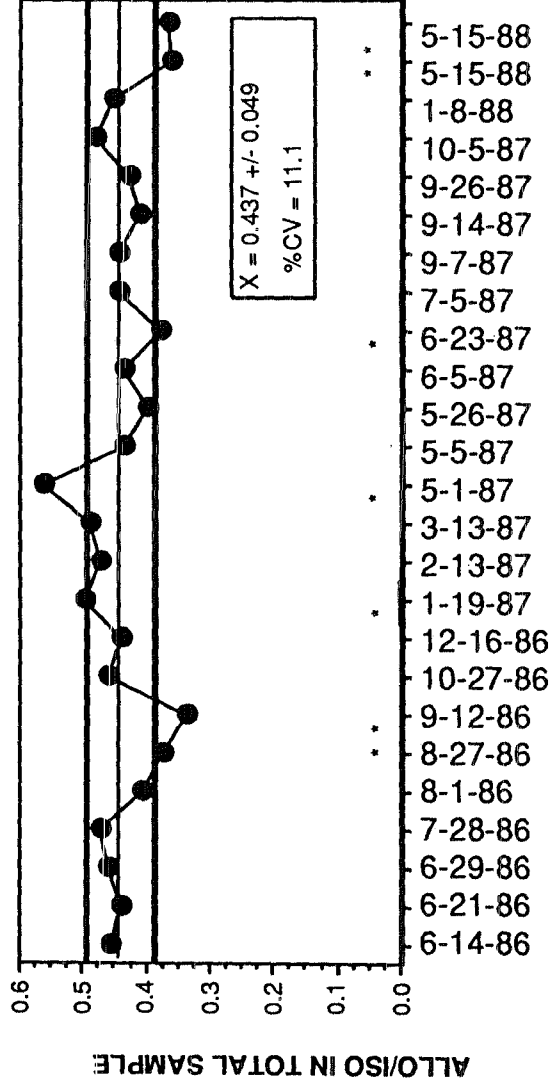


Fig 3-1. Plots showing precision of ALLO/ISO values obtained from both total (above) and free (below) samples of ILC-B molluscan shell powders. Light lines describe mean ALLO/ISO values, heavy lines describe the standard deviations of free or total ILC-B samples. (*) denotes ILC-B samples which lie outside the standard deviation envelope.

The plots in Fig. 3-1 show no long-term excursions from current mean University of Delaware laboratory values, although several ILC-B analyses deviate significantly (*i.e.* beyond the standard deviation of the mean). Each of these suspect ILC-B analyses is marked with a (*) in Fig. 3-1. Poor precision of these analyses could be ascribed to two factors: poor HPLC performance or contamination.

Suspect ILC-B samples noted in Fig. 3-1 do not fulfill all chromatographic criteria. For example, certain sample chromatograms have noisy baselines (9-12-87, 1-19-87); others show peak broadening (8-27-86, 5-1-87, 5-5-87, 7-5-87); or problems with integrator threshold setting (all 5-15-88 analyses). Of these chromatographic problems, peak broadening is the most common; however, it was not possible to eliminate all spurious ALLO/ISO data by removing only samples having high area/height ratios for ALLO, ISO or LEU. Chromatographic criteria, such as peak area/peak height values, provide another way to assess HPLC performance during each run.

HPLC performance can also be considered on the short-term, by comparing ALLO/ISO values from ILC standards run on a single HPLC column. During this project, samples were run on eight different HPLC columns. Mean (ALLO/ISO)TOTAL values for ILC-B standards run on each column range from 0.42 to 0.46. Coefficients of variation for these short-term averages are somewhat lower than those for the long-term average (Fig. 3-1); short-term %CVs range from 4% to 7%.

Contamination of samples by L-enantiomer amino acids is also possible, although contamination can be detected several ways. Sources of contamination include human contact (fingerprints, sneezing) and bacterial contamination of buffer solutions and HPLC lines. Contamination may be inferred in chromatograms showing highly unusual relative amino acid abundances. For example, fingerprint residue shows extraordinarily high abundances of acidic amino acids. Fingerprint residue can also contribute isoleucine, thus lowering the ALLO/ISO value in a sample. Since gloves are worn during all stages of sample preparation (from sample cutting through analysis), contamination through contact is not believed to be a problem. Contamination can also be detected in acid blanks run with each batch of samples.

3.3.5. Accuracy of ALLO/ISO Values from ILC-B Molluscan Shell Powders

Accuracy of ILC-B ALLO/ISO values calculated from this study can be determined by comparison with published data (Wehmiller, 1984). Mean values obtained from all studies are summarized in Table 3-3.

	ILC-B total samples	ILC-B free samples	Reference
This study	0.437 +/- 0.049	0.842 +/- 0.069	
UD Lab (1984)	0.578	0.880	Table 2
All laboratories	0.525 +/- 0.055	0.967 +/- 0.073	Table 3

Table 3-3. Comparison of mean ALLO/ISO values and standard deviations with published data. Tables are referenced from Wehmiller (1984).

Mean ILC-B ALLO/ISO values from this study are lower than all other published data, although standard deviations overlap. ALLO/ISO values determined at the UD lab differ from those obtained at other laboratories because of differences in instrumentation among laboratories, and because some workers calculate ALLO/ISO values using peak

heights. ALLO/ISO values obtained at UD (in 1984) differ from ILC-B values obtained in this study because different instruments were used to analyze the earlier samples. It should be noted that mean ILC-B ALLO/ISO values for total samples obtained by others working concurrently in the Univ. of Delaware Lab are nearly identical (L. York, pers. comm.) to the values calculated in this study.

3.4: Precision of Fossil Sample Analyses

The precision of amino acid fractions, Free/Total values and ALLO/ISO values in all fossil samples are considered in the following subsections. Amino acid concentrations are not considered in the fossil sample data set because of poor precision observed ILC-B molluscan shell analyses. Fossil sample data are divided into subsets corresponding to aminozones, although it may not yet be apparent why the data should be grouped in this context. The precision of data from each aminozone is calculated separately for each fossil locality. Fossil sample data and summaries of precision are tabulated in App. B.

Many fossil samples were rerun during this project. When comparing concentration data between initial and repeat analyses, I discovered that calculated concentrations were often much higher in repeat analyses. This problem will be discussed in detail in Section 3.6. Because of this lack of precision, only data obtained from initial analyses of free and total samples will be considered. ALLO/ISO values calculated from repeat analyses are listed in Appendix table B-1 for comparison.

During the initial stages of data interpretation, I thought that the analytical precision within an aminozone could be improved by removing all data which did not fulfill the criteria described in Section 3.2. These suspect samples were coded to identify the source of error (Appendix table B.1-1). Unfortunately, removal of suspect samples from the data set did not necessarily improve precision, and in many cases decreased precision. Statistical outliers in the data set did not exclusively correspond to "suspect" or low-quality chromatograms.

A second approach, assuming normal distribution of data points within each aminozone was considered. In this approach, amino acid fractions, free/total values and ALLO/ISO values from each aminozone were graphed on probability plots using the SYSTAT® statistical software package. Outliers were identified as points that did not fall along the general slope of the line, and were removed. Much more information is retained in each data subset using this method, and precision in each aminozone is improved. A comparison of descriptive statistics among data subsets is found in Appendix table B.2-1.

Caution should be exercised when using probability plots to delete outliers. In a probability plot, normally distributed data will show a generally straight sloping line, with no 'tails' or segments having a different slope. If tails are shown, it is important to determine whether these points are statistical outliers, or represent different trends in the data set which may become important later. By comparing the original data set with the filtered (*i.e.* outliers removed) data set, it was determined that outliers did not correspond exclusively with low quality chromatograms or with condition of the shell. This procedure is only useful for large data sets ($n > 20$), as it becomes difficult to distinguish outliers from tails or trends on plots constructed from smaller data sets. More information and illustrations of normally distributed data are found in Miller (1986).

3.4.1: Comparison of Fossil Sample and ILC Standard Data Run Concurrently

In an attempt to find a way to systematically remove all questionable fossil sample amino acid data from the data set, all fossil sample data that accompanied a "bad" ILC standard was removed. However, this action can result in the loss of otherwise

acceptable data. For example, Fig. 3-2 shows all samples from the youngest aminozone plotted with the ILC-B standard run concurrently. Outlier fossil sample values often accompany ILC-B standards that are greater than one standard deviation from the mean (denoted by a *). However, not all fossil sample values run with the "bad" ILC-B sample are outliers. A comparison of free and total fossil samples with the standard run 8-27-86 exemplify this problem. The ILC-B standards run 8-27-86 showed low ALLO/ISO values. The lowest fossil ALLO/ISO values for this aminozone were obtained from this HPLC run. However, not all fossil ALLO/ISO values in this HPLC run were low. This example indicates that standards are only one way to assess HPLC performance.

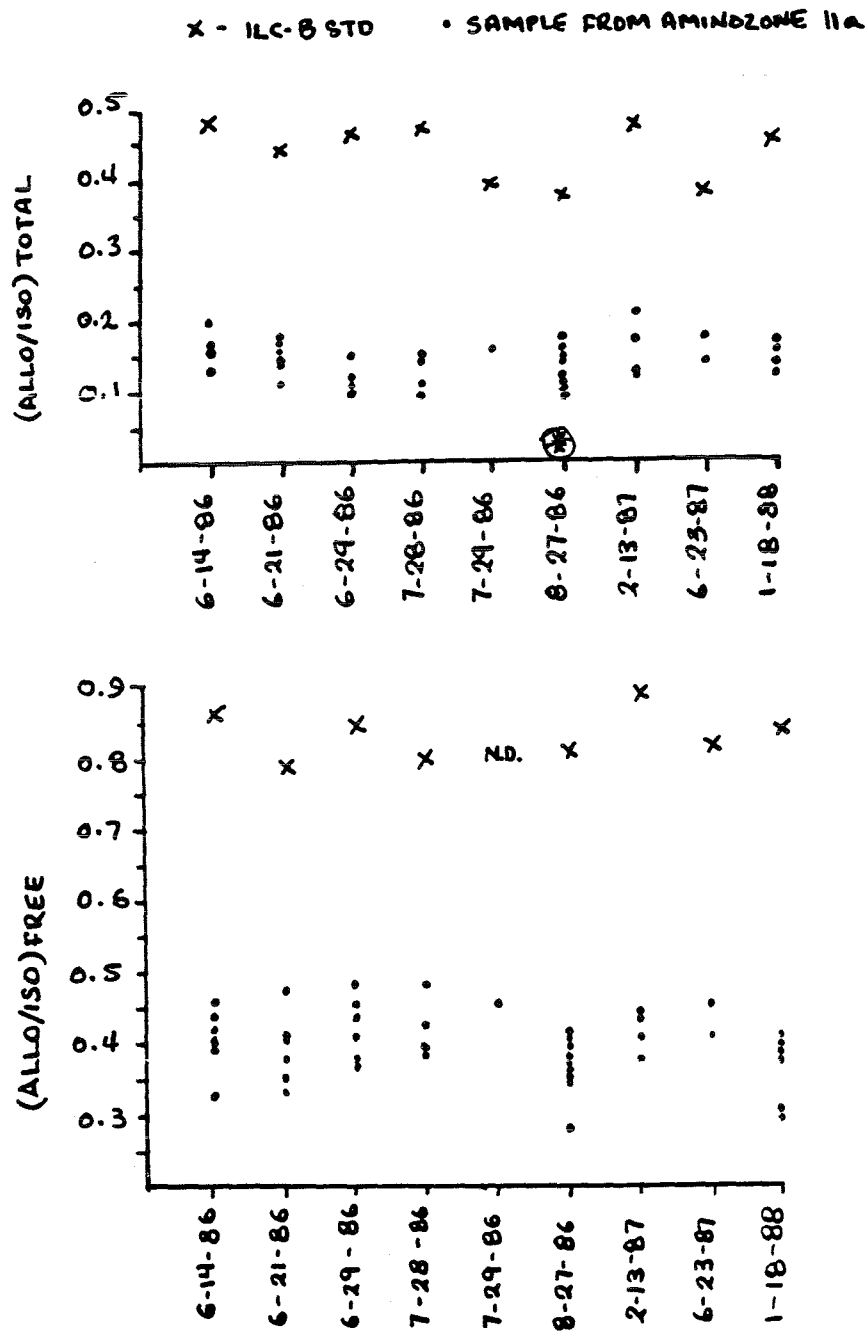


Fig. 3-2. Comparison of fossil sample ALLO/ISO values with ILC-B standard data run concurrently. Only fossil samples from aminozone IIa are shown. ALLO/ISO values from ILC-B standards that exceed one standard deviation from the mean are denoted with (*).

CHAPTER 4

ANALYTICAL METHODS II: ATOMIC ABSORPTION SPECTROMETRY, X-RAY DIFFRACTION, SCANNING ELECTRON MICROSCOPY AND WEIGHT GAIN/LOSS EXPERIMENTS

4.1: Introduction and Structure of Chapter

One focus of this project is to determine a qualitative relationship between the degree of shell preservation and amino acid data. Leaching and dissolution of both calcium carbonate and organic matrix can theoretically affect ALLO/ISO values and amino acid composition. If the hypothesis that the organic matrix serves as a template for calcium carbonate crystallization in molluscs (Weiner and Hood, 1975) is accepted, then it is reasonable to expect that alteration of shell carbonate during early diagenesis can affect amino acid composition. The following four techniques were used to determine physical and chemical changes in molluscan shell carbonate in order to relate these changes to variation in ALLO/ISO values and amino acid composition of the shells (Table 4-1). Methods for each technique are described here, and interpretations are discussed in Chapter Nine.

4.2: Atomic Absorption Spectrometry Methods: Calcium, Strontium, Manganese and Iron

Shell fragments (approximately 0.5 g) were cut from the molluscan shell hinge region. The discolored outer prismatic layer and inner chalky layer were removed with a dental drill. Shell fragments were cleaned in alternating rinses of 1N HCl and triple-distilled water, and extensively bored samples were agitated to remove debris. Shell fragments were dried overnight (150°C), dissolved in a known excess volume of 12N

fragments were dried overnight (150°C), dissolved in a known excess volume of 12N HCl (technical grade), and diluted to 10 ml volume; these are the concentrated samples.

TECHNIQUE	PURPOSE
Elemental analysis by flame atomic absorption spectrophotometry (Sr, Fe, Mn, Ca)	Detect authigenic mineral formation in shells, or ionic substitution in shell lattice structure
X-Ray Diffraction	Determine recrystallization of aragonite to calcite
Scanning Electron Microscopy	Observe microstructural alteration
Weight Gain/Loss	Determine relative porosity of shell fragments.

Table 4-1. Summary of techniques used to determine diagenetic changes in molluscan shell carbonate.

Concentrated samples were then diluted so that the concentration of each element was within the linear range of the instrument, as defined by a standard curve for that element. One ml concentrated sample was acidified with 0.1 ml 12N HCl and diluted to 10 or 20 ml. For Sr and Ca analyses, 1.0 ml of a 500 ppm LaCl₂/KCl solution was added to each sample to before dilution to prevent interference by ionization. These dilute samples used for atomic absorption spectrometry (AAS) analysis. Elemental data from fossil samples are found in Appendix C-1.

Standards were made from spectroscopically pure stock solutions (Fisher Scientific, Springfield, NJ; or Sigma Chemical Co., St. Louis, MO). Standard matrices were similar in composition to sample matrices. Operating parameters of the Perkin-Elmer model 5000 flame atomic absorption spectrometer are shown in Table 4-2. Sample concentrations were calculated using an equation obtained from linear regression

of the standard curves that showed the relationship between absorbance and standard concentration. Calculations of μg element/g shell were obtained using the following equation:

$$\mu\text{g element/g shell} = \frac{\text{sample conc.}(\mu\text{g/ml}) * \text{sample vol.}(\text{ml}) * \text{dilution factor}}{\text{shell weight (g)}}$$

PARAMETER	Ca	Fe	Sr	Mn
Fuel mix	C ₂ H ₂ /air	C ₂ H ₂ /air	N ₂ O/C ₂ H ₂	C ₂ H ₂ /air
Current	10 mA	30 mA	20 mA	20 mA
Slit width	0.7 nm	0.2 nm	0.4 nm	0.2 nm
Wavelength	422.7 Å	248.3 Å	460.7 Å	279.5 Å

Table 4-2. Operating parameters for elemental analyses using flame atomic absorption spectrometry.

4.2.1: Estimation of Dilution Error

Concentrated samples were diluted to ratios of 1:10 or 1:20 (Sr, Mg, Fe) or 0.3:100 (Ca). To estimate the error resulting from dilution, 10 samples of a standard mollusc shell powder (ILC-D) were diluted and analyzed as usual for each element. Precision is reported as % Coefficient of Variation (%CV; Table 4-3). Precision is low for Ca because a three-step dilution sequence was required to reduce Ca concentrations within the linear range of the instrument. Fe and Mn precision is low and non-reproducible; laboratory contamination probably contributed to the analytical error for these elements. For this reason, Fe and Mn data are reported in App. C-1 but are not considered in the interpretations. Sr concentrations show the highest precision, although a %CV of 9.5 is barely acceptable. Only Sr concentrations and Sr/Ca values will be

considered in the interpretations presented in Chapter Nine. Concentrations and precision estimates are presented in App. C-1.

ILC-D	Ca	Fe	Sr	Mn
Mean	428962	243.4	1899	1.0
Std. Dev.	73027	59.3	171.3	2.4
%C.V.	17.0	24.4	9.0	236
n	10	10	10	10

Table 4-2. Statistics describing 10 analyses of the ILC-D powder to determine dilution error. Concentrations are reported as $\mu\text{g} / \text{g}$ shell.

4.2.2. Comments For Future Work

Dilution of 100 shell samples for analysis of different elements is tedious work. Elemental analysis using AAS is not recommended for future work. Better data can be obtained with less effort using other methods such as ICP (inductively coupled plasma) spectroscopy because several elements can be analyzed simultaneously. EDAX (energy dispersive X-ray) analysis is time consuming if many elements are considered, but can be useful for a limited number of samples.

4.3: Scanning Electron Microscopy

Shell fragments were viewed by scanning electron microscopy (SEM) to identify textural modification of shell microstructure. Features that suggested diagenetic modification were noted, especially those features created by boring and encrusting organisms or by dissolution.

Fresh fracture faces were viewed using SEM. Fracture faces were oriented so that a cross-section of the shell was viewed perpendicular to growth lines. Shell

fragments were trimmed (except for the fracture to be viewed) with a dental drill, then ultrasonically cleaned in distilled water to remove dust.

Cleaned shell fragments were mounted on aluminum stubs with silver paint, and placed in a dessicator for 2 hours to ensure dryness. Mounted samples were coated in a Denton Vacuum Evaporator (DV-502) first with carbon, then with an amalgam composed of 60% gold, 40% palladium. Samples were viewed on a Cambridge Stereoscan Electron Microscope operated at 25 kV with an electron backscattering device. Photographs were taken using Poloroid Type 55 film.

4.4: X-Ray Diffraction Methods

Shell samples were analyzed by X-ray diffraction to determine the percent of calcite recrystallization in these originally aragonitic fossils. Calcite was not detected in any sample. All samples were analyzed except 87GP-345A through 87GP-353A (9 samples) which were sent to another laboratory for electron spin resonance dating.

Shell samples were prepared in the following manner. A fragment was removed from the hinge area, adjacent to the samples used for amino acid analysis. The outer prismatic and inner nacreous layers were removed with a dental drill. The remainder of the fragment was crushed to a fine powder with mortar and pestle, and the powder mounted on a glass slide with Vaseline. Analyses were performed using a General Electric X-ray diffractometer. The operating parameters were: copper radiation, source operated at 40 kV and 20 mA, nickel filter, and the time constant equal to 2X. The {111} aragonite peak at $26.2^{\circ}2\theta$ and the {104} calcite peak at $29.4^{\circ}2\theta$ were used for mineral identification. Samples were scanned from $20^{\circ}2\theta$ to $35^{\circ}2\theta$ so a baseline could be drawn for these peaks.

A set of standard powders consisting of different proportions of calcite and aragonite were prepared, to develop a standard curve relating the percentage of calcite in a sample to a peak intensity. Pure calcite rhombs were obtained from the Department of Geology teaching collection. Aragonite (sample no. 3324, from Jungapéo, State of Michoacán, Mexico) was donated by the Irénée du Pont Mineral Museum. Calcite proportions in each sample ranged from 100 to 1 percent by weight. Peak intensities were converted to a function R (below; Turekian and Armstrong, 1960); R values were plotted against percent calcite to define a standard curve (Fig. 4-1).

$$R = \frac{I_{\text{calcite}}}{I_{\text{aragonite}} + I_{\text{calcite}}} \quad I = \text{peak intensity (mm)}$$

— Data from Turekian and Armstrong (1960)

--- Data from this study. Line fit to the equation: $y = -0.26 + 0.58 \cdot \log(x)$ $r^2 = 0.87$

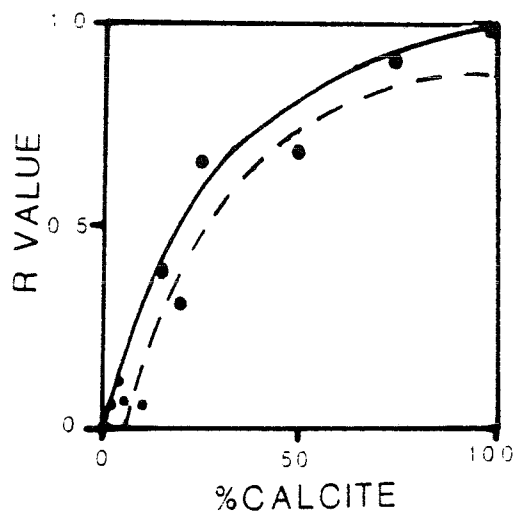


Fig. 4-1. Plot showing the relationship between % calcite and calculated R value for powder mixtures with varying proportions of calcite and aragonite. Data from Turekian and Armstrong (1960) and from this study are shown.

The standard curve obtained from this study is not adequate for quantitative determination in samples showing low % calcite (<10%). R values do not decrease systematically for mixtures having less than 10% calcite, and this curve differs in shape from curves published previously (Turekian and Armstrong, 1960; Davies and Hooper, 1963). The probable cause of non-reproducible behavior in these mixtures is non-homogeneity of calcite and aragonite grain sizes mounted on the glass slide. Greater accuracy may be obtained by first sieving calcite and aragonite powders before mixing. Aragonite/calcite powder mixture data used to construct Fig. 4-1 are found in App. C-2.

4.5: Water Weight Gain/Loss Experiments

The purpose of this experiment is to provide a relative comparison of effective porosity among shells of variable condition and age. Effective porosity is defined as the interconnected pore space within the solid shell, or voids through which water can percolate. Porous shells have greater surface area available for leaching of amino acids. Thus the leaching capacity of shell material may be assessed by a simple measurement of water weight gain.

Squares of shell material were cut from shell specimens representing all conditions (excellent, good, fair, poor) from all aminozones where available. A modern shell (collected from the beach) was also sampled for comparison. Shell samples were washed, air-dried and weighed. Each shell specimen was then placed in a labeled wide-mouth test tube, covered with distilled water and placed under a vacuum to evacuate all air from within the specimen. Shells remained under vacuum until conspicuous bubbling ceased, indicating that the shells were saturated (usually for 10 minutes). Shells were removed from the test tubes, their exteriors patted dry and were then

weighed three times, to four decimal places. This "water weight gain" step was repeated daily (usually for five or six days) until constant weight (to 0.002 g) was attained. Shell fragments were then placed in an oven to dry, for the "weight loss" step. Again, samples were weighed daily until constant weight was attained.

This experiment was conducted twice. On the first trial, three specimens (one modern, one from aminozone IIa in excellent condition, one from aminozone IIa in poor condition) were saturated, then placed in a low-temperature (100° C) for the weight loss step. After three cycles of saturation and heating in the low-temperature oven (lasting 41 days), these same shell samples were subjected to saturation and heating in a high-temperature oven (300°C) for another 26 days. Heating at high temperature destroyed organic matrix within shell samples, and represented more severe diagenetic conditions. This experiment, 67 days in duration, is called the long-term experiment.

In the second trial, a greater number of shells (n=14) representing all shell conditions (where available) in aminozones IIa, IIc, and IID were subjected to alternating saturation and heating (100°C only) for a period of 25 days. This is the short-term experiment.

Daily weighings were recorded and plotted against time (hours) elapsed since the initial weighing. The greatest error of these experiments involved weighing the wet shell specimens. Typical reproducibility of triplicate weighings was to 0.01 g, but was occasionally higher (0.2 g) in more porous specimens. Data for the water weight gain/loss experiments are tabulated in Appendix C-3.

CHAPTER 5

GEOLOGIC HISTORY OF THE PLEISTOCENE UNITS FOUND IN THE OUTER COASTAL PLAIN OF SOUTHEASTERN VIRGINIA

5.1 Introduction

The purpose of this chapter is to discuss different interpretations of the late Pleistocene exposures seen at Gomez Pit and nearby Womack Pit, both located south of Norfolk, Virginia. Womack Pit (now flooded), was located less than 1 km southeast of Gomez Pit. Exposures in Womack Pit were examined in earlier works (e.g. Oaks and Coch, 1963; 1973; Belknap, 1979; Mixon *et al.*, 1982) and type sections for several formations were described at this locality. Gomez Pit (also known as the Mears Corner locality) became an active quarry after the closure of Womack Pit; hence many of the later interpretations are based on these newer exposures (e.g. Cronin *et al.* 1981; Peebles, 1984; Mirecki, 1985; Spencer and Campbell, 1987; Wehmiller *et al.*, 1988). Both borrow pits exhibit similar lithostratigraphic sequences. Fig. 5-1 summarizes the stratigraphic frameworks of previous workers, and the relationship of these works to the Gomez Pit sections central to this study.

It is necessary to review in detail the physical stratigraphy of the Quaternary units in southeastern Virginia for two reasons. First, the physical stratigraphy of these exposures provide the basis for all geological interpretations. Second, all previous interpretations of the magnitude and timing of sea level change in

southeastern Virginia have been based on lithologic and paleontologic data. Using these data, all previous workers have interpreted the exposures at Gomez Pit and Womack Pit as representing deposition during one interglacial high sea stand. As will be presented in Chapter Six, amino acid data obtained from these same sections indicates that lithologic remnants of at least two high sea stands are preserved at the Gomez Pit locality.

5.2: Lithostratigraphy of Pleistocene Units in Southeastern Virginia (Oaks and Coch, 1973)

The first detailed lithostratigraphic studies of post-Miocene units of southeastern Virginia were presented as the dissertations of Robert Oaks and Nicholas Coch, who examined the strata of the inner and outer Coastal Plain, respectively. Detailed lithologic sections were published jointly by Oaks and Coch (1973). Four formations were recognized at the Womack Pit locality: the Great Bridge, Norfolk, Kempsville and Sand Bridge Formations. Type sections for the Great Bridge Formation (upper member), the Norfolk Formation (upper member) and Kempsville Formation are defined at Womack Pit (sections H and I, Oaks and Coch, 1973).

The Great Bridge Formation, which commonly occupies paleotopographic lows of the underlying Yorktown Formation, comprises two members. The lower member consists of fluvial sand and gravel, overlain by an upper member consisting of open bay-lagoonal clay, silt and fine sand. The upper surface of the Great Bridge Formation was mapped as having a maximum altitude of 4 ft (1.2 m) below mean sea level (MSL).

The Norfolk Formation, as defined by Oaks and Coch (1973) was divided into two members. The lower member consists of coarse sand and pebbles and was interpreted

as a beach environment. The lower member is laterally extensive west of the Fentress Rise, and was considered a stratigraphic marker near the Suffolk Scarp. The upper member of the Norfolk Formation is variable in composition, and has been divided into eight mappable facies (Oaks and Coch, 1973). The upper member generally consists of coarse beach sand and pebbles in the west (near the Suffolk Scarp) grading to sand and fine sand at the Fentress Rise. The fine sands and fossils of the Norfolk Formation at Womack Pit were deposited in a marine environment, seaward of a shoreline located at the Suffolk Scarp.

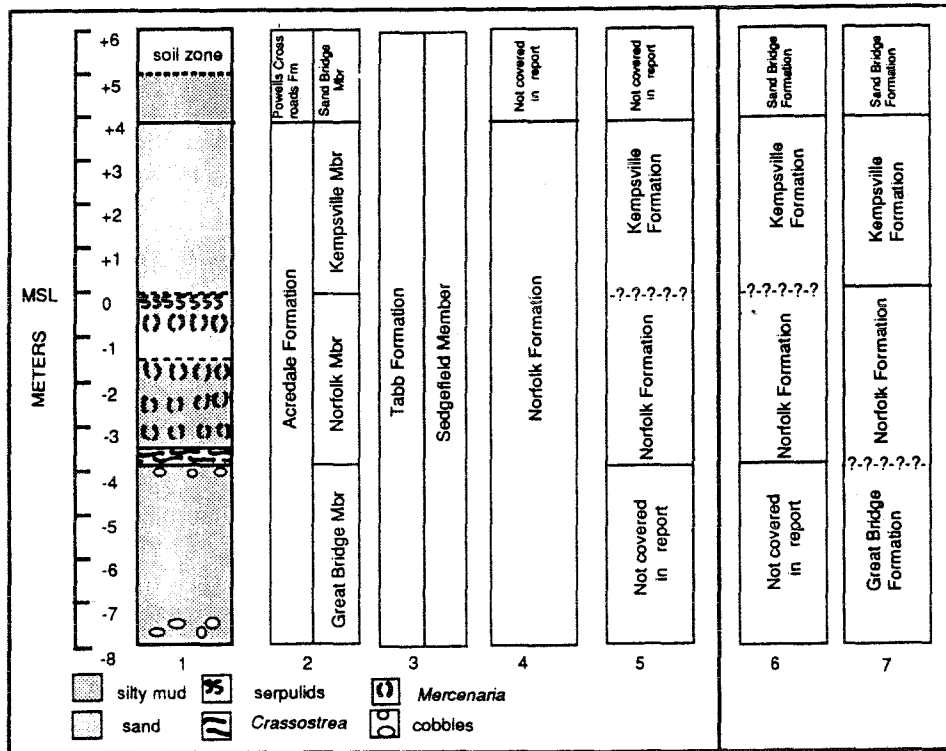


Fig. 5-1. A comparison of stratigraphic interpretations used to describe the late Pleistocene units of southeastern Virginia. Sections 2 through 5 are redrawn from published Gomez Pit sections. Sections 6 and 7 are redrawn from published Womack Pit sections. Section 1, composite section of Gomez Pit. Section 2, from Spencer and Campbell (1987). Section 3, from Peebles (1984). Section 4, from Darby (1983). Section 5, from Cronin *et al.* (1981). Section 6, from Mixon *et al.* (1982). Section 7, Oaks and Coch (1973).

Oaks and Coch (1973) found no lithologic evidence of a major break in the stratigraphic record between the Great Bridge and Norfolk Formations, and suggested that there was a close time relationship between the two units. Absence of weathering characteristics in the silty sands and clays were interpreted as evidence that the Great Bridge Formation had not stood above sea level for an extended period. There is a conformable relationship between the Great Bridge Formation and the Norfolk Formation. However, the contact between the upper member of the Great Bridge Formation and the overlying members of the Norfolk Formation is difficult to discern on the basis of lithology. In the type sections of the Great Bridge and Norfolk Formations, the contact between the upper member of the Great Bridge Formation and the lower members of the Norfolk Formation was obscured during drilling (sections H and I, Oaks and Coch, 1973).

The Kempsville Formation consists of fine to coarse sand with minor amounts of fine- pebble gravel. As defined by Oaks and Coch (1973), this formation was restricted to sand sediments forming several north-south trending arcuate ridges capping parts of the Fentress Rise (Plate 2, Oaks and Coch, 1973). These sediments were interpreted as beach and dune environments along a mainland coast. Belknap (1979) noted discrepancies in the placement of the Norfolk-Kempsville Formation boundary among several authors. As defined by Oaks and Coch (1973; Fig. 17D, p.61), the upper 1m of the Norfolk Formation was marked by a serpulid bioherm, overlain by a horizon of articulated *Mercenaria* . The lowest few meters of the Kempsville Formation contains disarticulated *Mercenaria* oriented convex-up, parallel to bedding planes. Mixon *et al.* (1982) included all fossiliferous strata as part of the Norfolk Formation.

A comparison of weathering characteristics of quartz grains and clays led Oaks and Coch (1973) to conclude that the Kempsville Formation was closer in age to overlying units (Londonbridge and Sand Bridge Formations) than to the Great Bridge and Norfolk Formations. A minor emergence (or lower sea stand) was inferred after the deposition of the Norfolk Formation (Oaks and Coch, 1973).

The Sand Bridge Formation occupies the highest stratigraphic position in Womack Pit and parts of Gomez Pit, and unconformably overlies the Norfolk and Kempsville Formations. Although the Sand Bridge Formation is laterally extensive east of the Suffolk Scarp, this formation thins at the Fentress Rise resulting in limited exposure at both Womack Pit and Gomez Pit. The Londonbridge Formation occupies a stratigraphic position between the Norfolk Formation and the Sand Bridge Formation, but was not exposed at all in Womack Pit (sections H and I; Oaks and Coch, 1973) or Gomez Pit.

The Sand Bridge Formation comprises two members. The lower member consists of clean to silty, fine to medium sand containing fossils indicating a marine environment. West of Fentress Rise, the lower member was deposited in a shallow, sandy lagoon. Open marine conditions are inferred from sediments and fossils of the lower member deposited east of the Fentress Rise. The upper member has been subdivided into four lithologic facies which together define a sand-ridge and mud-flat environment representing a barrier-lagoon complex extending east of the Fentress Rise (Oaks and Coch, 1973). Together, the Londonbridge (not exposed in these sections) and the Sand Bridge Formations represented deposition during one transgressive-regressive cycle.

Oaks and Coch (1973) interpreted these data in the context of rising and falling sea level. Two transgressive-regressive sedimentary sequences were deposited during late Pleistocene time. The oldest sequence consists of the Great Bridge, Norfolk and Kempsville Formations. The youngest sequence consists of the Londonbridge and Sand Bridge Formations.

The Great Bridge and Norfolk Formations were interpreted as being deposited during a sea level rise that reached a maximum during Norfolk time. A "minor emergence" or lower sea stand may have occurred between the deposition of the Norfolk Formation and the Kempsville Formation. Sea level then reached a minimum after the deposition of the Kempsville Formation. Finally, relative sea level rose reaching another maximum during deposition of the Londonbridge and lowest Sand Bridge Formation.

Few dated samples were available to Oaks and Coch during their research. Uranium series analyses of corals obtained from the Norfolk Formation (serpulid bed) ranged in age from 62 to 86 ka (p.70, Oaks and Coch, 1973). ¹⁴C dating of driftwood from the Kempsville Formation, and from peat of the Sand Bridge Formation all yielded ages exceeding 40 ka (p. 78, 97; Oaks and Coch, 1973). All units were interpreted as being deposited during Sangamonian or mid-Wisconsinan time.

5.3 Reinterpretations Considering Timing and Magnitude of Sea Level Rise.

The work presented by Oaks and Coch (1963, 1973) and Oaks *et al.* (1974) provide an extensive lithostratigraphic framework to which all later works are compared. However, it is difficult to reconcile the timing of sea level fluctuations with the deep-sea oxygen isotope curve (Shackleton and Opdyke, 1973) and dated, emerged coral terraces in Barbados (Fairbanks and Matthews, 1978). A conflict exists when the timing and magnitude of sea level change preserved in southeastern Virginia is compared to records of global sea level change.

Cronin *et al.* (1981) re-examined many Atlantic coastal plain localities (including Womack and Gomez Pits) in order to correlate the timing of these continental margin deposits with records of global sea level change. New uranium series age estimates of 62 +/- 4 ka (Womack Pit) and 75 +/- 5 ka (Gomez Pit) were calculated from analyses of corals collected within the serpulid bed of the Norfolk Formation (Cronin *et al.*, 1981). This cluster of uranium series ages is similar in age to the Worthing terrace in Barbados (72 ka; Fairbanks and Matthews, 1978); therefore the Norfolk and Kempsville Formations were interpreted to represent transgression and regression during oxygen isotope Substage 5a. Sea level estimates for Substage 5a range from -15 to -43 meters below MSL (Shackleton, 1987), yet the maximum altitudes of the Norfolk and Kempsville Formations are at or above present day sea level. Therefore, the conflict between timing and magnitude of sea level rise remains unresolved. It was suggested that hydro-isostasy (*i.e.* crustal adjustment to a redistribution of mass from continental ice to seawater) might be a mechanism resulting in uplift of these coastal plain units (Cronin, 1981).

Mixon *et al.* (1982) reconsidered the lithostratigraphy of these Late Pleistocene units in the context of a transgressive barrier island model. The nomenclature of Oaks and Coch (1973) was retained; however, two revisions to the stratigraphic framework of Oaks and Coch (1973) were proposed. First, the relationship between the Kempsville Formation and Sand Bridge Formation was redefined. Second, the age of the Norfolk Formation was reinterpreted. One feature of this work is that a hypothesis (i.e. a model of deposition during marine transgression) is used to interpret these complex lithologic exposures.

Mixon *et al.* (1982) re-interpreted the Kempsville Formation to include all back-barrier estuarine deposits west of Fentress Rise previously defined as Sand Bridge Formation. The relationship of the coarse sand unit capping the Fentress Rise (Kempsville Formation) to the silty sands exposed on the surface west of Fentress Rise (the Sand Bridge Formation) reflects a facies change within one transgressive sedimentary sequence, not the remnants of two high sea stands as inferred by Oaks and Coch (1973).

The Norfolk Formation was also re-interpreted by Mixon *et al.*, (1982). Although this unit was not renamed, the Norfolk Formation was divided into two units of different age: east of Suffolk scarp, these beds were less than 140 ka in age, and west of Suffolk scarp they were greater than 140 ka. The relationship between the Great Bridge Formation and the Norfolk Formation remains enigmatic. Although the Great Bridge Formation was recognized in the subsurface (6m below MSL; Fig. 2, Mixon *et al.*, 1982), its relationship to overlying units is not discussed.

Darby (1983) re-interpreted the lithostratigraphy of the units exposed at Gomez Pit and other nearby quarries. In this work, the Norfolk Formation was expanded to include the Norfolk, Kempsville and Sand Bridge Formations of Oaks and Coch (1973). The Kempsville and Sand Bridge terms were abandoned; instead, Darby (1983) reassigned these formations into five facies. The Norfolk Formation of Darby (1983) rests unconformably on the Great Bridge Formation, and a major hiatus was inferred between these two formations. Apparently, this hiatus is marked by a boulder and cobble layer, corresponding to the lowest boulder layer on Fig. 5-1. A second boulder layer was deposited above the hiatus, into a bay or lagoon (Norfolk Formation sediments) during a rising sea level. Darby (1983) proposed the mechanism of ice rafting, rather than fluvial processes for deposition of the boulders. However, these interpretations seem inconsistent with previously published data. A warm-temperate to subtropical marine environment, having ocean temperatures warmer than present day Virginia is inferred from ostracode (Valentine, 1971; Cronin *et al.*, 1981) and pollen (Cronin *et al.*, 1981) assemblage data obtained from the Norfolk Formation. Given a warm climate, it seems unlikely that ice rafting was a significant depositional process.

Peebles (1984) re-interpreted the lithostratigraphy of middle and upper Pleistocene units using a model describing the succession of fluvial, paludal, estuarine and marine sedimentary environments over a dissected coastal plain during a marine transgression. Here, the nomenclature of Oaks and Coch (1973) is not used. The Tabb Formation (Johnson, 1976) originally defined on the York River-James River peninsula is correlated to units exposed in Gomez Pit.

Peebles (1984) argued that the Great Bridge Formation was correlative with the late Pliocene Chowan River Formation (Blackwelder, 1981). Peebles (1984) eliminated the Norfolk Formation; strata previously assigned to this unit were reassigned in part to the Shirley Formation (Johnson and Berquist, in press) and the Tabb Formation (Johnson, 1976). The Shirley Formation and the Tabb Formation are separated by an unconformity. The Kempsville, Londonbridge and Sand Bridge Formation terms were also abandoned. These units represent facies within the Sedgefield and Lynnhaven Members of the Tabb Formation.

The Gomez Pit exposures reveal an almost complete section of the Sedgefield Member, Tabb Formation (Ref. section 1; Peebles, 1984). The base of the Sedgefield Member is marked by a pebble to cobble layer overlain by a dark mottled silty mud. This unit is overlain by a laterally extensive *Crassostrea* layer, which serves as a local stratigraphic marker. The *Crassostrea* layer is overlain by a fossiliferous sandy unit which coarsens upward and contains abundant articulated *Mercenaria*. A serpulid worm reef is locally prominent at midsection in Gomez Pit. Both articulated and disarticulated *Mercenaria* are found above the serpulid worm reef. However, as the sandy sediments coarsen upward above the serpulid bed, only shell ghosts and leached fragments of shells are present. Cross-bedded sands are found in some portions of this upper section. In other sections, a poorly sorted, dark silty sand unit overlies the *Mercenaria* unit. The dark silty sand unit may represent channels formed in the upper Sedgefield Member. The Sedgefield Member of the Tabb Formation was interpreted as representing deposition during a marine transgression (Peebles, 1984). Considering the superposition of sedimentary environments in the Gomez Pit section, it appears as if a nearly complete record of marine transgression has been preserved.

Spencer and Campbell (1987) proposed another stratigraphic framework based on the exposures at Gomez Pit and other nearby quarries. The type section of the Acredale Formation was defined at Gomez Pit. The Great Bridge, Norfolk and Kempsville Formations of Oaks and Coch (1973) represent different lithofacies of the Acredale Formation, and were reduced to member status. The Powells Crossroads Formation type section was defined at a different locality (Mt. Trashmore, near Virginia Beach). The Londonbridge and Sand Bridge Formations of Oaks and Coch (1973) represent lithofacies of the Powells Crossroads Formation, and were also reduced to member status. The Acredale and Powells Crossroads Formations each represent one transgressive-regressive sequence in the Spencer and Campbell (1987) model.

5.4: Lithostratigraphy of Related Field Sites in Virginia: Norris Bridge and Yadkin Pit

Data obtained from the Norris Bridge and Yadkin Pit localities will contribute significantly to the age estimates of several aminozones as discussed in Chapter Six. The geologic setting of these sites, and the lithostratigraphic relationship of these sites to the units observed in Gomez Pit will be considered in the following subsections.

5.4.1: The Norris Bridge Locality

The Norris Bridge locality is located on the north side of the Rappahannock River, east of the Whitestone Bridge in Virginia (Fig. 1-2). Exposures consist of fossiliferous sandy silt, overlain by a cross-bedded sandy unit (App. D.1-1). These units have been interpreted as a transgressive sequence (Cronin *et al.*, 1981; Mixon *et al.*, 1982).

The units at Norris Bridge have been interpreted in the context of lithostratigraphic frameworks defined in both the Norfolk area (Peebles, 1984) and the Delmarva Peninsula (Owens and Denny, 1979; Mixon *et al.* 1982; Mixon, 1985; Colman and Mixon, 1988). The nomenclature applied at Norris Bridge differs between these two lithostratigraphic frameworks. However, both support the idea that the Norris Bridge units represent an interglacial deposit older than oxygen isotope Stage 5. At present, there is no complete agreement on the age of the Norris Bridge (and correlative) units. Geologic evidence including geomorphic, paleontologic and magnetostratigraphic data constrain the age interpretations of the Norris Bridge site, and these data will be reviewed here. Amino acid and uranium series data will be considered in Chapter Six, using geologic data as a basis for discussion.

Considering nomenclature applied in southeastern Virginia, the Norris Bridge units have been interpreted as facies within the Shirley Formation by Peebles (1984). The Shirley Formation is a transgressive sedimentary package representing maximum high sea stand approximately 15 m above MSL (p. 114; Peebles, 1984). This package is older and slightly higher in elevation than the Tabb Formation (*i.e.* the units at Gomez Pit). Definition of the Shirley Formation is in Berquist and Johnson (1989), and described in the area southeast of Norfolk in Peebles (1984).

The Norris Bridge units have also been correlated with the Accomack Member of the Omar Formation, as defined on the Delmarva peninsula near Chincoteague, Virginia (Mixon *et al.*, 1982; Mixon, 1985). Two types of data support this cross-bay correlation. First, both localities show similar transgressive stratigraphic sequences (Mixon *et al.*, 1982). Second, the transgressive sequences on both sides of the bay underlie depositional surfaces ranging about 12 to 15 m above MSL (Mixon *et al.*, 1982).

Ostracode assemblage data and interpretations have been published for Norris Bridge (Cronin, 1979) and two other localities on the Delmarva Peninsula where the Omar Formation is exposed (Chincoteague, Virginia in Cronin (1988); Dirickson Creek ditch, Delaware in Cronin (1984)).

The Norris Bridge site, and samples from the Omar Formation (Accomack Member) at Chincoteague, Virginia both show similar ostracode assemblages. These assemblages differ from those of the Omar Formation (undivided) collected at Dirickson Creek ditch, Delaware. Ostracode assemblage data can be useful for correlation between localities; however, the timing of interglacial deposits cannot be

discerned strictly from these data because ostracode assemblages in marginal marine environments are both climate- and facies-dependent (T. Cronin, personal comm. 1989). Age interpretation of ostracode biostratigraphic data are dependent in part on uranium series and amino acid data, and these will be considered further in Chapter Six.

In addition to these data, paleomagnetic study of clays and silts collected from the Accomack Member near Chincoteague indicates normal magnetic polarity. The Accomack Member is considered to be of Brunhes age (< 730 ka) on the basis of stratigraphic relationships with adjacent units of late Pleistocene age (Liddicoat and Mixon, 1980).

5.4.2: The Yadkin Pit Locality

Yadkin Pit is located approximately 14 km west of Gomez Pit, near Deep Creek, Virginia (App. D.1-2). Lithologic sections from this locality have been described previously (Belknap, 1979, p. 466; Peebles, 1984, Fig. A50, ref. section 43; Spencer and Campbell, 1987, ref. section 21, p. 75). The exposures at Yadkin Pit are complex, and include several superposed unconformable lithostratigraphic units. In a manner analogous to Gomez Pit, several stratigraphic frameworks have been applied to the Yadkin Pit exposures (Fig. 5-2).

The Pliocene Yorktown Formation is the lowest unit exposed at Yadkin Pit, and is unconformably overlain by the late Pliocene Chowan River Formation, as interpreted by Blackwelder (1981) and Peebles (1984). The Chowan River Formation at Yadkin Pit is characterized by indurated silty sand with ferricrete nodules and abundant

mollusc fragments, including *Glycymeris subovata* , *Noetia limula* , and *Chesapecten* sp. The molluscan fauna, although possibly reworked, is distinct and easily discerned from molluscs in the overlying Pleistocene units.

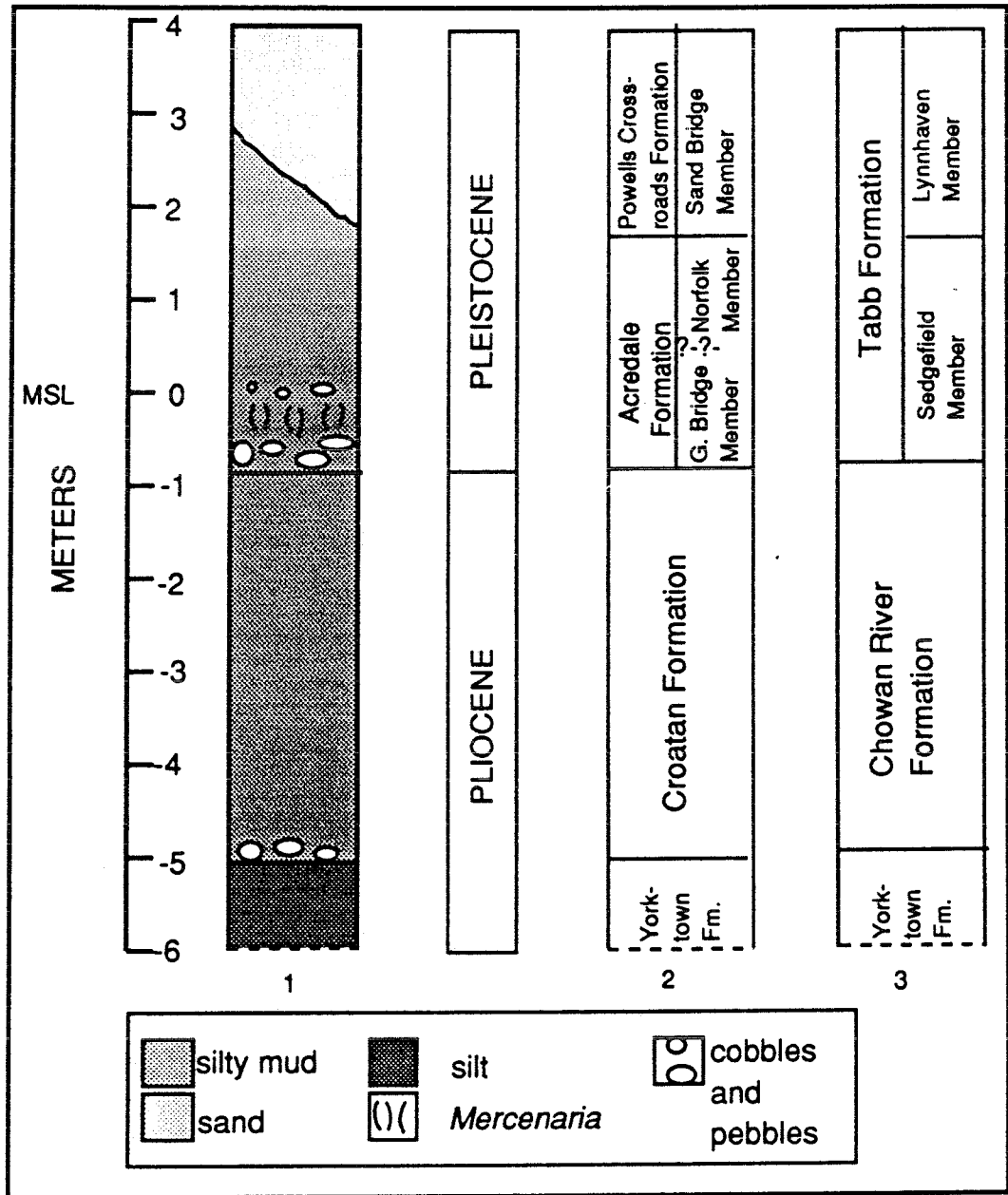


Fig. 5-2. A comparison of stratigraphic interpretations used in southeastern Virginia, as seen in Yadkin Pit. Section 1, composite lithologic section of Yadkin Pit. Section 2, Spencer and Campbell (1987). Section 3, Peebles (1984).

Spencer and Campbell (1987) retain an older stratigraphic term, the Croatan Formation, for this same late Pliocene unit (Fig. 5-2). The question of appropriate stratigraphic nomenclature cannot be answered using the limited exposures in Virginia because type sections for both the Chowan River Formation and the Croatan Formation are defined at extensive exposures in northeastern North Carolina. Reference is made to Blackwelder (1981) for discussion of late Pliocene lithostratigraphy in this region.

The Pleistocene stratigraphic frameworks of Peebles (1984) and Spencer and Campbell (1987) have been applied to the Yadkin Pit exposures (Fig. 5-2). These frameworks differ in their interpretation of timing of sea level change. In the Peebles (1984) model, the Sedgefield Member and Lynnhaven Member of the Tabb Formation together represent one transgressive-regressive episode. Minor regression is indicated by Lynnhaven channels entrenched into Sedgefield sediments; these channels are exposed near the top of Yadkin Pit (ref. section 43, Peebles, 1984). In the Spencer and Campbell (1987) model, members of the Acredale and Powells Crossroads Formations each represent one high sea stand. The Great Bridge and Norfolk Members of the Acredale Formation, representing a somewhat older high sea stand, are unconformably overlain by the Sandbridge Member of the Powells Crossroads Formation.

5.5: Comparison of Stratigraphic Frameworks Applied in Southeastern Virginia

Emerged continental marine Quaternary units of southeastern Virginia represent a partial record of interglacial sea level maxima. Recent interpretations have focused on correlation of this partial sedimentary record with the deep-sea oxygen isotope

curve, which provides a complete chronostratigraphic reference describing glacial to interglacial change. While the curve of Shackleton and Opdyke (1973) provides only a first-order approximation of sea level change, more recent work (Shackleton, 1987) focuses on the resolution of the sea level (or ice volume) component of the oxygen isotope curve.

Geologists face the problem of correlation of an incomplete sedimentary record preserved on continental margins with the complete record preserved in deep-sea basins. Correlation is hindered by the number and ephemeral nature of outcrop exposures, and the range and resolution of various dating methods.

5.5.1: Definition of Lithostratigraphic Frameworks in Southeastern Virginia

The philosophy of most works discussed in this chapter is to define a lithostratigraphic formation as encompassing a transgressive (or transgressive-regressive) sequence of lithofacies, bounded by unconformities formed during lowest sea levels. Oaks and Coch (1973) originally defined lithostratigraphic formations in this manner. They distinguished "major emergences" (or unconformities) which bounded each major transgressive sequence. However, they also recognized "minor emergences", apparently resulting from minor sea level fluctuations. Minor emergences also served as boundaries between formations.

Subsequent authors retained the nomenclature of Oaks and Coch (1973), but expanded or abandoned those formations which did not fit into a depositional model describing marine transgression. The net result was a body of literature that was muddled with overlapping lithostratigraphic terms. Peebles *et al.* (1984) and Spencer

and Campbell (1987) avoided the problem of usage by renaming the units exposed in the study area; however, the idea that each lithostratigraphic formation represents one transgressive-regressive event remains.

5.5.2: Definition of Biostratigraphic Frameworks in Southeastern Virginia

Biostratigraphic frameworks using ostracodes (Cronin, 1988) and molluscs (Blackwelder, 1981b) have been proposed for Quaternary deposits of the middle Atlantic coastal plain. Biostratigraphic information using foraminifera, calcareous nannofossils and pollen (Cronin *et al.*, 1981) are also routine components in investigations of marine cores collected from this region.

Biostratigraphers face the problem of correlation of marine deposits with nearshore facies equivalents. Planktonic foraminifera and calcareous nannoplankton are relatively sparse in nearshore deposits (Cronin *et al.*, 1984). Benthic organisms (foraminifera and ostracodes) show strong facies control by depth, salinity, substrate and water temperature (Cronin, 1979; Cronin *et al.*, 1984), effectively limiting the resolution of time in nearshore deposits. Molluscan biozones have been proposed for the middle Atlantic coastal plain (Blackwelder, 1981b), but this approach does not adequately resolve successive interglacial deposits during the late Pleistocene. Generally, biostratigraphic frameworks do not yet provide the resolution necessary to discern the partial record of interglacial deposits exposed on the coastal plain.

5.5.3: Definition of an Allostratigraphic Framework in Southeastern Virginia, and Its Relationship to Aminostratigraphy

The North American Code of Stratigraphic Nomenclature (1983) defines an

allostratigraphic unit, or alloformation, as a mappable stratiform body of sedimentary rock defined and identified on the basis of its bounding discontinuities. Genesis, geologic history and time span are inappropriate bases for definition of an alloformation, but may influence the choice of its boundaries. Boundaries which distinguish alloformations are disconformities.

Aminostratigraphy is defined (Miller and Hare, 1980) as correlation of fossiliferous strata over a limited geographic region (characterized by similar mean annual temperatures and seasonal temperature regimes) using amino acid enantiomeric ratios. The fundamental unit of aminostratigraphic classification is the aminozone, characterized by a cluster of statistically similar amino acid enantiomeric ratios. Un-calibrated amino acid enantiomeric ratios can be used to correlate strata, and to establish relative age relationships among superposed strata. If amino acid enantiomeric ratios are calibrated using an independent dating method, numerical age may be estimated using a non-linear model describing racemization kinetics.

It is proposed that amino acid enantiomeric ratios serve as the basis for definition of allostratigraphic units exposed in southeastern Virginia. The bounding discontinuities between alloformations are abrupt shifts in amino acid enantiomeric ratios, and these boundaries are also called disconformities. Disconformities often (but not always) coincide with disconformities defined using lithologic criteria, such as gravel and cobble lags and weathered (soil) horizons.

Allostratigraphic nomenclature has been applied previously to units in southeastern Virginia (Peebles *et al.*, 1984). In this work, each alloformation represents a sedimentary sequence deposited during marine transgression. The

bounding disconformities are coarse- grained fluvial lags deposited during lowest sea levels. Other data such as elevation and lithology are used to correlate exposures away from the type section of each alloformation. However, it will be shown in Chapter Six that at least two aminozones can be discerned in Gomez Pit exposures previously interpreted as representing one transgressive sequence. This apparent conflict highlights the utility of aminostratigraphy: that amino acid enantiomeric ratios can resolve superposed interglacial deposits representing stages of the more complete chrono- stratigraphic record described by the deep-sea oxygen isotope curve.

The definition of allostratigraphic formations using amino acid enantiomeric ratios is not without precedence. McCoy (1987a) defined alloformations on the basis of amino acid enantiomeric ratios in the Quaternary deposits the Bonneville Basin. Each alloformation (and aminozone) defined by McCoy (1987a) represents deposition during a single lake cycle. Both this work and the work of McCoy use amino acid ratios to discern successive marine or lacustrine cycles which are often lithologically indistinguishable.

CHAPTER 6

AMINOSTRATIGRAPHY OF THE PLEISTOCENE UNITS FOUND IN THE OUTER COASTAL PLAIN OF SOUTHEASTERN VIRGINIA

6.1: Introduction

A regional aminostratigraphic framework is presented using the Gomez Pit amino acid data, supplemented by other results from Yadkin Pit and Norris Bridge localities. This framework will be compared to lithostratigraphic interpretations discussed in Chapter Five. In this chapter, the spatial distribution of amino acid data is used to define four aminozones in the extensively sampled outcrops of Gomez Pit, and these aminozones are extended away from Gomez Pit to other localities. This approach (called aminostratigraphy) represents the fundamental use of amino acid data. Once aminozones are defined spatially, their ages can be calibrated using uranium series ages from coral samples collected from that same aminozone (section 6.4). Additional age estimates are presented using ESR analyses of molluscan shell carbonate (section 6.5). Geochronological use of amino acid enantiomeric values (as compared to stratigraphic use of these data) will be considered in detail in Chapter Seven. Here, age estimates are calculated from amino acid enantiomeric values using the non-linear isoleucine kinetic model (Wehmiller *et al.*, 1988; Boutin, 1989).

Belknap (1979) provided the first aminostratigraphic data and interpretations for this region, and his work serves as a basis for this study. Regional interpretations have been presented in Wehmiller *et al.* (1988), to which the reader is referred for a

review of Atlantic coastal plain aminostratigraphy. However, a more detailed examination of Gomez Pit aminostratigraphy follows in this chapter. Nomenclature defined in Wehmiller *et al.* (1988) will be used here; all fossil localities occur in Region II, and aminozones (a) through (e) -youngest to oldest- are defined.

Age estimates for each aminozone in Region II are based on the non-linear isoleucine kinetic model (Boutin, 1989), calibrated by uranium series solitary coral ages obtained from aminozone IIa strata at Gomez Pit. These age estimates are as follows: aminozone IIa, 70 KA (late Stage 5) or 125 KA (early Stage 5); aminozone IIc, approximately 250 KA (early Stage 7); aminozone II d, approximately 500 KA (Stage 13 or as young as Stage II); aminozone IIe, Pliocene (greater than 2 million years). The non-linear kinetic model of isoleucine epimerization is considered in Chapter Seven.

6.2: Aminostratigraphy of Gomez Pit

Four clusters of ALLO/ISO values, or aminozones, are recognized in Gomez Pit exposures (Table 6-1, Fig. 6-1, App. D.1-3). Resolution of these aminozones is best using amino acid data from total samples; free sample data shows lower resolution. Although frequency diagrams such as Fig. 6-1 represent a simplified version of the aminostratigraphy in Gomez Pit, the existence of four aminozones suggests a more complex geologic history than has been inferred previously using lithostratigraphic data. Each aminozone will be defined in this section, starting with the youngest aminozone, IIa. A synthesis of both litho- and aminostratigraphy will follow in section 6.6.

	AMINOZONE (ALLO/ISO)TOT			(ALLO/ISO)FREE			(D/LEU)TOT		
Gomez Pit Ila	0.141	(0.028)	57	0.394	(0.051)	52	0.224	(0.051)	9
Ilc	0.333	(0.032)	23	0.640	(0.052)	23	not available		
Ild	0.459	(0.037)	9	0.746	(0.044)	9	0.530	(0.007)	3
Ile	1.066	(0.052)	5	1.156	(0.143)	5	not available		
Yadkin Pit Ilc	0.263	(0.034)	9	0.491	(0.036)	8	0.37		2
Ile	1.087		1	1.238		1	0.880(0)		2
Norris Br. Ild	0.469	(0.050)	14	0.929	(0.115)	14	0.530	(0.022)	7
DCD, DE Ild	0.420	(0.065)	6	0.705	(0.015)	6	0.535		8
Chinco. VA Ild	0.443	(0.055)	4	0.775	(0.037)	4	0.57		25

Table 6-1. Statistics describing four aminozones found in southeastern Virginia and the Delmarva peninsula. Data are presented as "mean ALLO/ISO value (standard deviation) number of samples". D/L leucine values are from the following sources: Norris Bridge and Gomez Pit, Mirecki (1985); Yadkin Pit, Belknap (1979); Dirickson Creek Ditch, DE (DCD) and Chincoteague, VA sites (including CW-4, Mathews Field and T's Corner data), Wehmiller *et al.* (1988). All ALLO/ISO data were obtained by JEM for this project, except for DCD and the Chincoteague, VA sites in Boutin (1989).

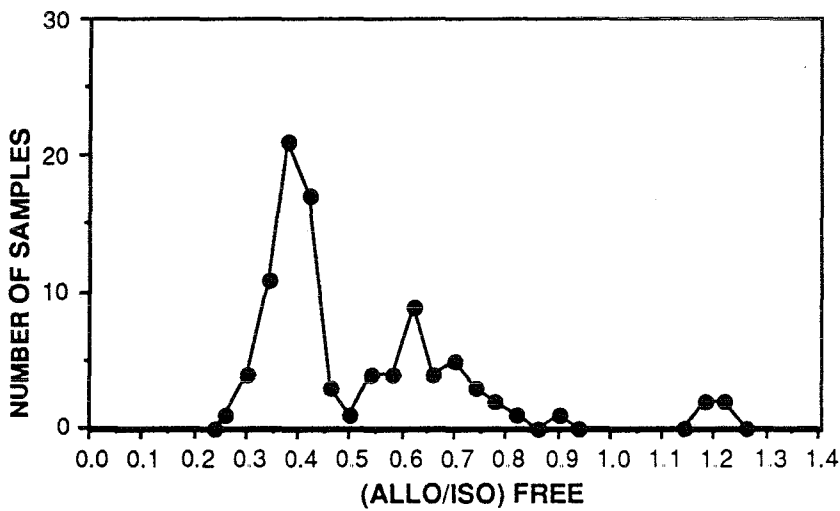
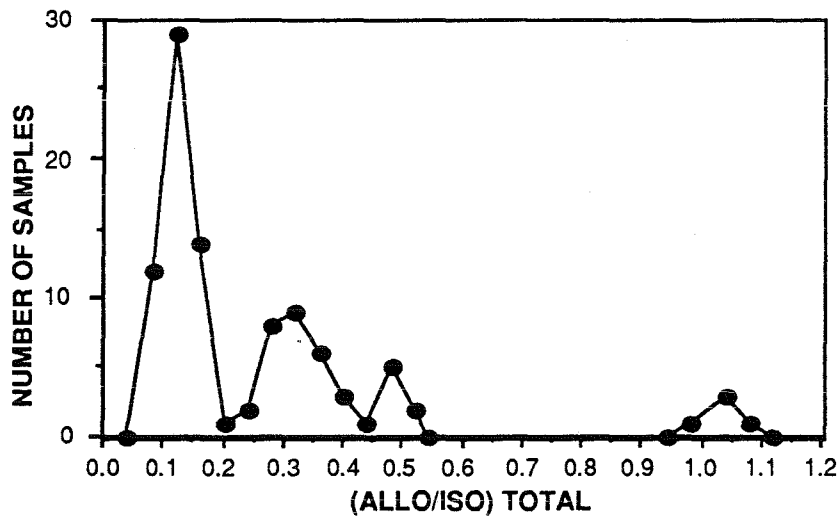


Fig. 6-1. Frequency diagrams showing the distribution of (ALLO/ISO)TOTAL and (ALLO/ISO)FREE values in Gomez Pit. Each peak represents an aminozone. Aminozones are not well resolved using (ALLO/ISO)FREE data. ALLO/ISO values are in grouped in units of 0.04.

The youngest aminozone, Ila includes the uppermost fossiliferous unit in Gomez Pit, and includes the serpulid bed and coral-bearing units dated by uranium series. This aminozone was also observed in the shallow subsurface at other nearby sand quarries (New Light and Womack Pits, Belknap, 1979; Wehmiller *et al.*, 1988). Conspicuous features in Gomez Pit aminozone Ila are several horizons of articulated *Mercenaria* (*e.g.* Fig. 6-2, App. D.1-3), which are laterally continuous on the outcrop scale (tens of meters).

Aminozone IIc lies stratigraphically below aminozone Ila in most sections of Gomez Pit (*e.g.* Fig. 6-3, App. D.1-3) and in the New Light and Womack Pit exposures. The contact between these two aminozones is best observed in Gomez Pit, and is distinct in that *Mercenaria* with (ALLO/ISO)TOTAL values of ca. 0.33 were collected within a laterally continuous *Crassostrea* (oyster) layer, and that other *Mercenaria* collected 10 cm or above the *Crassostrea* layer show (ALLO/ISO)TOTAL values of ca. 0.14 (UDAMS location 06045, Fig. 6-4, App. D.1-3). These two superposed clusters of amino acid data have been reported previously by Belknap (Fig. A49b, p. 465; 1979) at New Light Pit. The contact between aminozones Ila and IIc is well-defined in Gomez Pit, and is interpreted as the Ila/IIc disconformity. Surprisingly, lithologic evidence of a disconformity (*e.g.* obvious cobble and pebble lag deposits or evidence of weathering) is absent from the upper boundary of the *Crassostrea* layer.

Aminozone II d is characterized by ALLO/ISO values of ca. 0.46; however, it is difficult to correlate *Mercenaria* showing these ratios to any lithologic unit at Gomez Pit because some evidence suggests that II d shells are not in-place at Gomez Pit. First, shells representing aminozones Ila, IIc and II d coexist (*e.g.* UDAMS locations 06065, 06066 and 06067, Fig. 6-4). Second, II d shells are often (but not always) disartic-



Fig. 6-2. Gomez Pit exposure showing superposed aminozones IIa and IIc. Note that the contact between these aminozones occurs at the upper boundary of the *Crassostrea* (oyster) layer. UDAMS localities 06045 and 06031 are shown in the photograph.

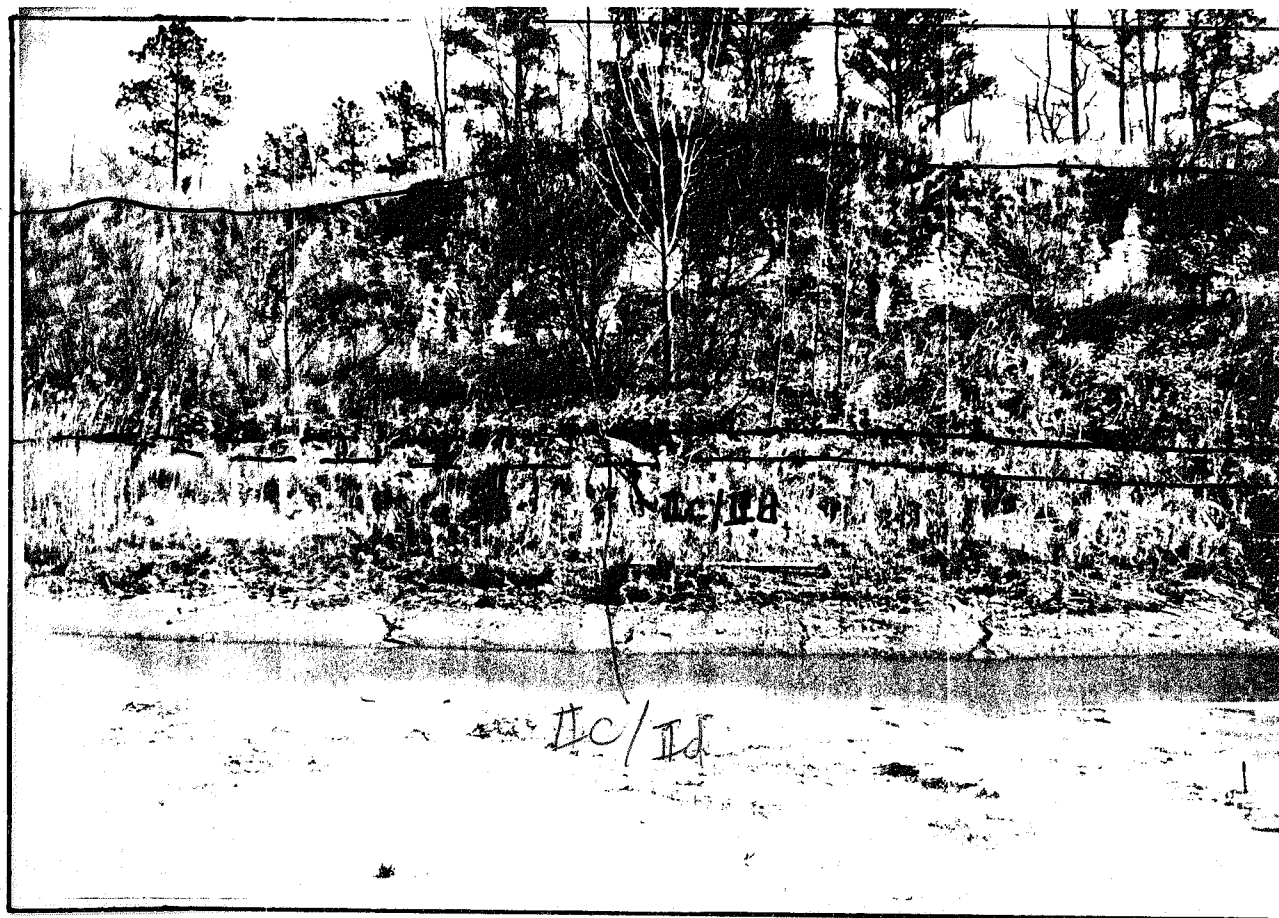


Fig. 6-3. Gomez Pit exposure showing aminozone IIa above the reworked horizon. Note that the *Crassostrea* layer thins to the left, and can be traced laterally to the IIc/IId disconformity. UDAMS localities 06067, 06066, 06065 and 06056 can be seen in this photograph.

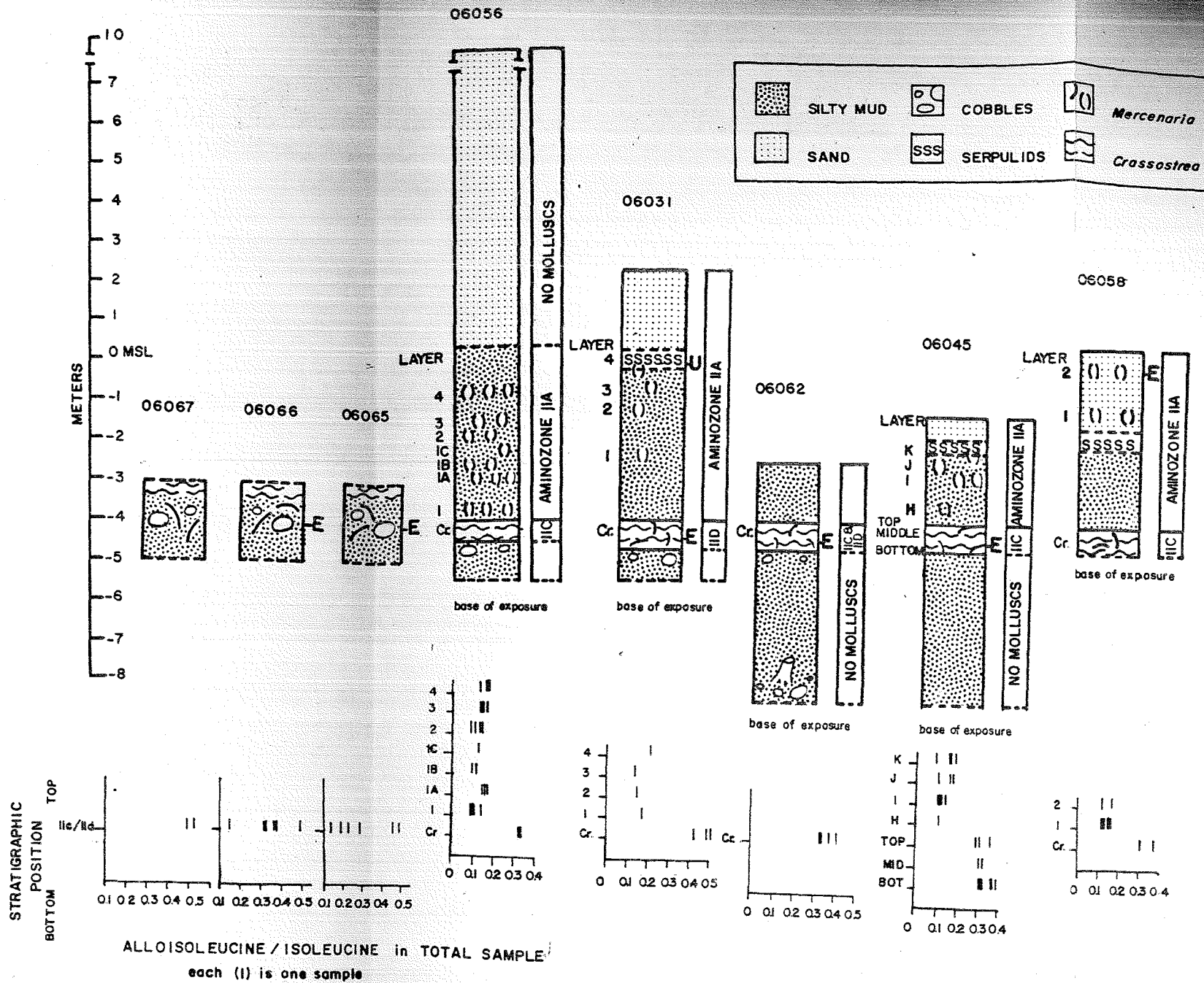


Fig. 6-4. Synthesis of lithostratigraphy and aminostratigraphy at Gomez Pit. The locations of corals for uranium series dates (-U) and molluscs for ESR analyses (-E) are shown. Aminozones are defined by the stratigraphic superposition of units characterized by increasing (ALLO/ISO)TOTAL values. A distinct break in (ALLO/ISO)TOTAL values occurs at the top of the *Crassostrea* layer (Cr.), and this is interpreted as the IIA/IIB disconformity. Molluscs showing (ALLO/ISO)TOTAL values representing aminozones IIA, IIC and IID coexist along one horizon (UDAMS locations 06065, 06066, 06067) and this horizon is called the IIC/IID disconformity. See text for further discussion.

ulated. Finally, cobbles and pebbles coexist with mollusc shells collected at UDAMS locations 06065, 06066 and 06067, and these clasts also underlie the *Crassostrea* layer in other measured sections of Gomez Pit (e.g. 06062 in Fig. 6-4). These lines of evidence support the interpretation of a disconformity lying immediately beneath the *Crassostrea* layer.

The spatial distribution of mollusc valves representing aminozones IIc and II d suggests the presence of an older disconformity or diastem, occurring at a lower stratigraphic level than the IIa/IIc disconformity in Gomez Pit. Two options are proposed (Fig. 6-5), comparing the occurrence of molluscs representing aminozones IIc and II d with lithologies from which these mollusc samples were taken.

Option 1. All molluscs representing aminozone II d are reworked within aminozone IIc. A disconformity or diastem is inferred where molluscs representing aminozones IIc and II d coexist (UDAMS locations 06065, 06066 and 06067). All lithologic units between the upper boundary of the *Crassostrea* layer and the Chowan River Formation (contact covered) are assigned to aminozone IIc, including the non-fossiliferous unit directly beneath the *Crassostrea* layer. A source for these older II d shells has not yet been exposed in or near Gomez Pit; however, in-place molluscs representing aminozone II d are found in Norris Bridge (Fig. 1-2).

Option 2. Molluscs representing aminozone II d are in-place, or have not been transported far from their source. A disconformity is inferred at the horizon marked by coexisting IIc and II d shells and cobbles (this is the IIc/II d horizon in Fig. 6-4 and Table 6-3). The non-fossiliferous unit below the *Crassostrea* layer is assigned to amino zone II d, and this unit extends down to the contact with the Chowan River Formation.

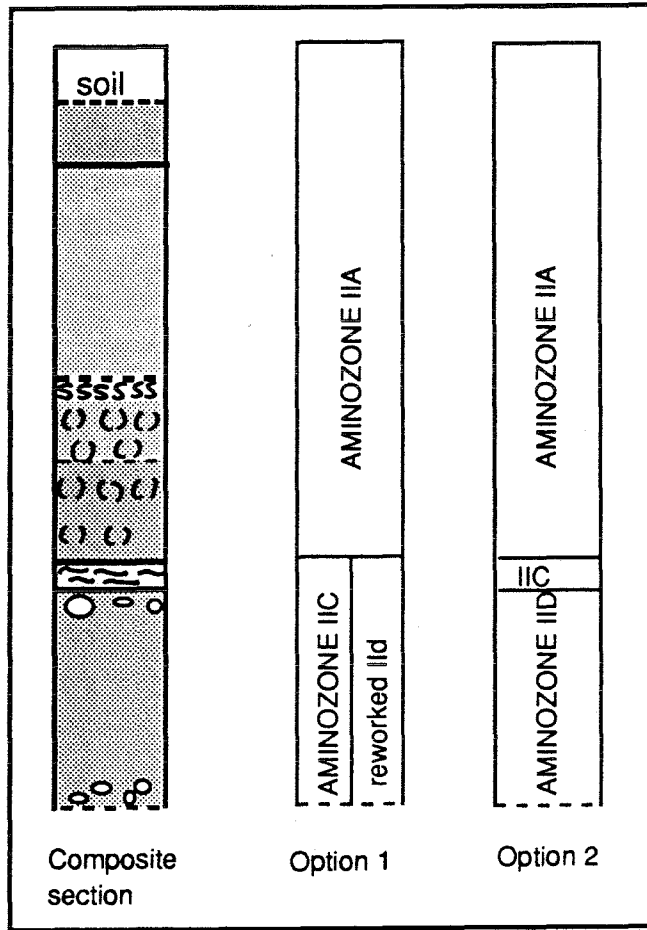


Fig. 6-5. Aminostratigraphic options describing the spatial relationship between aminozones IIC and IId as exposed in Gomez Pit. See text section 6.2 for discussion.

Resolution of the relationship between aminozones IIc and II d beyond these two options is not yet possible for the following reasons. First, IIc and II d shells coexist along a laterally traceable horizon at sites 06065, 06066 and 06067 (App. D.1-3) in Gomez Pit, occurring directly below the base of the *Crassostrea* layer. However, there are no mollusc fossils in the lithologic unit below the *Crassostrea* layer. Second, there is evidence supporting both reworking and in-place preservation of valves representing aminozone II d. If II d shells are reworked, disarticulated and articulated valves were redeposited during IIc time. If II d shells are in-place at the base of the *Crassostrea* layer, they were directly overlain by oysters and sediment during a IIc high sea stand. The depositional nature of II d shells will be discussed further in light of ESR data presented in sections 6.2.1 and 6.5.

Aminozone IIe is characterized by nearly racemic (ALLO/ISO)TOTAL values. At Gomez Pit, these highest (ALLO/ISO)TOTAL values are restricted to molluscs collected from limited exposure (UDAMS location 06054, App. B-1) of the late Pliocene Chowan River Formation (Blackwelder, 1981a) as interpreted at Gomez Pit by Peebles (1984). The contact between the Chowan River Formation and overlying Pleistocene units is not exposed in Gomez Pit, but can be seen in Yadkin Pit (App. D.1-2). It is not possible to estimate precisely the age of this unit from these extensively racemized samples. Instead, aminozone IIe, where exposed, serves as a base on which the late Pleistocene aminostratigraphic framework is built.

6.2.1: Evidence for reworked shells in Gomez Pit outcrops

Previous discussion in section 6.2 described evidence for one or more discontinuities or diastems in Gomez Pit outcrops. Data supporting these inferred breaks in

deposition include (1) lithologic evidence (pebble and cobble-sized lag deposits, lithofacies changes) and (2) that shells representing different aminozones coexist at or are adjacent to these apparent breaks in deposition. Amino acid data can be used to identify a disconformity or diastem, and also to infer timing of that break in deposition. To avoid ambiguity, there is a need to discuss the usage of the terms "disconformity" and "diastem" and the terms "reworked " and "transported".

Disconformity and diastem both refer to breaks in deposition, in which beds above and below the break are parallel. The distinction between disconformity and diastem is one of duration; the time represented by a diastem "involves only a brief interval of time" and is often "only deduced solely on paleontologic evidence" whereas a disconformity indicates erosion or non-deposition for "a significant interval of time", and is "usually marked by a visible and irregular or uneven erosion surface of appreciable relief" (terms in quotations from the Glossary of Geology, 3rd edition, 1987). Disconformities and diastems in coastal sequences result from non-deposition and erosion during low sea levels. The ability to distinguish a disconformity or diastem rests on the resolution of superposed interglacial deposits; the ability of amino acid enantiomeric data to resolve these deposits will be discussed in detail in section 6.6.

In the Gomez Pit outcrops located at UDAMS sites 06065, 06066 and 06067, a disconformity is inferred based on two features: cobble- and pebble-sized lag deposits coexisting in the same horizon as shells representing two aminozones, IIc and II d. Two stratigraphic options have been proposed for these exposures, each option specifying the relative timing of deposition of the IIc and II d molluscan shells (section 6.2). For example, Option 1 specifies that the older II d shells have been reworked (removed and redeposited) into a younger depositional unit containing in-place shells representing

aminozone IIc. In these discussions, the term "reworking" refers only to older shells found in a younger unit; the younger unit represents deposition during a subsequent high sea stand. In comparison, Option 2 specifies that IId shells are in-place, or have not been transported far from their source. In this usage, aminozone IId shells are not reworked into younger deposits; instead, IId shells define the uppermost boundary of a lithologic unit older than aminozone IIc. ESR data and uranium concentrations obtained from the IId shells in the IIc/IId horizon (Table 6-3, Appendix E) indicate that these shells have been removed from their original depositional environment. However, because the IId shells at sites 06065, 06066 and 06067 are stratigraphically below a well-defined stratigraphic unit containing shells from aminozone IIc (at other sections in Gomez Pit), the option of aminozone IId shells representing a lithologic unit must be considered.

In summary, reworked shells can be used to physically define a break in deposition. The use of reworked shell horizons to define the duration of a disconformity or diastem can be estimated from amino acid enantiomeric data, and also from other independent dating methods. In this study, attempts were made to obtain independent (ESR) age estimates for IIc and IId shells. Unfortunately, all IId shells at Gomez Pit appear to be transported, affecting the depositional and hence geochemical constraints necessary for ESR dating.

6.3: Aminostratigraphy of the Yadkin Pit and Norris Bridge Localities

Yadkin Pit and Norris Bridge localities were collected primarily to study diagenetic effects on amino acid data. These data expand the aminostratigraphic framework described at Gomez Pit, and also highlight conflicts between aminostrat-

framework described at Gomez Pit, and also highlight conflicts between aminostratigraphy and other dating methods.

Aminozones IIc and IIe are recognized at Yadkin Pit. A comparison of aminozone IIc data between Yadkin Pit and Gomez Pit shows statistically different ALLO/ISO values (Table 6-1). This difference is interpreted as a diagenetic effect, and will be discussed in detail in Chapter Eight. Previous analyses of Yadkin Pit molluscs using gas chromatographic methods yielded D/L leucine values that were consistent with aminozone IIc interpretation (defined at New Light Pit; Belknap, 1979, Fig. A50b, p. 466; Wehmiller *et al.*, 1988). Aminozone IIe is restricted to the late Pliocene Chowan River Formation as interpreted in Yadkin Pit by Blackwelder (1981a).

Only aminozone IIId is recognized at Norris Bridge. A comparison of aminozone IIId data among the Norris Bridge and Gomez Pit localities, and the Omar Formation as exposed at Dirickson Creek Ditch, DE and Chincoteague, VA show similar (ALLO/ISO)TOTAL and D/L leucine values (Table 6-1). The aminostratigraphic correlation among these sites will become important in the discussion of age options for aminozone IIId (section 6.6.3). Norris Bridge is one of few sites in region II where abundant, in-place, well-preserved molluscs representing aminozone IIId have been found. This site is also significant because uranium series and amino acid age estimates have been obtained from coral and mollusc fossils. Certain age estimates obtained by each of the dating methods are in conflict, and will be discussed in the following sections.

6.4: Calibration of ALLO/ISO Values in Southeastern Virginia

The amino acid racemization reaction is temperature-dependent. One way to place this aminostratigraphic framework into the context of time is through calibration of one or more aminozones using an independent dating method. Calibration of an aminozone "fixes" the curve defining racemization kinetics in time, thus enabling an estimate of numerical age from an ALLO/ISO value. Amino acid data are usually calibrated by uranium series analyses of corals that coexist with the molluscan fossils, and several uranium series analyses have been published from localities described in this study (Table 6-3, Fig. 6-4). In addition to these dates, age estimates have been calculated for mollusc samples using the electron spin resonance (ESR) dating method (Table 6-4).

6.4.1: Uranium Series Ages

Uranium series dating is based on the decay of parent uranium isotopes and concurrent growth of daughter products. The activity ratios of ^{230}Th to ^{234}U , and ^{231}Pa to ^{235}U are measured to determine age of a coral sample. The upper limit for age resolution using these nuclide pairs is 350,000 yrs ($^{230}\text{Th}/^{234}\text{U}$) and 150,000 yrs ($^{231}\text{Pa}/^{235}\text{U}$) (Ku, 1976). A third dating method is based on the disappearance of unsupported ^{234}U relative to ^{238}U . Sample age is calculated by comparing the $^{234}\text{U}/^{238}\text{U}$ value from a carbonate sample to the open ocean $^{234}\text{U}/^{238}\text{U}$ value of 1.15 (Ku, 1976). This technique is appropriate for older (up to 700,000 yrs) samples (Szabo, 1985). A detailed discussion of U-series systematics can be found elsewhere (Ku, 1976; Ivanovich, 1982).

Unrecrystallized corals can behave as a closed system with respect to U-series nuclides provided that void-filling contaminants containing detrital ^{230}Th and ^{231}Pa are removed (Ivanovich, 1982). Criteria used to evaluate U-series analyses include concordance of all three U-series dating methods, agreement of U-series ages with stratigraphic interpretation, and $^{230}\text{Th}/^{232}\text{Th}$ values > 20 , suggesting that post-depositional uptake of ^{232}Th and associated ^{230}Th is minimal (Ku, 1976).

Corals collected from the upper units of Gomez, New Light and Womack Pits (Table 6-2) consistently yield uranium series ages of approximately 70 ka, corresponding to Substage 5a of the deep-sea oxygen isotope record of Shackleton and Opdyke (1973). Although these ages are problematic when compared to global records of sea-level change, there is no geochemical evidence invalidating the results of these particular analyses. Use of these U-series dates for amino acid racemization calibration requires that aminozone IIa be defined as representing an age of 70 ± 5 ka.

LOCALITY	U-SERIES DATE (KA)	$^{230}\text{Th}/^{232}\text{Th}$
New Light Pit	74 +/- 4	25
Gomez Pit	79 +/- 5	24
Gomez Pit	69 +/- 4	31
Gomez Pit	67 +/- 4	20
Womack Pit	62 +/- 4	15

Table 6-2. Uranium series ages obtained from fossil corals collected from localities described in the text. Uranium series ages are calculated using decay of ^{234}U to ^{230}Th . The locations of corals collected from Gomez Pit are identified in Fig. 6-4. All dates are published in Szabo (1985).

6.5: Age Estimates Using the ESR (Electron Spin Resonance) Dating Method

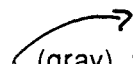
The ESR dating method is used to estimate age in a variety of geological samples, including fossil molluscs of Pleistocene age (e.g. Ikeya, 1981; Ikeya and Ohmura, 1983;

Radtke *et al.*, 1985; Millard *et al.*, 1988; Skinner, in press 1989). This method yields numerical ages (*c.f.* Colman *et al.*, 1988); however, many works combine ESR and uranium series methods to provide independent calibration of ESR age estimates. Theory and application of ESR techniques to Quaternary geology are reviewed in Hennig and Grün (1983).

The basis of ESR dating is that unpaired electron spin concentration increases linearly with time. Radioactive decay of U, Th and K in the shell and enclosing sediment and cosmic radiation results in damage to the crystal lattice of the sample. These resulting lattice defect sites are called paramagnetic centers, and can interact with a magnetic field. There is a linear increase in the number of paramagnetic centers with time until all crystal defects are saturated with unpaired electrons. The ESR signal is proportional to the number of paramagnetic centers, and represents the data from which age is calculated. A mathematical relationship between ESR age and background radiation is presented in Smart *et al.* (1988); a simplified version of this relationship is presented below:

$$\text{ESR Age} = \frac{\text{Accumulated Dose (rad)}}{\text{Mean Annual Dose (rad yr}^{-1}\text{)}}$$

where: Accumulated Dose (AD) = the radiation dose a sample has received since its formation. Also expressed in units of Gy

 (gray) where Gy=10⁻³ rad.

Mean Annual Dose = average radiation dose a sample receives per year.

The accumulated dose (AD) represents the "total concentration" of unpaired electrons trapped in a mollusc shell. AD measurements can show precision to 5% (Hennig and Grün, 1983); however, there is a developing body of literature which

describes optimum operating conditions of the ESR spectrometer with respect to mollusc samples, and considers different methods of ESR spectra interpretation (e.g. Molodkov, 1988; Katzenberger and Willems, 1988; Skinner, in press, 1989; Katzenberger *et al.*, in press, 1989). Standard methods for ESR spectrometric analysis of mollusc shells are still developing.

Calculation of the annual dose (*i.e.* rads yr⁻¹ "received " by the shell) consists of two components: (1) the external dose, representing the annual contribution resulting from radioactive decay of U, Th and K from enclosing sediments, and from cosmic radiation, and (2) the internal dose, representing the annual contribution resulting from radioactive decay of U, Th and K in the shell. To calculate external and internal dose components, U, Th and K concentrations are measured in both enclosing sediment and shell samples. If the fossil has been buried to a depth of several meters, the contribution of cosmic radiation to the internal dose is negligible.

Closed-system behavior of U, Th and K in both shell and sediment is intrinsic to accurate age estimates by the ESR dating method. In nature, closed-system behavior is not always the case. Molluscs in particular incorporate uranium throughout their burial history (Kaufman *et al.*, 1971). Several models describing post-depositional behavior of uranium in molluscs have been proposed, in the context of uranium series dating method (*e.g.* uranium trend dating; Szabo and Rosholt, 1969) and the ESR dating method (uranium uptake models, as discussed in Molodkov, 1988). Despite these attempts, it is still difficult to ascertain the timing of diagenetic uranium uptake in molluscs using their present day uranium and thorium elemental concentrations. If uranium uptake occurs during diagenesis of a late Pleistocene shell, the decay of incorporated ²³⁴U and ²³⁵U can result in an age assignment that is either too high or too low,

depending on the time of uranium incorporation. In light of the problems relating to uranium mobility in shells and sediment, Molodkov (1988) has suggested that present day uranium concentration in molluscs does not provide a reliable reflection of diagenetic behavior of uranium.

It has been estimated that 15% of the annual dose in molluscs is contributed by isotope decay within the mollusc shell (Molodkov, 1988); the remainder of the annual dose is contributed from sediments enclosing the shell. If a mollusc shell is removed from its original depositional environment, it becomes difficult to calculate an annual dose for the sample. Annual dose estimates will differ because the nuclide decay contributions vary with sediment type (*e.g.* sandy sediments, having lower uranium concentrations will contribute less to the internal dose). If the shell has been exposed, the contribution of cosmic radiation to the external dose becomes significant. Because it is difficult to assess the time spent by a reworked or transported shell in particular sedimentary environment, ESR age estimates are invalid if a sample has been displaced from its original depositional environment.

A qualitative example of the effect of shell transport on ESR age estimates can be inferred by comparison of ESR data obtained from in-place shells with data obtained from shells that may have been transported (sites 06065, 06066, 06031; Fig. 6-3, Table 6-3). ESR age estimates range from 93 ka to 125 ka for in-place molluscs; all valves showing (ALLO/ISO)TOTAL values typical of aminozone IIa. ESR age estimates of 220 ka and 262 ka were obtained from two in-place molluscs from the *Crassostrea* layer (UDAMS location 06062), and both valves showed (ALLO/ISO)TOTAL values typical of aminozone IIc. These ESR age estimates are in general agreement with amino acid racemization age estimates, and the comparison among dating methods will be

acid racemization age estimates, and the comparison among dating methods will be discussed further in Section 6.6.

In contrast, all ESR age estimates obtained from shells collected at 06065, 06066 and 06031 (IIc/II d horizon in Table 6-3) range from 86 to 136 ka, regardless of the (ALLO/ISO)TOTAL value. All ESR age estimates obtained from these particular samples are considered inaccurate in light of the physical evidence suggesting reworking or transport. Reworked/transported shells collected from the IIc/II d horizon do not show increasing ESR ages with increasing (ALLO/ISO)TOTAL values (Fig. 6-6a). These reworked/transported specimens also show increasing uranium concentrations with increasing (ALLO/ISO)TOTAL values, suggesting post-depositional uranium uptake has occurred in older valves (Fig. 6-6b). Post-depositional uranium uptake violates the closed-system assumption necessary for accurate estimation of age using ESR.

If the IIc/II d horizon does represent a disconformity or diastem, defined by reworked shells representing two aminozones, one particular sample (87GP-349A) is problematic. This sample shows an (ALLO/ISO)TOTAL value typical of aminozone IIa (0.189), and an ESR age estimate of 86 KA, yet this sample was collected from a stratigraphic position below aminozone IIa. By definition (section 6.2.1), this shell (87GP-349A) cannot be considered "reworked", since this older shell has not been redeposited into a younger unit. The presence of a shell from aminozone IIa at this lower stratigraphic level is probably the result of sampling error; sample 87GP-349A probably fell from the upper part of the section, and was sampled inadvertently.

SHELL SAMPLE	UDAMS LOC., LAYER	(ALLO/ISO)TOT, (AMINOZONE)	ESR AGE (KA) ESTIMATE
87GP-341A	06058, layer 2	0.155 (IIa)	93
87GP-342A	06058, layer 2	0.167 (IIa)	125
87GP-343A	06058, layer 2	0.151 (IIa)	101
87GP-344A	06058, layer 2	0.156 (IIa)	97
87GP-345A	06062, <i>Crassostrea</i>	0.328 (IIc)	220
87GP-346A	06062, <i>Crassostrea</i>	0.330 (IIc)	262
87GP-347A	06065, IIc/II d horizon	0.278 (IIc)	103
87GP-349A	06065, IIc/II d horizon	0.189 (IIa?)	86
87GP-351A	06066, IIc/II d horizon	0.353 (IIc)	111
87GP-352A	06066, IIc/II d horizon	0.308 (IIc)	136
87GP-353A	06066, IIc/II d horizon	0.311 (IIc)	118
87GP-135A	06031, IIc/II d horizon	0.510 (II d)	99

Table 6-3. Electron spin resonance age estimates and (ALLO/ISO)TOTAL values obtained from analyses of mollusc valves collected from Gomez Pit. Both techniques were performed on single mollusc valves or articulated valve pairs. Locations of mollusc valves used for ESR analyses are identified in Fig. 6-4. All ESR data from Skinner (in press, 1989); U, Th and K concentrations for most samples can be found in App. E.

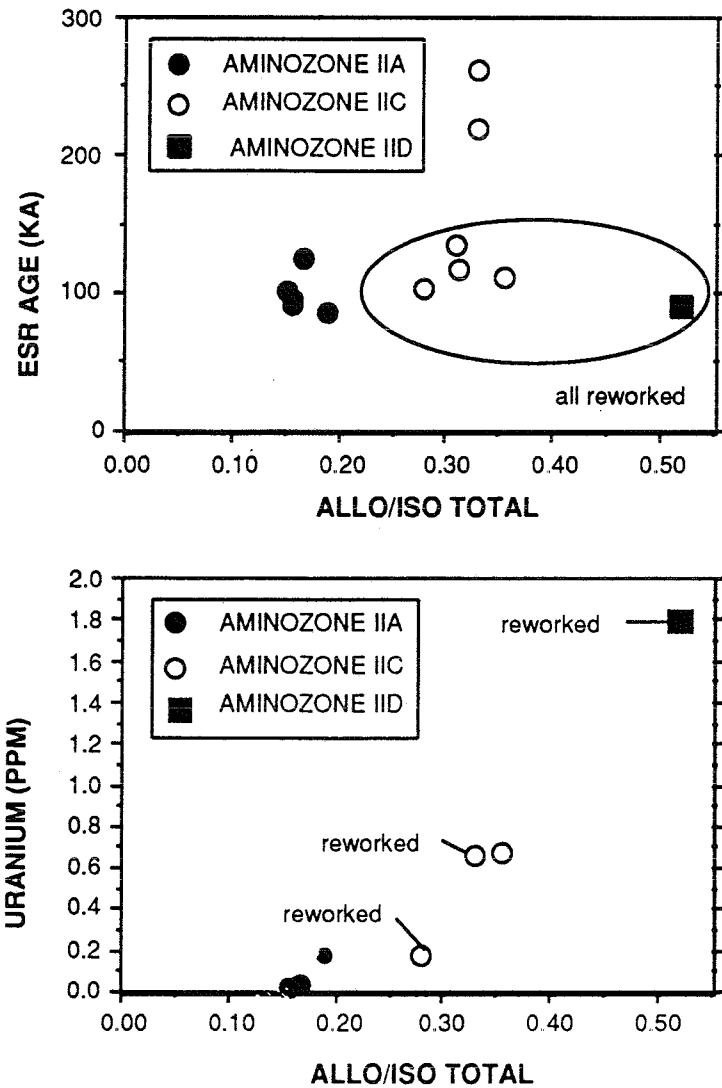


Fig. 6-6. A comparison of (ALLO/ISO)TOTAL values with ESR age estimates (a) and uranium concentrations (ppm; b) obtained from both in-place and reworked valves in Gomez Pit.

6.6: Age Options for Aminozones Defined in Southeastern Virginia

Dated, emerged coastal plain deposits are often interpreted in the context of the deep-sea oxygen isotope curve of Shackleton and Opdyke (1973), which provides a first-order approximation of sea levels during the Quaternary Period. Altitudes of paleo-shorelines on the coastal plain can also be compared to the uplifted terrace deposits dated by uranium series methods in New Guinea (Bloom *et al.*, 1974) and Barbados (Fairbanks and Matthews, 1978) which provide an independent record of high sea level events. These works provide a global perspective in which to interpret the high sea level record partially preserved in southeastern Virginia. All stratigraphic and geochronologic data discussed throughout the previous two chapters will be synthesized here, in order to propose reasonable age options for the aminozones in the context of global records of Late Pleistocene sea level change. A discussion of amino acid age estimates using a non-linear kinetic model of isoleucine epimerization will follow in Chapter Seven.

6.6.1: Aminozone IIa

Molluscs defining aminozone IIa at Gomez Pit coexist with corals yielding a mean uranium-series age of 70.2 ± 4 ka ($n=3$, mean of Gomez Pit analyses listed in Table 6-3). As discussed in section 6.3, these uranium-series ages are used to calibrate (ALLO/ISO)TOTAL values (approximately 0.14) that define aminozone IIa.

Aminozone IIa represents all or parts of several lithostratigraphic formations described in Chapter Five. Aminozone IIa encompasses the Norfolk Formation and the Kempsville Formation of Oaks and Coch (1973). Oaks and Coch (1973) interpreted a "major emergence" (or disconformity) between these two formations. No such discon-

formity is indicated from amino acid data because molluscs collected above and below their Norfolk Formation/Kempsville Formation contact (*c.f.* UDAMS locations 06058 and 06045, App. D.1-3 and Fig. 6-4) show similar (ALLO/ISO)TOTAL values. Later works (Mixon *et al.*, 1982; Peebles *et al.*, 1984; Spencer and Campbell, 1987) have interpreted the relationship between the Norfolk Formation and Kempsville Formation (or the equivalents defined in each stratigraphic framework) as conformable, and the contact between these two units represents a bio- or lithofacies change.

The Sedgefield Member of the Tabb Formation (Peebles *et al.*, 1984), as exposed at Gomez Pit encompasses both aminozone IIa and IIc. Apparently, two transgressive events are recorded in this single allostratigraphic unit (Wehmiller *et al.*, 1988).

The existence of approximate 70 ka uranium-series ages from emerged coastal plain deposits in southeastern Virginia remains problematic. It is difficult to reconcile aminozone IIa (at altitudes of 0 m to 10 m above present MSL) as representing Substage 5a, because all global models predict much lower sea levels at 70 KA. Sea level reductions of -15 m and -45 +/- 20 m (from present day sea level) are interpreted from dated terrace records in New Guinea (Bloom *et al.*, 1974) and Barbados (Fairbanks and Matthews, 1978), respectively. Although it is well known that deep-sea oxygen isotope curves contain both temperature and ice volume components, Chappell and Shackleton (1986) and Shackleton (1987) have taken a different approach by isolating the temperature component of oxygen isotope data, to better understand the ice volume (and hence sea level) record provided in deep-sea cores.

Although there is no consensus regarding a more precise estimate of Substage 5a sea level has been reached, all models imply that deposits of Substage 5a should not be

present at or above present MSL on stable coastlines. During the last 120 ka, only Substage 5e showed sea levels comparable to present MSL. To reconcile the Gomez Pit deposits with global sea level records, two scenarios have been proposed. Either late Pleistocene coastal plain deposits have been uplifted, or the uranium series ages are incorrect. Neither scenario has been accepted fully.

Pleistocene uplift of sedimentary units in the Atlantic coastal plain has been proposed by some workers and disputed by others. Cronin (1981) proposed that the mechanism of hydroisostasy can account for average uplift rates of 3cm/1000 yrs in the mid-Atlantic coastal plain, and therefore can broadly reconcile the altitude of these Substage 5a deposits with minimum estimates of sea level (*i.e.* -15m, from New Guinea terraces; Bloom *et al.*, 1974). In contrast, Peebles and Johnson (1984) find no geomorphic or structural evidence suggesting uplift during the Pleistocene in southeastern Virginia.

There is no geochemical evidence to invalidate the average age of 70 ka for Gomez Pit uranium series coral analyses. Mixon *et al.* (p. E14, 1982) speculated that these corals may have suffered post-depositional loss of thorium due to burial in permeable, detrital sediments. However, Szabo (1985) states that open-system conditions probably would not yield concordant ages from both $^{230}\text{Th}/^{234}\text{U}$ and $^{231}\text{Pa}/^{235}\text{U}$ methods.

If strata representing aminozone IIa are interpreted as representing deposition during Substage 5e (dated at approximately 120 ka), then the altitude of aminozone IIa is consistent with sea levels predicted for Substage 5e by the oxygen isotope curve (Shackleton, 1987). Colman and Mixon (1988) use this approach, and have tentatively

correlated deposits representing aminozone IIa on the southern Delmarva peninsula with oxygen isotope Substage 5e. In addition to these stratigraphic interpretations, ESR age estimates obtained from in-place IIa shells range from 93 ka to 125 ka (UDAMS location 06058, Table 6-3). These data represent the first geochemical indication that aminozone IIa records deposition during Substage 5e.

6.6.2. Aminozone IIc

Aminozone IIc has been interpreted to represent deposition during oxygen isotope stage 7 (Wehmiller *et al.*, 1988) using the non-linear model describing epimerization kinetics, loosely calibrated by the 70 ka uranium series coral analyses from aminozone IIa.

In Gomez Pit, the stratum that defines aminozone IIc consists of a 0.5 to 1m thick *Crassostrea* layer which shows (ALLO/ISO)TOTAL values of approximately 0.33. This layer has been included in the Norfolk Formation of Oaks and Coch (1973), Mixon *et al.* (1982) and Darby (1981); the Norfolk Member of the Acredale Formation of Spencer and Campbell (1987); and the Sedgefield Member of the Tabb Formation by Peebles *et al.* (1984). The disconformity between aminozones IIa and IIc (at the upper boundary of the *Crassostrea* layer) has not been recognized previously by lithostratigraphic methods.

As stated previously, the Sedgefield Member of the Tabb Formation (Peebles *et al.*, 1984) encompasses both aminozone IIa and IIc in Gomez Pit. It is possible that aminozone IIc can be correlated with the Shirley Formation (Peebles, 1984) although amino acid analyses from the type section of the Shirley Formation are required before this correlation is considered valid.

Independent age control for aminozone IIc is limited. An age of 187 ka +/- 20 ka has been obtained from uranium series analysis from a coral collected from Norris Bridge (aminozone IIc), and has been interpreted as representing deposition during oxygen isotope stage 7 (Cronin *et al.*, 1981; Szabo, 1985). For reasons discussed in section 6.6.3, this age estimate is rejected. ESR analyses of in-place molluscs from aminozone IIc (UDAMS location 06062, Fig. 6-4 and App. D.1-3) provide an age estimate of ca. 240 ka, consistent with Stage 7 interpretation.

The position of sea level during oxygen isotope Stage 7 is not well-defined. Estimates of sea level range from +30 m to -30 m MSL, based on terrace records from Barbados, Bermuda and New Guinea (summarized in Radtke, 1987). Shackleton (1987) compared $\delta^{18}O$ data among late Pleistocene interglacials and suggested that while Stage 7 sea levels are not well-defined, they probably did not reach levels as high as present day or Substage 5e.

Because calibration of Stage 7 is not widely available on the mid-Atlantic coastal plain, and sea levels are poorly understood during this interval, a Stage 7 age estimate for aminozone IIc is tentative. Aminozone IIc could be interpreted as representing Stage 9, and still be consistent with the non-linear model describing epimerization kinetics if aminozone IIa represents a Substage 5e high sea stand (Chapter Seven).

6.6.3: Aminozone IIc

Aminozone IIc has been interpreted to represent deposition during oxygen isotope Stage 11 or 13 (approximately 500 ka; Wehmiller *et al.*, 1988) using the non-linear model of epimerization kinetics, calibrated by the 70 ka uranium series coral analyses from aminozone IIa. In the mid-Atlantic coastal plain, IIc deposits are best observed at

the Norris Bridge site (App. D.1-2). The Norris Bridge site represents a major conflict between amino acid racemization and uranium series age estimates.

An age of 187 +/- 20 ka has been obtained from a coral collected at the Norris Bridge site (Szabo, 1985), and has been interpreted as representing oxygen isotope Stage 7. Because the Norris Bridge deposits are correlated with the Shirley Formation in southeastern Virginia (Peebles, 1984) and the Accomack Member of the Omar Formation (Mixon, 1985) using lithostratigraphic and geomorphic similarities, these correlative sites were also interpreted as representing oxygen isotope Stage 7 by Mixon *et al.* (1982).

(ALLO/ISO)TOTAL values for Norris Bridge, Dirickson Creek (Delaware; representing the Omar Formation, undivided) and Chincoteague (Virginia; representing the Accomack Member of the Omar Formation) all range between 0.42 and 0.47 (Table 6-1). These localities clearly indicate an aminozone older than IIc (characterized by ALLO/ISO values of approximately 0.33), and have therefore been assigned to aminozone IIId.

It has been difficult for workers to obtain reproducible data from corals collected from older stratigraphic units on the coastal plain. Considering uranium series analyses of a Norris Bridge coral sample, the $^{230}\text{Th}/^{232}\text{Th}$ value of 10.7 (Szabo, 1985) exceeds the guideline value of 20 used to distinguish post-depositional Th uptake (Ku, 1976). Multiple analyses of another coral sample from the Accomack Member of the Omar Formation (Szabo, 1985) shows excess ^{230}Th (relative to parent ^{234}U) in one trial. An age >340 ka has been inferred from uranium and thorium concentrations obtained in the second analysis of this Accomack Member coral sample (Szabo, 1985). In light of the

problems associated with dating corals in the range of 300-500 ka years, the analytical problems associated with the Norris Bridge and Accomack Member coral samples and the conflict of the 187 ka +/- 20 ka age with aminozone IId, a Stage 7 age estimate for aminozone IId cannot be accepted.

In Gomez Pit, molluscs showing (ALLO/ISO)TOTAL values of approximately 0.46 occur within a thin, discontinuous horizon directly beneath the *Crassostrea* layer at UDAMS locations 06065, 06066, 06067, 06031 and 06062. Because the spatial distribution of IId molluscs occurs within a discrete horizon directly beneath the *Crassostrea* horizon, and these IId molluscs are commonly associated with IIc molluscs and cobbles, two options have been proposed to explain the stratigraphic relationship of aminozone IId and coincident lithologic units (section 6.2).

The lithologic unit directly beneath the *Crassostrea* layer has been assigned to separate formation or member status in some stratigraphic frameworks. The Great Bridge Formation (Oaks and Coch, 1973) or the Great Bridge Member of the Acredale Formation (Spencer and Campbell, 1987) are both conformably overlain by the Norfolk Formation (or Member). The contact between the Great Bridge Formation (or Member) and the Norfolk Formation (or Member) is roughly coincident with the IIc/IId horizon (-4m to -8m below MSL). However, no significant passage of time is indicated at the contact between these two formations (or members) in either stratigraphic framework. Instead, the contact between these two units is interpreted as a biofacies (Spencer and Campbell, 1987) or lithofacies (Oaks and Coch, 1973) change.

Aminozone IId represents interglacial deposits that are older than those in aminozone IIc, because IId shells are characterized by higher (ALLO/ISO)TOTAL values,

and these shells are found with or stratigraphically below I1c shells. The question of which interglacial episode is represented by aminozone I1d remains. If aminozone I1d represents oxygen isotope Stage 11 or 13 (approximately 500 ka), then this aminozone will be difficult to calibrate independently because only the $^{234}\text{U}/^{238}\text{U}$ method of uranium series dating is valid in this age range.

6.6.4: Aminozone I1e

Aminozone I1e is characterized by nearly racemic (ALLO/ISO)TOTAL values. A mean (ALLO/ISO)TOTAL value of 1.06 has been calculated from samples from the Chowan River Formation, at its type locality (Colerain Beach; Fig. 1-2) on the Chowan River in North Carolina and from Chowan River Formation outcrops at Yadkin and Gomez Pits. Analyses from these four outcrops are generally reproducible, although 3 out of 14 samples show low (ALLO/ISO)TOTAL values. The Chowan River Formation has been interpreted as late Pliocene in age (Blackwelder, 1981a). Because these samples are extensively epimerized, no further age resolution is attempted.

There is some question about the stratigraphic relationship between Chowan River Formation and overlying Pleistocene units. The contact between the Chowan River Formation and Pleistocene units is not exposed in Gomez Pit. It will be useful in future studies to examine the stratigraphy in this "gap" between the Chowan River Formation and the Norfolk Formation, because this is where aminozone I1d is likely to be preserved.

6.7: Concluding Remarks

At present, the oxygen isotope curve obtained from deep-sea benthic foraminifera $\delta^{18}\text{O}$ values represents one way to estimate and compare late Pleistocene sea levels

along stable coastlines, where complete stratigraphic sequences are rarely preserved. Chappell and Shackleton (1986) and Shackleton (1987) have refined the original oxygen isotope curve of Shackleton and Opdyke (1973) by isolating a temperature component, to better understand the ice volume (and hence sea level) signal preserved in deep-sea cores. While no numerical estimates of sea level position (relative to present day) are proposed for stages older than Substage 5e, Shackleton (1987) noted that $\delta^{18}\text{O}$ values from Stages 1, 5e, 9 and 11 are similar, and were isotopically lighter than $\delta^{18}\text{O}$ values from Stages 7, 13, 15, 17 and 19. Shackleton (1987) suggested that this pattern reflects the magnitude of sea level rise for each interglacial, such that isotopically light interglacial episodes (*i.e.* having more negative $\delta^{18}\text{O}$ values) show higher sea levels. Apparently, excess ice remained during Stages 7, 13, 15, 17 and 19.

The hypothesis that only Stages 5e, 9 and 11 should be recorded on coasts experiencing low uplift rates may prove useful for the mid-Atlantic coastal plain. At present, late Pleistocene deposits of southeastern Virginia are believed by some to represent oxygen isotope Stage 5a (*e.g.* aminozone IIa at Gomez Pit) and Stage 7 (*e.g.* Norris Bridge unit and correlative Accomack Member of Omar Formation, and the Shirley Formation) largely on the basis of uranium series ages from Gomez Pit and Norris Bridge deposits. However, that these deposits are near present MSL is inconsistent with sea levels inferred from the oxygen isotope curve of Shackleton (1987) and dated terrace records.

In the following chapter, calibrated kinetic curves are used to calculate age from ALLO/ISO values. If a Substage 5e calibration (rather than Substage 5a) is used to calibrate aminozone IIa, age estimates for aminozone IIc and II d would become somewhat older (*i.e.* aminozone IIc would represent Stage 9 rather than Stage 7, and aminozone II d

would represent Stage 13). This revision would be consistent with the non-linear model, and also be in close agreement with the timing of interglacial deposition predicted by the oxygen isotope curve. This concept will be considered in greater detail in Chapter Seven.

Aminostratigraphic studies of the mid-Atlantic coastal plain have contributed to the understanding of Pleistocene sea levels in two ways. First, fossiliferous lithologic units of increasing relative age can be resolved in greater detail than has been described previously, using amino acid data. Second, now that lithologic units representing different interglacials are resolved, kinetic models of isoleucine epimerization provide one means of estimating age of Pleistocene deposits. The interpretation of each dated aminozone in the context of global models describing the chronology of sea level change during the Pleistocene is the subject of continuing work.

CHAPTER 7

AGE ESTIMATES FOR AMINOZONES DEFINED IN SOUTHEASTERN VIRGINIA USING THE NON-LINEAR MODEL OF ISOLEUCINE EPIMERIZATION

7.1: Introduction

In Chapter Six, the aminostratigraphy of Gomez Pit was presented, and age estimates based on other independent dating techniques (uranium series, ESR methods) and stratigraphic relationships were proposed. In this chapter, age estimates are calculated using the non-linear model of isoleucine epimerization (Wehmiller and Belknap, 1982; Wehmiller *et al.*, 1988; Boutin, 1989). Amino acid racemization age estimates calculated for interglacial deposits in southeastern Virginia will then be interpreted in the context of the deep-sea oxygen curve.

Age estimates can be calculated from amino acid data using a kinetic model which permits interpretation of ALLO/ISO values in the context of two variables: changing temperature during burial history, and changing rates of epimerization during diagenesis. A more extensive discussion of the non-linear kinetic models of leucine and isoleucine racemization and their development can be found in Wehmiller and Belknap (1978, 1982), Wehmiller (1982) and Boutin (1989).

7.2: Modeling Temperature History

An understanding of the temperature dependence of the epimerization reaction is

required in order to calculate age from ALLO/ISO values. Laboratory pyrolysis experiments using several molluscan genera (Hare, 1971; Bada and Schroeder, 1972; Mitterer, 1975; Keenan, 1982; Rahaim, 1987 and McCoy, 1987b) have defined a relationship between epimerization (or in the case of D/L leucine, racemization) rate and temperature (generally 60°C to 160°). Reaction rates defined at these higher temperatures can be extrapolated to lower temperatures using Arrhenius plots. Two modified Arrhenius equations describe the relationship between racemization rate and temperature in molluscan fossils:

$$(1) \quad \log k \text{ (yr}^{-1}\text{)} = 15.77 - 5939/T^{\circ}\text{K} \quad (\text{Bada and Schroeder, 1972})$$

or

$$(2) \quad \log k \text{ (yr}^{-1}\text{)} = 17.29 - 6417/T^{\circ}\text{K} \quad (\text{Mitterer, 1975})$$

Either of these equations can be used to calculate the racemization rate (k), and calculation using either equation agree within a few percent.

Terrestrial deposits of Pleistocene age have been subjected to fluctuating temperatures resulting from climate change. While it is difficult (if not impossible) to know precise temperatures of a deposit at any given time during burial history, the integrated effect of all temperatures during burial history can be modeled. The EQT (or Effective Quaternary Temperature) is a number that represents the effect of all temperatures endured by a molluscan fossil during its burial history (Wehmiller *et al.*, 1977; Wehmiller and Belknap, 1978, 1982). In order to model temperature history and calculate an EQT, both timing and intensity of temperature change must be determined. The timing of temperature change is estimated from the deep-sea oxygen isotope curve of Shackleton and Opdyke (1973). Intensity of temperature change can

be estimated from local paleoclimate data, including palynological and microfossil assemblages, interglacial sea surface temperatures proposed for oxygen isotope Stage 5e (CLIMAP, 1984) and full-glacial climate reconstructions proposed for the last 18 ka (COHMAP, 1988).

In calculating the EQT, the rate constant (k) is calculated for each temperature; this rate constant is then weighted to an extent dependent on the duration of each temperature estimated through burial history. Weighted average rate constants can be calculated from equation (1) or (2) at 5 ka intervals, facilitated by a Macintosh spreadsheet program written by John Wehmiller.

Two concepts underlie the use of EQT as a representation of temperatures during burial history. First, latitudinal temperature gradients during the past were similar to present latitudinal temperature gradients, as shown by current mean annual air temperature (CMAT; Wehmiller and Belknap, 1982). Second, terrestrial samples older than Substage 5e (125 ka) have experienced approximately equal proportions of warm interglacial and cold glacial climate, so the EQT will not change substantially after Stage 5e time. However, samples of Substage 5a age versus Substage 5e age cannot be interpreted in the context of the same EQT because younger Substage 5a deposits have endured a proportionally longer interval of cold climate (Wehmiller, 1982; Wehmiller *et al.*, 1988).

7.3: The Quantitative Non-Linear Model of Isoleucine Epimerization

The rate of epimerization of L-isoleucine to D-alloisoleucine does not follow first-order kinetics in molluscs and foraminifera. The pathway which describes changing

rates of epimerization consists of two linear segments of different slope, joined by a transition zone (Fig. 7-1).

Non-linearity of the kinetic pathway is most likely the result of two diagenetic reactions proceeding in molluscan shell organic matrix: epimerization of L-isoleucine to D-alloisoleucine, and hydrolysis of the protein to form free amino acids and polypeptides. The works of Kriausakul and Mitterer (1978; 1980a,b; 1983; 1984) have clarified the relationship between these two reactions. Changes in amino acid composition, and changes in distribution of amino acids between free and peptide-bound states over time will be considered in Chapter Eight.

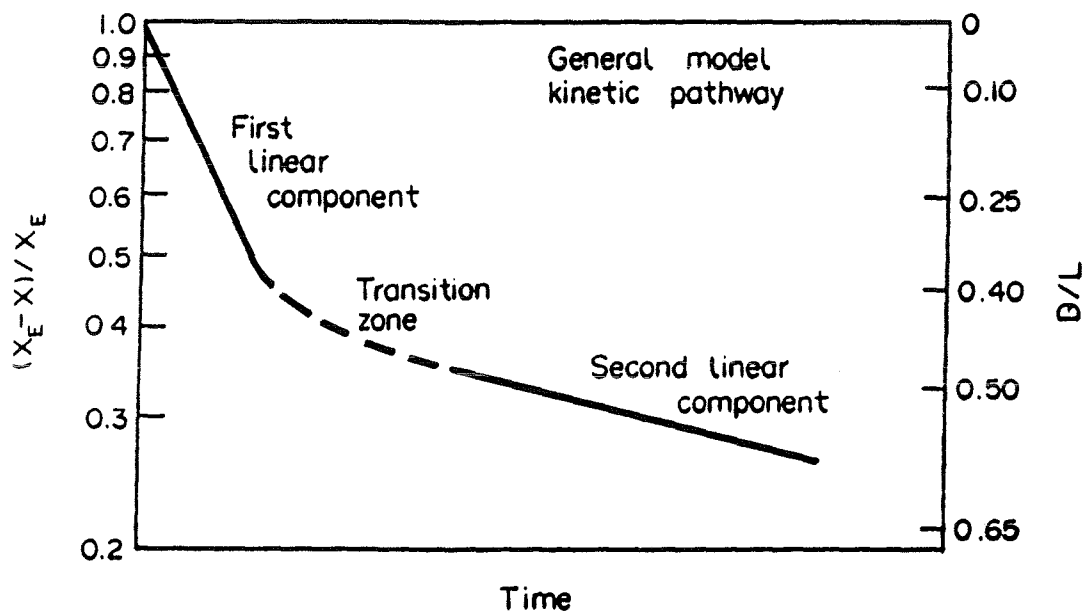


Fig. 7-1. The non-linear curve describing changing rates of the epimerization reaction over time. From Wehmiller (1986).

Molluscan shells hydrolyze, releasing lower molecular weight peptides and free amino acids. Kriausakul and Mitterer (1980a), using dipeptides and fossil *Mercenaria* showed that the extent of epimerization (as indicated by ALLO/ISO values) differs among free amino acids, interior amino acids within the protein chain, and terminal amino acids. Furthermore, free amino acids show the most extensive epimerization (*i.e.* the highest ALLO/ISO values) yet these high ALLO/ISO values do not correspond to a rapid epimerization rate for free amino acids, as determined in kinetic experiments. This observation led Kriausakul and Mitterer (1984) to propose a mechanism relating the epimerization and hydrolysis reactions in protein. In this mechanism, terminal amino acids epimerize at a greater rate than do interior and free amino acids. These extensively epimerized terminal amino acids are cleaved during hydrolysis, resulting in extensively epimerized free amino acids and polypeptides.

The equation which describes quantitatively the non-linear pathway for isoleucine epimerization, for each value of EQT is as follows:

$$(3) \quad y = a + b (\ln t),$$

where: $y = X_E - X$ and $X_E = \text{allo}/(\text{allo} + \text{iso})$ in total sample at equilibrium
 $X = \text{allo}/(\text{allo} + \text{iso})$ in total sample at time t
 a and b are constants

The value of X_E is determined using an equilibrium (ALLO/ISO)TOTAL value of 1.4, and has been calculated at 0.5833 (Boutin, 1989). Values for the constant a are unique for each EQT and molluscan genus (Appendix F). Values for the constant b have been determined from the venerid bivalve genera *Mercenaria*, *Chione*, and *Protothaca*,

all of which show essentially identical epimerization paths (App. F, this work, and Boutin, 1989). The constant b may also be taxon-dependent

When the age of one aminozone is known from an independent dating method, the age of a second aminozone can be estimated using equation (4), provided that both aminozones share a similar temperature history.

$$(4) \quad \frac{y_1}{y_2} = \frac{a + b (\ln t_1)}{a + b (\ln t_2)}$$

The values for y1 and t1 are from the calibrated aminozone, where t1 is known from an independent dating method. Equation (4) is solved for t2.

7.4: Amino Acid Epimerization Age Estimates for Aminozones IIc and II d in Southeastern Virginia

In the following discussion, age estimates are proposed based on a range of y1 values obtained from aminozone IIa (the calibrated aminozone), and y2 values obtained from either aminozone IIc or II d. Table 7-1 lists the maximum, mean and minimum (ALLO/ISO)TOTAL values for each aminozone, and the corresponding values of y. Age estimates are not calculated directly for aminozone IIa, because this aminozone (and the 70.2 ka uranium series coral date obtained from this aminozone) serves as calibration for older aminozones IIc and II d. It is important to note that a large range of (ALLO/ISO)TOTAL values exists for aminozone IIa; the %CV for aminozone IIa in Gomez Pit is 19.8% (Table 6-1). It is unlikely that the minimum (ALLO/ISO)TOTAL value shown for aminozone IIa (*i.e.* 0.087 in Table 7-1) is representative. As stated in section 3.4.1, lowest (ALLO/ISO)TOTAL values for aminozone IIa seem to reflect analytical difficulties, because these samples often accompany ILC-B standards also

showing low (ALLO/ISO)TOTAL values. Therefore, age estimates using minimum (ALLO/ISO)TOTAL (or y1) values for aminozone IIa are not preferred; these estimates are included for the sake of completeness.

	highest value		mean value		minimum value	
	(A/I)TOT	y	(A/I)TOT	y	(A/I)TOT	y
Aminozone IIa	0.198	0.712	0.141	0.758	0.087	0.863
Aminozone IIc	0.396	0.515	0.333	0.569	0.243	0.607
Aminozone IId	0.517	0.415	0.459	0.467	0.416	0.496

Table 7-1. Range of (ALLO/ISO)TOTAL values and corresponding y values for each aminozone defined in Gomez Pit. Age estimates presented in Table 7-2 are calculated using equation (4) and these data.

In section 6.6, age options for each aminozone were presented, based on stratigraphic and paleontological data for many sites in the mid-Atlantic coastal plain. In the following subsections, numerical age estimates calculated from amino acid data are presented. As discussed in section 6.6, the numerical ages of aminozones IIc and IId calculated using the non-linear kinetic model of isoleucine epimerization depend on the choice of calibration used for aminozone IIa. Uranium series coral ages indicate that aminozone IIa is approximately 70.2 ka. However, comparison of the stratigraphy of these aminozones with both the deep-sea oxygen isotope curve and lithostratigraphic record preserved in and around the southern Chesapeake Bay (Colman and Mixon, 1988) suggests that aminozone IIa is best reconciled with oxygen isotope stage 5e, dated at 120 ka. Therefore, age estimates for aminozones IIc and IId are presented, using either 70.2 ka or 120 ka calibration.

It is important to emphasize that a temperature history for an aminozone of 70.2 ka will differ from a temperature history for an aminozone of 120 ka. If aminozone IIa

is younger, it will have spent proportionally less time in warmer (early Stage 5) climate. Therefore, age estimates based on the 70.2 ka calibration for aminozone IIa must incorporate a colder EQT of 7° (and corresponding a and b constants in equation 3) than used for a 120 ka calibration, which is interpreted in terms of an EQT of 8° . Aminozones IIc and IId have been subjected to approximately equal durations of warm and cool climate, and are interpreted in terms of an EQT of 8° in this region.

7.4.1: Age Estimates Using Aminozone IIa Calibrated By 70.2 ka Mean Uranium Series

Date

y ₂ values from aminozone IIc	Calibrated values for y ₁ from aminozone IIa		
	maximum	mean	minimum
maximum	231	279	278
mean	196	196	193
minimum	154	153	153

y ₂ values from aminozone IIc	Calibrated values for y ₁ from aminozone IIa		
	maximum	mean	minimum
maximum	534	529	533
mean	381	381	381
minimum	314	316	316

Table 7-2. The range of age estimates (in ka) calculated for aminozone IIc (above) and aminozone IIc (below) in Gomez Pit using maximum, mean and minimum values of y₁ and y₂ as applied to the non-linear kinetic model of isoleucine epimerization. Aminozone IIa values are calibrated by the uranium series coral ages (mean equals 70.2 ka) obtained from Gomez Pit. All ages are calculated using an EQT of 7° for aminozone IIa, and an EQT of 8° for aminozones IIc and IIc (see section 7.4 for discussion). Best age estimates for each aminozone are highlighted.

7.4.2: Age Estimates Using Aminozone IIa Calibrated By Substage 5e (120 ka) High Sea Stand

y ₂ values from aminozone IIc	Calibrated values for y ₁ from aminozone IIa		
	maximum	mean	minimum
maximum	382	458	648
mean	278	340	396
minimum	222	277	414

y ₂ values from aminozone II d	Calibrated values for y ₁ from aminozone IIa		
	maximum	mean	minimum
maximum	668	797	1.054
mean	506	599	819
minimum	427	510	712

Table 7-3. The range of age estimates (in ka) calculated for aminozone IIc (above) and aminozone II d (below) in Gomez Pit using maximum, mean and minimum values of y₁ and y₂ as applied to the non-linear kinetic model of isoleucine epimerization. Aminozone IIa values are calibrated hypothetically by the age of the oxygen isotope substage 5e high sea stand. All ages are calculated using an EQT of 8°. Best age estimates for each aminozone are highlighted.

7.5: Summary

If aminozone IIa at Gomez Pit is calibrated by the mean uranium series age of 70.2 ka, then the resultant age for aminozone IIc ranges from 153 ka to 231 ka. This age range coincides with that of oxygen isotope stage 7, and overlaps with the two ESR age estimates of 220 ka and 262 ka (Table 6-3) obtained from in-place shells from aminozone IIc in Gomez Pit. The age estimate for aminozone IIc at Yadkin Pit (mean y_2 of 0.647) is calculated as 119 ka. This age estimate is substantially younger than aminozone IIc shown elsewhere in southeastern Virginia. The apparent age of the Yadkin Pit samples is believed to represent the effects of diagenetic leaching, and this factor will be discussed in Chapter Eight.

Using the same calibration, the age estimate for aminozone II d at Gomez Pit ranges from 316 ka to 534 ka, corresponding to oxygen isotope stages 9, 11 or 13. The wide range in ages for aminozone II d in Gomez Pit reflects the wide range in ALLO/ISO values obtained from these particular samples, and this point will be considered in detail in Chapter Eight. Based on mean ALLO/ISO values for Gomez Pit aminozone II d, the preferred age range for this unit is either oxygen isotope stages 11 or possibly 13. The age estimate for aminozone II d at Norris Bridge (mean y_2 value of 0.449) is calculated as 427 ka, corresponding to oxygen isotope stage 11.

If aminozone IIa at Gomez Pit is calibrated by the age of oxygen isotope substage 5e high sea stand (120 ka), then the resultant age for aminozone IIc ranges from 340 ka to 414 ka, corresponding to oxygen isotope stages 9 or 11. Similarly, the age estimate for aminozone IIc in Yadkin Pit is calculated as 222 ka.

Using a 120 ka calibration, the age for aminozone IId at Gomez Pit ranges from 599 ka to 712 ka, corresponding to oxygen isotope stages 15, 17 or 19. The age estimate for aminozone IId at Norris Bridge is calculated as 660 ka, corresponding approximately to oxygen isotope stage 19. It should be noted that the age estimate of aminozone IId at Norris Bridge and correlative localities is constrained by magnetostratigraphic data. The normal magnetic polarity signature of the Norris Bridge sediments suggests an age younger than the Brunhes-Matuyama boundary, dated at 760 ka. Therefore, amino acid age estimates for aminozone IId that exceed 760 ka (Table 7-3) should be considered inaccurate. Fig. 7-3 summarizes the age estimates based on amino acid data (using both 70.2 ka and 120 ka calibrations) and compares these age estimates with the chronology of the oxygen isotope curve.

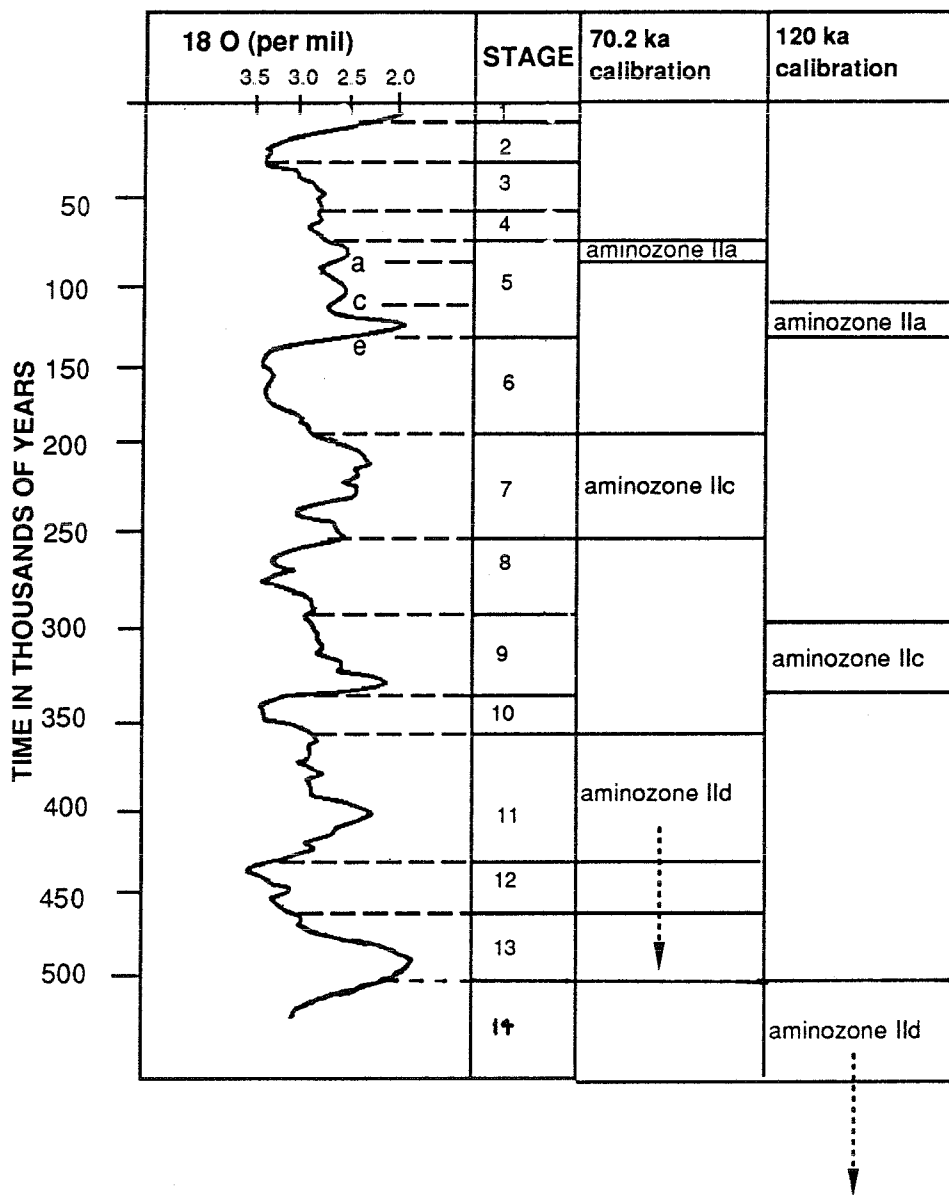


Fig. 7-2. Relationship between the oxygen isotope curve and age assignments for aminozones defined in southeastern Virginia. Amino acid age estimates are determined by calibration of aminozone IIa by either uranium series coral ages (70.2 ka) or the age of oxygen isotope substage 5e high sea stand (120 ka).

CHAPTER 8

DIAGENETIC MODIFICATION OF MOLLUSC SHELL: ANALYSIS OF AMINO ACID COMPOSITION, ELEMENTAL CONCENTRATIONS, MINERALOGY AND TEXTURES IN LATE CENOZOIC MOLLUSCS

8.1: Introduction

The use of well-preserved fossils is usually a prerequisite for amino acid studies to ensure the highest possible analytical precision. In this study, mollusc fossils exhibiting a wide range of preservational characteristics were chosen specifically to correlate differences in shell chemistry with degree of preservation; the goal of this study is to define chemical criteria on which amino acid data can be evaluated. The effects of protein hydrolysis and subsequent leaching of amino acids may affect amino acid composition and hence the precision of the amino acid racemization dating method. With the development of criteria to recognize the effects of these diagenetic processes, it may be possible to quantify the effects of leaching as a function of shell condition, or of time. The majority of molluscs used in this study were analyzed for amino acid concentrations (HPLC) and Sr, Fe, Mn and Ca (AAS) to detect subtle diagenetic change in both organic matrix and shell carbonate. Selected specimens were also observed by scanning electron microscopy (SEM) and used in the weight gain/loss experiments to observe physical changes in shell structure with condition or with time. Laboratory methods for each technique are described in Chapters Two and Four. The results and interpretations of each technique follow in this chapter.

Considering amino acid data, it seems reasonable to expect that a relationship exists between the structural integrity of the mollusc shell and its amino acid composition. Weiner and Hood (1975) hypothesize that an amino acid sequence of -ASP-(dipeptide)-ASP- at least partially defines a nucleation site for CaCO₃ in molluscs. Their work has shown that a space defined by the -COO- groups of ASP in the peptide chain is very similar to Ca²⁺-Ca²⁺ interatomic distance in the CaCO₃ lattice. Hydrolysis of the peptide chain near the nucleation site can conceivably result in diagenetic decalcification of the mollusc shell. To date, diagenetic effects on amino acid data have been investigated on foraminifera (Müller, 1984) and mollusks (Weiner and Hood, 1975; Weiner and Lowenstam, 1980; Rahaim, 1986; Boutin, 1989).

Considering Sr concentration data, several works have shown increased Sr concentrations and Sr/Ca values in single aragonitic mollusc genera over time (Pilkey and Goodell, 1964; Ragland *et al.*, 1969; Estes, 1972). Initially, increased Sr content and Sr/Ca values in older Cenozoic mollusks was interpreted as evidence of biochemical evolution (Hallam and Price, 1966). However, subsequent work focused on Sr/Ca variations resulting from post-depositional alteration of mollusc shells (Schroeder, 1969; Srivastava, 1975; Walls *et al.*, 1977; Ragland *et al.*, 1979) or the relationship between Sr/Ca in skeletal carbonates to their surrounding aqueous environment (Kinsman and Holland, 1969; Burchard and Fritz, 1978; Baker *et al.*, 1982). The use of Sr/Ca values of carbonate fossils as indicators of paleosalinity or paleochemistry shows some promise because Sr distribution coefficients between shell carbonate and seawater are well-established (Lorenz and Bender, 1980; Graham *et al.*, 1982; Chivas *et al.*, 1985).

SEM is commonly used to observe microstructural alteration resulting from taphonomic processes. While the effects of dissolution, leaching, abrasion and boring are clearly evident in Quaternary molluscs (section 8.2.2, this work; Benamy, 1980; Walker, 1979), the effect of these destructive processes can also be observed in modern bivalves present in Ca^{2+} -undersaturated bottom- or pore-waters (Alexandersson, 1979; Lewy, 1981; Aller, 1982). Additionally, endolithic organisms such as sponges (Driscoll, 1970), gastropods (Carriker, 1978; Poulicek, 1986), fungi (Jones and Pemberton, 1986) and macrophytes (Lukas, 1979) degrade shell structure through the burial process. The extent of physical degradation of shell structure cannot be considered time-dependent, but can define a classification based on quality of shell preservation.

The final technique used to investigate shell condition involves a measurement of void volume (or porosity) in shell fragments of differing condition. Increased porosity, measured as the weight of water gained by a shell fragment after soaking, can suggest greater susceptibility of a shell to leaching. This simple measurement of void volume within a shell may also be used to define shell condition.

8.2: Definition of Shell Quality

Before analysis, all mollusc valves were assigned a subjective grade of excellent, good, fair or poor based on the physical appearance of the mollusc. The premise of these assignments is that of a field geologist choosing mollusc samples from outcrop for future analysis. Ideally, one would choose the best preserved samples, although these samples may not always be available. Table 8-1 and Figure

8-1 compare these physical criteria among excellent, good, fair and poor samples collected from all aminozones.

Degradation of shell integrity is not solely a function of time. All grades of shell were found in aminozone IIa in Gomez Pit, and this population of shells serves as the primary test of amino acid variation with shell condition. However, in the older aminozones at Gomez Pit, it was not possible to find shells exhibiting excellent characteristics. These samples tended to be of lesser quality, and most showed very similar (fair or poor) preservational characteristics. In contrast, molluscs from aminozone IIc at Norris Bridge were unusually well preserved. Preservation of shells in the older units seems related to the enclosing sediment type. If groundwater flows readily through coarser grained sediments, shells are poorly preserved. In contrast, the Norris Bridge shells are preserved in an estuarine silt; the water table is perched above this unit, possibly resulting in reduced groundwater flow through the fossiliferous unit and thus better preservation of these older shells.

EXCELLENT CONDITION

Hinge ligament present
Natural tan coloration present
No borings by molluscs, *Cliona*
No pitting of surface (prismatic) layer
No staining by Fe oxides or pyrite
Growth lines may show relief
Shell does not flake apart when cut
Interior usually nacreous

FAIR CONDITION

Hinge ligament may be partially present
Shell has lost all natural coloration
Shell shows limited boring
Pitting on shell interior or exterior
Outer prismatic layer mostly intact
Staining may be extensive
Growth lines show varying relief
Shell may flake apart when cut
Interior and exterior may be chalky

GOOD CONDITION

Hinge ligament usually present
Coloration begins to fade to white
No borings by molluscs, *Cliona*
No pitting of surface (prismatic) layer
Little or no staining by Fe oxides or pyrite
Growth lines may show relief
Shell does not flake apart when cut
Interior is rarely nacreous

POOR CONDITION

Hinge ligament usually absent
Shell has lost all natural coloration
Obvious boring by *Cliona*, epibionts
Shell shows extensive pitting
Outer prismatic layer mostly removed
Staining may be extensive
Interior and exterior are chalky
Shell may flake, or is friable
Interior and exterior usually chalky

Table 8-1. Characteristics defining subjective grades of shell preservation used in this study.

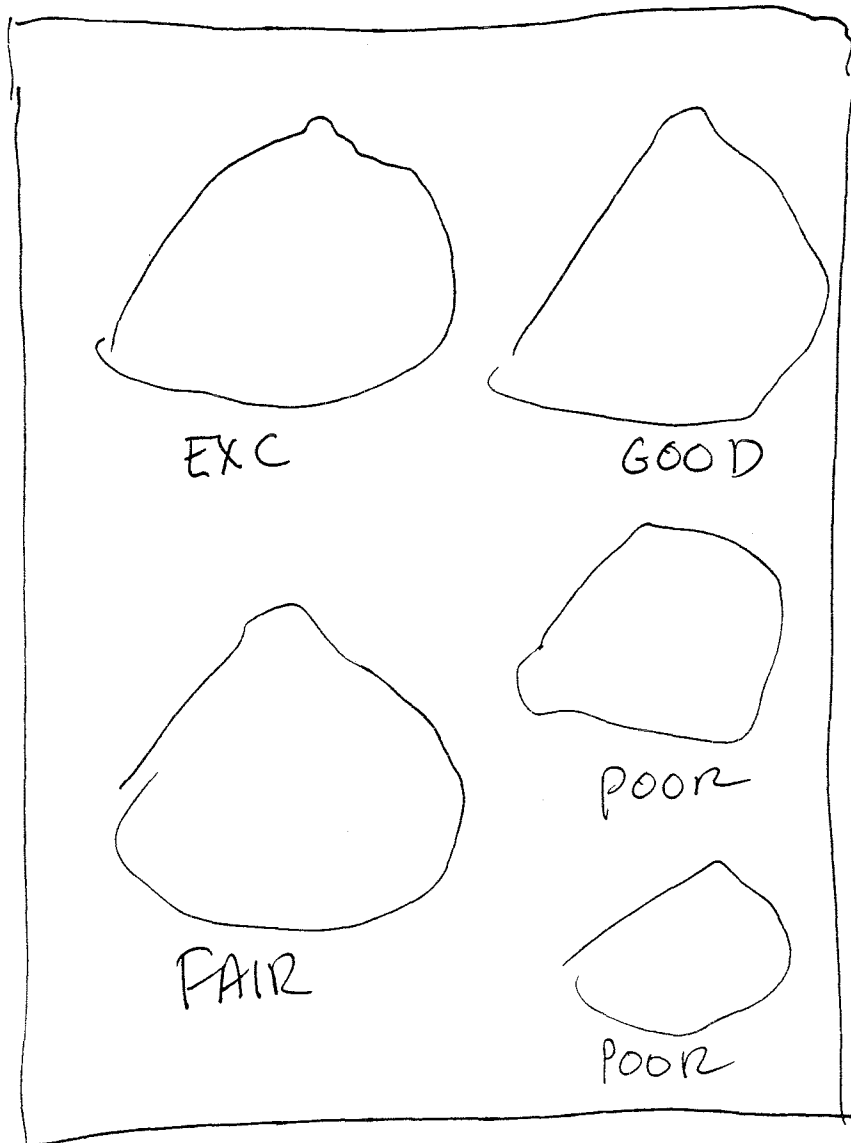


plate in the making.

Fig. 8-1. Examples of shell qualities used in this work. Samples 85GP-153B (excellent), 84GP-141B (good), 85GP-163B (fair), 85GP-259B and 85YP-189B (both poor) are shown.

8.2.1: Relationship Between Shell Condition and Shell Porosity: Water Weight Gain/Loss Experiments

Simple measurements of water weight gain by soaking, and water weight loss by heating were performed on representative shell fragments to provide an approximate measure of shell porosity. Apparent porosity is defined here as representing the void volume in a shell fragment available for contact with water. Shells having greater porosity also have greater exposed surface area, and would be the best samples to show the effects of leaching on amino acid and elemental composition.

In this study, only selected specimens were used in the water weight gain/loss experiments, representing the range of conditions found in aminozone IIa. Because weight gain/loss measurements were not performed on each shell used for this study, one is not able to correlate apparent porosity with either amino acid or element data. However, a qualitative relationship exists between apparent porosity and shell condition; lesser quality shells consistently show greater apparent porosity. Therefore, the criteria used to grade shells by visible condition (Table 8-1) are appropriate physical characteristics for recognizing the effect of leaching in mollusc shells.

In both long- and short-term weight gain/loss experiments, raw data obtained from weighings were normalized by conversion to % change from initial weight (or apparent porosity), enabling a comparison among shell fragments of different size. A comparison of modern shell with two shells from aminozone IIa (excellent and poor condition) shows that a fossil shell (aminozone IIa) in excellent condition resembles a modern shell with respect to apparent porosity; however, a poor quality fossil shell of the same age shows at least three times apparent porosity. Also, carbonate is lost

during the experiment, indicated by the general downward slope of the weight change curve.

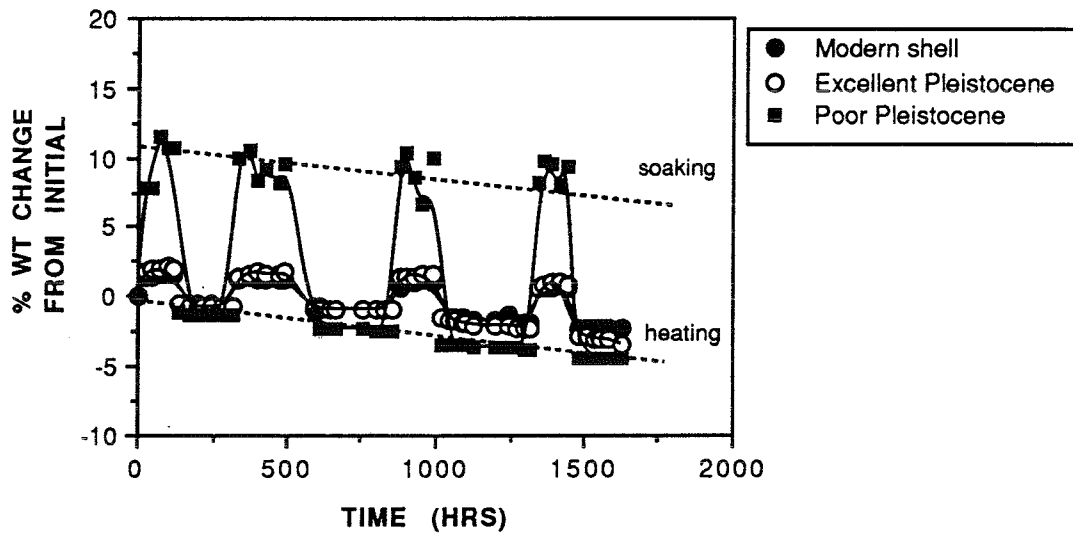


Fig. 8-2. Comparison of % weight change from initial weight in the long-term (2 month) water weight gain/loss experiment. Shells used in this experiment were modern *Mercenaria* (86L-319); a specimen from aminozone IIa showing excellent condition (85GP-260A, A/I total 0.095) and a shell from aminozone IIa showing poor condition (85GP-241A, A/I total 0.141).

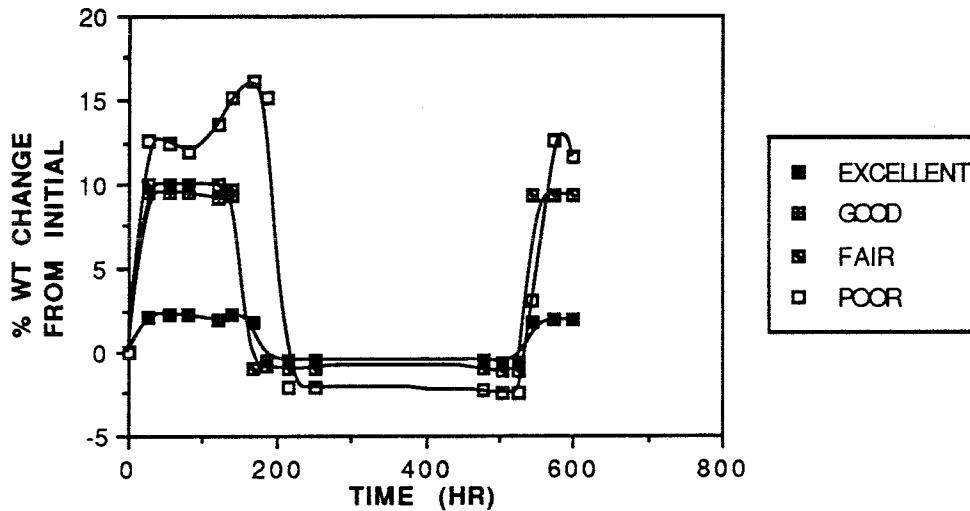


Fig. 8-3. Comparison of % weight change from initial weight in the short-term (approximately one month) experiment. All grades of shell condition in aminozone IIa are represented: excellent condition (85GP-153A, A/I TOTAL 0.114); good condition (85GP-141A; shell broke apart after 250 hours, A/I TOTAL 0.134); fair condition (85GP-183A, A/I TOTAL 0.198); poor condition (85GP-182A, A/I TOTAL 0.113).

A comparison of apparent porosities (% weight change from initial) among all shell conditions from aminozone IIa is shown in Fig. 8-3. This figure shows the differences in apparent porosity among conditions, especially at the extremes of excellent versus poor condition. Both of these figures show that weight gain measurements, used as a qualitative estimate of shell porosity, correlate well with shell condition. Lesser quality shells show greater porosity, and shells having greater porosity are likely to be leached. Therefore, shell quality (as defined in section 8.2) does serve as an adequate context in which to judge the chemical effects of leaching.

The relationship between shell age and shell porosity cannot be discerned clearly. The only shell condition common to all aminozones is "poor", and % weight change from these poor-quality specimens ranges from 7% to 18%. There is no increase in apparent porosity with age in these specimens.

8.2.2: Relationship Between Shell Age and Shell Microtextures: SEM Observations

Previous work has focused on alteration the prismatic structures in *Mercenaria* (*i.e.* the structures which compose the outermost layer of the shell; Fig. 8-4) as an indicator of diagenetic alteration (Benamy, 1980). An attempt was made in this work to discern diagenetic textural change in the structures found in the homogeneous layer of *Mercenaria* (*i.e.* the dense, lamellar layer found in shell cross-sections) as a function of condition, since this is the region of the shell that is routinely sampled for amino acid analyses. Unfortunately, this region of the shell is difficult to work with using SEM because crystalline components of the homogeneous layer are not clearly defined. Consequently, it was not possible to define clearly a

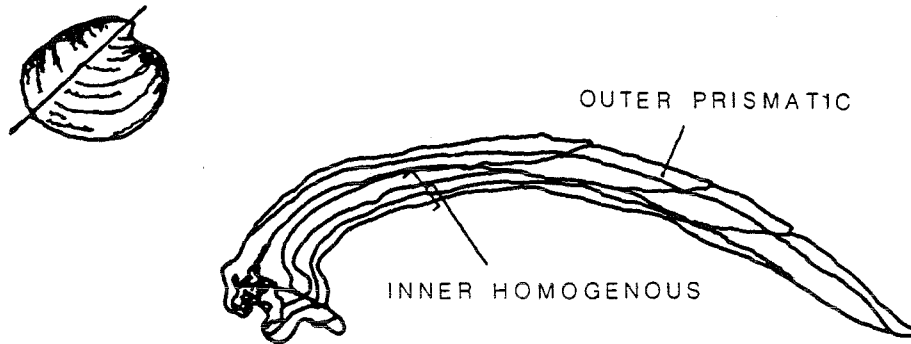
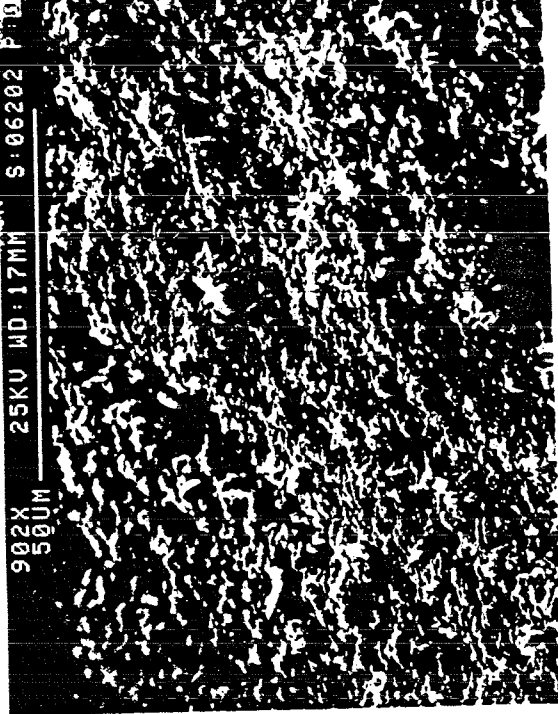


Fig. 8-4. Diagrammatic cross-section of *Mercenaria* , showing the location of outer prismatic, and homogeneous layers in the shell. Redrawn from Kennish (1980).

relationship between structural degradation with lesser shell quality in aminozone IIa.

A commonly occurring feature of lesser quality shells is their tendency to flake apart along lamellae. These lamellae represent regions of incremental growth, although the time represented by these increments can vary (Kennish, 1980). Microstructural evidence suggests that carbonate dissolution (accompanied by removal of organic matrix) occurs preferentially on the margins of shell lamellae, resulting in a plane of weakness along which shells can flake apart (Fig. 8-5). The specimens shown in Fig. 8-5 occur in aminozones IIa (85GP-186A) and II d (85GP-321A), and also represent "good" and "poor" grades of shell condition, respectively.



85GP-186A Ammonoite 11a
good condition



87GP-321A Ammonoite 11d
poor condition

Fig. 8-5. Photomicrographs of lamellar features in the homogeneous layer of *Mercenaria*. Shown here are samples 85GP-186A (aminozone 11a, good condition, A/I TOTAL 0.172; left) and 87GP-321A (aminozone 11d, poor condition, A/I TOTAL 0.492). See text for discussion.

Removal of organic matrix represents one example of textural change by leaching. Estes (1972) also suggests that the boundary between the outer prismatic layer and the homogeneous layer in Mercenaria is a pathway through which water can travel.

8.3: A Generalized Model of Diagenetic Hydrolysis and Epimerization

The relationship between the amino acid epimerization reaction and protein hydrolysis has been qualitatively established, and is discussed in section 7.3. The following points summarize this relationship. First, epimerization rate depends on the position of an amino acid in the protein chain. Epimerization rate decreases as follows: terminal amino acid rate > interior amino acid rate > free amino acid rate.

Second, protein hydrolysis exerts a rate-controlling function on the epimerization reaction. As protein hydrolysis proceeds early in diagenesis,

High molecular weight protein \longrightarrow low molecular weight polypeptide \longrightarrow free amino acid

and a greater proportion of terminal amino acids appear in the low molecular weight polypeptide state. These terminal amino acids racemize relatively rapidly, and are then cleaved to the free form.

Protein hydrolysis probably begins very early in the burial process (Kriausakul and Mitterer, 1980). The most labile peptide bonds are hydrolyzed, yielding a population of polypeptide fragments of varying molecular weight. This early diagenetic stage is marked by a relatively rapid apparent isoleucine epimerization rate (Fig. 7-1). At some point, hydrolysis of the labile peptide bonds is complete. A

population of hydrolysis-resistant polypeptide fragments remain, and this later diagenetic stage is marked by slower apparent isoleucine epimerization rate.

It is important to distinguish between actual and apparent epimerization rates when considering the diagenetic reactions of mollusc shell proteins (*c.f.* Lajoie *et al.*, 1980). The actual isoleucine epimerization rate of terminal, interior or free amino acids is not necessarily equal to the apparent rates of epimerization shown by ALLO/ISO values in the free, total or bound (found by difference, total minus free) samples. Figure 8-6 summarizes the diagenetic pathway resulting from both epimerization and hydrolysis reactions occurring in mollusc shell amino acids.

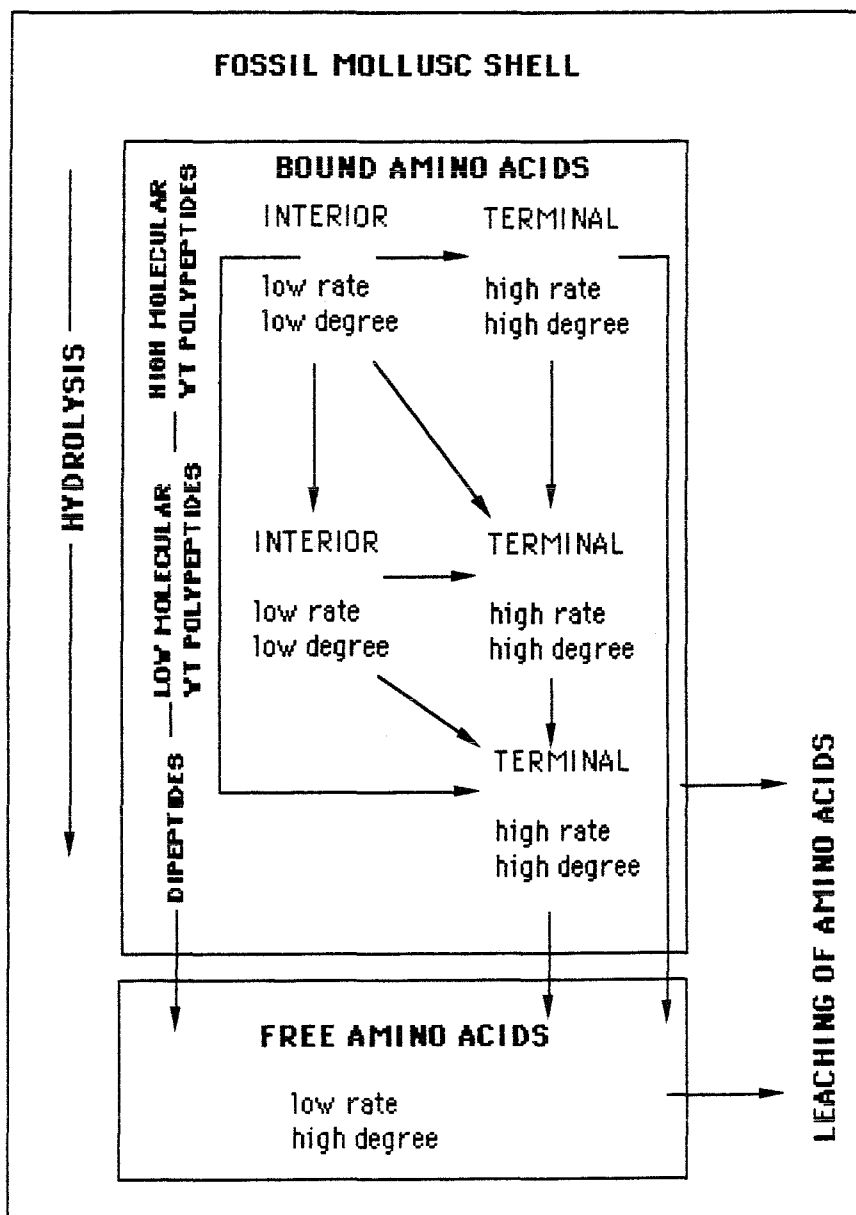


Fig. 8-6. Diagenetic processes of epimerization, protein hydrolysis and amino acid leaching in mollusc shell. Redrawn from Boutin (1989).

8.4: Toward a Leaching Model for Molluscan Shell Amino Acids

Removal of amino acids from fossils during burial has been recognized, but the process remains unquantified. Those works that do recognize leaching as a significant diagenetic process do so either by definition of a "leaching index" molecule or ratio, or through comparison of amino acid composition between modern and fossil shell.

γ -Carboxyglutamic acid has been used as an indicator of leaching intensity in fossil bone samples (King, 1978; King and Bada, 1979). γ -Carboxyglutamic acid is found in non-collagenous protein of modern bone samples, and its concentration in modern bone decreases as a function of leaching time in laboratory experiments (King, 1978). γ -Carboxyglutamic has not yet been observed in fossil molluscs.

Weiner and Lowenstam (1980) have used the ratio of glycine to alanine (GLY/ALA) in the nondialyzable (>12,000 mw) fraction of several types of molluscs as an indicator of diagenetic change in the organic matrix. Lower GLY/ALA values seem to characterize better preserved specimens, although no mechanism was proposed for this phenomenon.

Another approach used to determine the extent of amino acid loss is by comparison of amino acid abundances between modern and fossil genera. Hare and Mitterer (1969) and Hare *et al.* (1975) compared amino acid distribution in total, free and bound (total minus free) samples of *Mercenaria* among modern, Pleistocene and Miocene age shells. Their comparison shows that a considerable portion of the amino acid content has been lost by Pleistocene time. The Gomez Pit data set (Fig. 8-7) when averaged, shows that amino acid abundances in total samples from each aminozone have decreased substantially when compared to modern concentrations.

Free amino acid concentrations increase to a point, then slowly decrease. By aminozone Ila time, 57% of all amino acids have been lost, and the free amino acids account for about one quarter of the total sample concentration. Total sample abundances in older aminozones IIc and II d show that ca. 70% of the amino acids have been lost, and free amino acids account for about half of the total sample. Total sample amino acid abundances in aminozone IIe (Pliocene) have decreased 79% from modern samples, and free amino acids account for 39% of total sample concentration. It should be noted that these percentages are only approximate due to large standard deviations about each mean concentration value.

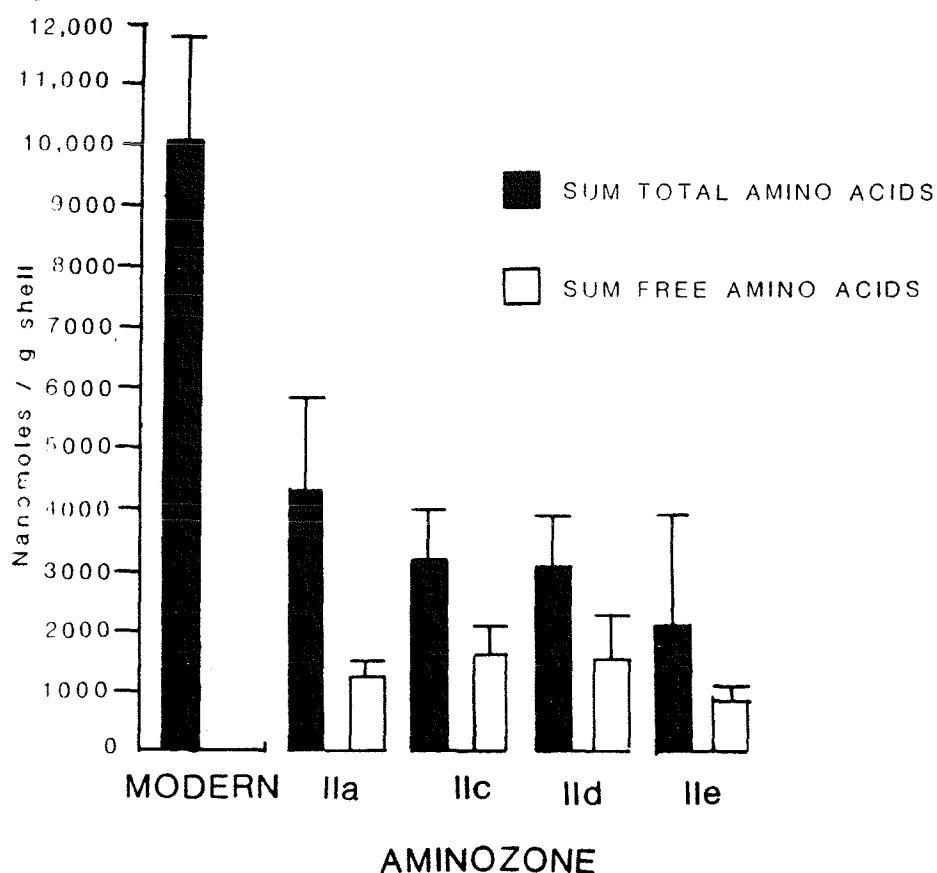


Fig. 8-7. Amino acid abundances for free and total samples for all aminozones in Gomez Pit. Histogram shows mean values and standard deviations for total and free amino acid concentrations (nanomoles/g shell) of all aminozones in Gomez Pit.

It is most important in these studies is to quantify the effect of leaching on isoleucine epimerization. Müller (p. 35, 1984) describes the effect of leaching on ALLO/ISO values of planktonic foraminifera, stating that "... as leaching selectively removes the most extensively epimerized [free ALLO] isoleucine fraction it lowers the total ALLO/ISO ratios.". Certain comparisons within the Gomez Pit, Yadkin Pit and Norris Bridge data sets support this hypothesis.

8.5: Variations in Amino Acid Composition with Condition

Three data subsets were examined for differences in amino acid composition with condition: aminozone IIa in Gomez Pit (8.5.1); aminozone IIc at Gomez Pit and Yadkin Pit (8.5.2); and aminozone IId at Gomez Pit and Norris Bridge (8.5.3). The data set for aminozone IIa had the largest population of samples (n=60 before removal of outliers) although the number of samples was not distributed equally among all conditions (excellent, n=13; good, n=18; fair, n=18; poor, n=11; App. G). Because not all shell conditions were represented in Gomez Pit aminozones IIc and IId, the Yadkin Pit and Norris Bridge sites were used for comparison. The Yadkin Pit samples cannot be correlated directly to Gomez Pit aminozone IIc using ALLO/ISO total values. However, if the leaching of amino acids proceeds as described by Müller (1984), then Yadkin Pit molluscs represent leached examples from aminozone IIc.

8.5.1: Gomez Pit Aminozone IIa

Amino acid concentrations and fractions from each shell quality in aminozone IIa are shown in histogram form (Figs. 8-8, 8-9; Appendix G). The following general conclusions can be drawn from the distributions of amino acids in aminozone IIa

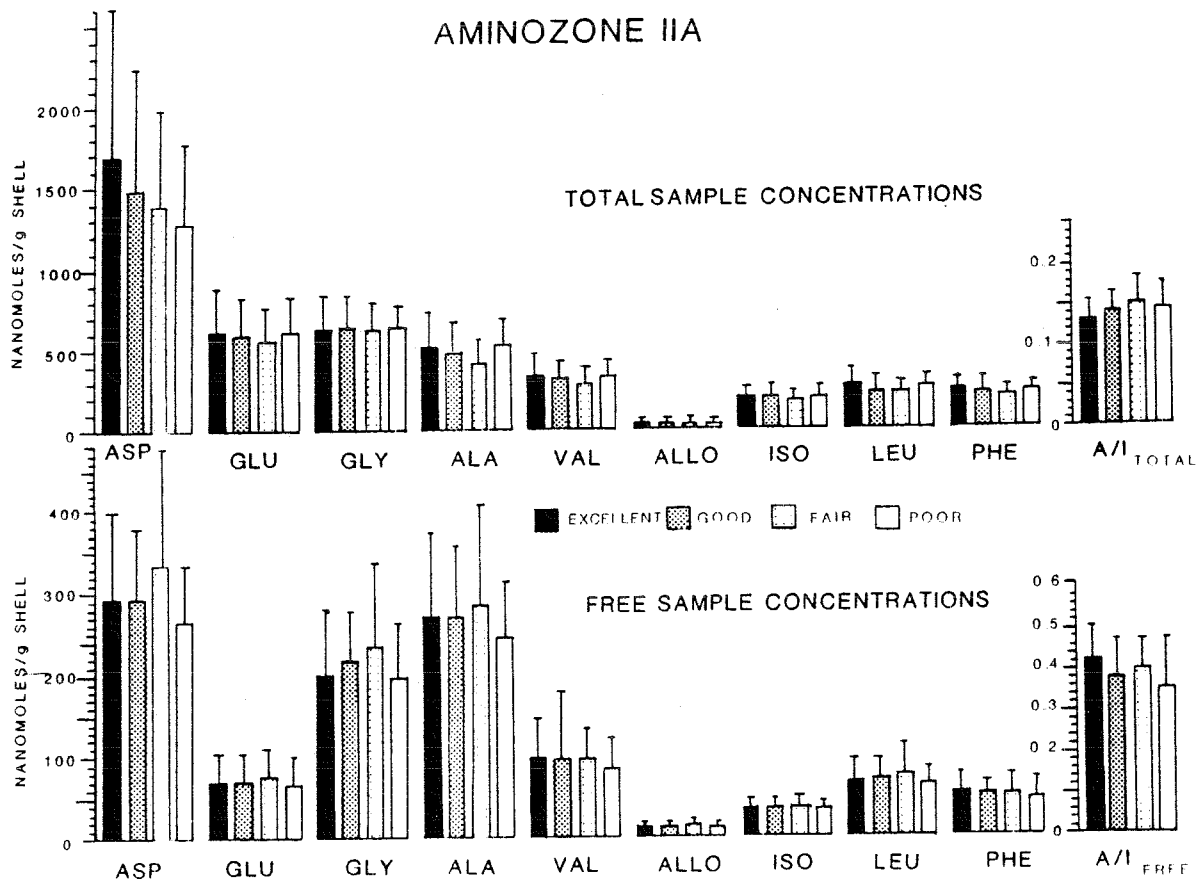


Fig. 8-8. Comparison of amino acid concentrations by shell condition in both total and free samples. All molluscs were collected from aminozone IIA in Gomez Pit. Condition was graded using the criteria listed in Table 8-1. Data used to construct this figure are found in Appendix G.

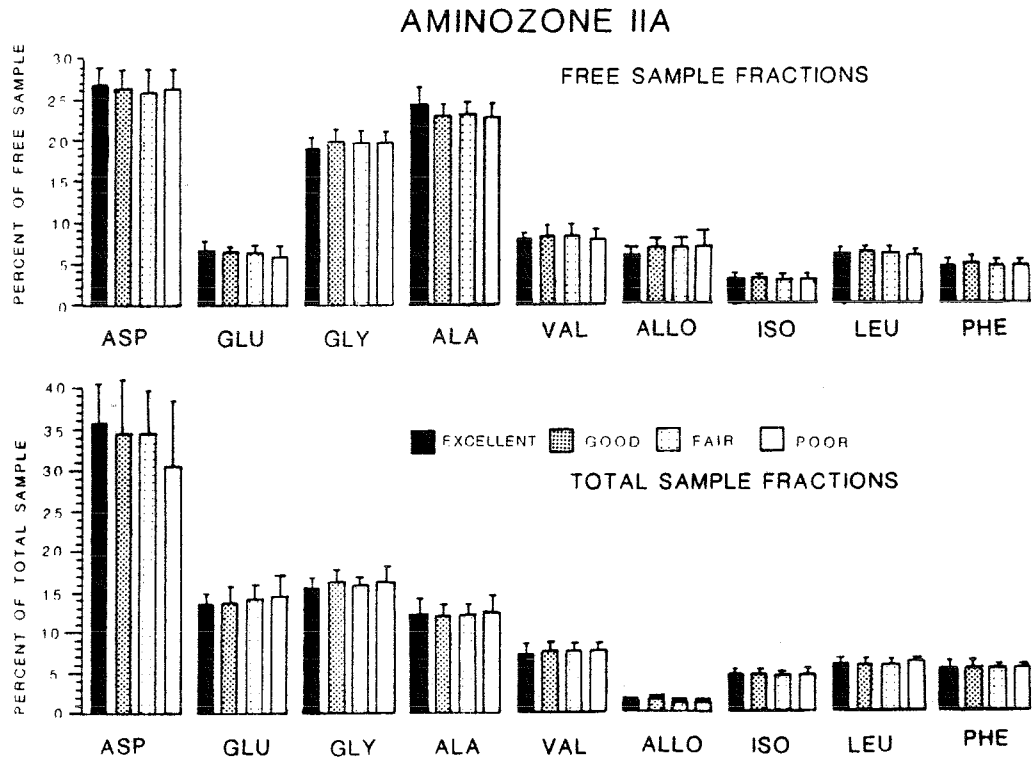


Fig. 8-9. Comparison of amino acid fractions by shell condition in both total and free samples. All molluscs were collected from aminozone Iia in Gomez Pit. Data used to construct this figure are found in Appendix G.

molluscs. First, mean ALLO/ISO values in free samples are greater than ALLO/ISO values in total samples. Second, labile amino acids (those amino acids which form relatively weak peptide bonds such as ASP, GLY and ALA; Hare *et al.*, 1975) show higher concentrations (Fig. 8-8) and relative abundances (Fig. 8-9) in free samples than do amino acids forming more stable peptide bonds such as GLU, VAL, ISO, LEU and PHE. Amino acids appearing most readily in free samples are also most extensively racemized. The preferential appearance of ASP, GLY, ALA and LEU in free samples is generally consistent with apparent racemization rates of amino acids determined previously for Gomez Pit shells (Mirecki, 1985), where D/L values decrease in the order: ASP > ALA > PHE, LEU > GLU, VAL.

Considering the amino acid concentration variations among different conditions of shell, amino acid concentrations show no statistically significant differences in either free or total samples (Fig. 8-8). Comparison of amino acid concentrations was made using the one-way ANOVA (ANalysis Of VAriance) method, in which the mean values of each normally distributed population (μ) were tested using the null hypothesis μ (excellent) = μ (good) = μ (fair) = μ (poor). The null hypothesis was accepted (significance level of 0.99) for all amino acid concentrations in both free and total samples. It is apparent that large standard deviations (typically showing coefficients of variation of 35%) in these concentration measurements obscure any subtle diagenetic signal. These variations are slightly higher than those shown for ILC-B standard concentration measurements, which typically show coefficients of variation of 25% to 35% for total concentrations, and 40% for free concentrations.

Considering amino acid fractions (defined in section 3.3.2), there are again no statistically significant differences in free or total samples among different condi-

tions of shell in aminozone IIa (Fig. 8-9). Shells collected from aminozone IIa do not seem to show gross compositional variation resulting from differences in shell quality.

Considering ALLO/ISO values in free and total samples, there again seems to be no systematic reduction of ALLO/ISO value in poor quality, leached shells. To discern any kind of systematic variation in ALLO/ISO values within aminozone IIa, the data were considered in two ways. First, ALLO/ISO values in both free and total values were compared by condition (Fig. 8-8). No statistically significant variation in free or total ALLO/ISO values was discerned using the ANOVA method described previously.

In the second approach, ALLO/ISO values from molluscs collected adjacent to a vertically restricted "leached facies" in Gomez Pit were compared with ALLO/ISO values from molluscs collected down-section. G. Johnson (pers. comm., 1983) and Darby (1983) have recognized leached, in-place shells and shell ghosts in upper strata (MSL to +3m) in Gomez Pit (Fig. 8-10; also above the oxidized zone at site 06056; App. D.1-3). A plot of ALLO/ISO value versus stratigraphic position in aminozone IIa (Fig. 8-11) shows no trend of decreasing ALLO/ISO values closer to the leached zone. It also appears that variations of ALLO/ISO values in aminozone IIa are not necessarily related to instrumental variation. Aminozone IIa samples were analyzed successively from top to bottom of the outcrop; ILC-B standard powder analyses accompanying each batch of IIa samples are also shown in Fig. 8-11. Variation of ALLO/ISO values in the ILC-B samples does not correspond with the slight reduction of ALLO/ISO values near the base of aminozone IIa.

8.5.2: Comparison of Amino Acid Data Between Gomez Pit IIc and Yadkin Pit IIc

Shells analyzed from these two localities are both ranked as poor. However, the Yadkin Pit shells were the most poorly preserved specimens of the collection. Valves from aminozone IIc in Gomez Pit are intact, although chalky in appearance; valves from aminozone IIc in Yadkin Pit are friable, and were difficult to extract from the outcrop intact. The Yadkin Pit shells were analyzed because they exhibit "worst case" preservation characteristics. Mean amino acid concentrations and fractions from both sites are shown in Fig. 8-12, and tabulated in Appendix G.

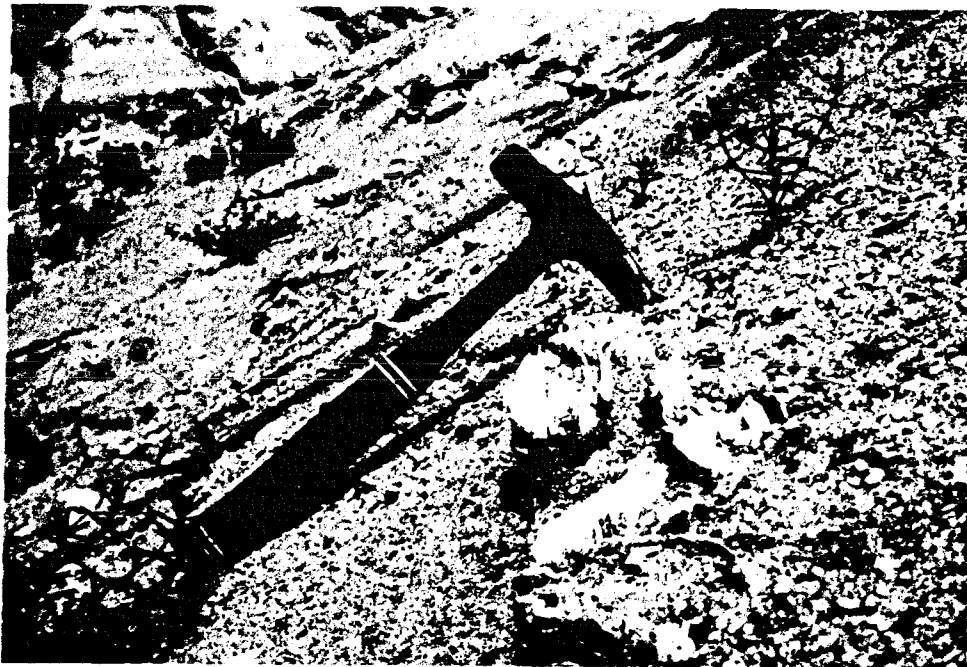


Fig. 8-10. Photograph of leached, in-place *Mercenaria* collected from the upper part (approximately +1m above MSL) of aminozone IIa in Gomez Pit.

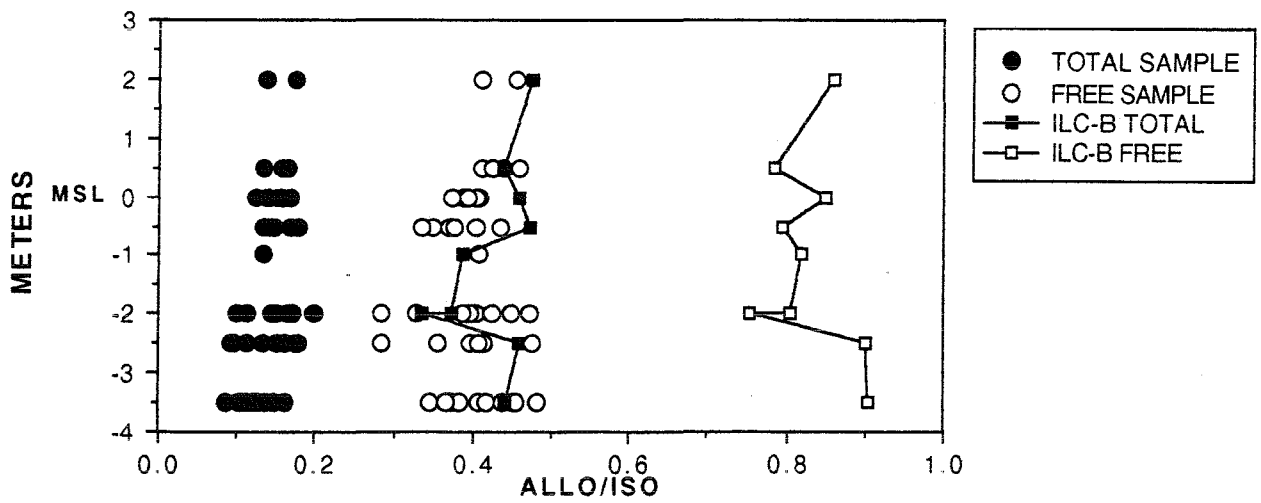


Fig. 8-11. Plot of (ALLO/ISO)TOTAL (•) and (ALLO/ISO)FREE (○) values versus stratigraphic position in aminozone IIa. ALLO/ISO value from ILC-B standard powders with these IIa samples are shown for comparison.

Fig. 8-12 shows no statistically significant differences in either amino acid concentrations or fractions between the Gomez Pit and Yadkin Pit data sets. The lack of statistical significance is due in part to large standard deviations in the concentration measurements, typically showing % coefficients of variation around 30%. It can be noted that the concentration of each amino acid in the total and free samples is consistently lower in Yadkin Pit than in Gomez Pit valves. Concentrations of labile amino acids ASP, GLY and ALA are 12% to 23% lower, and ALLO concentrations are 39% lower in the total samples of friable Yadkin Pit valves. Because ALLO only accounts for about 1% of the total amino acid composition in shells of aminozone IIc age, small reductions in ALLO concentration will significantly affect ALLO/ISO values in free and total samples. It should be noted that a reduction of (ALLO/ISO)_{total} values in Yadkin Pit shells ($A/I = 0.261$ in YP IIc compared to 0.334 in GP IIc) is only discerned in these "worst case" examples. A similar reduction of ALLO/ISO values in Yadkin Pit free samples is observed ($A/I = 0.463$ in YP IIc compared to 0.627 in GP IIc) probably the result of leaching "free" alloisoleucine molecules from the shell, consistent with the effect described by Müller (1984) and Boutin (1989).

127

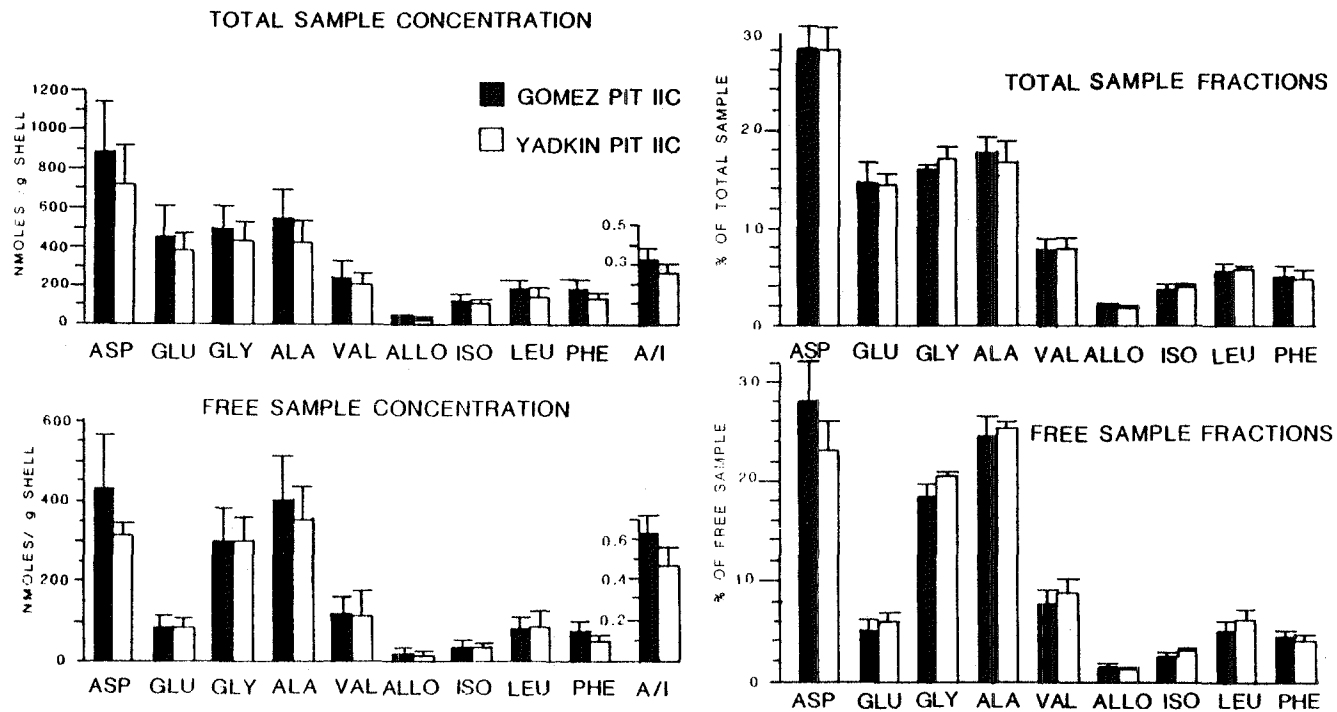


Fig. 8-12. Comparison of amino acid concentrations (left) and amino acid fractions (right) between valves collected from Yadkin Pit and Gomez Pit, both representing aminozone IIC. Yadkin Pit IIC samples show extensive structural degradation when compared to Gomez Pit IIC shells. Data used to compile this table are found in Appendix G.

8.5.3: Comparison of Amino Acid Data Between Norris Bridge Ild and Gomez Pit Ild

The Norris Bridge shells show physical preservation characteristics unlike any other Pleistocene mollusc from the mid-Atlantic coastal plain. Although the original coloration of the outer prismatic layer has faded or been obscured by pyritization (shell conditions are sometimes graded fair or good in Appendix B), Norris Bridge shells often show original purple coloration along the ventral margin, and no sign of structural weakness between lamellae when cut in cross-section. Scanning electron microscopy of the prismatic layer of these shells (Benamy, 198~~0~~³) also revealed unusual preservation of individual crystallites. Textural observations of the Norris Bridge shells suggests that these fossils are unusually well-preserved in comparison to other *Mercenaria* of the same age.

Amino acid concentrations and fractions from Norris Bridge and Gomez Pit shells are plotted in histogram form in Fig. 8-13. The only systematic difference between these two data subsets is that Norris Bridge Ild shells show higher amino acid concentrations in total samples; amino acid concentrations in free samples do not differ significantly. It is difficult to distinguish leaching criteria in these data sets because of high variability in Gomez Ild data, where % coefficients of variation are at least 27% in total sample concentrations, and range between 43% and 65% for free sample concentrations (Appendix G).

A comparison of total and free sample fractions between Gomez Pit and Norris Bridge shells representing aminozone Ild shows differences in amino acid composition, but these differences are difficult to interpret in the context of the leaching process. Fraction data from free and total samples show that Gomez Pit Ild shells are

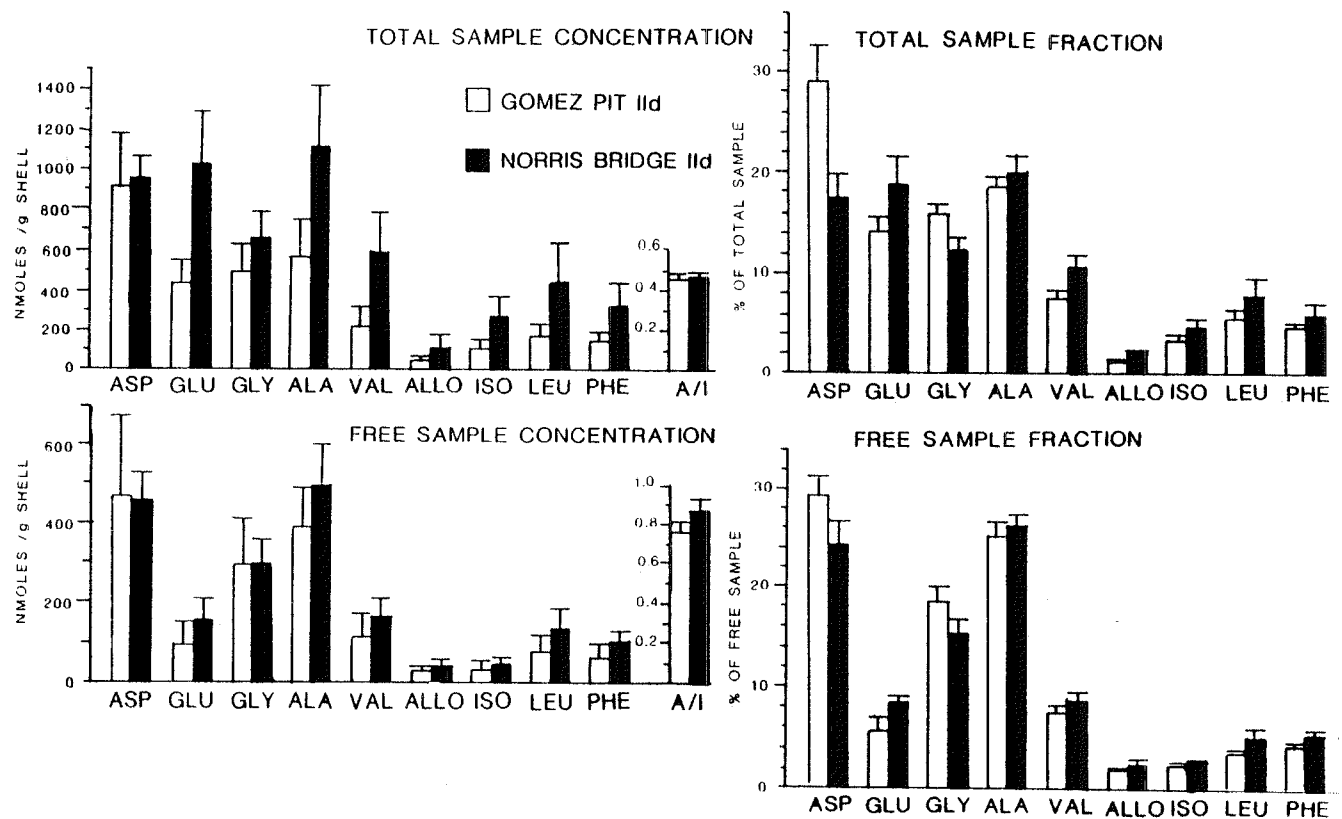


Fig. 8-13. Comparison of amino acid concentrations (left) and amino acid fractions (right) between valves collected from Gomez Pit and Norris Bridge, representing aminozone II d. Norris Bridge II d shells appear to be uniquely well-preserved in comparison to Gomez Pit II d. Data used to compile this table are found in Appendix G.

"enriched" in the labile amino acids ASP and GLY, and that all other amino acid fraction data are similar between the two sites (Fig. 8-13). If Gomez Pit shells from aminozone IId are extensively leached, it is surprising that this process did not remove a discernable portion (either in concentration or relative fractions) of labile amino acids.

ALLO/ISO values in total samples do not vary significantly between Gomez Pit and Norris Bridge IId shells. However, ALLO/ISO values in free samples are significantly higher in Norris Bridge samples than in Gomez Pit IId samples (0.874 +/-0.061 versus 0.759 +/-0.045, respectively). This observation is consistent with leaching and removal of free ALLO. ALLO abundances are still low in aminozone IId (approximately 1.5% of the total fraction, 2.3% of the free fraction) so that small reductions in ALLO content by leaching can substantially reduce ALLO/ISO values of the Gomez Pit valves. Unfortunately, corresponding reductions in the free sample concentration of other amino acids in leached Gomez Pit IId samples is not observed.

8.6: Variations in Amino Acid Composition With Time

The dominant diagenetic processes affecting mollusc shell amino acid concentrations and fractions over time are conversion of peptide-bound amino acids to the free form by hydrolysis (accompanied by epimerization of terminal amino acids), and loss of amino acids by leaching. Mean values for each amino acid in both free and total samples from aminozones in Gomez Pit are shown in histogram form in Figs. 8-14 and 8-15 (tabulated in Appendix G). A comparison of amino acid distribution among total, free and bound (found by difference, total minus free) samples is shown in Table 8-2, which has also been calculated from data tabulated in Appendix G. Because aminozones IIa, IIc, II d and II e are superposed in Gomez Pit, these strata serve as a general model for amino acid diagenesis. Mean values of these amino acid concentrations show significant variability, so that the record of diagenesis preserved in the Gomez Pit section should be considered qualitative.

8.6.1: Changes in Amino Acid Concentrations and Their Distribution in Free and Bound States.

Amino acid concentrations in total samples show marked decrease during earliest diagenesis. Amino acid concentrations in total samples are reduced to at least half of modern concentrations by aminozone IIa time, with the exception of ALLO which is accumulating in both the free and bound form. Labile amino acids (*e.g.* ASP, GLY, ALA) do not show especially high reductions in total sample concentration when compared to more "tenacious" GLU and VAL concentrations, when modern and aminozone IIa shells are compared. Although peptide bond strengths differ based on the constituent amino acids, it seems that peptide bond hydrolysis overcomes differences in all bond strengths during earliest diagenesis.

30 132

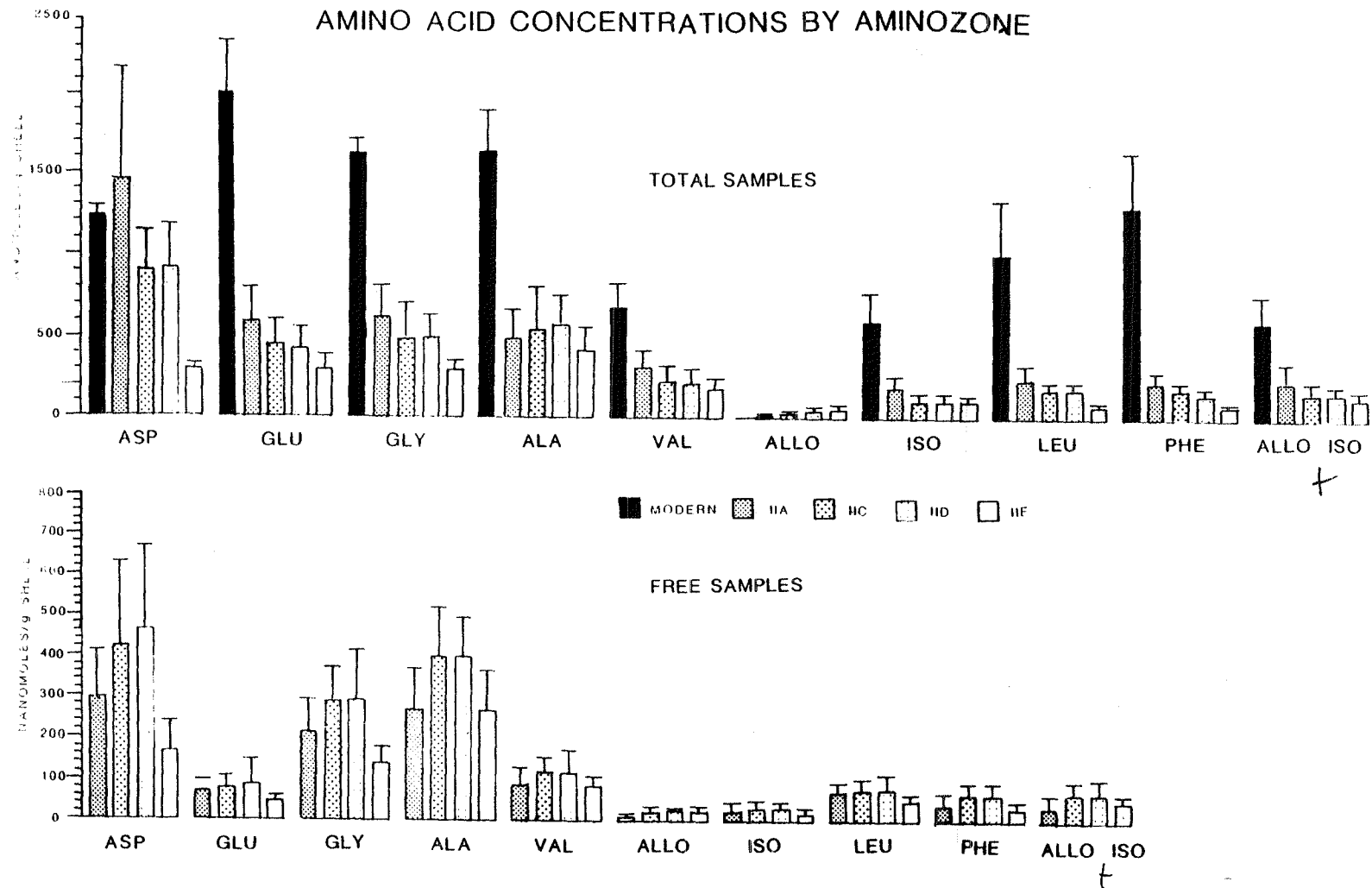


Fig. 8-14. Comparison of amino acid concentrations among valves from all aminozones in Gomez Pit. Data used to compile this table are found in Appendix G.

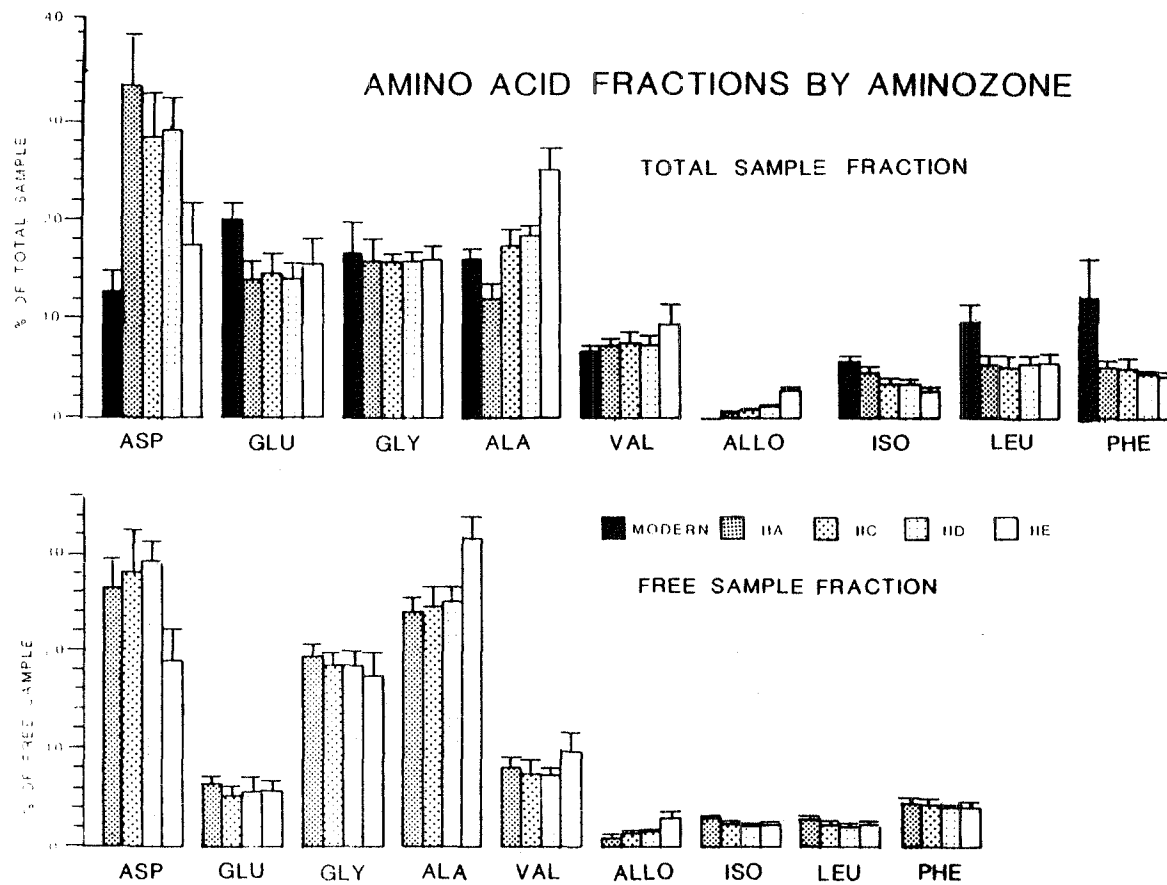


Fig. 8-15. Comparison of amino acid fractions among valves from all aminozones in Gomez Pit. Data used to compile this table are found in Appendix G.

133

Apparently, roughly half of the amino acid concentration of modern shells is lost through hydrolysis and subsequent removal by leaching, all occurring prior to aminozone IIa time. However, most of the remaining amino acids in aminozone IIa samples exist in the peptide-bound state (Table 8-~~1~~²). A sample calculation can reinforce this point:

Modern LEU concentration (total sample)	984 nmole/g shell
Aminozone IIa LEU concentration (total sample)-	<u>242 nmole/g shell</u>
LEU lost	742 nmole/g shell
LEU distribution in aminozone IIa: total sample 242 nmole/g shell	
	free sample 69 nmole/g shell (29% of total)
	bound sample 173 nmole/g shell (71% of total)

The amino acids that remain at aminozone IIa time represent hydrolysis-resistant polypeptides or protein consisting mostly of bound rather than free amino acids (Table 8-~~2~~² *# OK as Table 8-2*). With the exception of ALA, GLY and ALLO, more than 70% of each amino acid exists in the bound form at aminozone IIa time.

Total sample amino acid concentrations continue to decrease through aminozone IIc time. With the exception of ALA and ALLO, total sample amino acid concentrations decrease 20% to 40% from aminozone IIa to aminozone IIc time, and ALA and ALLO concentrations increase during this same time interval. ALLO increases as a result of ISO epimerization, and increasing ALA concentrations may result from decarboxylation of ASP (Schroeder, 1975) or decomposition of SER (Vallentyne, 1964). By aminozone IIc time, the distribution of amino acids between free and bound states is approximately equal. Labile amino acids GLY and ALA show greater proportions in the free state, and hydrolysis-resistant amino acids LEU and PHE show greater proportions in the bound state (Table 8-~~2~~² *Table 8-2*).

AMINO ZONE	TOTAL FREE BOUND (nanomoles/g shell)			%FREE	%BOUND
ASP MODERN	1230	---	1230	0	100
IIA	1455	299	1155	21	79
IIC	883	427	456	48	52
IID	908	464	444	51	49
IIE	301	165	136	55	45
GLU MODERN	2003	---	2003	0	100
IIA	595	72	523	12	88
IIC	459	84	375	18	82
IID	438	93	345	21	79
IIE	294	49	245	17	83
GLY MODERN	1628	---	1628	0	100
IIA	625	215	410	34	66
IIC	490	289	201	59	41
IID	495	290	205	59	41
IIE	294	49	245	17	83
ALA MODERN	1635	---	1635	0	100
IIA	492	269	223	55	45
IIC	548	399	149	73	27
IID	579	464	400	69	31
IIE	294	267	27	91	9
VAL MODERN	685	---	685	0	100
IIA	312	93	219	30	70
IIC	241	120	121	50	50
IID	234	118	116	50	50
IIE	178	84	94	47	53
ALLO MODERN	---	---	---	0	0
IIA	26	13	13	50	50
IIC	38	25	13	66	34
IID	46	29	17	63	37
IIE	54	25	29	47	53
ISO MODERN	594	---	594	0	100
IIA	187	34	153	18	82
IIC	116	39	77	34	66
IID	110	37	73	34	66
IIE	106	21	85	20	80
LEU MODERN	984	---	984	0	100
IIA	242	69	173	29	71
IIC	175	81	94	46	54
IID	177	83	94	47	53
IIE	49	50	--	100	0
PHE MODERN	1284	---	1284	0	100
IIA	217	51	166	24	76
IIC	173	74	99	43	57
IID	151	67	84	44	56
IIE	76	35	41	46	54

Table 8-~~2~~⁵ Distribution of amino acids in total, free and bound (found by difference, total minus free) in all amino zones defined in Gomez Pit. Data used to compile this table are found in Appendix G.

OK as Table 8-2

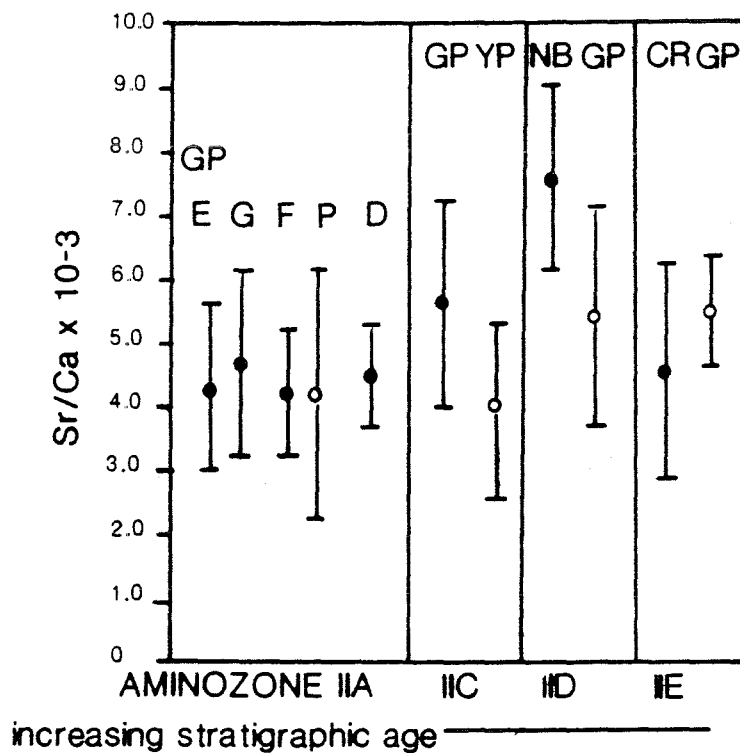
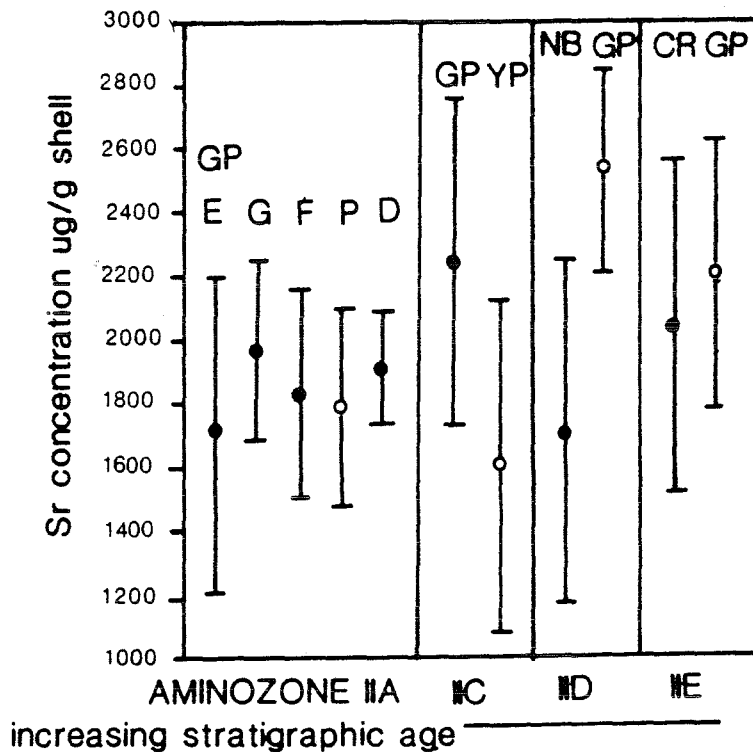
Both free and total sample amino acid concentrations remain almost constant between aminozone IIc and aminozone II d time. Consequently, the distribution of each amino acid between the free and bound states remains essentially constant (Table 8-2).

By aminozone IIe time, total sample amino acid concentrations have been reduced to 5% to 25% of modern concentrations. ASP, ALA and LEU exist predominantly in the free state, while GLU and GLY are predominantly peptide-bound. It is difficult to interpret these data in the context of diagenetic reactions because the amino acid composition of these oldest shells probably reflects the combined effect of hydrolysis, leaching and decomposition reactions.

8.7: Sr Concentrations and Sr/Ca Values with Time, and Condition

Most of the molluscs reported in this study were analyzed for Sr, Mn, Fe and Ca, to develop chemical criteria that would reflect progressive alteration of shell carbonate. Sr probably occupies a lattice site in the aragonite crystal structure, due in part to similar ionic radii of ^{Sr and Ca} these two cations. Onuma *et al.* (1979) showed that Sr partitions preferentially to shell aragonite from extrapallial fluid in molluscs. Walls *et al.* (1977) showed that Sr in mollusc shell aragonite was not easily removed (i.e. not exchangeable) from mollusc shell material when subjected to mild (1N) ammonium acetate leaches. Because Sr seems to be readily incorporated into new shell aragonite, and not easily removed from aragonite once it is has been precipitated, Sr concentrations and Sr/Ca values were used here as a "tracer" for aragonite alteration. Strontianite (SrCO₃) has a lower solubility than aragonite (as shown by lower K_{sp} values; p. 243, Stumm and Morgan, 1981) in freshwater, so that

176
 Fig. 8-15a and b. Sr concentrations ($\mu\text{g/g}$ shell), and Sr/Ca values for mollusc valves from Gomez Pit (GP), Yadkin Pit (YP), the Chowan River Formation (CR) and Norris Bridge (NB). E, G, F and P denote conditions of shell in aminozone IIa. D denotes analyses of ILC-D standard powder, made from aminozone IIa shells. Data used to construct these diagrams are found in Appendix C; ILC-D data are summarized in Table 4-3.



extensive dissolution of shell carbonate can result in increasing Sr/Ca values. This trend has been observed by others, as discussed in section 8.1. Mn and Fe were also measured in these same shells, to detect precipitation of metal oxides or authigenic minerals in shell microcavities. Mn concentrations were low (not exceeding 29.3 $\mu\text{g/g}$ shell) and could not be correlated with shell condition. Fe concentrations were very variable, and also could not be correlated with shell condition. In addition, the 24.4 % coefficient of variation of Fe content in ILC-D standard samples was unacceptable (Table 4-3). Mn and Fe concentrations in mollusc shells are not considered because of poor analytical reproducibility of the ILC-D standard.

There is no statistically significant increase in either Sr content or Sr/Ca values among shells of different conditions in aminozone IIa (Fig. 8-16). As with amino acid data, mollusc shell Sr and Ca concentrations from aminozone IIa show high % coefficients of variation (24 to 43%), which is higher than the variability observed in analyses of the ILC-D shell powder (Table 4-3). High variability in these data probably obscures any diagenetic signal preserved in Sr and Ca analyses of these aminozone IIa shells.

The comparison of data among sites representing aminozones IIc and II d (discussed in sections 8.5.2 and 8.5.3) is used for comparison of Sr concentration and Sr/Ca data. Sr concentrations show no systematic variation with condition in aminozones IIc, II d and II e (Fig. 8-16a). That is, leached specimens (such as YP IIc and GP II d) do not always show higher Sr concentrations than better preserved specimens of the same age. Sr/Ca values are also lower in those shells showing more extensive dissolution (shown in Fig. 8-16b by YP in aminozone IIc, and GP in

aminozone IId), contrary to the expected trend of increasing Sr/Ca values based on comparative solubilities of strontianite and aragonite.

The Sr/Ca data set from all sites do follow the general trend of increasing Sr/Ca values with time. Sr/Ca values from aminozone IIa do not differ substantially from those values in modern shells (Sr/Ca = 0.0047 for *Mercenaria*, in Walls *et al.*, 1977). However, Sr/Ca values from best-case shells in aminozones IIc and IId do increase with time.

CHAPTER NINE

CONCLUSIONS AND FUTURE WORK

Work performed at the Gomez Pit locality exemplifies the utility of amino acid racemization dating techniques. Four aminozones have been recognized at Gomez Pit, each characterized by a distinct cluster of ALLO/ISO values. Each aminozone is characterized by a cluster of ALLO/ISO values obtained from total samples (representing bulk amino acid composition), and from free samples (representing the labile fraction) of the organic matrix in fossil mollusc shells. The stratigraphic relationships among these aminozones are complex, in that aminozones IIc and II d show evidence of reworking; however, all four aminozones are found in stratigraphic superposition. Aminozones IIa, IIc and possibly II d represent deposition during successive high sea levels during the Quaternary period.

Age estimates can be inferred for each aminozone using the non-linear kinetic model of isoleucine epimerization which has been calibrated by a reliable uranium-series date. Aminozone IIa, dated by uranium-series methods at 70.2 ka, serves as calibration for older aminozones in the mid-Atlantic region. Using this calibration, aminozone IIc is correlative with oxygen-isotope Stage 7, and aminozone II d is correlative with Stages 11 or possibly 13. The age of aminozone IIe is constrained largely by lithostratigraphic and paleontologic evidence. Shells from aminozone IIe show ALLO/ISO values that are almost at equilibrium. These shells have been collected from the Chowan River Formation, which is interpreted as Pliocene in age, and no further attempt is made to discern the age of these extensively racemized shells.

A second age option has been proposed for the Gomez Pit sequence, intended as another hypothesis which can be used to reconcile the age of the southeastern Virginia deposits with the deep-sea oxygen isotope curve. In this second option, the age of aminozone IIa is estimated at 120 ka, concurrent with the Substage 5e high sea stand. Given this theoretical calibration of aminozone IIa, the age estimate for aminozone IIc is Stage 9, and the age estimate for aminozone II d ranges from Stage 15 to Stage 19. The upper age limit for this aminozone is constrained by the Brunhes-Matuyama magnetostratigraphic boundary dated at 760 ka.

It should be emphasized that both of these age options represent hypotheses that can be supported by data presented in this text. The cluster of 70 ka uranium-series coral dates from Quaternary units in southeastern Virginia has been problematic in that these deposits, existing near present-day sea level, do not correspond with a high sea stand predicted by the oxygen isotope curve. Only with continued sampling and analysis of new outcrops, using several different dating methods can the conflict in this region be resolved.

The relationship between amino acid composition and condition of fossil shell cannot yet be interpreted quantitatively (in terms of a leaching model), but the following trends in amino acid data have been observed. No systematic difference in amino acid concentrations or relative fractions is shown in a comparison of amino acid data among all shell conditions from aminozone IIa. Although leaching and removal of amino acid molecules has probably occurred to a greater extent in poor quality shells from aminozone IIa, it is not possible to statistically resolve a "leaching signature" from the aminozone IIa data set.

Only by comparison of "worst-case" shells (i.e. those shells exhibiting the poorest physical characteristics in the entire collection) obtained from Yadkin Pit aminozone IIc with Gomez Pit aminozone IIc shells can definite effects of leaching can be observed. A marked reduction of ALLO/ISO values in both total samples (0.333 in Gomez Pit versus 0.263 in Yadkin Pit) and free samples (0.640 in Gomez Pit versus 0.491 in Yadkin Pit) is consistent with the removal of extensively racemized free amino acids (specifically ALLO) in leached shells. Apparently, the severity of leaching (indicated by friable texture in Yadkin Pit shells) was great enough to alter the composition of the "refractory" polypeptides which define the total sample.

A more subtle example of leaching is shown by the comparison of Norris Bridge IId shells with Gomez Pit IId shells. Both of these sites have similar ALLO/ISO values in total samples (0.459 for Gomez Pit versus 0.469 for Norris Bridge). However, ALLO/ISO values from free samples differ significantly between these two sites (0.746 for Gomez Pit versus 0.929 for Norris Bridge). The difference in ALLO/ISO values from free samples is interpreted as a preferential loss of free ALLO in the Gomez Pit shells from aminozone IId. However, leaching is not as severe in these Gomez Pit shells, and Norris Bridge shells seem to show unusually fine physical preservation. The differences in physical quality between these two sets of shells representing aminozone IId is not great enough to affect bulk composition. However, leaching of free ALLO in the Gomez Pit IId shells has proceeded even though these shells are still intact.

Weiner and Lowenstam (1980) have proposed that ALLO/ISO values and GLY/ALA values in mollusc shells serve as an indicator of subtle diagenetic change. The data presented from aminozones IIc and IId confirm the utility of ALLO/ISO values as such an indicator. There seems to be no relationship between GLY/ALA values and condition in

aminozones defined in this work, possibly due to variation of concentrations of these two amino acids.

Using these data, leaching can only be recognized from ALLO/ISO values if there is a relatively non-leached reference specimen from each aminozone (within each geographic region) with which non-leached specimens can be compared. The conclusions presented in this work represent an empirical approach for the recognition of leaching in shells. A more quantitative leaching model is needed, based on hydrolysis rates and solubilities of each amino acid, and the distribution of amino acids between free and bound phases. The data presented here do not offer the precision from which a quantitative leaching model can be formulated.

Removal of amino acids from the shell by leaching is a significant process that seems to dominate earliest diagenesis. Comparison of data from modern and aminozone IIa shells shows that at least half of the initial concentration for each amino acid has been lost by aminozone IIa time. There seems to be no preferential loss of any particular amino acid during earliest diagenesis. Those amino acids that are hydrophilic (*e.g.* GLY, ASP) are lost by percentages similar to hydrophobic residues (*e.g.* GLU, VAL). Apparently, by aminozone IIa time molluscan shell organic matrix is composed of a more "refractory" population of polypeptides. That is, only polypeptides bound by hydrolysis-resistant peptide bonds still exist in the shell. This observation is consistent with the distribution of amino acids between free and bound phases; despite the loss of at least half of the molluscan shell amino acid concentration by aminozone IIa time, approximately 60 to 70 percent of amino acids in aminozone IIa shells are in the bound state. In future work, it will be interesting to quantify amino acid composition of shells having ages less than 70 ka, since these shells undergo extensive diagenetic loss of amino acids

in temperate climates.

Loss of amino acids by leaching continues after aminozone IIa time for most amino acids, but at a much slower (apparent) rate. Exceptions to this process are ALLO and ALA concentrations, which increase through aminozone IIc time. ALLO concentrations increase as a result of diagenetic epimerization; ALA concentrations increase, possibly due to decomposition of SER or decarboxylation of ASP. GLY/ALA values can increase during diagenesis due to loss of amino acid -R groups, resulting in breakdown of amino acids to GLY. Because ALA and GLY concentrations change as a result of many types of diagenetic reactions, the use of GLY/ALA values as an indicator of shell quality requires further investigation. Lack of precision in these data prohibit the use of GLY/ALA values as an indicator of shell quality.

REFERENCES CITED

Abelson, P.H. , 1954, Organic constituents of fossils: Carnegie Institute of Washington Yearbook 53, p. 97-101.

Aller, R.C., 1982, Carbonate dissolution in nearshore terrigenous muds: The role of physical and biological reworking: Journal of Geology, v. 90, p. 79-95.

Alexandersson, E.T., 1979, Marine maceration of skeletal carbonates in the Skagerrak, North Sea: Sedimentology, v. 26, p. 853-857.

Baker, P.S., Gieskes, J.M., Elderfield, H., Diagenesis of carbonates in deep-sea sediments: Evidence from Sr/Ca and interstitial dissolved Sr²⁺ data: Journal of Sedimentary Petrology, v. 52(1), p. 71-82.

Bada, J.L., and Schroeder, R.A., 1978, Racemization of isoleucine in calcareous marine sediments: Kinetics and mechanism: Earth Science and Planetary Letters, v. 15, p. 1-11.

Benamy, E., 1983, Physical alteration of the structure of the hard-shelled clam *Mercenaria*, [M.S. thesis]: Newark, Delaware, University of Delaware, 226p.

Benson, J.R., and Hare, P.E., 1975, O-phthalaldehyde: Fluorogenic detection of primary amines in the picomole range. Comparison with fluorescamine and ninhydrin: Proceedings of the National Academy of Sciences, U.S.A., v. 72(2), p. 619-622.

Belknap, D.F., 1979, Application of amino acid geochronology to stratigraphy of the late Cenozoic marine units of the Atlantic coastal plain [Ph.D. thesis]: Newark, Delaware, University of Delaware, 550 p.

Blackwelder, B.W., 1981a, Stratigraphy of the upper Pliocene and lower Pleistocene marine and estuarine deposits of northeastern North Carolina and southeastern Virginia: U.S. Geological Survey Bulletin 1502-B, 16 p.

Blackwelder, B.W., 1981b, Late Cenozoic stages and molluscan zones of the U.S. middle Atlantic coastal plain: Journal of Paleontology Memoir 12, v. 55 (Part II of II), p. 1-34.

Boutin, B.S., 1989, On the quantitative aspects of amino acid diagenetic racemization in fossil Quaternary mollusks [M.S. thesis]: Newark, Delaware, University of Delaware, 130p.

- Burchard, B., and Fritz, P., 1978, Sr uptake in shell aragonite from the freshwater gastropod *Limnaea stagnalis* : Science, v. 199: 291-292.
- Carriker, M.R., 1978, Ultrastructural analysis of dissolution of shell of the bivalve *Mytilus edulis* by the accessory boring organ of the gastropod *Urosalpinx cinera*: Marine Biology, v. 48, p. 105-134.
- Chappell, J. and Shackleton, N.J., 1986, Oxygen isotopes and sea-level: Nature, v. 324, p. 137-140.
- Chivas, A.R., DeDeckker, P., and Shelley, J.M.G., 1985, Sr content of ostracodes indicates lacustrine paleosalinity: Nature, v. 316: 251-253.
- CLIMAP Project Members, 1984, The last interglacial ocean: Quaternary Research, v. 21, P. 123-224.
- COHMAP Members, 1988, Climatic changes of the last 18 ka: Observations and model simulations: Science, v. 241, p. 1043-1052.
- Colman, S.M., Pierce, K.L., and Birkeland, P.W., 1987, Suggested terminology for Quaternary dating methods: Quaternary Research, v. 28, p. 314-319. —
- Colman, S.M. and Mixon, R.B., 1988, The record of major Quaternary Sea-level changes in a large coastal plain estuary; Chesapeake Bay, eastern United States: Paleogeography, Paleoclimatology, Paleoecology, v. 68, p. 99-116.
- Cronin, T.M., 1979, Late Pleistocene marginal marine ostracodes from the southeast Atlantic coastal plain and their paleoenvironmental implications: Geographie, Physique et Quaternaire, v. 3, no. 2, p. 121-173.
- Cronin, T.M., 1981, Rates and possible causes of neotectonic vertical crustal movements of the emerged southeast U.S. Atlantic coastal plain: Geological Society of America Bulletin, v. 92 (part I), p. 812-833.
- Cronin, T.M., 1988, Evolution of marine climates of the U.S. Atlantic coast during the past four million years: Philosophical Transactions of the Royal Society of London, B, v. 318, p. 661-678.
- Cronin, T.M., Szabo, B.J., Ager, T.A., Hazel, J.E., and Owens, J.P., 1981, Quaternary climates and sea levels: U.S. Atlantic coastal plain: Science, v. 211, p. 233-240.
- Cronin, T.M., Bybell, L.M., Poore, R.Z., Blackwelder, B.W., Liddicoat, J.C., and Hazel, J.E., 1984, Age and correlation of emerged Pliocene and Pleistocene deposits, U.S. Atlantic coastal Plain: Paleogeography, Paleoclimatology, Paleoecology, v. 48, p. 263-284.

- Darby, D.A., 1983, Sedimentology, diagenesis and stratigraphy of Pleistocene coastal deposits in southeastern Virginia: Annual Virginia Field Conference (15th), Old Dominion University, 37 p.
- Davies, T.T., and Hooper, P.R., 1963, Determination of the calcite-aragonite ratio in mollusc shells by x-ray diffraction: Mineralogical Magazine, v. 33, p. 609-612.
- Driscoll, E.G., 1970, Selective bivalve destruction in marine environments,: A field study: Journal of Sedimentary Petrology, v. 40 (3), p. 895-905.
- Estes, E.L. III, 1972, Diagenetic Alteration of *Mercenaria mercenaria* as determined by laser microprobe analysis [Ph.D. thesis]: Chapel Hill, North Carolina, University of North Carolina, 95p.
- Fairbanks, R.G., and Matthews, R.K., 1978, The marine oxygen isotope record in Pleistocene coral, Barbados, West Indies: Quaternary Research, v. 10, p. 181-196.
- Graham, D.W., Bender, M.L., Williams, D.F., Keigwin, L.D., Jr., 1982, Strontium-calcium ratios in Cenozoic planktonic foraminifera: Geochimica et Cosmochimica Acta, v. 46, p. 1281-1292.
- Hallam, A., and Price, N.B., 1966, Strontium contents of recent and fossiliferous aragonitic cephalopod shells: Nature, v. 212, p. 25-27.
- Hare, P.E., 1971, Effect of hydrolysis on racemization rate of amino acids: Carnegie Institution of Washington Yearbook 72, p. 256-258.
- Hare, P.E., and Mitterer, R.M., 1969, Laboratory simulation of amino acid diagenesis in fossils: Carnegie Institution of Washington Yearbook 1967, p. 205-208.
- Hare, P.E., Miller, G.H. and Tuross, N.C., (1975) Simulation of natural hydrolysis of proteins in fossils: Carnegie Institution of Washington Yearbook 74, p. 609-612.
- Hare, P.E., St. John, P.A., and Engel, M.H., 1985, Ion-exchange separation of amino acids in Barrett, G.C., ed. Chemistry and biochemistry of amino acids: London, Chapman and Hall, p. 415-425.
- Hennig, G.J., and Grün, R., 1983, ESR dating in Quaternary geology: Quaternary Science Reviews, v. 2, p. 157-238.
- Ikeya, M., and Ohmura, K., 1983, Dating of fossil shells with ESR: Journal of Geology, v. 89, p. 247-251.
- Ivanovich, M., 1982, U-series disequilibria: applications to geochronology, in Ivanovich, M., and Harmon, R.S. eds., Uranium series Disequilibrium, Applications to Environmental Problems: Oxford, U.K., Clarendon Press, 569 p.

- Johnson, G.H., 1976, Geology of the Mulberry Island, Newport News North and Hampton Quadrangles, Virginia: Virginia Division of Mineral Resources Report of Investigations 41, 72 p.
- Johnson, G.H. and Berquist, C.R., 1989, Geology and mineral resources of the Brandon and Norge quadrangles, Virginia: Publication 87, Virginia Minerals, 28 p.
- Jones, B. and Pemberton, S.G., 1987, The role of fungi in the diagenetic alteration of spar calcite: Canadian Journal of Earth Sciences, v. 24, p. 903-914.
- Katzenberger, O., and Willems, N., 1988, Interferences encountered in the determination of accumulated dose (AD) of mollusc samples: Quaternary Science Reviews, v. 7, p. 485-490.
- Katzenberger, O., Debuyst, R., DeCanniere, P., Dejehet, F., Apers, D., and Barabas, M., in press, Temperature experiments on mollusk samples: An approach to ESR signal identification: International Journal of Radiation Applications and Instrumentation, Part A.
- Kaufman, A., Broeker, W.S., Ku, T.-L., and Thurber, D.L., 1971, The status of U-series methods of mollusk dating: Geochimica et Cosmochimica Acta, v. 35, p. 1155-1183.
- Keenan, E., 1982, Amino acid racemization dating: Theoretical considerations and practical applications [Ph.D. thesis]: Newark, Delaware, Univ. of Delaware, 351 p.
- Kennish, M.J., 1980, Shell microgrowth analysis, *in* Skeletal Growth of Aquatic Organisms, eds. D.C. Rhodes and R.A. Lutz, Plenum Press, New York, p. 255-293.
- King, K., 1978, γ -carboxyglutamic acid in fossil bone and its significance for amino acid dating: Nature, v. 273, p. 41-43.
- King, K., and Bada, J.L., 1979, Effect of in-situ leaching on amino acid racemization rates in fossil bones: Nature, v. 281, p. 135-137.
- Kinsman, D.J.J., and Holland, H.D., 1969, The co-precipitation of cations with calcium carbonate, IV: The co-precipitation of Sr²⁺ with aragonite between 16° and 96°C: Geochimica et Cosmochimica Acta, v. 33, p. 1-17.
- Kriausakul, N., and Mitterer, R.M., 1978, Comparison of isoleucine epimerization in a model dipeptide and fossil protein: Geochimica et Cosmochimica Acta, v. 44 (5), p. 753-758.
- Kriausakul, N. and Mitterer, R.M. 1980a, Some factors influencing the epimerization of isoleucine in peptides and proteins, *in* Biogeochemistry of Amino Acids, eds. Hare, P.E., Hoering, T.C. and King, K., Jr.: New York, John Wiley and Sons, p. 283-296.

- Kriausakul, N. and Mitterer, R.M., 1980b, Isoleucine epimerization in peptides and proteins: Kinetic factors and applications to fossil proteins: *Science*, v. 201, p. 1011-1014.
- Kriausakul, N. and Mitterer, R.M., 1984, Comparison of rates and degrees of isoleucine epimerization in dipeptides and tripeptides: *Organic Geochemistry*, v. 7 (1), p. 91-98.
- Ku, T.-L., 1976, The U-series method of age determination: *Annual Review of Earth and Planetary Science*, v. 4, p. 347-379.
- Lajoie, K.R., Kennedy, G.L. and Wehmler, J.F. (1980c) Inter- and Intrageneric trends in apparent amino acid relative racemization kinetics in Quaternary mollusks, *in Biogeochemistry of Amino Acids*, eds. Hare, P.E., Hoering, T.C. and King, K., Jr.: New York, John Wiley and Sons, p. 305-340.
- Lehninger, A.L., 1975, *Biochemistry*, Worth Publishing Co., p. 100.
- Lewy, Z., 1981, Maceration of calcareous skeletons: *Sedimentology*, v. 28, p. 893-895.
- Liddicoat, J.C., and Mixon, R.B., 1980, Paleomagnetic investigation of Pleistocene sediments in the Delmarva peninsula, central Atlantic coastal plain: *Geological Society of America abstracts with programs*, v. 12(2), p. 70.
- Lorens, R.B. and Bender, M.L., (1980) The impact of solution chemistry on *Mytilus edulis* calcite and aragonite: *Geochimica et Cosmochimica Acta*, b. 44, p. 1265-1278.
- Lukas, K.J., 1979, The effects of marine microphytes on carbonate substrates: *SEM/1979/II*, p. 447-455.
- McCoy, W.D., 1987a, Quaternary aminostratigraphy of the Bonneville basin, western United States: *Geological Society of America Bulletin*, v. 98, p. 99-112.
- McCoy, W.D., 1987b, The precision of amino acid geochronology and paleothermometry: *Quaternary Science Reviews*, v. 6, p. 43-54.
- Millard, H.T., and Muhs, D.R., 1988, ESR dating of Pleistocene fossil molluscs from San Nicholas Island, California: *Geological Society of America abstracts with programs*, Denver National Meeting, p. A346.
- Miller, G., Brigham, J.K., and Clark, P., 1982, Alteration of total Aile/Ile ratios by different methods of sample preparation, *in* Miller, G., ed., *Amino acid geochronology lab reports of current activities*, Jan. 1981 - May 1982, Boulder, Colorado, INSTAAR, University of Colorado, p. 9-20.

Miller, G.H. and Hare, P.E., 1980, Amino acid geochronology: Integrity of the carbonate matrix and potential of molluscan fossils: *in* Biogeochemistry of Amino Acids, eds. Hare, P.E., Hoering, T.C. and King, K., Jr.: New York, John Wiley and Sons, p. 415-444.

Miller, R.J., 1986, Beyond ANOVA: Basics of applied statistics, New York, John Wiley and Sons, p.16.

Mirecki, J.E., 1985, Amino acid racemization dating of coastal plain sites, southeastern Virginia and northeastern North Carolina [M.S. thesis]: Newark, Delaware, University of Delaware, 118p.

Mitterer, R.M., 1975, Ages and diagenetic temperatures of Pleistocene deposits of Florida based on isoleucine epimerization in *Mercenaria* : Earth and Planetary Letters, v. 28, p. 275-282.

Mitzuani, T., and Mitzuani, A., 1977, Adsorption of cationic biological materials on controlled pore glass: Analytical Biochemistry, v. 83, p. 216-221.

Mitzuani, T., and Mitzuani, A., 1978, Estimation of adsorption of drugs and proteins on glass surfaces with controlled pore glass as a reference: Journal of Pharmaceutical Science, v. 67(8), p. 1102-1105.

Mixon, R.B., Szabo, B.J., and Owens, J.P., 1982, U-series dating of mollusks and corals, and age of Pleistocene deposits, Chesapeake Bay Area, Virginia and Maryland: U.S. Geological Survey Professional Paper 1067-E, 18p.

Mixon, R.B., 1985, Stratigraphic and geomorphic framework of the uppermost Cenozoic deposits in the southern Delmarva peninsula, Virginia and Maryland: U.S. Geological Survey Professional Paper 1067-G, 51p.

Molodkov, A., ESR Dating of Quaternary shells: Recent advances: Quaternary Science Reviews, v. 7, p. 477-484.

Müller, P.J., 1984, Isoleucine epimerization in; Quaternary planktonic foraminifera: Effects of diagenetic hydrolysis and leaching, and Atlantic-Pacific intercore correlations: Meteor Forsch.-Ergebnisse, Reihe C, no. 38, Seite 25-47.

North American Commission on Stratigraphic Nomenclature, 1983, North American stratigraphic code: AAPG Bulletin, v. 67(5), p. 841-875.

Oaks, R.Q., and Coch, N.K., 1973, Post-Miocene stratigraphy and morphology, southeastern Virginia: Virginia Division of Mineral Resources Bulletin 82, 135p.

- Oaks, R.Q., Coch, N.K., Sanders, J.E., and Flint, R.F., 1974, Post-Miocene shorelines and sea levels, southeastern Virginia, *in* Oaks, R.Q., and DuBar, J.R., eds., Post-Miocene stratigraphy, central and southern Atlantic coastal plain, Salt Lake City, Utah State University Press, p. 53-87.
- Onuma, N., Masuda, F., Masataka, H. and Wada, K., 1979, Crystal structure control on trace element partition in mollusc shell formation: *Geochemical Journal*, v. 13, 187-189.
- Owens, J.P., and Denny, C.S., 1979, Upper Cenozoic of the central Delmarva peninsula, Maryland and Delaware: U.S. Geological Survey Professional Paper 1067-A, 53 p.
- Parente, E.S., 1987, Studies on the high-performance ion-exchange chromatography of proteins [Ph.D. thesis], Newark, Delaware, University of Delaware, 199p.
- Parris, N.A., 1984, Instrumental liquid chromatography. A practical manual on HPLC chromatographic methods, 2nd ed., Amsterdam, Elsevier Press, 432p.
- Peebles, P.C., 1984, Late Cenozoic landforms, stratigraphy and history of sea level oscillations of southeastern Virginia and northeastern North Carolina [Ph.D. thesis], Williamsburg, Virginia, College of William and Mary, 231p.
- Peebles, P.C., Johnson, G.H., and Berquist, C.R., 1984, The middle and late Pleistocene stratigraphy of the outer coastal plain, southeastern Virginia and northeastern North Carolina: *Virginia Minerals*, v. 30(2), p. 13-22.
- Pilkey, O.H. and Goodell, H.G., 1964, Comparison of the composition of Recent and fossil mollusk shells: *Geological Society of America Bulletin*, v. 75, p. 217-228.
- Poulicek, M., 1986, Shell matrix weathering in marine sediments: *Proceedings of the 8th International Malacological Conference, Budapest, 1983*, p. 201-205.
- Radtke, U., 1987, Paleo-sea levels and discrimination of the last and penultimate interglacial fossiliferous deposits by absolute dating methods and geomorphological investigations: *Berliner Geographische Studien*, v. 25, p. 313-342.
- Radtke, U., Mangini, A., and Grün, R., 1985, ESR dating of marine fossil shells: *Nuclear Tracks*, v. 10, p. 879-884.
- Ragland, P.C., Pilkey, O.H. and Blackwelder, B.W., 1969, Comparison of the Sr/Ca ratio of fossil and Recent mollusc shells: *Nature*, v. 224, p. 1223-1224.
- Ragland, P.C., Pilkey, O.H. and Blackwelder, B.W., 1979, Diagenetic changes in the elemental composition of unrecrystallized mollusk shells: *Chemical Geology*, v. 25, p. 123-134.

- Rahaim, S.D., 1986, The aminostratigraphy of the Sankaty Sand, Nantucket Island, Massachusetts [M.S. thesis]: Newark, Delaware, University of Delaware, 121 p.
- Schroeder, J.H., 1969, Experimental dissolution of Ca, Mg and Sr from Recent biogenic carbonates: A model of diagenesis: *Journal of Sedimentary Petrology*, v. 39(3), p. 1057-1073.
- Schroeder, R.A., 1975, Absence of β -alanine and γ -aminobutyric acid in cleaned foraminiferal shells: Implications for use as a chemical criterion to indicate removal of non-indigenous amino acid contaminants: *Earth Science and Planetary Letters*, v. 25, p. 274-278.
- Shackleton, N.J., 1987, Oxygen isotopes, ice volume and sea level: *Quaternary Science Reviews*, v. 6, p. 183-190.
- Shackleton, N.J., and Opdyke, N.P., 1973, Oxygen isotope and paleomagnetic stratigraphy of equatorial Pacific core V28-238: Oxygen isotope temperatures and ice volumes on a 10⁵ and 10⁶ year time scale: *Quaternary Research*, v. 3, p. 39-55.
- Skinner, A., in press, ESR dosimetry and dating in aragonitic molluscs: *International Journal of Radiation Applications and Instrumentation, Part A*.
- Smart, P.L., Smith B.W., Chandra, H., Andrews, J.N., and Symons, M.C.R., 1988, An intercomparison of ESR and uranium series ages for Quaternary speleothem calcites: *Quaternary Science Reviews*, v. 7, p. 411-416.
- Spencer, R.S., and Campbell, L.D., 1987, The fauna and paleoecology of the late Pleistocene marine sediments of southeastern Virginia: *Bulletins of American Paleontology*, v.92(327), 84p.
- Srivastava, N.K., 1975, Early diagenetic changes in Recent molluscan shells: *Neues Jahrbuch Geol. Paläontologische Abh.*, 148(3), p. 380-403.
- Stumm, W. and Morgan, J., 1982, *Aquatic Chemistry*, John Wiley and Sons, New York, p. 243.
- Szabo, B.J., 1985, Uranium series dating of fossil corals from marine sediments of the U.S. Atlantic coastal plain: *Geological Society of America Bulletin*, v. 96, p.398-406.
- Turekian, K.K. and Armstrong, R.L., 1960, Mg, Sr and Ba concentrations and calcite-aragonite ratios of some Recent molluscan shells: *Journal of Marine Research*, v. 8(3), p. 133-151.
- Valentine, P.C., 1971, Climatic implications of a late Pleistocene ostracode assemblage from southeastern Virginia: *U.S. Geological Survey Professional Paper 683-D*, 28p.

- Vallentyne, J.R., 1969, Pyrolysis of amino acids in Pleistocene *Mercenaria* shells: *Geochimica et Cosmochimica Acta*, v. 33, 1453-1458.
- Veeh, H.H., and Burnett, W.C., 1982, Carbonate and phosphate sediments, *in* Ivanovich, M. and Harmon, R.S., eds. *Uranium series Disequilibrium: Applications to Environmental Problems*, Oxford, U.K., Clarendon Press, p. 459-480.
- Walker, B.M., 1979, Shell dissolution: Destructive diagenesis in a meteoric environment: *Scanning Electron Microscopy/1979/II*, p. 463-468.
- Walls, R.A., Ragland, P.C. and Crisp, E.L., 1977, Experimental and natural early diagenetic mobility of Sr and Mg in biogenic carbonates: *Geochimica et Cosmochimica Acta*, v. 41, p. 1731-1737.
- Wehmiller, J.F., 1982, A review of amino acid racemization studies in Quaternary mollusks: Stratigraphic and geochronologic applications in coastal and interglacial sites, Pacific and Atlantic coasts, United States, United Kingdom, Baffin Island and tropical islands: *Quaternary Science Reviews*, v.1, p. 83-120.
- Wehmiller, J.F., 1984, Interlaboratory comparison of amino acid enantiomeric ratios in fossil Pleistocene mollusks: *Quaternary Research*, v. 22, p. 109-120.
- Wehmiller, J.F., and Belknap, D.F., 1978, Alternative kinetic models for interpretation of amino acid enantiomeric ratios in Pleistocene mollusks; examples from California, Washington and Florida: *Quaternary Research*, v. 9, p. 330-348.
- Wehmiller, J.F., and Belknap, D.F., 1982, Amino acid age estimates, Quaternary Atlantic coastal plain; comparison with U-series dates, biostratigraphy and paleomagnetic control: *Quaternary Research*, v. 18, p. 311-336.
- Wehmiller, J.F., 1986, Amino Acid Racemization Chronology, *in* Proceedings of the Workshop "Dating Young Sediments", Beijing, Peoples's Republic of China, September 1985, p.139-158.
- Wehmiller, J.F., Belknap, D.F., Boutin, B.S., Mirecki, J.E., Rahaim, S.D., York, L.L., 1988, A review of the aminostratigraphy of Quaternary mollusks from the U.S. Atlantic coastal plain: *Geological Society of America Special Paper 227*, p. 69-109.
- Weiner, S. and Hood, L., 1975, Soluble protein of the organic matrix of mollusk shells: a potential template for shell formation: *Science*, v. 190, p. 987-990.
- Weiner, S. and Lowenstam, H.A., 1980, Well-preserved fossil mollusk shells: Characterization of mild diagenetic processes, *in* Hare, P.E., Hoering, T.C. and King, K., Jr., eds. *Biogeochemistry of Amino Acids*, John Wiley and Sons, New York, p. 95-107.

APPENDICES

APPENDIX A: ILC-B data and Experiments

- Appendix A.1: Total and Free ILC-B Concentration data
- Appendix A.2: Total and Free ILC-B Fraction data
- Appendix A.3: Free/Total Values for ILC-B Samples
- Appendix A.4: Hydrolysis Experiment Data
- Appendix A.5: Glassware Adsorption Data

APPENDIX B: Amino Acid Concentrations From Molluscan Shell Data

APPENDIX C: Elemental Concentrations, X-Ray Diffraction and Water Weight Gain/Loss Experimental Data

- Appendix C.1: Sr, Ca, Mn, Fe concentrations($\mu\text{g/g}$ shell) in mollusc shells by flame atomic absorption spectrometry
- Appendix C.2: R values for calcite/aragonite mixtures, obtained from X-ray diffraction
- Appendix C.3: Water weight gain/loss data

APPENDIX D: Stratigraphic Sections

- Appendix D.1: Norris Bridge site, Whitestone,
Yadkin Pit site, Deep Creek, VA
Gomez Pit site, Mears Corner, VA (in pocket)

APPENDIX E: Electron Spin Resonance Data

APPENDIX F: Values of Constants for Age Calculations Using the Non-Linear Kinetic Model for Isoleucine

APPENDIX G: Mean values of Amino Acid Concentrations and Fractions by Shell Condition and Shell Age

APPENDIX A

ILC-B DATA AND EXPERIMENTAL DATA

- Appendix A.1: Total and free ILC-B concentration data
- Appendix A.2: Total and free ILC-B fraction data
- Appendix A.3: Free/total values for ILC-B samples
- Appendix A.4: Hydrolysis experiment data
- Appendix A.5: Glassware adsorption data

TABLE A.1-1: ILC-B TOTAL SAMPLE CONCENTRATIONS

RUNDATE	SAMPLE NO.	UDAALAB NO	ASP	THR	SER	GLU	GLY	ALA	VAL
5/15/88	C-B5/11T(OLD)	880215	897.2	88.4	69.5	588.1	784.4	450.9	371.6
5/15/88	C-B5/11T(NEW)	880217	602.6	99.5	77.5	655.0	745.9	627.8	414.2
1/18/88	ILC-B12/10T	870791	669.1	103.0	47.0	499.6	382.0	500.6	297.6
10/5/87	ILC-B10/1T	870752	803.9	89.9	58.6	472.9	407.5	504.2	302.0
9/26/87	ILC-B9/13T	870706	864.3	36.7	44.5	449.9	408.9	494.3	298.9
9/14/87	ILC-B9/1T	870587	688.3	47.3	37.9	352.9	316.0	387.9	233.3
9/07/87	ILC-B7/27T	870551	505.5	35.0	20.0	276.5	241.4	286.2	168.7
7/5/87	ILC-B6/24T	870461	875.5	145.4	41.7	501.5	436.6	503.4	345.6
6/23/87	ILC-B6/17T	870441	349.0	43.2	25.5	202.8	188.9	228.6	134.4
6/5/87	ILC-B5.30T	870393	696.7	68.7	40.7	362.4	299.2	345.7	220.6
5/26/87	ILC-B5.23T	870363	695.9	77.9	26.4	356.0	318.4	367.3	231.4
5/5/87	ILC-B5.1T	870279	472.5	37.0	37.0	262.1	239.9	273.7	180.3
5/1/87	ILC-B4/16T	870219	1009.0	63.5	70.3	503.7	457.6	571.0	305.8
3/13/87	ILC-B3/6T	870148	547.0	65.6	38.6	293.0	254.2	321.5	188.2
2/13/87	ILC-B1/28T	870062	865.6	85.9	58.4	559.5	443.0	527.9	320.7
1/19/87	ILC-B1/12T	870007	716.0	85.6	42.1	363.3	326.4	393.2	238.8
12/16/87	ILCB12/4T	860848	1230.3	101.8	71.6	637.9	537.0	654.8	410.0
10/27/86	ILCB10/19T	860744	517.8	65.4	34.1	286.1	302.6	347.6	196.5
9/12/86	ILC-B8/27T	860618	1048.1	174.0	133.9	706.1	631.8	689.7	413.5
8/27/86	ILC-B8/23T	860577	826.8	87.3	43.0	460.6	408.5	503.1	293.5
7/29/86	ILC-B7/12T	860469	784.4	92.1	50.8	472.2	393.1	460.5	282.4
7/28/86	ILC-B6/30T	860418	686.4	71.7	36.2	377.1	332.1	399.3	227.0
6/29/86	ILC-B6/15T	860377	813.0	77.0	43.7	505.1	437.0	533.9	310.1
6/21/86	ILCB-6/10T	860357	617.0	66.9	34.2	363.6	311.2	385.8	229.2
6/14/86	ILCB-6/6T	860313	1079.8	121.1	55.6	584.4	482.0	601.0	354.2
		MEAN	754.5	81.2	49.5	443.7	403.4	454.4	278.8
		STD. DEV.	202.6	32.2	22.6	130.8	144.6	120.0	77.3
		%C.V.	26.8	39.6	45.6	29.5	35.8	26.4	27.7

152

TABLE A.1-1: ILC-B TOTAL SAMPLE CONCENTRATIONS, CONTINUED

RUN DATE	SAMPLE NO.	MET	ALLO	ISO	LEU	TYR	PHE	A/I AREA	A/I HT
5/15/88	I-B5/11T(OLD)	50.3	55.2	146.1	267.1	157.7	241.9	0.36	0.42
5/15/88	I-B5/11T(NEW)	57.5	64.2	175.2	316.7	130.0	283.1	0.37	0.42
1/18/88	ILC-B12/10T	36.0	54.6	121.2	208.7	172.1	183.9	0.45	0.49
10/5/87	ILC-B10/1T	0.0	63.8	132.2	223.5	118.2	200.1	0.48	0.51
9/26/87	ILC-B9/13T	56.1	54.2	126.6	221.2	105.2	189.6	0.43	0.48
9/14/87	ILC-B9/1T	31.9	41.2	99.6	171.6	50.1	146.7	0.41	0.47
9/07/87	ILC-B7/27T	47.3	28.9	65.2	119.8	112.2	97.6	0.44	0.51
7/5/87	ILC-B6/24T	1.6	65.1	146.7	241.2	41.8	204.7	0.44	0.50
6/23/87	ILC-B6/17T	22.8	21.4	56.5	93.9	52.5	82.9	0.38	0.46
6/5/87	ILC-B5.30T	32.7	40.7	93.6	172.2	74.7	150.8	0.43	
5/26/87	ILC-B5.23T	0.0	39.9	100.4	172.0	48.9	146.5	0.40	
5/5/87	ILC-B5.1T	10.9	32.8	75.1	134.5	35.1	96.7	0.44	
5/1/87	ILC-B4/16T	0.0	66.5	118.4	228.4	218.6	193.5	0.56	0.62
3/13/87	ILC-B3/6T	0.0	39.9	81.9	145.6	41.3	111.9	0.49	0.53
2/13/87	ILC-B1/28T	0.0	65.0	137.9	252.1	244.5	208.3	0.47	0.54
1/19/87	ILC-B1/12T	43.1	49.2	99.1	189.1	100.7	151.6	0.50	
12/16/87	ILCB12/4T	58.0	74.3	168.4	295.9	158.1	244.7	0.44	0.48
10/27/86	ILCB10/19T	8.5	37.4	81.2	144.7	126.9	118.7	0.46	0.52
9/12/86	ILC-B8/27T	86.4	58.4	174.2	315.7	319.5	265.8	0.34	0.38
8/27/86	ILC-B8/23T	24.4	48.0	129.1	1189.7	106.2	178.2	0.37	0.45
7/29/86	ILC-B7/12T	0.0	52.7	135.6	232.1	154.6	186.9	0.39	0.47
7/28/86	ILC-B6/30T	49.0	47.2	99.8	175.5	170.7	140.8	0.47	0.57
6/29/86	ILC-B6/15T	72.9	56.6	123.1	220.4	203.1	193.1	0.46	0.54
6/21/86	ILCB-6/10T	52.1	42.1	96.2	170.0	168.6	144.0	0.44	0.50
6/14/86	ILCB-6/6T	82.7	71.5	156.4	282.3	219.9	238.9	0.48	0.52
	MEAN	33.0	50.8	117.6	207.3	132.4	176.0	0.44	
	STD. DEV.	27.4	13.4	32.6	56.8	70.0	52.3	0.05	
	%C.V.	82.9	26.4	27.8	28.3	52.9	30.0	11.50	

153

TABLE A.1-2: ILC-B FREE SAMPLE CONCENTRATIONS

RUN DATE	SAMPLE NO	UDAALAB NO	ASP	THR	SER	GLU	GLY	ALA	VAL
5-15-88	B5/11F (OLD)	880216	508.8	16.1	14.7	101.2	289.3	397.4	152.2
5-15-88	B5/11F (NEW)	880218	468.5	22.5	19.2	101.6	290.7	399.1	142.0
1-18-88	ILC-B12/10F	870808	425.8	47.4	25.3	152.4	255.7	385.7	154.5
10-5-87	ILC-B10/1F	870753	241.9	21.7	21.0	83.5	211.2	318.1	124.8
9-26-87	ILC-B9/13F	870707	432.9	30.7	37.2	119.6	270.6	382.4	151.0
9-14-87	ILC-B9/1F	870588	202.2	15.9	16.9	50.7	116.1	162.2	68.9
9-7-87	ILC-B7/27F	870554	245.1	22.8	9.2	69.6	159.4	230.8	91.0
7-5-87	ILC-B6/24F	870469	299.2	48.4	10.8	81.0	177.2	239.9	110.3
6-23-87	ILC-B6/17F	870450	344.3	48.8	20.2	94.2	220.8	322.0	138.8
6-5-87	ILC-B5/30F	870404	699.7	64.2	28.0	156.4	357.8	496.9	210.9
5-26-87	ILC-B5/23F	870364	514.4	42.6	18.2	107.9	221.5	298.3	130.8
5-5-87	ILC-B5/1F	870286	468.7	39.9	39.9	123.7	267.9	378.4	156.7
5-1-87	ILC-B4/16F	870231	177.7	14.4	14.4	45.1	119.4	170.7	70.6
3-13-87	ILC-B3/6F	870158	363.4	43.5	19.1	90.3	212.0	311.2	118.6
2-13-87	ILC-B1/28F	870008	177.8	23.1	10.7	40.9	100.0	145.4	54.7
1-19-87	ILC-B1/12F	870015	300.6	21.0	13.5	82.8	167.0	259.9	105.2
12-16-87	ILC-B12/4F	860854	297.5	17.9	12.3	74.4	180.3	264.0	106.9
10-27-86	ILC-B10/19F	860754	442.6	27.2	26.6	119.9	265.2	388.8	152.3
9-12-86	ILC-B8/27F	860629	225.1	15.4	12.2	68.2	152.5	218.5	92.1
8-27-86	ILC-B8/23F	860587	403.2	42.5	33.0	107.4	248.9	363.3	144.6
8-1-86	ILC-B7/12F	860480	755.4	93.2	87.4	195.9	458.2	648.9	260.0
7-28-86	ILC-B6/30F	860429	185.7	24.0	8.2	49.9	123.2	178.4	66.1
6-29-86	ILC-B6/15F	860386	447.2	44.9	16.9	119.5	283.9	399.1	165.4
6-21-86	ILC-B6/10F	860367	180.7	18.4	8.8	46.9	104.6	151.8	58.4
6-16-86	ILC-B6/6F	860325	648.8	76.9	36.2	161.3	413.2	600.9	244.2
		MEAN	378.3	35.3	22.4	97.8	226.7	324.5	130.5
		STD. DEV.	161.6	19.9	16.1	39.2	91.1	128.5	52.4
		% C.V.	42.7	56.4	71.7	40.1	40.1	39.5	40.1

154

TABLE A.1-2: ILC-B FREE SAMPLE CONCENTRATIONS, CONTINUED

RUN DATE	SAMPLE NO.	UDAALABNO	MET	ALLO	ISO	LEU	TYR	PHE	AI FREE AREA	AI FREE HT
5-15-88	B5/11F (OLD)	880216	38.1	31.4	41.0	120.1	100.2	93.6	0.77	
5-15-88	B5/11F (NEW)	880218	46.3	31.3	41.1	120.7	113.3	100.8	0.76	
1-18-88	ILC-B12/10F	870808	30.4	36.1	43.0	109.8	118.1	88.9	0.84	0.93
10-5-87	ILC-B10/1F	870753	0.0	30.3	38.6	94.3	79.4	69.7	0.78	0.90
9-26-87	ILC-B9/13F	870707	72.9	36.2	42.3	110.8	117.3	88.9	0.85	0.94
9-14-87	ILC-B9/1F	870588	19.3	15.6	20.3	49.4	48.5	37.3	0.77	0.89
9-7-87	ILC-B7/27F	870554	27.6	21.7	26.9	67.5	67.0	47.6	0.80	0.92
7-5-87	ILC-B6/24F	870469	40.7	28.5	30.6	78.0	81.9	61.3	0.93	
6-23-87	ILC-B6/17F	870450	38.7	28.3	34.7	93.5	84.8	68.4	0.82	0.90
6-5-87	ILC-B5/30F	870404	50.8	53.5	63.5	161.2	161.1	126.4	0.84	
5-26-87	ILC-B5/23F	870364	33.1	28.2	36.1	95.5	106.4	75.8	0.78	
5-5-87	ILC-B5/1F	870286	56.4	42.7	46.1	117.4	114.6	86.2	0.93	
5-1-87	ILC-B4/16F	870231	21.5	16.9	19.2	46.2	44.8	32.8	0.88	0.98
3-13-87	ILC-B3/6F	870158	34.9	32.8	36.9	94.1	79.2	67.5	0.89	
2-13-87	ILC-B1/28F	870008	28.8	14.5	16.4	47.7	37.9	28.7	0.89	0.99
1-19-87	ILC-B1/12F	870015	27.5	28.1	26.5	70.9	69.7	53.6	1.06	1.03
12-16-87	ILC-B12/4F	860854	29.8	28.5	31.5	79.6	74.8	57.7	0.91	0.98
10-27-86	ILC-B10/19F	860754	39.4	39.5	44.0	109.2	124.7	94.0	0.90	0.94
9-12-86	ILC-B8/27F	860629	18.9	19.9	26.5	64.8	68.9	54.9	0.75	0.84
8-27-86	ILC-B8/23F	860587	41.6	34.2	42.5	108.7	100.6	78.4	0.81	
8-1-86	ILC-B7/12F	860480	77.3	62.2	76.1	193.1	204.4	152.0	0.82	
7-28-86	ILC-B6/30F	860429	18.0	16.6	21.3	53.4	44.2	34.5	0.80	
6-29-86	ILC-B6/15F	860386	41.0	38.5	45.4	123.7	123.7	94.5	0.85	0.96
6-21-86	ILC-B6/10F	860367	15.2	14.0	17.8	45.7	43.4	34.8	0.79	0.93
6-16-86	ILC-B6/6F	860325	69.1	58.6	68.1	180.2	180.3	136.7	0.86	0.96
	MEAN		36.7	31.5	37.5	97.4	95.5	74.6	0.84	
	STD. DEV.		18.0	12.7	14.9	39.1	41.8	31.9	0.07	
	% C.V.		49.1	40.2	39.8	40.1	43.8	42.8	8.20	

155

TABLE A.2-1: ILC-B TOTAL FRACTION

RUN DATE	SAMPLE NO.	UDAALAB NO.	FRAC ASP	FRAC GLU	FRAC GLY	FRAC ALA
5-15-88	D-B5/11T(NEW)	880217	0.161	0.176	0.200	0.168
5-15-88	D-B5/11T(OLD)	880215	0.241	0.158	0.211	0.121
1-8-88	ILC-B12/10T	870791	0.230	0.172	0.131	0.172
10-5-87	ILC-B10/1T	870752	0.265	0.156	0.135	0.167
9-26-87	ILC-B9/13T	870706	0.286	0.149	0.135	0.163
9-14-87	ILC-B9/1T	870587	0.294	0.151	0.135	0.166
9-7-87	ILC-B7/27T	870551	0.280	0.153	0.134	0.159
7-5-87	ILC-B6/24T	870461	0.277	0.159	0.138	0.159
6-23-87	ILC-B6/17T	870441	0.263	0.153	0.142	0.172
6-5-87	ILC-B5/30T	870393	0.302	0.157	0.130	0.150
5-26-87	ILC-B5/23T	870363	0.299	0.153	0.137	0.158
5-5-87	ILC-B5/1T	870279	0.277	0.154	0.141	0.160
5-1-87	ILC-B4/16T	870219	0.290	0.145	0.132	0.164
3-13-87	ILC-B3/6T	870148	0.286	0.153	0.133	0.168
2-13-87	ILC-B1/28T	870062	0.253	0.164	0.130	0.155
1-19-87	ILC-B1/12T	870007	0.289	0.147	0.132	0.159
12-16-86	ILC-B12/4T	860848	0.295	0.153	0.129	0.157
10-27-86	ILC-B10/19T	860744	0.254	0.140	0.148	0.170
9-12-86	ILC-B8/27T	860618	0.241	0.162	0.145	0.158
8-27-86	ILC-B8/23T	860577	0.279	0.155	0.138	0.170
7-29-86	ILC-B7/12T	860469	0.264	0.159	0.132	0.155
7-28-86	ILC-B6/30T	860418	0.273	0.150	0.132	0.159
6-29-86	ILC-B6/15T	860377	0.254	0.158	0.136	0.167
6-21-86	ILC-B6/10T	860357	0.259	0.153	0.131	0.162
6-14-86	ILC-B6/6T	860313	0.282	0.153	0.126	0.157
	MEAN		0.268	0.155	0.140	0.161
	STD. DEV.		0.029	0.008	0.020	0.010
	%C.V.		10.800	4.800	14.100	6.200

RUN DATE	SAMPLE NO.	FRAC VAL	FRAC ALLO	FRAC ISO	FRAC LEU	FRAC PHE
5-15-88	D-B5/11T(NEW)	0.111	0.017	0.047	0.085	0.035
5-15-88	D-B5/11T(OLD)	0.100	0.015	0.039	0.072	0.042
1-8-88	ILC-B12/10T	0.102	0.019	0.042	0.072	0.059
10-5-87	ILC-B10/1T	0.100	0.021	0.044	0.074	0.039
9-26-87	ILC-B9/13T	0.099	0.018	0.042	0.073	0.035
9-14-87	ILC-B9/1T	0.100	0.018	0.043	0.073	0.021
9-7-87	ILC-B7/27T	0.094	0.016	0.036	0.066	0.062
7-5-87	ILC-B6/24T	0.109	0.021	0.046	0.076	0.013
6-23-87	ILC-B6/17T	0.101	0.016	0.043	0.071	0.040
6-5-87	ILC-B5/30T	0.096	0.018	0.041	0.075	0.032
5-26-87	ILC-B5/23T	0.099	0.017	0.043	0.074	0.020
5-5-87	ILC-B5/1T	0.106	0.019	0.044	0.079	0.021
5-1-87	ILC-B4/16T	0.088	0.019	0.034	0.066	0.063
3-13-87	ILC-B3/6T	0.098	0.021	0.043	0.076	0.022
2-13-87	ILC-B1/28T	0.094	0.019	0.040	0.074	0.072
1-19-87	ILC-B1/12T	0.096	0.020	0.040	0.076	0.041
12-16-86	ILC-B12/4T	0.098	0.018	0.040	0.071	0.038
10-27-86	ILC-B10/19T	0.096	0.018	0.040	0.071	0.062
9-12-86	ILC-B8/27T	0.095	0.013	0.040	0.072	0.073
8-27-86	ILC-B8/23T	0.099	0.016	0.044	0.064	0.036
7-29-86	ILC-B7/12T	0.095	0.018	0.046	0.078	0.052
7-28-86	ILC-B6/30T	0.090	0.019	0.040	0.070	0.068
6-29-86	ILC-B6/15T	0.097	0.018	0.038	0.069	0.063
6-21-86	ILC-B6/10T	0.096	0.018	0.040	0.071	0.071
6-14-86	ILC-B6/6T	0.092	0.019	0.041	0.074	0.057
	MEAN	0.098	0.018	0.041	0.073	0.045
	STD. DEV.	0.005	0.002	0.003	0.004	0.018
	%C.V.	5.200	10.200	7.200	5.900	39.900

TABLE A.2-2: ILC-B FREE FRACTION

RUN DATE	SAMPLE NO.	UDAALAB NO.	FRAC ASP	FRAC GLU	FRAC GLY	FRAC ALA
5-15-88	C-B5/11F(OLD)	880216	0.293	0.058	0.167	0.229
5-15-88	D-B5/11F(NEW)	880218	0.276	0.060	0.171	0.235
1-18-88	ILC-B12/10F	870808	0.258	0.092	0.155	0.233
10-5-87	ILC-B10/1F	870753	0.200	0.069	0.174	0.262
9-26-87	ILC-B9/13F	870707	0.265	0.073	0.166	0.234
9-14-87	ILC-B9/1F	870588	0.280	0.070	0.161	0.224
9-7-87	ILC-B7/27F	870554	0.255	0.072	0.166	0.241
7-5-87	ILC-B6/24F	870469	0.271	0.073	0.160	0.217
6-23-87	ILC-B6/17F	870450	0.256	0.070	0.164	0.239
6-5-87	ILC-B5/30F	870404	0.301	0.067	0.154	0.214
5-26-87	ILC-B5/23F	870364	0.341	0.072	0.147	0.198
5-5-87	ILC-B5/1F	870286	0.278	0.073	0.159	0.224
5-1-87	ILC-B4/16F	870231	0.254	0.065	0.171	0.244
3-13-87	ILC-B3/6F	870158	0.274	0.068	0.160	0.235
2-13-87	ILC-B1/28F	870071	0.284	0.065	0.160	0.232
1-19-87	ILC-B1/12F	870015	0.275	0.076	0.153	0.237
12-16-87	ILC-B12/4F	860854	0.266	0.066	0.161	0.236
10-27-86	ILC-B10/19F	860754	0.267	0.072	0.160	0.235
9-12-86	ILC-B8/27F	860629	0.244	0.074	0.165	0.237
8-27-86	ILC-B8/23F	860587	0.263	0.070	0.163	0.237
7-28-86	ILC-B6/30F	860429	0.255	0.068	0.169	0.245
6-29-86	ILC-B6/15F	860386	0.260	0.070	0.165	0.232
6-21-86	ILC-B6/10F	860367	0.276	0.072	0.160	0.232
6-16-86	ILC-B6/6F	860325	0.258	0.064	0.164	0.239
	MEAN		0.268	0.155	0.137	0.161
	STD.DEV.		0.028	0.007	0.014	0.01
	% C.V.		10.4	4.52	10.2	6.2
	FRAC VAL	FRAC ALLO	FRAC ISO	FRAC LEU	FRAC PHE	
5-15-88	C-B5/11F(OLD)	0.088	0.018	0.024	0.069	0.054
5-15-88	D-B5/11F(NEW)	0.084	0.018	0.024	0.071	0.059
1-18-88	ILC-B12/10F	0.094	0.022	0.026	0.066	0.054
10-5-87	ILC-B10/1F	0.103	0.025	0.032	0.078	0.058
9-26-87	ILC-B9/13F	0.092	0.022	0.026	0.068	0.054
9-14-87	ILC-B9/1F	0.095	0.022	0.028	0.068	0.052
9-7-87	ILC-B7/27F	0.095	0.023	0.028	0.070	0.050
7-5-87	ILC-B6/24F	0.100	0.026	0.028	0.071	0.055
6-23-87	ILC-B6/17F	0.103	0.021	0.026	0.070	0.051
6-5-87	ILC-B5/30F	0.091	0.023	0.027	0.069	0.054
5-26-87	ILC-B5/23F	0.087	0.019	0.024	0.063	0.050
5-5-87	ILC-B5/1F	0.093	0.025	0.027	0.070	0.051
5-1-87	ILC-B4/16F	0.101	0.024	0.027	0.066	0.047
3-13-87	ILC-B3/6F	0.089	0.025	0.028	0.071	0.051
2-13-87	ILC-B1/28F	0.087	0.023	0.026	0.076	0.046
1-19-87	ILC-B1/12F	0.096	0.026	0.024	0.065	0.049
12-16-87	ILC-B12/4F	0.095	0.025	0.028	0.071	0.051
10-27-86	ILC-B10/19F	0.092	0.024	0.027	0.066	0.057
9-12-86	ILC-B8/27F	0.100	0.022	0.029	0.070	0.059
8-27-86	ILC-B8/23F	0.094	0.022	0.028	0.071	0.051
7-28-86	ILC-B6/30F	0.091	0.023	0.029	0.073	0.047
6-29-86	ILC-B6/15F	0.096	0.022	0.026	0.072	0.055
6-21-86	ILC-B6/10F	0.089	0.021	0.027	0.070	0.053
6-16-86	ILC-B6/6F	0.097	0.023	0.027	0.072	0.054
	MEAN	0.098	0.018	0.042	0.073	0.046
	STD.DEV.	0.005	0.002	0.003	0.004	0.018
	% C.V.	5.10	11.1	7.1	5.48	39.1

APPENDIX A.3: ILC-B FREE/TOTAL VALUES

SAMPLE	F/T ASP	F/T GLU	F/T GLY	F/T ALA	F/T VAL	F/T ALLO	F/T ISO	F/T LEU	F/T PHE
B5/11T(NEW)	0.778	0.155	0.390	0.836	0.343	0.488	0.235	0.381	0.356
B5/11T(OLD)	0.567	0.172	0.369	0.881	0.410	0.568	0.281	0.450	0.387
ILC-B12/10T	0.636	0.305	0.669	0.771	0.519	0.660	0.355	0.526	0.484
ILC-B10/1T	0.301	0.176	0.518	0.631	0.413	0.474	0.292	0.422	0.349
ILC-B9/13T	0.501	0.266	0.662	0.774	0.505	0.668	0.334	0.501	0.469
ILC-B9/1T	0.294	0.144	0.368	0.418	0.295	0.379	0.204	0.288	0.254
ILC-B7/27T	0.485	0.252	0.660	0.807	0.539	0.750	0.412	0.563	0.488
ILC-B6/24T	0.342	0.162	0.406	0.477	0.319	0.438	0.209	0.323	0.299
ILC-B6/17T	0.987	0.465	1.169	1.408	1.033	1.322	0.614	0.996	0.826
ILC-B5/30T	1.004	0.432	1.196	1.438	0.956	1.314	0.678	0.936	0.838
ILC-B5/23T	0.739	0.303	0.696	0.812	0.565	0.707	0.359	0.555	0.517
ILC-B5/1T	0.992	0.472	1.117	1.383	0.869	1.302	0.614	0.873	0.892
ILC-B4/16T	0.176	0.090	0.261	0.299	0.231	0.254	0.162	0.202	0.169
ILC-B3/6T	0.664	0.308	0.834	0.968	0.630	0.822	0.450	0.646	0.604
ILC-B1/28T	0.205	0.073	0.226	0.275	0.170	0.222	0.119	0.189	0.138
ILC-B1/12T	0.420	0.228	0.512	0.661	0.441	0.572	0.268	0.375	0.354
ILC-B12/4T	0.242	0.117	0.336	0.403	0.261	0.384	0.187	0.269	0.236
ILC-B10/19T	0.855	0.419	0.876	1.118	0.775	1.057	0.541	0.755	0.792
ILC-B8/27T	0.215	0.097	0.241	0.317	0.223	0.341	0.152	0.205	0.206
ILC-B8/23T	0.488	0.233	0.609	0.722	0.493	0.712	0.329	0.573	0.440
ILC-B7/12T	0.569	0.264	0.699	0.823	0.523	0.711	0.353	0.526	0.486
ILC-B6/30T	0.271	0.132	0.371	0.447	0.291	0.351	0.214	0.304	0.245
ILC-B6/15T	0.550	0.236	0.650	0.748	0.533	0.680	0.369	0.561	0.489
ILC-B6/10T	0.293	0.129	0.336	0.394	0.255	0.332	0.185	0.269	0.242
ILC-B6/6T	0.601	0.276	0.857	1.000	0.689	0.819	0.435	0.638	0.572
MEAN	0.527	0.236	0.601	0.744	0.491	0.653	0.334	0.493	0.445
STD. DEV.	0.258	0.117	0.285	0.339	0.233	0.319	0.154	0.226	0.215
% C.V.	48.9	49.6	47.4	45.6	47.5	48.8	46.1	45.8	48.3

158

APPENDIX A.4: DATA AND DESCRIPTION OF HYDROLYSIS EXPERIMENT

Appendix A.4 shows the results of the hydrolysis experiment. The purpose of this experiment was to determine changes in total hydrolyzate amino acid concentration resulting from variation in hydrolysis time. Samples of the ILC-A standard powder were prepared as total samples and hydrolyzed for periods of 2 to 90 hours. Results (concentration of amino acid versus hydrolysis time) are shown in Fig. A.4-1, and tabulated in Table A.4-1.

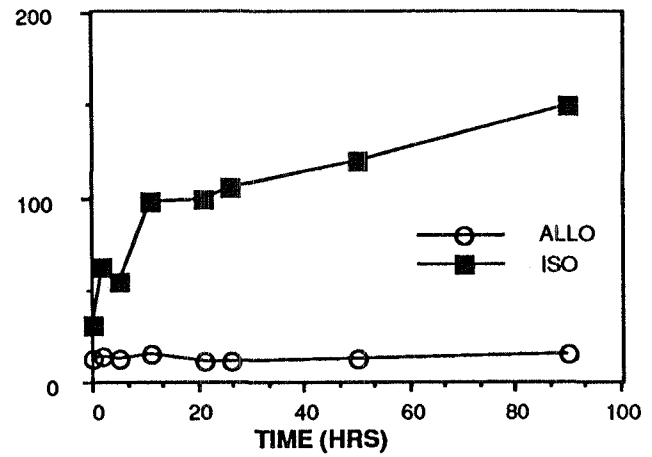
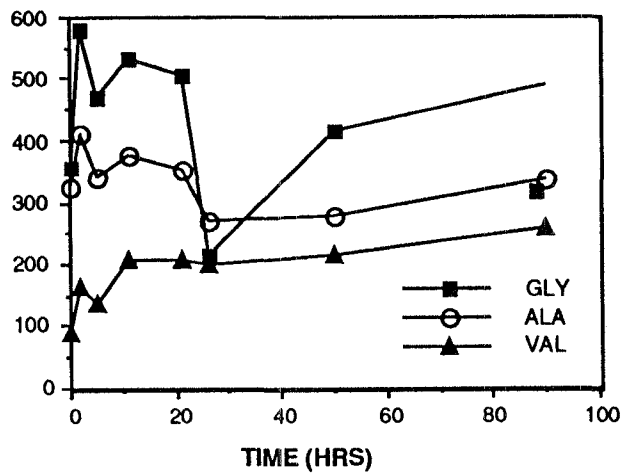
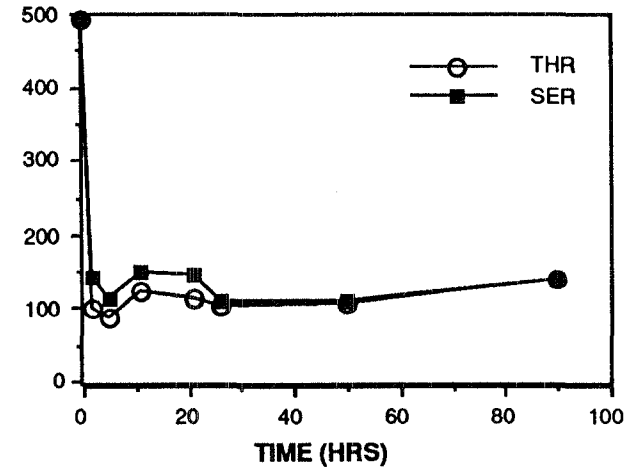
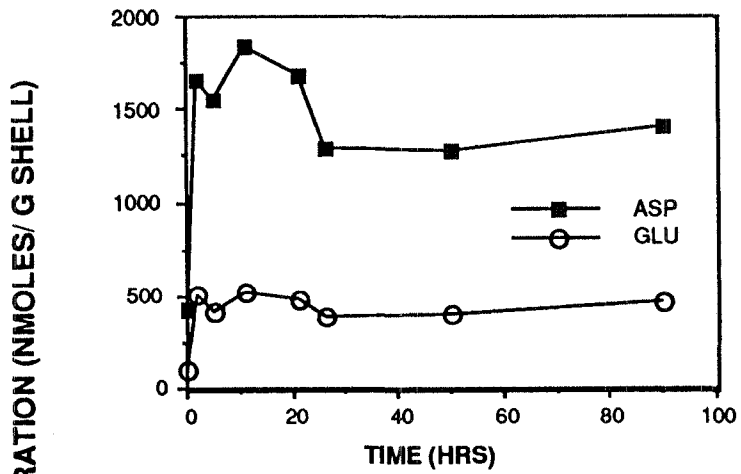


Fig. A.4-1. Results of hydrolysis experiment. Amino acid concentrations were obtained from ILC-A standard powders, hydrolyzed for periods of 2 to 90 hours.

09)

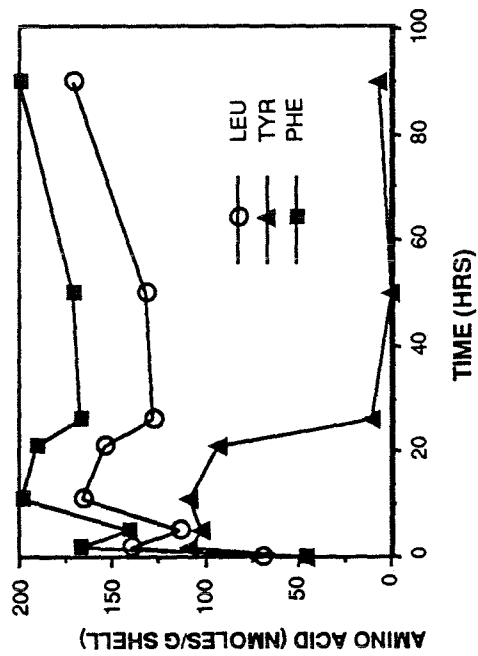
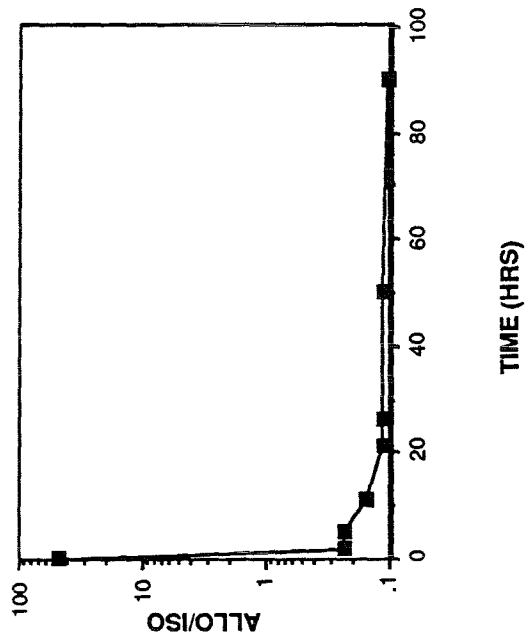


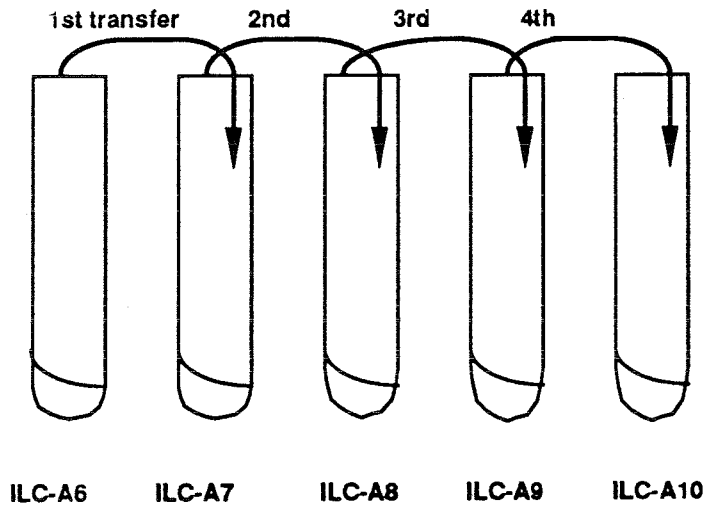
Fig. A.4-1. Continued.

TABLE A.4-1: ILC-A DATA USED TO CONSTRUCT FIG. A.4-1

SAMPLE NO.	TIME	ASP	THR	SER	GLU	GLY	ALA	VAL
ILC-A (FREE)	0.000	428.1	493.1	493.1	110.8	358.1	325.8	89.2
ILC-A 2HRS	2.000	1663.5	100.6	143.5	513.7	582.0	413.4	162.9
ILC-A 5HRS	5.000	1561.9	87.0	114.9	413.3	471.8	339.5	138.8
ILC-A 11HRS	11.000	1843.2	125.6	151.7	519.5	533.5	377.8	209.4
ILC-A 21HRS	21.000	1687.3	114.2	147.8	488.2	506.8	354.4	208.0
ILC-A 26HRS	26.000	1299.7	104.2	111.1	396.9	216.5	271.6	198.8
ILC-A 50HRS	50.000	1280.4	108.3	111.8	400.0	416.8	276.6	214.1
ILC-A 90HRS	90.000	1413.2	141.6	139.7	467.3	491.2	335.9	259.6
SAMPLE NO.	TIME	MET	ALLO	ISO	LEU	TYR	PHE	ALLO/ISO
ILC-A (FREE)	0.000	0.0	12.8	31.2	69.7	46.4	46.4	0.41
ILC-A 2HRS	2.000	31.6	14.6	63.2	140.3	108.1	167.7	0.23
ILC-A 5HRS	5.000	23.3	12.7	55.0	113.9	102.4	141.2	0.23
ILC-A 11HRS	11.000	8.6	15.3	98.3	166.3	108.1	198.6	0.16
ILC-A 21HRS	21.000	8.5	11.2	99.4	153.9	92.3	190.9	0.11
ILC-A 26HRS	26.000	0.0	12.3	105.5	128.7	10.0	166.7	0.12
ILC-A 50HRS	50.000	0.0	13.7	119.9	132.0	0.0	171.8	0.11
ILC-A 90HRS	90.000	0.0	15.8	150.2	170.8	6.0	199.9	0.11

162

APPENDIX A.5: GLASS WALL ADSORPTION EXPERIMENT



AMINO ACID	ILC-A6	ILC-A7	ILC-A8	ILC-A9	ILC-A10	ILC-A8/30T (CONTROL)
FRACTION						
ASP	0.335	0.403	0.397	0.416	0.455	0.405
GLU	0.153	0.141	0.142	0.143	0.135	0.140
GLY	0.141	0.139	0.139	0.142	0.144	0.147
ALA	0.105	0.094	0.091	0.088	0.088	0.097
VAL	0.090	0.075	0.072	0.072	0.060	0.074
ALLO	0.001	0.003	0.000	0.000	0.004	0.004
ISO	0.051	0.040	0.043	0.033	0.033	0.040
LEU	0.064	0.052	0.064	0.055	0.041	0.045
PHE	0.060	0.051	0.052	0.051	0.039	0.049
ALLO/ISO	0.021	0.079	0.020	0.020	0.129	0.104
AMINO ACID ONCENTRATION	ILC-A6	ILC-A7	ILC-A8	ILC-A9	ILC-A10	ILC-A8/30T (CONTROL)
ASP	168.8	125.2	87.6	97.3	1121.9	1222.8
GLU	77.2	43.9	31.2	33.4	333.8	423.6
GLY	70.7	43.2	30.8	33.1	356.0	444.5
ALA	52.9	29.3	20.0	20.5	217.2	294.1
VAL	45.5	23.4	15.9	16.9	149.1	222.6
ALLO	0.5	1.0	0.0	0.0	9.8	12.5
ISO	25.5	12.4	9.5	7.7	80.9	119.8
LEU	32.0	16.2	14.1	12.9	100.5	136.0
PHE	30.0	15.8	11.5	11.9	96.7	147.1
ALLO/ISO	0.021	0.079	0.000	0.000	0.129	0.104

APPENDIX B

AMINO ACID CONCENTRATIONS IN FREE AND TOTAL SAMPLES FROM FOSSIL MOLLUSC SHELLS

Each sample in Appendix B is coded to identify possible problems with data from a particular free or total sample. If there is no code for a sample, then the quality of the chromatogram from that sample was satisfactory. Codes used in the "COMMENTS" column are as follows:

1. Quantitative data (nmoles/g shell) in the total sample from this shell fragment showed poor reproducibility during rerun. Only ALLO/ISO values should be used.
2. Quantitative data (nmoles/g shell) in the free sample from this shell fragment showed poor reproducibility during rerun. Only ALLO/ISO values should be used.
3. All data are poor. Sample data should be disregarded.
4. The ILC-B mollusc powder standard accompanying this batch of fossil samples showed ALLO/ISO values beyond the one standard deviation for all standards (*c.f.* Fig. 3-1).
5. Evidence of amino acid contamination was found in the HCl blank accompanying this batch of samples.

AMINOZONE IIA: GOMEZ PIT
AMINO ACID CONCENTRATIONS, FREE AND TOTAL SAMPLES

SAMPLE NO.	FREE ASP	TOTAL ASP	FREEGLU	TOTAL GLU	FREEGLY	TOTAL GLY	FREE ALA	TOTAL ALA
84GP-137A	373.3	1219.7	88.6	590.7	270.6	601.0	349.6	455.6
84GP-138B	315.4	972.8	74.5	380.6	241.9	469.9	311.9	354.6
84GP-140B	86.4	2411.6	19.5	929.2	51.3	941.9	71.2	770.1
84GP-141A	67.1	1372.5	17.1	511.8	50.3	635.7	55.3	412.1
85GP-153A	346.0	3515.2	67.0	1161.5	223.4	1378.0	302.6	999.4
85GP-154A	404.9	2199.4	74.3	598.1	263.4	790.9	356.4	557.5
85GP-154B	414.0	2402.0	79.5	773.8	253.9	982.4	363.7	705.1
85GP-163A2	517.2	604.8	130.9	276.0	343.8	292.1	405.9	238.2
85GP-167A	338.2	4951.6	109.8	1961.5	259.1	2111.3	388.2	280.5
85GP-174A	317.5	1519.7	63.3	554.6	186.0	625.9	244.0	476.0
85GP-176A	276.3	1271.3	71.3	545.9	190.7	489.1	266.6	232.8
85GP-178A	224.3	1680.5	50.2	588.6	153.2	703.0	206.4	515.8
85GP-180A	197.3	983.3	47.3	608.9	135.5	541.9	165.3	485.3
85GP-181A2	716.5	1243.9	114.6	370.6	386.9	460.3	507.0	328.6
85GP-182A	225.3	1648.2	40.6	559.3	145.5	701.6	186.8	523.9
85GP-183A	298.5	1031.0	89.7	542.3	275.6	566.4	282.7	424.1
85GP-184A	312.2	1046.0	76.6	378.3	254.2	493.8	279.1	349.0
85GP-185A	230.0	1360.5	65.5	561.0	209.2	661.8	214.3	492.2
85GP-186A	365.4	734.2	72.6	252.9	268.2	332.8	271.5	239.1
85GP-187A	388.9	3072.9	77.1	950.2	216.1	1538.5	363.8	937.8
85GP-237A	422.3	3322.7	149.8	1020.7	329.4	973.2	449.9	760.2
85GP-239A	397.4	1771.8	83.2	615.3	205.5	659.7	165.5	512.7
85GP-240A	572.1	1608.9	109.2	543.8	332.3	687.9	430.7	456.6
85GP-241A	195.4	1304.2	34.8	683.8	132.6	668.3	168.9	532.8
85GP-243A	2668.4	839.3	788.5	352.9	2047.3	435.6	2248.8	330.2
85GP-244A	145.9	1253.3	26.1	440.0	102.1	525.9	124.7	393.1
85GP-251A	329.7	1850.1	88.2	579.1	234.1	661.7	312.3	488.3
85GP-256A	215.5	973.7	52.5	353.7	101.3	434.3	201.5	328.6
85GP-258A	457.6	1714.6	145.9	908.6	473.6	948.8	509.5	769.5
85GP-259A	229.3	2120.3	51.6	719.8	163.9	802.6	217.1	622.5
85GP-260A	260.5	2344.2	55.1	723.0	162.3	824.7	235.5	603.8
85GP-264A	281.5	2923.6	61.4	843.0	204.8	992.6	245.9	648.5
85GP-264B	396.2	1643.7	124.7	554.3	336.6	632.0	353.1	417.5
85GP-266A	259.2	3041.6	48.9	925.8	175.7	1001.3	197.6	760.9
85GP-267A	75.7	1542.6	26.8	518.3	66.1	545.5	70.7	424.7
85GP-269A	212.0	654.0	50.1	227.8	158.2	272.4	192.4	208.4
85GP-270A	268.9	1153.3	52.2	462.4	176.9	542.2	199.0	409.0

APPENDIX B: AMINO ACID CONCENTRATIONS FROM MOLLUSC SHELL SAMPLES

165

AMINOZONE IIA: GOMEZ PIT
 AMINO ACID CONCENTRATIONS, FREE AND TOTAL SAMPLES, CONTINUED

SAMPLE NO.	FREE ASP	TOTAL ASP	FREEGLU	TOTAL GLU	FREEGLY	TOTAL GLY	FREE ALA	TOTAL ALA
85GP-271A	229.2	1169.4	38.8	428.1	148.3	548.1	156.7	392.2
85GP-273A	154.8	1012.2	32.8	398.4	104.8	462.9	137.7	387.4
85GP-274A	271.1	1030.0	68.0	414.9	229.5	497.0	252.3	386.2
85GP-275A	375.4	2195.0	72.3	669.1	246.9	839.8	319.5	556.7
85GP-276A	318.1	1378.3	79.8	534.4	236.2	600.2	279.0	429.4
85GP-277A	279.8	1308.1	47.5	416.2	192.3	561.4	233.9	380.6
85GP-278A	313.5	1636.4	93.4	668.5	269.4	775.6	292.7	553.9
86GP-282A2	278.7	1641.8	93.2	802.9	272.3	1124.4	326.9	879.1
85GP-285A	331.2	1317.9	109.0	529.9	248.2	550.8	386.4	461.0
87GP-330A	345.1	1412.0	98.9	521.3	281.1	569.5	375.2	429.3
87GP-331A	312.5	639.2	80.1	291.0	275.9	383.9	318.4	344.9
87GP-338A	330.6	851.2	91.3	859.1	267.8	788.4	323.6	347.3
87GP-339A	316.1	873.8	90.7	848.2	259.9	798.4	317.8	608.7
87GP-340A	368.3	1133.2	74.7	643.7	231.0	661.1	315.6	646.5
87GP-341A	339.1	857.1	76.8	817.3	254.9	808.1	305.8	614.6
87GP-342A	264.2	777.1	59.6	597.1	193.4	529.8	279.9	318.0
87GP-343A	256.0	810.2	69.6	561.5	181.9	492.9	247.6	451.7
87GP-344A	229.6	669.2	53.6	404.1	197.1	422.4	219.1	403.1
JW88-51-1	183.2	674.6	38.5	343.1	146.9	441.5	175.2	366.4
JW88-51-2	186.1	716.7	97.0	996.6	150.9	441.3	179.6	459.3

APPENDIX B: AMINO ACID CONCENTRATIONS FROM MOLLUSC SHELL SAMPLES

146

AMINOZONE IIA: GOMEZ PIT
AMINO ACID CONCENTRATIONS, FREE AND TOTAL SAMPLES, CONTINUED

APPENDIX B: AMINO ACID CONCENTRATIONS FROM MOLLUSC SHELL
 SAMPLES

SAMPLE NO	FREE VAL	TOTAL VAL	FREE ALLO	TOTAL ALLO	FREE ISO	TOTAL ISO	FREE LEU	TOTAL LEU
84GP-137A	106.4	301.5	19.0	24.7	46.6	184.9	86.3	266.5
84GP-138B	98.6	177.0	15.0	23.5	40.6	113.2	78.7	163.2
84GP-140B	21.3	471.6	3.7	49.1	8.3	292.4	16.4	362.4
84GP-141A	22.3	238.3	3.6	22.6	8.4	168.7	16.2	214.6
85GP-153A	93.5	691.8	14.4	49.8	32.8	434.9	69.7	519.3
85GP-154A	108.8	370.9	18.9	31.6	41.8	258.2	86.6	297.5
85GP-154B	110.2	462.2	19.1	36.2	39.4	293.9	83.1	350.3
85GP-163A2	143.4	152.9	24.6	13.8	54.2	85.3	113.2	114.7
85GP-167A	156.6	1214.8	21.2	100.3	52.1	688.8	108.9	879.0
85GP-174A	70.8	209.3	5.6	20.5	29.0	190.7	58.7	229.3
85GP-176A	93.0	301.3	12.0	21.5	32.5	178.2	72.5	224.3
85GP-178A	515.8	354.5	9.6	28.0	25.0	222.4	50.5	268.7
85GP-180A	55.6	349.6	1.3	30.7	3.7	172.1	41.6	225.3
85GP-181A2	137.1	182.5	26.8	3.8	56.4	23.4	121.5	160.8
85GP-182A	55.5	310.6	8.9	23.8	21.9	210.6	40.2	244.8
85GP-183A	125.0	271.0	16.7	28.9	41.5	142.7	85.5	200.2
85GP-184A	113.5	182.2	15.4	19.8	39.1	120.8	85.8	146.9
85GP-185A	89.0	282.2	12.8	27.7	32.2	170.4	69.2	225.3
85GP-186A	68.9	119.3	12.3	13.8	37.2	80.2	64.6	104.8
85GP-187A	91.4	504.1	9.8	36.8	34.5	369.7	79.4	450.6
85GP-237A	160.8	615.2	17.9	38.0	46.4	275.1	104.9	347.7
85GP-239A	80.5	330.7	12.0	21.0	28.7	203.9	58.8	244.3
85GP-240A	126.6	294.1	17.1	19.2	47.8	203.6	85.5	245.1
85GP-241A	55.8	370.3	8.9	37.7	31.3	218.9	69.5	309.8
85GP-243A	924.1	211.6	117.5	19.3	340.7	120.7	702.6	163.4
85GP-244A	36.5	276.9	7.0	20.1	16.6	175.6	30.6	197.5
85GP-251A	105.9	323.6	13.2	21.9	38.3	213.9	83.8	244.7
85GP-256A	193.5	193.5	9.3	15.8	23.6	118.5	46.4	139.9
85GP-258A	235.6	539.8	24.5	42.6	68.9	285.6	181.3	399.6
85GP-259A	70.9	417.4	9.4	24.9	25.1	285.9	54.0	313.0
85GP-260A	64.2	394.5	10.8	26.5	26.2	279.0	52.9	314.3
85GP-264A	79.4	398.9	11.7	26.6	29.8	267.9	61.5	337.1
85GP-264B	165.2	265.5	21.8	20.6	51.4	182.8	104.4	238.1
85GP-266A	66.2	492.9	10.3	39.4	26.5	273.4	58.2	311.3
85GP-267A	26.6	280.5	4.2	24.3	8.9	163.6	22.8	211.2
85GP-269A	64.6	123.5	8.9	10.8	23.6	75.0	45.2	91.6
85GP-270A	66.9	269.5	8.7	22.5	24.9	153.8	49.1	185.6

167

**AMINOZONE IIA: GOMEZ PIT
AMINO ACID CONCENTRATIONS, FREE AND TOTAL SAMPLES, CONTINUED**

SAMPLE NO	FREE VAL	TOTAL VAL	FREE ALLO	TOTAL ALLO	FREE ISO	TOTAL ISO	FREELEU	TOTAL LEU
85GP-271A	44.3	197.7	7.5	19.9	19.8	143.2	37.1	169.2
85GP-273A	38.6	215.3	5.2	22.3	15.4	133.4	29.8	167.8
85GP-274A	102.0	243.1	13.9	20.2	34.4	143.4	75.2	178.4
85GP-275A	83.1	317.9	15.8	30.3	34.5	227.6	64.4	274.6
85GP-276A	89.0	273.2	14.2	25.9	34.6	165.5	66.2	205.6
85GP-277A	107.0	195.8	10.8	22.8	24.7	138.1	44.9	177.8
85GP-278A	123.1	340.7	18.2	33.2	43.1	208.7	82.3	268.5
86GP-282A2	141.1	565.7	17.1	45.5	46.8	308.7	97.3	401.9
85GP-285A	147.9	299.6	18.0	27.0	43.3	151.4	97.0	207.4
87GP-330A	156.4	313.0	21.1	23.8	46.3	173.8	96.1	223.7
87GP-331A	103.4	165.4	17.7	16.3	43.1	94.2	85.6	130.4
87GP-338A	118.5	383.4	15.2	32.7	40.6	236.5	80.5	296.2
87GP-339A	124.7	431.7	17.8	33.2	45.1	271.4	86.7	314.5
87GP-340A	113.8	188.4	18.6	30.3	45.7	223.1	89.4	270.5
87GP-341A	85.4	346.0	15.0	34.4	37.0	221.8	72.3	284.2
87GP-342A	73.8	298.7	12.2	27.9	31.1	166.8	60.2	216.1
87GP-343A	83.3	261.0	13.5	23.4	35.9	154.9	66.2	196.6
87GP-344A	71.6	230.4	12.8	21.4	33.0	137.0	61.1	183.3
JW88-51-1	47.1	194.4	5.9	11.7	20.0	106.5	38.4	153.4
JW88-51-2	69.8	300.0	7.8	22.5	25.7	125.6	47.4	201.7

APPENDIX B: AMINO ACID CONCENTRATIONS FROM MOLLUSC SHELL SAMPLES

168

**AMINOZONE IIA: GOMEZ PIT
AMINO ACID CONCENTRATIONS, FREE AND TOTAL SAMPLES, CONTINUED**

SAMPLE NO.	FREE PHE	TOTAL PHE	ALLO/ISO FREE	ALLO/ISO TOT	A/I FREE	A/I TOT RERUN	CONDITION	LAYER/UDAMS	COMMENTS
84GP-137A	57.6	213.9	0.407	0.134	0.419	0.158	E	2/06031	1, 2
84GP-138B	59.4	141.0	0.371	0.209	0.423	0.177	F	4/06031	1, 2
84GP-140B	13.8	376.6	0.448	0.168			F	1/06031	
84GP-141A	11.2	190.9	0.435	0.134			G	3/06031	
85GP-153A	63.3	532.7	0.438	0.114	N/A	0.119	E	1/06045	1
85GP-154A	73.6	303.0	0.452	0.112			G	1/06045	
85GP-154B	70.5	355.2	0.483	0.123	N/A	0.124	E	1/06045	
85GP-163A2	86.8	96.9	0.455	0.161	0.367	0.161	F	1/06045	2
85GP-167A	88.8	577.6	0.407	0.148	N/A	0.161	G	1/06045	1
85GP-174A	84.8	157.5	0.192	0.107	0.436	N/A	E	1/06045	
85GP-176A	49.6	224.4	0.368	0.120			E	1/06045	
85GP-178A	55.8	214.7	0.384	0.126			F	1/06045	
85GP-180A	39.4	246.5	0.357	0.179			G	J/06045	
85GP-181A2	105.4	248.0	0.475	0.160			F	J/06045	
85GP-182A	34.4	244.2	0.407	0.113			P	J/06045	
85GP-183A	62.0	168.8	0.404	0.198			F	K/06045	5
85GP-184A	50.7	133.4	0.393	0.163			G	K/06045	5
85GP-185A	41.7	188.7	0.397	0.163			G	K/06045	5
85GP-186A	46.8	86.8	0.329	0.172			G	K/06045	5
85GP-187A	64.5	398.2	0.284	0.100			G	K/06045	
85GP-237A	79.5	331.5	0.368	0.138			E	1/06056	4
85GP-239A	50.4	230.1	0.418	0.103			F	1/06056	4, 1
85GP-240A	69.2	221.8	0.357	0.094	0.352	0.093	F	1B/06056	4, 1, 2
85GP-241A	40.5	230.8	0.283	0.173	0.418	0.141	P	1A/06056	4, 1, 2
85GP-243A	467.8	127.6	N/A	0.160	0.345	0.113	E	1B/06056	4, 2
85GP-244A	25.1	207.5	N/A	0.114	0.422	0.120	E	1C/06056	4, 2
85GP-251A	59.7	323.1	0.345	0.102			G	1/06056	4, 2
85GP-256A	34.8	128.4	0.396	0.134	0.422	0.159	E	1A/06056	4, 2
85GP-258A	87.1	207.3	0.356	0.149			F	1A/06056	4
85GP-259A	40.1	317.8	0.374	0.087	0.433	0.108	P	1/06056	4
85GP-260A	44.2	321.8	0.415	0.095			E	1/06056	4
85GP-264A	47.1	321.5	0.393	0.099			F	2/06056	
85GP-264B	76.5	205.3	0.423	0.112			P	2/06056	
85GP-266A	42.7	339.4	0.387	0.144			G	2/06056	2
85GP-267A	8.1	198.8	0.471	0.149			E	2/06056	1, 2
85GP-269A	32.4	91.7	0.377	0.143			G	3/06056	
85GP-270A	43.5	184.2	0.349	0.147			G	3/06056	

APPENDIX B: AMINO ACID CONCENTRATIONS FROM MOLLUSC SHELL SAMPLES

169

**AMINOZONE IIA: GOMEZ PIT
AMINO ACID CONCENTRATIONS, FREE AND TOTAL SAMPLES, CONTINUED**

SAMPLE NO.	FREE PHE	TOTAL PHE	ALLO/ISO FREE	ALLO/ISO TOT	AI FREE	AI TOT RERUN	CONDITION	LAYER/UDAMS	COMMENTS
85GP-271A	1.1	179.8	0.377	0.139			F	2/06031	1, 2
85GP-273A	23.5	157.0	0.337	0.167			F	3/06056	2
85GP-274A	45.4	163.2	0.403	0.141			F	3/06056	
85GP-275A	52.6	51.1	0.459	0.133			G	3/06056	5
85GP-276A	54.0	192.7	0.411	0.157			F	4/06056	5
85GP-277A	45.0	157.0	0.437	0.165			F	4/06056	5
85GP-278A	62.5	223.4	0.424	0.159			G	4/06056	5
86GP-282A2	45.4	324.6	0.365	0.148	0.405	N/A	P	4/06056	5
85GP-285A	71.0	182.3	0.415	0.175			F	06054	2
87GP-330A	102.0	201.8	0.456	0.137	N/A	0.131	G	06054	4
87GP-331A	56.7	105.2	0.410	0.173			E	2/06058	4, 1
87GP-338A	65.8	284.0	0.374	0.138			G	2/06058	
87GP-339A	64.5	306.3	0.395	0.122			G	1/06058	
87GP-340A	74.2	275.7	0.408	0.139	N/A	0.146	E	1/06058	
87GP-341A	60.7	265.4	0.404	0.155			P	1/06058	
87GP-342A	53.1	209.0	0.393	0.167			F	1/06058	
87GP-343A	56.8	180.1	0.374	0.151			F	1/06058	
87GP-344A	48.7	158.4	0.387	0.156			G	1/06058	
JW88-51-1	28.5	128.0	0.293	0.109			P	1/06058	
JW88-51-2	40.9	177.4	0.301	0.179			P	?	?

APPENDIX B: AMINO ACID CONCENTRATIONS FROM MOLLUSC SHELL SAMPLES

172

AMINOZONE IIC: GOMEZ PIT
AMINO ACID CONCENTRATIONS, FREE AND TOTAL SAMPLES

APPENDIX B: AMINO ACID CONCENTRATIONS FROM MOLLUSC SHELL SAMPLES

SAMPLE NO.	FREE VAL	TOTAL VAL	FREE ALLO	TOTAL ALLO	FREE ISO	TOTAL ISO	FREE LEU	TOTAL LEU
85GP-148A	66.3	157.7	16.1	33.5	25.0	84.8	49.0	130.7
85GP-147A	157.7	289.8	34.4	47.8	49.6	132.2	113.1	220.3
85GP-150A	53.8	274.4	11.8	42.4	18.7	130.3	39.8	195.2
85GP-156A	65.7	143.2	16.1	26.6	28.2	73.9	51.5	107.8
85GP-157A	333.3	858.2	52.1	117.3	96.3	364.1	256.7	626.7
85GP-158A	159.9	152.9	40.2	29.2	62.0	97.5	112.0	115.8
85GP-159A	156.2	171.7	37.8	27.1	54.5	69.5	106.4	126.2
85GP-161A	66.8	145.8	17.1	25.7	23.5	83.3	46.2	105.8
85GP-169A2	130.0	306.1	29.6	43.9	41.5	158.1	91.9	221.2
85GP-170A	124.2	222.9	29.3	35.3	44.6	112.4	104.5	159.5
85GP-245A	79.0	167.9	23.6	28.8	31.4	88.8	65.9	128.6
85GP-255A	106.0	229.0	25.2	34.3	38.4	104.4	82.6	153.9
87GP-327A	97.2	210.0	21.9	36.8	31.3	88.5	67.9	147.7
87GP-328A	85.4	295.6	16.7	43.8	26.6	113.3	59.4	211.6
87GP-329A	104.4	146.6	20.0	19.6	32.0	64.1	72.8	103.4
87GP-329B	112.2	180.8	20.6	27.7	33.2	71.5	71.3	129.9
87GP-332A	110.3	215.9	21.6	34.6	36.1	112.8	69.5	149.2
87GP-333A	142.6	406.7	26.8	58.0	44.1	177.9	94.8	279.8
87GP-345A	175.2	339.6	38.0	57.8	54.8	176.5	120.3	261.4
87GP-346A	420.6	217.2	17.4	34.9	30.7	105.8	62.0	155.9

SAMPLE NO.	FREE ASP	TOTAL ASP	FREE GLU	TOTAL GLU	FREE GLY	TOTAL GLY	FREE ALA	TOTAL ALA
85GP-148A	369.7	782.2	67.2	337.4	214.5	421.2	523.6	472.8
85GP-147A	692.3	1158.7	124.3	543.2	409.0	639.5	537.9	682.2
85GP-150A	256.9	1383.9	45.9	555.9	145.7	670.2	183.4	705.2
85GP-156A	297.4	577.6	46.7	264.4	172.3	307.7	233.6	324.3
85GP-157A	946.6	2649.0	237.7	1505.7	716.0	1535.8	559.1	1959.1
85GP-158A	945.5	782.0	125.1	303.2	467.3	389.1	588.4	366.0
85GP-159A	681.9	761.1	104.7	314.8	404.4	356.1	540.7	377.6
85GP-161A	326.6	775.1	48.2	277.6	192.8	396.6	254.2	391.9
85GP-169A2	735.6	1577.3	100.9	644.0	374.4	705.9	477.5	736.2
85GP-170A	587.4	1246.6	100.2	477.8	339.6	509.3	420.1	537.4
85GP-245A	410.1	848.6	76.0	359.1	225.5	419.4	350.1	488.1
85GP-255A	417.9	793.6	85.9	422.2	306.9	470.3	400.3	544.3
87GP-327A	393.2	971.4	69.0	396.4	224.5	448.8	304.0	512.2
87GP-328A	210.6	831.8	61.3	521.5	181.2	526.8	232.4	577.7
87GP-329A	343.0	700.6	66.3	275.0	236.0	364.5	293.9	343.6
87GP-329BT	453.2	797.9	71.2	329.5	268.2	418.2	348.6	425.1
87GP-332A	437.5	1035.7	79.2	391.1	280.1	463.9	355.0	490.7
87GP-333A	549.8	1321.9	113.7	655.5	337.5	706.6	447.2	839.5
87GP-345A	397.7	777.5	112.4	625.5	365.2	589.0	587.2	826.2
87GP-346A	321.4	648.5	57.2	382.6	184.0	415.6	322.1	570.7

171

**AMINOZONE IIC: GOMEZ PIT
AMINO ACID CONCENTRATIONS, FREE AND TOTAL SAMPLES, CONTINUED**

**APPENDIX B: AMINO ACID CONCENTRATIONS FROM MOLLUSC SHELL
SAMPLES**

SAMPLE NO.	FREE PHE	TOTAL PHE	ALLO/ISO FREE	ALLO/ISO TOT	A/FR RERUN	A/ TOT RERUN	CONDITION	UDAMS SITE	COMMENT
85GP-148A	46.5	124.5	0.647	0.396	0.618	0.396	P	IOTTOM/06045	1
85GP-147A	96.2	201.3	0.693	0.361	0.693	0.362	P	IOTTOM/06045	
85GP-150A	35.9	203.1	0.630	0.325			P	IOTTOM/06045	
85GP-156A	44.7	95.3	0.572	0.359			P	IOTTOM/06045	1
85GP-157A	184.7	504.1	0.541	0.322			P	MIDDLE/06045	1
85GP-158A	117.9	122.5	0.647	0.300	0.647	0.298	P	MIDDLE/06045	1,2
85GP-159A	105.1	118.3	0.694	0.390	N/A	0.363	P	TOP/06045	1,2
85GP-161A	105.1	309.2	0.728	0.309			P	TOP/06045	1,2
85GP-169A2	90.0	248.0	0.715	0.278			P	IOTTOM/06045	1,2
85GP-170A	105.2	484.6	0.657	0.314			P	IOTTOM/06045	
85GP-245A	67.6	139.3	0.751	0.324			P	0/06056	
85GP-255A	67.5	158.2	0.657	0.329			P	0/06056	
87GP-327A	50.6	141.6	0.701	0.416			P	06062	4
87GP-328A	38.2	146.5	0.626	0.387			P	06062	4
87GP-329A	53.6	94.6	0.625	0.306	0.578	0.321	P	06059	2,4
87GP-329B	58.2	115.5	0.621	0.388			P	06059	4
87GP-332A	65.0	161.1	0.598	0.307			P	IOTTOM/06061	
87GP-333A	82.4	248.8	0.608	0.326			P	IOTTOM/06061	
87GP-345A	108.1	261.4	0.693	0.328			P	06062	
87GP-346A	57.9	148.9	0.566	0.330			P	06062	

172

APPENDIX B: AMINO ACID CONCENTRATIONS FROM MOLLUSC SHELL SAMPLES

**AMINOZONE IIC: YADKIN PIT
AMINO ACID CONCENTRATIONS, FREE AND TOTAL SAMPLES**

SAMPLE NO.	FREE ASP	TOTAL ASP	FREEGLU	TOTAL GLU	FREEGLY	TOTAL GLY	FREE ALA	TOTAL ALA
85YP-189A	269.5	718.5	59.1	349.0	228.7	457.5	276.0	435.3
85YP-190A	302.8	646.0	110.6	476.0	355.1	509.7	413.7	541.1
85YP-190A2	362.3	328.1	137.6	201.8	429.7	246.1	517.1	274.2
85YP-193A	312.9	1085.3	79.3	542.8	259.1	608.2	308.3	601.3
85YP-193A2	290.6	815.3	77.1	429.1	264.5	526.0	338.6	521.2
87YP-334A	335.4	561.2	82.0	325.9	314.0	393.3	371.4	381.0
87YP-335A	343.4	762.4	64.7	294.7	254.6	342.7	308.8	321.9
87YP-336A	299.6	797.3	93.0	380.7	280.4	434.9	323.2	387.9
87YP-337A	151.4	768.7	35.6	344.0	126.6	388.3	157.8	354.6

SAMPLE NO.	FREE VAL	TOTAL VAL	FREE ALLO	TOTAL ALLO	FREE ISO	TOTAL ISO	FREE LEU	TOTAL LEU
85YP-189A	88.4	219.0	16.9	30.9	32.3	106.4	54.2	137.3
85YP-190A	179.5	282.9	23.8	32.0	54.4	109.2	125.1	191.6
85YP-190A2	222.2	115.1	15.8	14.7	65.6	46.0	150.5	77.0
85YP-193A	109.6	278.1	17.6	35.0	37.4	143.0	78.1	207.7
85YP-193A2	107.8	238.3	16.8	33.4	35.1	112.4	71.5	160.4
87YP-334A	133.4	121.0	20.7	22.9	43.3	92.2	91.4	134.4
87YP-335A	91.3	159.1	17.4	22.0	31.3	111.8	61.2	139.8
87YP-336A	89.2	210.3	20.5	25.2	41.7	104.8	87.8	140.3
87YP-337A	51.6	178.5	7.6	19.4	15.2	88.1	34.3	125.2

SAMPLE NO.	FREEPHE	TOTAL PHE	A/I FREE	A/I TOTAL	A/I FR RERUN	A/I TOT RERUN	CONDITION	UDAMS LOC	COMMENTS
85YP-189A	41.9	125.1	0.521	0.291			P	1/06046	2
85YP-190A	61.6	113.5	0.437	0.293			P	1/06046	4
85YP-190A2	76.7	28.3	0.253	0.315	0.504	0.354	P	1/06046	1, 2
85YP-193A	52.6	179.4	0.471	0.243			P	1/06046	4
85YP-193A2	53.7	142.8	0.476	0.297			P	1/06046	2
87YP-334A	63.9	112.1	0.478	0.248			P	06071	4
87YP-335A	55.5	152.1	0.555	0.219	0.464	0.226	P	2/06072	2, 4
87YP-336A	62.4	127.1	0.493	0.241	0.436	0.208	P	2/06072	4
87YP-337A	23.1	113.0	0.496	0.220			P	2/06072	

173

**GOMEZ PIT SAMPLES FROM SITES 06065, 06066, 06067
(IIC/IID DISCONFORMITY): FREE AND TOTAL AMINO ACID CONCENTRATIONS**

APPENDIX B: AMINO ACID CONCENTRATIONS FROM MOLLUSC SHELL SAMPLES

SAMPLE NO.	FREE ASP	TOTAL ASP	FREEGLU	TOTAL GLU	FREEGLY	TOTAL GLY	FREE ALA	TOTAL ALA
87GP-320A	502.6	1018.5	93.6	518.1	305.4	516.4	461.6	691.2
87GP-321A	300.4	1014.9	55.0	569.1	218.1	633.8	227.0	751.0
87GP-322A	240.8	1641.4	47.3	563.6	151.1	648.5	207.5	550.0
87GP-323A	761.2	1304.8	111.6	471.3	455.8	656.6	627.9	742.6
87GP-324A	418.5	642.2	77.0	271.3	303.3	328.2	404.5	382.4
87GP-325A	475.3	969.6	70.4	376.1	270.4	485.2	394.4	556.4
87GP-326A	155.5	655.5	31.6	295.2	109.2	361.8	151.9	421.3
87GP-347A	323.8	641.7	85.3	470.6	288.6	475.4	400.7	500.6
87GP-348A	269.7	744.0	74.4	698.7	223.5	592.7	282.3	693.7
87GP-349A	311.1	808.7	60.6	545.6	203.1	555.0	276.5	280.8
87GP-350A	298.4	926.3	60.6	649.0	220.0	730.0	294.8	590.6
87GP-351A	371.0	732.6	47.2	557.6	265.8	490.4	365.1	579.3
87GP-352A	547.3	770.8	258.5	802.8	415.2	655.8	555.4	768.0
87GP-353A	442.0	773.6	163.6	589.9	262.0	484.6	410.7	567.7

SAMPLE NO	FREE VAL	TOTAL VAL	FREE ALLO	TOTAL ALLO	FREE ISO	TOTAL ISO	FREE LEU	TOTAL LEU
87GP-320A	141.33	288.84	33.07	53.48	40.03	103.41	94.15	195.32
87GP-321A	83.53	308.96	16.96	56.94	23.96	155.76	58.63	224.63
87GP-322A	58.85	282.37	10.32	25.86	20.97	176.46	38.55	231.18
87GP-323A	177.16	256.17	43.99	53.08	56.10	170.53	120.95	178.28
87GP-324A	141.96	182.77	27.94	31.47	44.24	82.07	96.58	132.05
87GP-325A	99.59	193.75	26.57	41.05	33.73	91.11	68.84	
87GP-326A	41.60	143.85	12.14	32.16	16.29	65.78	34.52	110.92
87GP-347A	130.98	217.10	21.94	34.88	41.48	125.28	90.28	166.67
87GP-348A	94.15	344.06	14.57	38.63	38.07	171.79	69.06	244.16
87GP-349A	81.67	283.98	13.10	31.14	32.02	164.47	63.80	215.82
87GP-350A	86.34	332.52	13.62	28.11	35.24	192.03	66.55	257.21
87GP-351A	125.02	317.68	22.24	48.81	36.93	138.09	50.91	216.32
87GP-352A	193.44	415.02	36.26	62.00	61.48	201.32	141.03	310.36
87GP-353A	136.10	285.74	27.42	43.22	43.62	139.17	99.09	207.49

174

**GOMEZ PIT SAMPLES FROM SITES 06065, 06066, 06067
 (IIC/IID DISCONFORMITY): FREE AND TOTAL AMINO ACID CONCENTRATIONS
 CONTINUED**

SAMPLE NO.	FREEPHE	TOTAL PHE	ALLO/ISO FREE	ALLO/ISO TOT	AI FR RERUN	LOCATION	CONDITION
87GP-320A	75.6	164.8	0.826	0.517	P	06067	4
87GP-321A	40.7	186.0	0.707	0.492	P	06067	4
87GP-322A	33.2	246.1	0.492	0.147	P	06066	4
87GP-323A	101.7	181.6	0.784	0.494	P	06066	4
87GP-324A	74.7	122.8	0.632	0.384	P	06066	4
87GP-325A	63.5	136.5	0.786	0.455	P	06065	4
87GP-326A	22.9	97.9	0.746	0.489	P	06065	4
87GP-347A	64.2	167.0	0.529	0.278	P	06065	
87GP-348A	53.7	197.5	0.383	0.225	P	06065	
87GP-349A	49.8	188.0	0.409	0.189	G	06065	
87GP-350A	52.6	228.3	0.387	0.146	G	06065	
87GP-351A	72.9	209.3	0.602	0.353	P	06066	
87GP-352A	94.1	236.8	0.590	0.308	P	06066	
87GP-353A	80.7	189.1	0.629	0.311	P	06066	

APPENDIX B: AMINO ACID CONCENTRATIONS FROM MOLLUSC SHELL
 SAMPLES

175

APPENDIX B: AMINO ACID CONCENTRATIONS FROM MOLLUSC SHELL SAMPLES

**AMINOZONE IID: GOMEZ PIT
AMINO ACID CONCENTRATIONS. FREE AND TOTAL SAMPLES**

SAMPLE NO.	FREE ASP	TOTAL ASP	FREEGLU	TOTAL GLU	FREEGLY	TOTAL GLY	FREE ALA	TOTAL ALA			
84GP-135A	N/A	553.8	N/A	393.4	N/A	390.4	N/A	390.2			
84GP-136A	N/A	544.0	N/A	281.7	N/A	304.3	N/A	347.8			
84GP-139A	662.1	1141.4	216.0	638.7	449.7	657.3	632.2	795.7			
87GP-327A	393.2	971.4	69.0	396.4	224.5	448.8	304.0	512.2			
	FREE VAL	TOTAL VAL	FREE ALLO	TOTAL ALLO	FREE ISO	TOTAL ISO	FREELEU	TOTAL LEU			
84GP-135A	N/A	212.2	N/A	41.5	N/A	80.4	N/A	154.1			
84GP-136A	N/A	141.0	N/A	30.5	N/A	69.0	N/A	122.8			
84GP-139A	186.3	354.1	45.2	68.3	59.4	163.9	135.2	281.1			
87GP-327A	97.2	210.0	21.9	36.8	31.3	88.5	67.9	147.7			
	FREE PHE	TOTAL PHE	A/I FREE	A/I TOTAL	A/I FR RERUN	A/I TOT RERUN	CONDITION	LOCATION	COMMENTS		
84GP-135A	N/A	120.2	N/A	0.5	0.7	0.5	P	1/06031	2		
84GP-136A	N/A	99.1	N/A	0.4	0.8	0.4	P	1/06031	2		
84GP-139A	112.4	228.3	0.8	0.4			P	1/06031			
87GP-327A	50.6	141.6	0.7	0.4			P	06062	4		

176

**AMINOZONE IID: NORRIS BRIDGE
AMINO ACID CONCENTRATIONS, FREE AND TOTAL SAMPLES**

APPENDIX B: AMINO ACID CONCENTRATIONS FROM MOLLUSC SHELL
SAMPLES

SAMPLE NO.	FREE ASP	TOTAL ASP	FREEGLU	TOTAL GLU	FREEGLY	TOTAL GLY	FREE ALA	TOTAL ALA
83NB-10B	357.4	900.0	100.202	879.603	217.1	649.6	364.8	905.1
83NB-12B	439.7	887.9	146.980	816.328	289.2	567.9	452.6	852.5
83NB-25A	452.4	1086.0	162.994	1468.851	241.2	877.7	485.7	1349.2
83NB-56A	566.5	819.5	200.799	1027.421	353.2	624.3	607.6	941.6
83NB-126B	461.1	1061.9	207.755	909.598	367.9	623.4	589.7	1527.3
	FREE VAL	TOTAL VAL	FREE ALLO	TOTAL ALLO	FREE ISO	TOTAL ISO	FREE LEU	FREE PHE
83NB-10B	97.4	464.2	26.920	86.544	32.3	195.4	73.5	302.4
83NB-12B	166.4	437.8	36.465	90.849	45.0	181.5	121.1	298.3
83NB-25A	144.7	703.9	44.399	164.886	45.8	337.2	126.8	544.2
83NB-56A	208.8	498.5	54.351	107.517	61.8	229.4	175.2	371.3
83NB-126B	210.7	868.4	55.914	192.308	63.8	415.1	189.6	741.8
	FREE PHE	TOTAL PHE	A/I TOTAL	A/I FREE	CONDITION	LOCATION		
83NB-10B	57.6	245.2	0.443	0.832	G	06000		
83NB-12B	91.8	266.5	0.501	0.811	G	06000		
83NB-25A	108.1	519.3	0.489	0.969	G	06000		
83NB-56A	124.8	335.1	0.469	0.880	F	06000		
83NB-126B	131.0	317.5	0.463	0.876	G	06000		

177

**AMINOZONE IIE: GOMEZ PIT
AMINO ACID CONCENTRATIONS, FREE AND TOTAL SAMPLES**

SAMPLE NO.	FREE ASP	TOTAL ASP	FREE GLU	TOTAL GLU	FREE GLY	TOTAL GLY	FREE ALA	TOTAL ALA		
86GP-290A	299.6	354.6	64.3	323.2	206.3	327.2	444.7	538.6		
86GP-303A	130.6	271.0	55.8	416.9	168.5	377.5	246.9	497.2		
86GP-304A	138.9	307.7	33.5	167.6	121.5	233.5	224.8	370.9		
86GP-314A	129.8	271.3	49.1	268.4	124.0	252.6	220.1	371.5		
	FREE VAL	TOTAL VAL	FREE ALLO	TOTAL ALLO	FREE ISO	TOTAL ISO	FREE LEU	TOTAL LEU		
86GP-290A	122.3	204.8	38.5	65.0	32.0	61.6	76.0	127.6		
86GP-303A	108.9	267.7	29.8	71.6	23.4	62.5	57.7	147.9		
86GP-304A	52.1	84.6	12.2	24.8	13.9	23.4	31.8	53.8		
86GP-314A	79.1	157.8	25.4	49.1	21.3	46.4	47.5	90.6		
	FREE PHE	TOTAL PHE	A/I FREE	A/I TOTAL	A/I FR RERUN	A/I TOT RERUN	CONDITION	LOCATION	COMMENT	
86GP-290A	55.8	94.4	1.19	1.05			P	06054		
86GP-303A	33.0	92.2	1.27	1.14			P	06054		
86GP-304A	22.4	49.9	0.88	0.98			P	06054		
86GP-314A	32.8	66.3	1.20	1.06			P	06054		

178

**AMINOZONE IIE: YADKIN PIT
AMINO ACID CONCENTRATIONS, FREE AND TOTAL SAMPLES**

SAMPLE NO.	FREE ASP	TOTAL ASP	FREE GLU	TOTAL GLU	FREE GLY	TOTAL GLY	FREE ALA	TOTAL ALA	
86YP-318A 2	125.0	628.3	40.5	510.1	99.0	496.3	200.2	914.3	
	FREE VAL	TOTAL VAL	FREE ALLO	TOTAL ALLO	FREE ISO	TOTAL ISO	FREE LEU	TOTAL LEU	
86YP-318A2	55.2	312.3	20.6	110.6	16.3	101.7	40.8	225.0	
	FREE PHE	TOTAL PHE	A/I FREE	A/I TOTAL VI	FREE RERUN A/I	TOT RERUN	CONDITION	UDAMS LOC	CONDITION
86YP-318A2	32.3	183.5	1.238	1.087	1.161	1.064	P	06046	4.000

APPENDIX B: AMINO ACID CONCENTRATIONS FROM MOLLUSC SHELL SAMPLES

179

**AMINOZONE IIE: CHOWAN RIVER FORMATION, NORTH CAROLINA
AMINO ACID CONCENTRATIONS, FREE AND TOTAL SAMPLES**

APPENDIX B: AMINO ACID CONCENTRATIONS FROM MOLLUSC SHELL
SAMPLES

SAMPLE NO	FREE ASP	TOTAL ASP	FREEGLU	TOTAL GLU	FREEGLY	TOTAL GLY	FREE ALA	TOTAL ALA
JW-85-09A	325.2	509.5	118.7	516.5	189.8	369.1	355.0	592.9
JW-85-10A	228.9	262.4	50.0	236.9	174.7	197.5	302.3	301.1
JW-85-11A	136.9	199.4	51.5	145.1	85.8	107.4	154.8	180.9
JW-85-17A	213.0	293.9	75.2	247.1	150.4	197.8	249.8	292.7
JW-85-19A	415.3	741.8	130.5	761.7	242.4	558.1	469.1	834.7
JW-85-23A	155.4	171.6	45.2	134.5	91.9	127.7	167.6	179.1
JW-85-24A	121.6	159.5	45.3	101.6	95.3	94.7	152.1	153.1
JW-85-28A	191.4	251.9	83.7	260.2	171.1	226.9	299.7	331.4
SAMPLE NO.	FREE VAL	TOTAL VAL	FREE ALLO	TOTAL ALLO	FREE ISO	TOTAL ISO	FREE LEU	TOTAL LEU
JW-85-09A	195.1	412.2	74.8	134.7	58.5	127.9	131.9	250.6
JW-85-10A	161.2	196.2	48.9	63.9	40.4	61.3	91.6	115.6
JW-85-11A	94.7	123.2	33.0	42.6	25.4	43.6	59.7	87.9
JW-85-17A	147.9	196.9	53.0	62.7	44.2	70.6	90.5	128.3
JW-85-19A	249.1	572.5	103.7	217.6	80.2	202.6	179.9	394.6
JW-85-23A	70.8	102.4	25.2	33.3	25.6	38.8	51.6	72.2
JW-85-24A	85.1	93.1	29.5	30.6	24.8	34.2	61.3	68.7
JW-85-28A	146.3	180.4	46.1	57.4	37.5	55.7	86.7	112.5
SAMPLE NO.	FREE PHE	TOTAL PHE	A/I FREE	A/I TOTAL	UDAMS LOC	CONDITION	COMMENT	
JW-85-09A	107.0	187.1	1.277	1.052	07069	G		
JW-85-10A	66.3	84.5	1.212	1.042	07069	G		
JW-85-11A	49.2	70.6	1.319	0.977	07069	F		
JW-85-17A	72.6	109.9	1.119	0.888	07069	F		
JW-85-19A	162.6	350.3	1.293	1.074	07070	G	1,2	
JW-85-23A	43.3	119.2	0.987	1.293	07069	F		
JW-85-24A	43.4	59.6	1.190	0.860	07069	G		
JW-85-28A	53.6	78.8	1.228	1.030	07070	P		

180

APPENDIX C

APPENDIX C.1: Sr, Ca, Mn, Fe Concentrations ($\mu\text{g/g}$ shell) in mollusc shells by flame atomic absorption spectrometry

APPENDIX C.2: R values for calcite-aragonite mixtures, obtained from X-ray diffraction

APPENDIX C.3: Water weight gain/loss data

Appendix C.1: Element analyses using atomic absorption spectrophotometry

Table C.1-1. Ca, Fe, Mn and Sr concentrations ($\mu\text{g/g}$ shell) in mollusc shells. Refer to Chapter 4.1 for flame atomic absorption spectrophotometry methods. N.d. indicates that the element was not detected.

SAMPLE NO.	Ca	Fe	Mn	Sr	Sr/Ca	CONDITION
83NB-10B	454012	20.2	1.0	1330	2.9e-3	G
83NB-126A	291686	42.7	9.5	2206	7.6e-3	G
83NB-12B	396083	35.5	6.6	2266	5.7e-3	F
83NB-25A	157129	n.d.	n.d.	1018	6.5e-3	G
83NB-56A	359715	34.8	4.1	1653	4.6e-3	F
84GP-135A	279439	60.9	0.4	2405	8.6e-3	P
84GP-136A	430535	77.4	0.5	2797	6.5e-3	P
84GP-137A	474867	104.1	7.3	1894	4.0e-3	E
84GP-138A	400958	88.5	n.d.	1914	4.8e-3	F
84GP-139A	317915	58.3	6.1	2658	8.4e-3	P
84GP-140A	367173	83.4	3.0	2355	6.4e-3	F
84GP-141A	342009	37.6	n.d.	1806	5.3e-3	G
85GP-147A	610516	70.9	2.2	2551	4.2e-3	P
85GP-148A	455279	86.2	26.0	2253	4.9e-3	P
85GP-150A	458638	67.8	5.3	2521	5.5e-3	P
85GP-153A	416621	57.8	n.d.	2486	6.0e-3	G
85GP-154A	988314	47.9	3.4	2422	2.5e-3	G
85GP-154B	1232692	204.0	15.1	2435	2.0e-3	E
85GP-156A	639065	18.7	n.d.	3008	4.7e-3	P
85GP-157A	472830	23.4	n.d.	2291	4.8e-3	P
85GP-158A	414423	192.8	1.7	2277	5.5e-3	P
85GP-159A	360107	n.d.	n.d.	2388	6.6e-3	P
85GP-161A	306347	71.7	n.d.	2288	7.5e-3	P
85GP-163A	523793	44.4	n.d.	1821	3.5e-3	F
85GP-167A	406341	102.5	8.5	2074	5.1e-3	G
85GP-169A	291515	49.5	4.8	2472	8.5e-3	P
85GP-170A	390352	312.6	n.d.	2550	6.5e-3	P
85GP-174A	440242	189.3	n.d.	2195	5.0e-3	E
85GP-176A	330455	17.8	n.d.	1674	5.1e-3	E
85GP-178A	373792	59.8	17.8	2018	5.4e-3	F
85GP-180A	412479	310.9	n.d.	2170	5.3e-3	G
85GP-181A	430992	33.8	4.1	2533	5.9e-3	F
85GP-182A	398915	168.0	n.d.	1490	3.7e-3	P
85GP-183A	802008	45.0	n.d.	1828	2.3e-3	F
85GP-184A	477282	89.6	1.4	2235	4.7e-3	G
85GP-185A	459889	59.2	n.d.	2345	5.1e-3	G

TABLE C.1-1, CONTINUED

SAMPLE NO	Ca	Fe	Mn	Sr	Sr/Ca	CONDITION
85GP-186A	404327	n.d.	n.d.	1947	4.8e-3	G
85GP-187A	350792	62.9	n.d.	1986	5.7e-3	G
85GP-237A	387409	27.1	5.3	1522	3.9e-3	E
85GP-239A	418947	51.7	5.0	1591	3.8e-3	F
85GP-240A	414645	131.7	0.3	1368	3.3e-3	F
85GP-241A	432790	146.6	6.4	1572	3.6e-3	P
85GP-243A	396590	62.4	3.1	1538	3.9e-3	E
85GP-244A	359621	64.1	5.3	1273	3.5e-3	E
85GP-245A	411633	166.6	n.d.	1153	2.8e-3	P
85GP-251A	221562	348.9	n.d.	2002	9.0e-3	G
85GP-255A	387864	28.3	9.1	1583	4.1e-3	P
85GP-256A	414504	missing	n.d.	777	1.9e-3	E
85GP-258A	430314	97.4	3.7	1613	3.7e-3	F
85GP-259A	338279	33.7	4.4	1660	4.9e-3	P
85GP-260A	405900	30.7	4.0	1333	3.3e-3	E
85GP-264A	missing	47.4	n.d.	1972		F
85GP-264B	649723	203.9	n.d.	1926	3.0e-3	P
85GP-266A	417827	6.7	4.2	1636	3.9e-3	G
85GP-267A	375916	166.6	0.4	1394	3.7e-3	E
85GP-269A	2485064	358.3	10.3	9506	3.8e-3	G
85GP-270A	394626	60.7	5.0	1739	4.4e-3	G
85GP-271A	431773	50.6	n.d.	1649	3.8e-3	F
85GP-273A	370061	269.1	n.d.	1505	4.1e-3	F
85GP-274A	416820	75.3	1.9	1617	3.9e-3	F
85GP-275A	390361	1.6	0.5	1424	3.6e-3	G
85GP-276A	420750	184.4	n.d.	1828	4.3e-3	F
85GP-277A	432998	196.5	n.d.	1397	3.2e-3	F
85GP-278A	404077	127.0	n.d.	1619	4.0e-3	G
85YP-189A	517127	6.2	n.d.	794	1.5e-3	P
85YP-190A	517484	21.9	8.5	2180	4.2e-3	P
85YP-193A	417778	198.9	15.6	1941	4.6e-3	P
86GP-282A	391497	85.4	19.6	1652	4.2e-3	P
86GP-285A	406482	51.4	13.4	2070	5.1e-3	F
86GP-290A	356837	86.1	10.1	2142	6.0e-3	P
86GP-303A	314744	31.4	19.5	1566	5.0e-3	P
86GP-304A	491030	99.7	29.3	2080	4.2e-3	P
86GP-314A	381754	94.8	9.0	2486	6.5e-3	P
86GP-318A	399465	37.1	11.2	2661	6.7e-3	P
87GP-320A	260940	110.1	n.d.	2201	8.4e-3	P
87GP-321A	324818	58.6	n.d.	3178	9.8e-3	P
87GP-322A	286979	103.0	n.d.	2326	8.1e-3	P
87GP-323A	387291	54.7	n.d.	2170	5.6e-3	P
87GP-324A	missing	38.6	0.2	2047		P
87GP-324B	355501	missing	missing	2308	6.5e-3	P
87GP-325A	437122	72.1	0.5	2468	5.6e-3	P
87GP-326A	268006	59.1	0.4	2368	8.8e-3	P
87GP-327A	368120	44.9	missing	2493	6.8e-3	P
87GP-328A	434864	49.8	n.d.	1786	4.1e-3	P
87GP-329A	333558	45.8	0.3	3055	9.2e-3	P
87GP-330A	412420	72.5	n.d.	1911	4.6e-3	G
87GP-331A	142908	0.0	n.d.	1024	7.2e-3	E
87GP-332A	376664	68.8	n.d.	1305	3.5e-3	P
87GP-333A	353926	50.0	n.d.	2277	6.4e-3	P
87GP-334A	368337	25.3	n.d.	1754	4.8e-3	P
87YP-335A	412017	69.0	n.d.	1978	4.8e-3	P
87YP-336A	262756	68.7	n.d.	1473	5.6e-3	P
87YP-337A	405753	22.9	n.d.	1010	2.5e-3	P
JW85-09	568411	17.9	6.9	1603	2.8e-3	G
JW85-10	358324	10.5	4.0	2528	7.1e-3	G
JW85-11	442628	15.3	5.9	1519	3.4e-3	F
JW85-17	554561	12.5	0.4	1572	2.8e-3	G
JW85-19	446975	30.6	0.6	2417	5.4e-3	G
JW85-23	540027	104.8	n.d.	1624	3.0e-3	F
JW85-24	387173	20.9	0.2	2158	5.6e-3	G
JW85-28	435252	47.4	n.d.	2769	6.4e-3	P

APPENDIX C.2: R values calculated for calcite-aragonite mixtures

R values were calculated as $R = I(\text{calcite})/I(\text{calcite} + \text{aragonite})$ where I = peak intensity (Turekian and Armstrong, 1960). See Chapter 4.3 for discussion of a standard curve for % calcite determination.

% CALCITE	R VALUE	% CALCITE	R VALUE
100	1	10	0.060
75	0.899	5	0.069
50	0.680	4	0.16
25	0.670	3	0.059
20	0.319	2	0.056
15	0.380	1	not detected

Table C.2-1. R values calculated for calcite/aragonite mixtures.

APPENDIX C.3: Water weight gain/loss data

TIME (HRS)	86L-319	86GP-260A	85GP-241A	TIME (HRS)	86L-319	86GP-260A	85GP-241A
0.0	4.8059 g	3.7315 g	3.0095 g	880.0	4.8404 g	3.7869 g	3.2913 g
24.0	4.8746	3.8016	3.2453	900.5	4.8524	3.7871	3.3200
48.0	4.8787	3.8060	3.2453	925.0	4.8524	3.7838	3.2668
75.0	4.8876	3.8090	3.3568	951.0	4.8622	3.7947	3.2118
99.0	4.8816	3.8105	3.3317	992.0	4.8532	3.7920	3.3087
122.0	4.8839	3.8086	3.3307	1018.0	4.7365	3.6763	2.9089
138.0	4.7836	3.7105	2.9746	1044.5	4.7333	3.6696	2.9053
174.0	4.7801	3.7086	2.9726	1065.5	4.7314	3.6666	2.9048
196.0	4.7785	3.7077	2.9726	1092.5	4.7364	3.6645	2.9041
222.0	4.7764	3.7070	2.9706	1104.5	4.7288	3.6612	2.9038
247.0	4.7769	3.7068	2.9712	1127.0	4.7279	3.6557	2.9009
281.0	4.7751	3.7049	2.9722	1199.0	4.7269	3.6544	2.9003
315.0	4.7749	3.7052	2.9699	1247.5	4.7417	3.6527	2.9011
340.5	4.8634	3.7863	3.3078	1271.5	4.7123	3.6506	2.8983
375.0	4.8717	3.7935	3.3268	1299.0	4.7114	3.6504	2.8976
399.5	4.8640	3.7993	3.2607	1321.0	4.7119	3.6507	2.8977
425.0	4.8639	3.7935	3.2864	1344.5	4.8370	3.7591	3.2581
470.0	4.8680	3.7914	3.2587	1367.5	4.8334	3.7650	3.3046
493.0	4.8681	3.7973	3.2997	1391.5	4.8331	3.7713	3.2947
589.5	4.7682	3.6999	2.9731	1415.0	4.8434	3.7677	3.2482
613.0	4.7679	3.6997	2.9420	1441.0	4.8354	3.7608	3.2938
641.0	4.7665	3.6988	2.9403	1480.0	4.7016	3.6249	2.8798
661.0	4.7665	3.6983	2.9403	1511.0	4.7014	3.6243	2.8800
754.0	4.7629	3.6972	2.9390	1535.0	4.7003	3.6179	2.8766
801.5	4.7625	3.6959	2.9365	1559.0	4.6998	3.6191	2.8796
826.5	4.7627	3.6967	2.9372	1582.0	4.6990	3.6163	2.8764
852.0	4.7622	3.6992	2.9366	1626.0	4.6994	3.6066	2.8784

Table C.3-1. Raw data from long-term weight gain/loss experiment. Shown above are the results of daily weighings (in grams) of modern (86L-319), excellent quality Pleistocene (aminozone IIa; 86GP-260A) and poor quality Pleistocene (aminozone IIa; 86GP-241A) shell fragments.

APPENDIX C, CONTINUED

TIME (HR)	85GP-176A	84GP-137	85GP-153A	85GP-185A	85GP-141A	83NB-10B	85GP-181A
0.0	2.6003 g	2.4488 g	3.2222 g	1.5612 g	1.5245 g	3.9062 g	2.4100 g
26.0	2.6571	2.5433	3.2902	1.7368	1.6690	3.9740	2.4772
56.0	2.6705	2.5460	3.2966	1.7341	1.6681	3.9735	2.4784
79.0	2.6568	2.5426	3.2934	1.7304	1.6683	3.9711	2.4792
121.0	2.6577	2.5429	3.2824	1.7328	1.6634	3.9693	2.4740
140.0	2.6585	2.5453	3.2932	1.7307	1.6662	3.9648	2.4802
167.0	2.5911	2.4394	3.2803	1.5532	1.5143	3.8935	2.4005
187.0	2.5903	2.4402	3.2089	1.5543	1.5145	3.8928	2.4011
214.0	2.5886	2.4379	3.2061	1.5519	1.5127	3.8903	2.3994
252.0	2.5885	2.4386	3.2071	1.5526	1.5136	3.8908	2.3976
479.5	2.5862	2.4367	3.2049	1.5508	1.2966	3.8893	2.3968
503.5	2.5852	2.4356	3.2034	1.5494	1.2949	3.8881	2.3950
525.5	2.5851	2.4345	3.2031	1.5467	1.2951	3.8876	2.3951
546.0	2.6427	2.5361	3.2772	1.7266	1.4205	3.9536	2.6975
575.0	2.6536	2.5356	3.2823	1.7308	1.4186	3.9501	2.4697
600.5	2.6491	2.5373	3.2827	1.7272	1.4199	3.9586	2.4722
CONDITION AMINOZONE	EXCELLENT IIA	EXCELLENT IIA	GOOD IIC	GOOD IIA	GOOD IIC	GOOD IID	FAIR IIA
TIME (HRS)	85GP-183A	85GP-138A	83NB-56A	85GP-156A	85GP-147A	85GP-182A	85GP-139A
0.0	2.3017 g	2.8292 g	2.4939 g	2.5367 g	1.8175 g	2.3913 g	2.2634 g
26.0	2.5312	3.0451	2.5736	2.7100	1.8993	2.6913	2.385
56.0	2.5306	3.0487	2.5826	2.7126	1.8952	2.6889	2.3873
79.0	2.5316	3.0480	2.5762	2.7050	1.8930	2.6775	2.3855
121.0	2.5313	3.0507	2.5767	2.6986	1.8868	2.7136	2.3822
140.0	2.5260	3.0485	2.5639	2.6951	1.8912	2.7536	2.3785
167.0	2.2814	2.8168	2.4785	2.5158	1.8122	2.7762	2.2538
187.0	2.2830	2.8189	2.4789	2.5155	1.8124	2.7536	2.2532
214.0	2.2797	2.8142	2.4767	2.5144	1.8111	2.3424	2.2518
252.0	2.2812	2.8158	2.4761	2.5147	1.8157	2.3419	2.2536
479.5	2.2793	2.8137	2.4762	2.5128	1.8114	2.3356	2.2521
503.5	2.2752	2.8112	2.4733	2.5118	1.8108	2.3327	2.2503
525.5	2.2753	2.8113	2.4735	2.5121	1.8108	2.3317	2.2504
546.0	2.5191	3.0369	2.5500	2.6755	1.8890	2.4659	2.3734
575.0	2.5179	3.0408	2.5483	2.6767	1.8851	2.6938	2.3682
600.5	2.5171	3.0395	2.5554	2.6724	1.8840	2.6677	2.3716
CONDITION AMINOZONE	FAIR IIA	FAIR IID	FAIR IID	POOR IIC	POOR IIC	POOR IIA	POOR IID

Table C.3-2. Raw data from short-term weight gain/loss experiment. Shown above are the results of daily weighings (in grams) of selected molluscs shells used in this project.

APPENDIX D
STRATIGRAPHIC SECTIONS

APPENDIX D.1-1: Norris Bridge site, Whitestone, Virginia

APPENDIX D.1-2: Yadkin Pit site, Deep Creek, Virginia

APPENDIX D.1-3: Gomez Pit, Mears Corner, Virginia (in pocket)

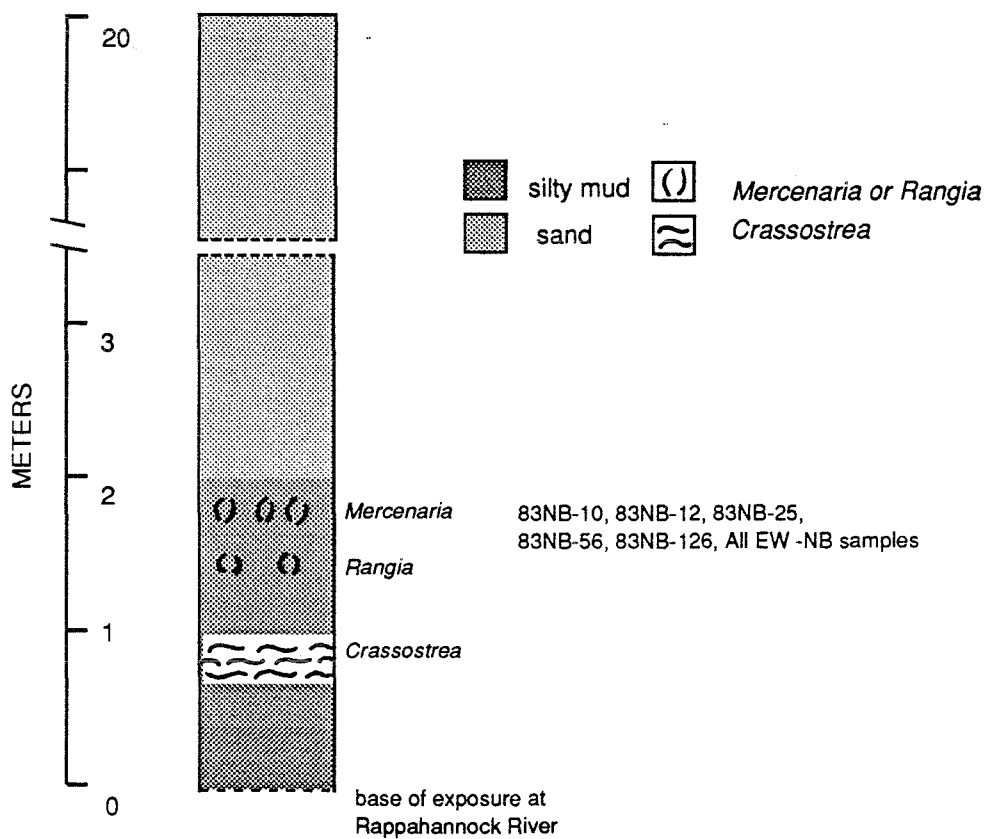


Fig. D.1-1. Stratigraphic section of the Norris Bridge site. Located on the north bank of the Rappahannock River, east of Norris (or Whitestone) Bridge; Irvington, VA 1:24,000 quad map. 37°38'00" North, 76°24'31" West.

APPENDIX D

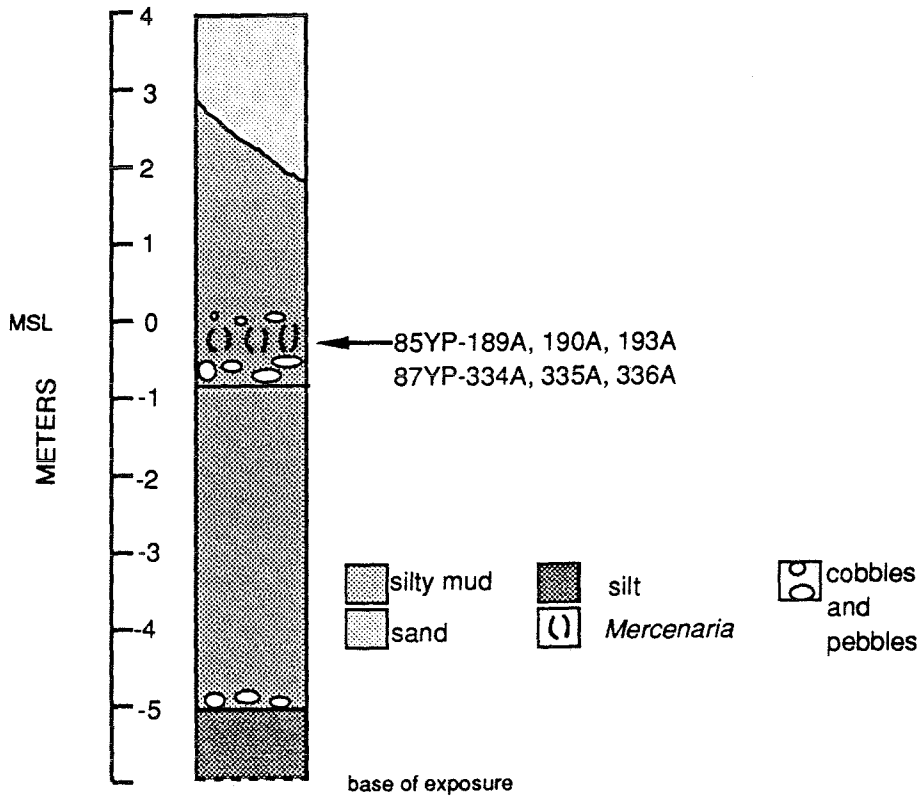


Fig. D.1-2. Stratigraphic section of the Yadkin Pit site. Located off of Dowdy Lane, in the Deep Creek area south of the City of Chesapeake; Norfolk South 1:24,000 quad map. 36° 45' 30" North, 76°22' 00" West

APPENDIX E

ELECTRON SPIN RESONANCE DATA

Tables E.1-1 and E.1-2 show element concentrations used to calculate internal and external doses for ESR dating. An example of ESR age calculation can be found in Smart *et al.*, (1988). All ESR dates from the Gomez Pit site are found in Skinner (in press, 1989).

SHELL SAMPLE	UDAMS LOC., LAYER	Uranium mg/kg	Age ka
87GP-341A	06058, layer 2	0.03	93
87GP-342A	06058, layer 2	0.04	125
87GP-343A	06058, layer 2	(a)	101
87GP-344A	06058, layer 2	(a)	97
87GP-345A	06062, <i>Crassostrea</i>	0.67	220
87GP-346A	06062, <i>Crassostrea</i>	(a)	262
87GP-347A	06065, Ilc/Ild discon.	(a)	103
87GP-349A	06065, Ilc/Ild discon.	0.18	86
87GP-351A	06066, Ilc/Ild discon.	0.68	111
87GP-352A	06066, Ilc/Ild discon.	(a)	136
87GP-353A	06066, Ilc/Ild discon.	(a)	118
87GP-135A	06031, Ilc/Ild discon.	1.88	99

Table E.1-1. Uranium concentrations used to calculate internal dose in shell samples for ESR dating. (a) means that uranium concentrations have not been measured in these samples. It was assumed that these samples would have similar uranium concentrations to other valves found in the same horizon.

Appendix E, continued.

UDAMS LOC. NUMBER	U mg/kg	Th mg/kg	K mg/kg
06058	1.15	2.9	0.76
06052	0.2	1.9	0.69
06065	0.5	2.2	1.08
06066	0.7	1.1	0.95

Table E.1-2. Element concentrations in sediment from each UDAMS site from which shells were analyzed. These data are used to calculate external dose.

APPENDIX F

VALUES OF CONSTANTS FOR AGE CALCULATIONS USING THE NON-LINEAR KINETIC MODEL OF ISOLEUCINE EPIMERIZATION

The following table lists values for the constants a and b of the non-linear kinetic model of isoleucine epimerization (Table 5, Boutin, 1989). These constants are used in the equation $y = a + b (\ln t)$, in order to calculate age from amino acid data. For more information on the development of the non-linear kinetic model, see Wehmiller *et al.* (1988) and Boutin (1989).

EQT (°C)	a	b
7.0	0.3461	-0.1542
7.5	0.3329	-0.1542
8.0	0.3183	-0.1542
9.0	0.2905	-0.1542
10.0	0.2627	-0.1542
11.0	0.2349	-0.1542
12.0	0.2071	-0.1542
13.0	0.1793	-0.1542
13.5	0.1660	-0.1542
14.0	0.1527	-0.1542
15.0	0.1250	-0.1542
16.0	0.0971	-0.1542
17.0	0.0693	-0.1542
18.0	0.0416	-0.1542
19.0	0.0135	-0.1542
20.0	-0.0145	-0.1542
20.5	-0.0284	-0.1542
21.0	-0.0419	-0.1542

Table F.1-1. Values of constants a and b for the kinetic equation for isoleucine epimerization.

APPENDIX G

TOTAL AMINO ACID CONCENTRATIONS BY CONDITION: AMINOZONE IIA

ASPARTIC ACID				GLUTAMIC ACID			
	MEAN	S.D.	%C.V. n		MEAN	S.D.	%C.V. n
E	1690.5	922.9	54.6 13	E	613.1	256.9	41.8 13
G	1476.8	766.4	51.9 17	G	589.8	216.0	36.6 17
F	1375.9	582.1	42.3 18	F	548.8	184.2	33.6 18
P	1271.2	494.5	38.9 11	P	657.8	175.2	26.6 11
GLYCINE				ALANINE			
	MEAN	S.D.	%C.V. n		MEAN	S.D.	%C.V. n
E	623.6	203.5	32.6 12	E	515.5	216.3	42.0 12
G	633.0	196.9	31.1 16	G	484.6	178.0	36.0 17
F	609.2	187.5	30.8 18	F	457.0	144.5	31.6 18
P	642.9	130.6	20.3 01	P	530.7	157.5	29.6 11
VALINE				ALLOISOLEUCINE			
	MEAN	S.D.	%C.V. n		MEAN	S.D.	%C.V. n
E	330.2	167.1	50.6 13	E	29.4	9.8	37.3 13
G	310.2	111.6	35.9 17	G	26.6	7.9	29.7 17
F	286.5	130.7	36.1 18	F	24.8	9.8	39.5 18
P	333.5	96.5	28.9 11	P	27.8	9.1	32.7 11
ISOLEUCINE				LEUCINE			
	MEAN	S.D.	%C.V. n		MEAN	S.D.	%C.V. n
E	191.5	65.5	32.7 12	E	258.8	106.1	41.1 12
G	194.8	75.1	38.6 17	G	238.8	86.6	36.3 17
F	168.7	68.6	40.6 18	F	223.0	75.8	34.0 18
P	199.4	60.5	30.3 11	P	259.2	66.5	25.6 11
PHENYLALANINE				ALLO/ISO IN TOTAL SAMPLE			
	MEAN	S.D.	%C.V. n		MEAN	S.D.	%C.V. n
E	220.6	84.7	38.4 12	E	0.131	0.022	16.8 13
G	218.3	97.8	44.8 17	G	0.142	0.022	15.3 18
F	202.6	64.7	31.9 18	F	0.152	0.031	20.4 18
P	232.4	58.2	25.0 11	P	0.142	0.033	23.2 11

Table G.1-1. Statistics describing mean, standard deviation (S.D.), coefficient of variation (%C.V.) and number of samples (n) of *Mercenaria* total sample amino acid concentrations (nanomole/g shell) collected from aminozone IIA in Gomez Pit. The physical condition of the shell was judged as excellent, good, fair or poor by the criteria listed in Chapter 8.

APPENDIX G, CONTINUED

FREE AMINO ACID CONCENTRATIONS BY CONDITION: AMINOZONE IIA

ASPARTIC ACID					GLUTAMIC ACID				
	MEAN	S.D.	%C.V.	n		MEAN	S.D.	%C.V.	n
E	294.0	106.0	36.0	12	E	69.6	32.1	46.1	12
G	293.6	83.7	28.5	18	G	71.1	23.1	32.5	18
F	331.7	152.4	45.9	18	F	76.9	34.6	45.0	18
P	262.1	68.7	26.2	11	P	66.0	28.7	43.5	11
GLYCINE					ALANINE				
	MEAN	S.D.	%C.V.	n		MEAN	S.D.	%C.V.	n
E	199.4	80.3	40.2	12	E	270.2	104.6	38.7	12
G	218.0	60.4	27.7	18	G	269.1	87.5	32.6	18
F	233.5	101.8	43.6	18	F	284.0	123.1	43.4	18
P	198.0	66.1	33.3	11	P	244.7	67.9	27.7	11
VALINE					ALLOISOLEUCINE				
	MEAN	S.D.	%C.V.	n		MEAN	S.D.	%C.V.	n
E	97.7	47.0	48.2	12	E	13.0	5.6	43.1	12
G	93.7	35.3	37.7	18	G	13.2	5.5	41.7	18
F	93.6	37.6	40.2	16	F	14.3	6.4	44.7	18
P	83.4	37.2	44.6	11	P	12.0	4.7	39.1	11
ISOLEUCINE					LEUCINE				
	MEAN	S.D.	%C.V.	n		MEAN	S.D.	%C.V.	n
E	32.6	12.3	37.7	12	E	66.9	25.1	37.5	12
G	33.6	12.5	37.2	18	G	70.0	22.4	32.0	18
F	35.6	15.1	42.4	18	F	73.8	38.2	51.7	18
P	31.6	10.4	32.9	11	P	62.9	22.5	35.7	11
PHENYLALANINE					ALLO/ISO IN FREE SAMPLE				
	MEAN	S.D.	%C.V.	n		MEAN	S.D.	%C.V.	n
E	54.0	23.0	42.6	12	E	0.411	0.040	9.7	12
G	52.3	17.7	33.8	18	G	0.389	0.046	11.8	18
F	51.9	22.7	43.8	17	F	0.400	0.037	9.2	18
P	45.7	13.8	30.2	11	P	0.376	0.063	16.7	11

Table G.1-2. Statistics describing mean, standard deviation (S.D.), coefficient of variation (%C.V.) and number of samples (n) of *Mercenaria* free sample amino acid concentrations (nanomole/g shell) collected from aminozone Iia in Gomez Pit. The physical condition of the shell was judged as excellent, good, fair or poor by the criteria listed in Chapter 8.

APPENDIX G, CONTINUED

TOTAL SAMPLE AMINO ACID FRACTIONS BY CONDITION: AMINOZONE IIA

ASPARTIC ACID				GLUTAMIC ACID			
	MEAN	S.D.	%C.V. n		MEAN	S.D.	%C.V. n
E	0.359	0.044	12.2 13	E	0.136	0.012	8.8 13
G	0.342	0.067	20.9 18	G	0.137	0.019	13.8 17
F	0.344	0.050	45.9 19	F	0.141	0.018	12.8 19
P	0.304	0.080	26.3 7	P	0.146	0.025	17.1 6

GLYCINE				ALANINE			
	MEAN	S.D.	%C.V. n		MEAN	S.D.	%C.V. n
E	0.155	0.012	7.7 12	E	0.121	0.020	16.5 12
G	0.161	0.015	9.3 18	G	0.120	0.014	11.7 17
F	0.159	0.010	6.3 19	F	0.120	0.013	10.8 19
P	0.163	0.019	11.6 6	P	0.126	0.018	14.3 7

VALINE				ALLOISOLEUCINE			
	MEAN	S.D.	%C.V. n		MEAN	S.D.	%C.V. n
E	0.072	0.011	15.3 13	E	0.006	0.001	16.7 13
G	0.075	0.012	16.0 18	G	0.007	0.001	14.3 18
F	0.075	0.012	16.0 19	F	0.007	0.001	14.3 18
P	0.077	0.008	10.4 7	P	0.006	0.002	33.3 7

ISOLEUCINE				LEUCINE			
	MEAN	S.D.	%C.V. n		MEAN	S.D.	%C.V. n
E	0.046	0.005	10.9 13	E	0.058	0.006	10.3 13
G	0.046	0.006	13.0 18	G	0.057	0.007	12.3 18
F	0.045	0.004	8.9 18	F	0.058	0.006	10.3 19
P	0.046	0.006	13.0 7	P	0.061	0.006	9.8 7

PHENYLALANINE			
	MEAN	S.D.	%C.V. n
E	0.053	0.008	15.1 13
G	0.054	0.010	18.5 17
F	0.052	0.006	11.5 18
P	0.054	0.004	13.5 7

Table G.1-3. Statistics describing mean, standard deviation (S.D.), coefficient of variation (%C.V.) and number of samples (n) of *Mercenaria* total sample amino fractions (nanomole/g shell) collected from aminozone IIA in Gomez Pit. The physical condition of the shell was judged as excellent, good, fair or poor by the criteria listed in Chapter 8.

APPENDIX G, CONTINUED

FREE SAMPLE AMINO ACID FRACTIONS BY CONDITION: AMINOZONE IIA

ASPARTIC ACID					GLUTAMIC ACID				
	MEAN	S.D.	%C.V.	n		MEAN	S.D.	%C.V.	n
E	0.267	0.021	7.9	13	E	0.064	0.011	17.2	13
G	0.265	0.027	10.2	18	G	0.064	0.006	9.4	18
F	0.265	0.035	13.2	16	F	0.063	0.009	14.3	19
P	0.263	0.021	8.0	7	P	0.059	0.010	16.9	7

GLYCINE					ALANINE				
	MEAN	S.D.	%C.V.	n		MEAN	S.D.	%C.V.	n
E	0.189	0.014	7.4	12	E	0.242	0.012	4.9	13
G	0.197	0.015	7.6	18	G	0.239	0.015	6.3	18
F	0.195	0.010	6.3	17	F	0.241	0.014	5.8	17
P	0.196	0.013	6.6	7	P	0.238	0.016	6.7	7

VALINE					ALLOISOLEUCINE				
	MEAN	S.D.	%C.V.	n		MEAN	S.D.	%C.V.	n
E	0.080	0.008	10.0	12	E	0.012	0.001	8.3	12
G	0.083	0.013	15.7	18	G	0.013	0.002	15.4	16
F	0.083	0.015	18.1	18	F	0.012	0.001	8.3	18
P	0.079	0.012	15.2	7	P	0.011	0.001	9.1	6

ISOLEUCINE					LEUCINE				
	MEAN	S.D.	%C.V.	n		MEAN	S.D.	%C.V.	n
E	0.030	0.003	10.0	13	E	0.062	0.006	9.7	13
G	0.031	0.003	13.0	17	G	0.063	0.006	9.5	18
F	0.030	0.003	10.0	18	F	0.060	0.007	11.7	17
P	0.032	0.005	15.6	7	P	0.059	0.004	6.8	6

PHENYLALANINE				
	MEAN	S.D.	%C.V.	n
E	0.047	0.005	10.6	11
G	0.049	0.007	14.3	17
F	0.046	0.006	11.5	18
P	0.048	0.004	8.3	7

Table G.1-4. Statistics describing mean, standard deviation (S.D.), coefficient of variation (%C.V.) and number of samples (n) of *Mercenaria* free sample amino fractions (nanomole/g shell) collected from aminozone IIA in Gomez Pit. The physical condition of the shell was judged as excellent, good, fair or poor by the criteria listed in Chapter 8.

APPENDIX G, CONTINUED

AMINOZONE IIC: COMPARISON BY CONDITION
 GOMEZ PIT IIC VERSUS YADKIN PIT IIC
 AMINO ACID CONCENTRATIONS OF FREE AND TOTAL SAMPLES

TOTAL SAMPLE CONCENTRATIONS

GOMEZ PIT		YADKIN PIT	
ASP	883.0 (258.7) 29.3% 25	720.3 (205.2)	28.4% 9
GLU	458.7 (153.6) 33.5 25	371.6 (101.0)	27.1 9
GLY	489.8 (117.8) 24.0 25	434.1 (107.5)	24.7 9
ALA	548.1 (151.4) 27.6 25	424.3 (109.3)	25.7 9
VAL	241.4 (81.5) 33.7 25	200.2 (61.7)	30.8 9
ALLO	37.9 (10.8) 24.5 25	26.2 (7.0)	26.8 9
ISO	116.1 (38.3) 33.0 25	108.5 (16.6)	15.3 8
LEU	175.2 (58.1) 33.2 25	146.0 38.0	26.0 9
PHE	173.4 (57.3) 33.0 24	133.2 (23.7)	17.8 8
A/I	0.334 (0.045) 13.5 26	0.261 (0.041)	15.7 9

FREE SAMPLE CONCENTRATIONS

GOMEZ PIT		YADKIN PIT	
ASP	437.3 (140.2) 28.3% 24	314.6 (30.5)	9.7% 8
GLU	83.5 (29.7) 35.9 24	82.1 (29.7)	36.1 9
GLY	289.2 (89.3) 29.0 24	298.3 (66.0)	22.1 8
ALA	399.2 (119.2) 29.0 26	357.1 (77.3)	21.6 8
VAL	120.0 (35.4) 29.5 23	119.2 (52.3)	43.6 9
ALLO	24.6 (8.0) 32.5 25	18.7 (2.7)	14.5 8
ISO	38.9 (11.5) 29.6 25	39.4 (8.0)	20.3 7
LEU	81.1 (26.4) 67.8 25	83.8 (35.8)	43.7 9
PHE	74.3 (24.1) 32.3 24	55.9 (7.6)	13.8 7
A/I	0.627 (0.076) 12.1 26	0.463 (0.090)	19.4 9

Table G.1-5. Comparison of Gomez Pit and Yadkin Pit total fractions representing aminozone IIC. Data are presented as Mean (Std. Dev.) Coefficient of variation, number of samples.

APPENDIX G, CONTINUED

AMINOZONE IIC: COMPARISON BY CONDITION
 GOMEZ PIT IIC VERSUS YADKIN PIT IIC
 AMINO ACID FRACTIONS OF FREE AND TOTAL SAMPLES

TOTAL SAMPLE FRACTIONS

GOMEZ PIT			YADKIN PIT		
ASP	0.284 (0.049)	17.3% 26	0.282 (0.035)	12.4%	9
GLU	0.146 (0.019)	13.0 25	0.146 (0.010)	6.8	9
GLY	0.158 (0.007)	4.4 25	0.171 (0.011)	6.4	9
ALA	0.175 (0.016)	9.1 26	0.168 (0.021)	12.5	9
VAL	0.077 (0.012)	15.6 26	0.078 (0.012)	15.4	9
ALLO	0.012 (0.002)	16.7 26	0.010 (0.001)	10.0	9
ISO	0.037 (0.006)	16.2 26	0.040 (0.004)	10.0	9
LEU	0.056 (0.008)	14.3 26	0.058 0.005	8.6	9
PHE	0.053 (0.008)	14.3 24	0.047 (0.012)	25.5	9

FREE SAMPLE FRACTIONS

GOMEZ PIT			YADKIN PIT		
ASP	0.283 (0.041)	14.5% 26	0.233 (0.031)	13.3%	9
GLU	0.053 (0.008)	15.1 24	0.062 (0.007)	11.3	9
GLY	0.185 (0.013)	7.0 25	0.213 (0.004)	1.9	9
ALA	0.246 (0.019)	7.7 24	0.256 (0.007)	2.7	9
VAL	0.076 (0.013)	17.1 25	0.089 (0.014)	14.3	9
ALLO	0.016 (0.002)	12.5 26	0.014 (0.002)	14.3	9
ISO	0.025 (0.003)	12.0 25	0.030 (0.003)	10.0	9
LEU	0.052 (0.008)	15.4 25	0.062 (0.010)	16.1	9
PHE	0.046 (0.006)	15.4 25	0.062 (0.010)	16.1	9

Table G.1-6. Comparison of Gomez Pit and Yadkin Pit free fractions representing aminozone Iic. Data are presented as Mean (Std. Dev.) Coefficient of variation, number of samples.

APPENDIX G, CONTINUED

TOTAL AMINO ACID CONCENTRATIONS BY AMINOZONE: GOMEZ PIT ONLY

ASPARTIC ACID					GLUTAMIC ACID				
	MEAN	S.D.	%C.V.	n		MEAN	S.D.	%C.V.	n
MOD	1230.4	58.2	4.7	5	MOD	2002.8	337.8	16.9	5
IIA	1454.8	707.6	48.6	59	IIA	595.1	208.0	34.9	59
IIC	883.0	258.7	29.3	25	IIC	458.7	153.6	33.5	25
IID	908.2	265.8	29.3	9	IID	437.8	121.1	27.7	9
IIE	301.1	34.3	11.4	4	IIE	294.0	90.2	30.7	4
GLYCINE					ALANINE				
	MEAN	S.D.	%C.V.	n		MEAN	S.D.	%C.V.	n
MOD	1628.0	78.1	4.8	5	MOD	1634.8	252.2	15.4	5
IIA	625.1	180.8	28.9	56	IIA	491.6	172.1	35.0	59
IIC	489.8	117.8	24.0	25	IIC	548.1	151.4	27.6	25
IID	495.0	132.0	26.7	9	IID	578.7	171.3	29.6	9
IIE	297.7	57.9	19.4	4	IIE	424.3	109.3	25.7	4
VALINE					ALLOISOLEUCINE				
	MEAN	S.D.	%C.V.	n		MEAN	S.D.	%C.V.	n
MOD	685.2	137.9	20.1	5	MOD	0.0	0.0	0.0	5
IIA	311.7	119.7	38.4	59	IIA	26.2	9.0	34.3	59
IIC	241.4	81.5	33.7	25	IIC	37.9	10.8	28.5	25
IID	234.3	73.3	31.3	9	IID	46.0	12.7	27.6	9
IIE	178.1	66.9	37.4	4	IIE	53.8	20.7	38.4	4
ISOLEUCINE					LEUCINE				
	MEAN	S.D.	%C.V.	n		MEAN	S.D.	%C.V.	n
MOD	594.3	161.0	27.1	5	MOD	984.5	346.8	35.2	5
IIA	186.9	67.9	36.3	58	IIA	242.2	84.1	34.7	59
IIC	116.1	38.3	33.0	25	IIC	175.2	58.1	33.2	25
IID	109.8	41.9	38.1	9	IID	176.9	56.2	31.8	8
IIE	105.6	36.0	34.3	4	IIE	48.5	15.9	32.7	4
PHENYLALANINE					ALLO/ISO IN TOTAL SAMPLE				
	MEAN	S.D.	%C.V.	n		MEAN	S.D.	%C.V.	n
MOD	1284.1	536.7	41.8	5	MOD	- - -	- - -	- - -	5
IIA	216.6	77.6	35.8	58	IIA	0.141	0.028	19.7	60
IIC	173.4	57.3	33.0	24	IIC	0.334	0.045	13.5	26
IID	150.7	43.4	28.8	9	IID	0.459	0.037	8.7	9
IIE	75.8	18.6	24.5	4	IIE	1.066	0.052	4.9	5

TABLE G.2-1. Statistics describing total sample *Mercenaria* amino acid concentrations (nanomoles/g shell) from all aminozones in Gomez Pit.

APPENDIX G, CONTINUED

FREE AMINO ACID CONCENTRATIONS BY AMINOZONE: GOMEZ PIT ONLY

ASPARTIC ACID					GLUTAMIC ACID				
	MEAN	S.D.	%C.V.	n		MEAN	S.D.	%C.V.	n
IIA	299.4	111.4	37.2	59	IIA	71.6	29.3	40.9	59
IIC	427.3	140.2	28.3	24	IIC	83.5	29.7	35.9	24
IID	464.3	206.7	44.5	7	IID	92.5	60.2	65.1	7
IIE	164.8	75.5	45.8	5	IIE	48.6	12.1	24.9	5
GLYCINE					ALANINE				
	MEAN	S.D.	%C.V.	n		MEAN	S.D.	%C.V.	n
IIA	215.2	79.4	36.8	59	IIA	269.3	98.6	36.6	59
IIC	289.2	83.9	29.0	24	IIC	399.2	119.2	29.0	26
IID	290.4	126.3	43.5	7	IID	399.9	187.3	46.8	7
IIE	143.9	43.0	29.9	5	IIE	267.3	100.5	37.5	5
VALINE					ALLOISOLEUCINE				
	MEAN	S.D.	%C.V.	n		MEAN	S.D.	%C.V.	n
IIA	92.5	38.3	41.3	57	IIA	13.2	5.6	42.0	59
IIC	120.0	35.4	29.5	23	IIC	24.6	8.0	32.5	25
IID	118.1	52.5	44.4	7	IID	28.6	12.8	44.8	7
IIE	83.5	31.4	37.6	5	IIE	25.3	9.9	39.1	5
ISOLEUCINE					LEUCINE				
	MEAN	S.D.	%C.V.	n		MEAN	S.D.	%C.V.	n
IIA	33.6	12.8	37.9	59	IIA	69.2	28.3	40.8	59
IIC	38.9	11.5	29.6	25	IIC	81.1	26.4	67.8	25
IID	37.3	15.9	42.6	7	IID	82.9	35.7	43.1	7
IIE	21.4	7.1	33.1	5	IIE	50.7	17.0	33.4	5
PHENYLALANINE					ALLO/ISO IN TOTAL SAMPLE				
	MEAN	S.D.	%C.V.	n		MEAN	S.D.	%C.V.	n
IIA	51.3	19.6	38.2	57	IIA	0.395	0.047	11.9	59
IIC	74.3	24.1	32.3	24	IIC	0.627	0.076	12.1	26
IID	66.8	32.3	48.3	7	IID	0.759	0.045	5.9	7
IIE	35.3	12.3	34.8	5	IIE	1.156	0.143	12.4	5

TABLE G.2-2. Statistics describing free sample *Mercenaria* amino acid concentrations (nanomoles/g shell) from all aminozones in Gomez Pit. Concentration data for free samples from modern shells is not included because analyses showed only negligible amounts of amino acids.

APPENDIX G, CONTINUED

TOTAL AMINO ACID FRACTIONS BY AMINOZONE: GOMEZ PIT ONLY

ASPARTIC ACID				GLUTAMIC ACID			
	MEAN	S.D.	%C.V. n		MEAN	S.D.	%C.V. n
MOD	0.126	0.023	18.3 5	MOD	0.200	0.016	8.0 5
IIA	0.342	0.059	17.3 57	IIA	0.139	0.018	13.0 55
IIC	0.284	0.049	17.3 26	IIC	0.146	0.019	13.0 25
IID	0.291	0.035	12.0 9	IID	0.141	0.014	9.9 9
IIE	0.176	0.040	22.7 5	IIE	0.157	0.024	15.3 5
GLYCINE				ALANINE			
	MEAN	S.D.	%C.V. n		MEAN	S.D.	%C.V. n
MOD	0.166	0.030	18.1 5	MOD	0.163	0.011	5.9 5
IIA	0.159	0.013	8.2 55	IIA	0.121	0.015	12.4 54
IIC	0.158	0.007	4.4 25	IIC	0.175	0.016	9.1 26
IID	0.159	0.008	5.0 9	IID	0.185	0.010	5.4 9
IIE	0.161	0.013	8.1 5	IIE	0.253	0.022	8.7 5
VALINE				ALLOISOLEUCINE			
	MEAN	S.D.	%C.V. n		MEAN	S.D.	%C.V. n
MOD	0.068	0.004	5.9 5	MOD	0.0	0.0	0.0 5
IIA	0.075	0.011	14.7 57	IIA	0.006	0.001	16.1 56
IIC	0.077	0.012	15.6 26	IIC	0.012	0.002	16.7 26
IID	0.075	0.009	12.0 9	IID	0.015	0.002	13.2 9
IIE	0.095	0.021	22.1 5	IIE	0.029	0.006	20.7 5
ISOLEUCINE				LEUCINE			
	MEAN	S.D.	%C.V. n		MEAN	S.D.	%C.V. n
MOD	0.058	0.008	13.8 5	MOD	0.096	0.021	21.9 5
IIA	0.046	0.005	10.9 56	IIA	0.058	0.006	10.3 57
IIC	0.037	0.006	16.2 26	IIC	0.056	0.008	14.3 26
IID	0.035	0.005	14.3 9	IID	0.057	0.008	14.0 8
IIE	0.027	0.005	18.5 5	IIE	0.058	0.010	17.2 5
PHENYLALANINE							
	MEAN	S.D.	%C.V. n				
MOD	0.123	0.040	32.5 5				
IIA	0.053	0.007	13.2 55				
IIC	0.053	0.008	14.3 24				
IID	0.048	0.003	6.3 9				
IIE	0.044	0.006	13.6 5				

TABLE G.2-3. Statistics describing total sample *Mercenaria* amino acid fractions (nanomoles/g shell) from all aminozones in Gomez Pit.

APPENDIX G, CONTINUED

FREE AMINO ACID FRACTIONS BY AMINOZONE: GOMEZ PIT ONLY

ASPARTIC ACID					GLUTAMIC ACID				
	MEAN	S.D.	%C.V.	n		MEAN	S.D.	%C.V.	n
IIA	0.265	0.027	9.2	54	IIA	0.063	0.009	14.3	56
IIC	0.283	0.041	14.5	26	IIC	0.053	0.019	15.1	24
IID	0.293	0.020	6.8	7	IID	0.057	0.014	24.6	7
IIE	0.193	0.028	14.5	5	IIE	0.059	0.009	15.3	5
GLYCINE					ALANINE				
	MEAN	S.D.	%C.V.	n		MEAN	S.D.	%C.V.	n
IIA	0.194	0.014	7.2	55	IIA	0.240	0.014	5.8	55
IIC	0.185	0.013	7.0	25	IIC	0.246	0.019	7.7	24
IID	0.186	0.013	6.9	7	IID	0.252	0.015	5.9	7
IIE	0.173	0.019	11.0	5	IIE	0.317	0.022	6.9	5
VALINE					ALLOISOLEUCINE				
	MEAN	S.D.	%C.V.	n		MEAN	S.D.	%C.V.	n
IIA	0.082	0.012	14.6	55	IIA	0.012	0.001	8.3	52
IIC	0.076	0.013	17.1	25	IIC	0.016	0.002	12.5	26
IID	0.075	0.006	8.0	7	IID	0.018	0.001	5.5	7
IIE	0.099	0.019	19.2	5	IIE	0.030	0.007	23.3	5
ISOLEUCINE					LEUCINE				
	MEAN	S.D.	%C.V.	n		MEAN	S.D.	%C.V.	n
IIA	0.031	0.003	9.7	55	IIA	0.061	0.006	9.8	54
IIC	0.025	0.003	12.0	25	IIC	0.052	0.008	15.4	25
IID	0.024	0.002	8.3	7	IID	0.053	0.005	9.4	7
IIE	0.025	0.003	12.0	5	IIE	0.061	0.008	13.1	5
PHENYLALANINE									
	MEAN	S.D.	%C.V.	n					
IIA	0.047	0.006	12.8	54					
IIC	0.046	0.006	13.0	24					
IID	0.042	0.002	4.8	7					
IIE	0.042	0.006	14.3	5					

TABLE G.2-4. Statistics describing free sample *Mercenaria* amino acid fractions (nanomoles/g shell) from all aminozones in Gomez Pit. Free amino acid concentrations and fractions were negligible in modern shells and were excluded.